University of New Mexico
UNM Digital Repository

Nuclear Engineering ETDs | Engineering ETDs

6-23-2015

Space-Time Kinetics of the AGN-201M Research Reactor at the University of New Mexico

Douglas Bowen

Follow this and additional works at: https://digitalrepository.unm.edu/ne_etds

Recommended Citation
Bowen, Douglas. "Space-Time Kinetics of the AGN-201M Research Reactor at the University of New Mexico." (2015).
https://digitalrepository.unm.edu/ne_etds/13

This Dissertation is brought to you for free and open access by the Engineering ETDs at UNM Digital Repository. It has been accepted for inclusion in Nuclear Engineering ETDs by an authorized administrator of UNM Digital Repository. For more information, please contact disc@unm.edu.

www.manaraa.com

Douglas G. Bowen

Candidate

Nuclear Engineering

Department

This dissertation is approved, and it is acceptable in quality and form for publication:

Aproved by the Dissertation Committee:

Dr. Cassiano De Oliviera, Chairperson

Dr. Robert Busch

Dr. Anil K. Prinja

Dr. Sedat Goluoglu

www.manaraa.com

Space-Time Kinetics of the AGN-201M Research Reactor at the University of New Mexico

by

Douglas G. Bowen

B.S. Nuclear Engineering, University of New Mexico, 1995
M.S. Nuclear Engineering, University of New Mexico, 1997

DISSERTATION

Submitted in Partial Fulfillment of the

Requirements for the Degree of

Doctor of Philosophy
Engineering

The University of New Mexico

Albuquerque, New Mexico

May 2015

www.manaraa.com

©2015, Douglas G. Bowen

www.manaraa.com

Acknowledgements

I have been working on my Ph.D. since 2002 when I worked as a Nuclear Criticality Safety Engineer (NCSE) at Los Alamos National Laboratory (LANL). This personal goal ended up taking much more time than anticipated. A career change from a NCSE at LANL to Senior Research and Development Staff at Oak Ridge National Laboratory (ORNL) strongly motivated me to complete my dissertation. I am extremely grateful for the support that ORNL provided me for these efforts. I am also extremely grateful to many of my ORNL colleagues, who supported me above and beyond what was expected for a research topic which was unrelated to our ORNL work activities. Specifically, I would like to thank Dr. Michael Dunn, group leader of the ORNL Nuclear Data and Criticality Safety Group, for the support and advice he provided me. In addition, Dr. Lester Petrie, Dr. Mark Williams, Dr. Matt Jessee, Dr. Dorothea Wiarda, Mr. Joel Risner, and Mr. Charles Daily provided me with significant and timely advice regarding the various modules of the SCALE package I struggled with along the way. A very sincere thank you goes to Dr. Cihangir Celik who provided me with significant support and assistance, helping me to generate multigroup cross sections for use with the EVENT code. His help saved me a great many months of time and for that I am extremely grateful. Dr. Luiz Leal provided invaluable technical advice and manuscript reviews – I am grateful to Dr. Leal and his wife, Tuca, for all their support. I appreciate the help of Larry Wetzel and Mackenzie Gorham for sharing their work on the AGN-201 research reactor – their work was invaluable for this project.

I would also like to thank my committee members with whom it has been an immense pleasure and honor to work with since I began these efforts. I have worked with Dr. Anil Prinja since I was a undergraduate student in ChNE in the early 1990s and it is always an honor to work alongside him. My committee chair, Dr. Cassiano De Oliviera provided a great deal of technical advice and EVENT code support for my research. I am appreciative to Dr. Sedat Goluoglu from the University of Florida at Gainesville for his support and expertise in this subject matter. Dr. Robert Busch provided me valuable AGN-201M experimental data and a great deal of advice and support throughout this period. Dr. Busch has been a guiding light in my career and I consider it to be a distinct honor to continue working together on various collaborations.

Dissertations cannot be completed without significant dedication and sacrifice. Most of all, I would like to acknowledge and thank my wife, Linda, my son, Ryan, and my daughter, Kelsey, for their love, extreme patience, and enduring support for which I am eternally grateful.

www.manaraa.com

Space-Time Kinetics of the AGN-201M Research Reactor at the University of New Mexico

by

Douglas G. Bowen

B.S. Nuclear Engineering, University of New Mexico, 1995
M.S. Nuclear Engineering, University of New Mexico, 1997

Ph.D., Engineering, University of New Mexico, 2015

Abstract

A series of experimental measurements were performed on the AGN-201M reactor (AGN) at the University of New Mexico. Steady-state measurements were made with the AGN in various delayed critical configurations. These delayed critical configurations are defined by moving the coarse and fine control rods to unique positions in the core. These experiments also provided data for control rod integral and differential reactivity worth estimates. Thermal flux measurments taken radially in the glory hole region of the AGN reactor were also compiled for this work. A series of time-dependent experiments were performed in conjunction with the

www.manaraa.com

steady-state measurements that involved prompt jump measurements, operations at delayed critical, and prompt drop measurements. A total of 36 steady-state and 11 time-dependent configurations were compiled for this work. The EVENT (**EVE**n parity **N**eutron **T**ransport) radiation transport code was chosen to analyze and verify the steady-state and time-dependent experimental configurations on the AGN. Complex AGN models were developed to test the EVENT code and the case-dependent multigroup cross-sections. The neutron cross-section libraries used are based on the ENDF/B-VII.1 library.

The AGN EVENT model results compared well to the steady-state and time-dependent experimental configurations. The EVENT analysis for the AGN delayed critical configurations resulted in an average computational bias of -0.0048% for P_{11} calculations and +0.0119% for P_{13} calculations utilizing 2-group neutron cross sections. The AGN EVENT thermal flux calculations also compare well to the experimental data, although the magnitude of the maximum thermal and total flux results calculated by EVENT are somewhat greater than expected. The EVENT transient calculation results using the diffusion theory approximation (P_1) and 2-group cross sections compare well with the 11 AGN time-dependent experimental configurations. Rod drop configurations with EVENT indicate six-group Keepin and Brady data are consistent with the AGN experimental data.

www.manaraa.com

The EVENT radiation transport code has proven to be an excellent tool for AGN research reactor analysis. More experiments are recommended to provide additional data for more rigorous analyses using the EVENT code. It is recommended these analyses consider AGN geometric and material uncertainties to allow for more complex analyses to be peformed on the AGN research reactor.

www.manaraa.com

Table of Contents

Chapter 1 – Introduction and Background 1
1.1 Introduction 1
1.2 Goals of this Work 5
1.3 Literature Review 9
Chapter 2 – Description of the AGN-201M Research Reactor 20
2.1 AGN-201M General Specifications 20
2.2 Core Specifications 24
2.2.1 Fuel Plates 24
2.2.2 Reactor Control 28
2.2.3 Thermal Fuse and Glory Hole 32
2.3 Reflector and Shielding Specifications 33
2.3.1 Graphite Reflector 33
2.3.2 Reactor Shielding 34
2.3.3 Instrumentation and Safety Systems 35
2.3.3.1 Neutron Detectors 35
2.3.3.2 AGN-201M Reactor Safety Interlocks and Radiation Monitoring 35
Chapter 3 – Computer Code Descriptions 37

www.manaraa.com

3.1 Introduction 37
3.2 SCALE Code Package 38
3.2.1 SCALE/KENO-VI AGN Model Development 40
3.2.2 Neutron Cross-Section Library Generation 41
3.3 MCNP6 Monte Carlo Radiation Transport Code 49
3.4 GEM Pre-Processor for EVENT 50
3.4.1 NETGEN 51
3.5 EVENT Radiation Transport Code 52
3.6 Visualization Applications 62
3.7 Mathematica 63
Chapter 4 – EVENT Model Development 64
4.1 Introduction 64
4.2 AGN Reactor Configuration and Materials 66
4.3 Control Element Operational Specifications 68
4.4 Background for AGN Experimental Analysis 69
4.4.1 Effective Multiplication Factor 70
4.4.2 Definition of Reactivity 73
4.4.3 Point Kinetics Equations 75
4.4.4 Estimation of the Effective Delayed Neutron Fraction 83
4.4.4.1 Prompt Method to Estimate β_{eff} 86
4.4.4.2 MCNP6 Calculation to Estimate β_{eff} 89
4.5 EVENT Model Descriptions 92
4.5.1 MCNP6 AGN Model 92
4.5.2 Detailed EVENT NETGEN Model 94
4.5.3 Simplified EVENT NETGEN Model 100
4.5.4 Detailed EVENT RZ Model 105
4.5.5 Simplified EVENT RZ Model 111
4.6 AGN-201M Wetzel Calculations 115
Chapter 5 – AGN-201M Experimental Verifications 118
5.1 Description of AGN-201M Experiments 118

www.manaraa.com

5.2 AGN Delayed Critical Verifications 124
5.3 AGN-201M Flux Measurement Analysis 128
5.3.1 Neutron Flux Visualization Calculations 134
5.4 AGN-201M Time Dependent Calculations 139
5.4.1 Experimental Transient Configurations 139
5.4.2 EVENT Time Dependent Calculation Methodology 142
5.4.2.1 General Discussion 142
5.4.2.2 EVENT Model Description 150
5.4.3 Transient Modeling with the EVENT RZ Model 153
5.4.4 Transient Modeling with the EVENT NETGEN Model 157
5.4.5 Transient Sequence Results 164
5.4.5.1 EVENT RZ Model Delayed Neutron Parametric Study 173
5.4.6 Material Sensitivities and Experimental Uncertainties 176
Chapter 6 – Conclusions 182
6.1 Future Work 185
Appendix A – EVENT 2-D Model Testing 187
A.1 MCNP6 XY Model 187
A.1.1 Model Specifications and Results 187
A.2 EVENT XY Model 192
A.2.1 Model Specifications and Results 192
A.2.2 Angular Flux Expansion and Order of Scattering Anisotropy for EVENT XY Model 196
A.3 EVENT RZ Model 198
A.3.1 Model Specifications and Results 198
A.3.2 Angular Flux Expansion and Order of Scattering Anisotropy for EVENT RZ Model 202
A.3.3 Cross-Section Parametric Study with EVENT RZ Model 204
A.4 EVENT Time Dependent Calculation Testing 206
Appendix B – AGN Reactor Experiment Logs 214
Appendix C – Model Input Files 220

www.manaraa.com

C.1 Introduction 220
C.2 SCALE Models 220
C.2.1 Generation of the Multigroup Cross Sections 220
C.3 MCNP6 Models 228
C.3.1 MCNP XY Model and 3-D Model 228
C.3.2 MCNP6 XY AGN Model Input File 230
C.3.3 MCNP6 3-D AGN Model Input File 230
C.4 EVENT XY and RZ Models 232
C.4.1 Detailed EVENT XY Model 233
C.4.2 Detailed EVENT RZ Model 235
C.4.3 Simplified EVENT RZ Model 239
C.4.4 EVENT RZ Transient Input Files 241
C.4.4.1 EVENT RZ Transient – Eigenvalue File 241
C.4.4.2 EVENT RZ Transient 244
C.5 EVENT NETGEN Models 252
C.5.1 Detailed EVENT NETGEN Model 253
C.5.2 Simplified EVENT NETGEN Model 264
C.5.3 EVENT NETGEN Transient Input Files 268
C.5.3.1 EVENT NETGEN Transient – Eigenvalue File 268
C.5.3.2 EVENT NETGEN Transient – Time-Dependent File 272
C.5.4 EVENT Transient Testing Files 281
C.5.4.1 EVENT U-Polyethylene Cylinder Transient Input Files 281
C.5.5 *Mathematica* Notebook File 286
References 290

www.manaraa.com

List of Figures

Figure 1. Illustration of the AGN Reactor Unit [2] 2

Figure 2. Illustration of the AGN Reactor Core [2] 3

Figure 3. Rod Drop Power Profile for the ISU AGN-201 11

Figure 4. AGN-201M Source Drive Configuration [8] 22

Figure 5. AGN-201 Thermal Fuse [7] 23

Figure 6. AGN-201M Fuel Plate Stack [8] 26

Figure 7. Core Cross Section Illustrations of the Control Rod Locations 27

Figure 8. Illustration of Fuel Plate Geometry 27

Figure 9. Illustration of the Upper Core Fuel Plate Geometry 28

Figure 10. Photo of the Control Element Drives and Element 31

Figure 11. Photograph of the Control Element Drives 31

Figure 12. Illustration of the AGN-201M Rod Drive Mechanism [8] 32

Figure 13. Codes Used to Prepare the AGN Calculation Methodology 38

Figure 14. AGN Neutron Flux Spectrum 46

www.manaraa.com

Figure 15. ^{1}H, ^{12}C and ^{16}O Absorption and Scattering Cross Section Plot 47

Figure 16. ^{235}U and ^{238}U Absorption and Fission Cross Section Plot.....47

Figure 17. Illustration of the Delayed Critical Window.....73

Figure 18. Neutron Population Components in Analytic Solution.....82

Figure 19. Neutron Population with a Step Increase in Reactivity 82

Figure 20. MCNP6 Kinetic Parameter Results 91

Figure 21. MCNP6 and Prompt Method β_{eff} Results.....91

Figure 22. MCNP6 3-D Model for EVENT Model Verification.....93

Figure 23. 3-D EVENT NETGEN Model with Vertical Glory Hole 98

Figure 24. 3-D EVENT NETGEN Model Showing Control Elements.....98

Figure 25. Core Region Illustration of NETGEN Control Rod Position.....99

Figure 26. Simplified EVENT NETGEN Model Configuration (XY) 103

Figure 27. Simplified EVENT NETGEN Model Configuration (YZ).....104

Figure 28. EVENT RZ Model Region and Mesh Definitions 107

Figure 29. EVENT RZ Model Illustrations.....108

Figure 30. Core Region Illustration of RZ Model Control Rod Position.....109

Figure 31. Simplified EVENT RZ Model for Experimental Analysis.....113

Figure 32. Simplified EVENT RZ Model Configuration 114

Figure 33. AGN-201M Experimental Data – Transient Sequence #1.....123

Figure 34. AGN-201M Experimental Transient Data 124

Figure 35. AGN-201M Delayed Critical Analysis Results.....128

Figure 36. Comparison of EVENT Flux Results with Experiment 133

www.manaraa.com

Figure 37. EVENT NETGEN Group 1 Neutron Flux Illustration 136

Figure 38. EVENT NETGEN Group 2 Neutron Flux Illustration 137

Figure 39. AGN EVENT RZ Neutron Flux Illustrations 138

Figure 40. EVENT Time Dependent Calculation Methodology.....145

Figure 41. UNM AGN Fine Control Rod Calibration Curve [8] 147

Figure 42. UNM AGN Coarse Control Rod Calibration Curve [8] 148

Figure 43. Equating AGN Control Rod Positions to a Reactivity Change....149

Figure 44. Equating AGN Control Rod Position to Reactivity Change.....150

Figure 45. EVENT RZ Annular Control Element Calibration Curve 155

Figure 46. EVENT NETGEN Fine Control Rod Calibration Curve.....161

Figure 47. EVENT NETGEN Coarse Control Rod Calibration Curve.....161

Figure 48. EVENT Transient Model Results – Transient Sequence 1.....168

Figure 49. EVENT Transient Model Results – Transient Sequence 2.....168

Figure 50. EVENT Transient Model Results – Transient Sequence 3.....169

Figure 51. EVENT Transient Model Results – Transient Sequence 4.....169

Figure 52. EVENT Transient Model Results – Transient Sequence 5.....170

Figure 53. EVENT Transient Model Results – Transient Sequence 6.....170

Figure 54. EVENT Transient Model Results – Transient Sequence 7.....171

Figure 55. EVENT Transient Model Results – Transient Sequence 8.....171

Figure 56. EVENT Transient Model Results – Transient Sequence 9.....172

Figure 57. EVENT Transient Model Results – Transient Sequence 10.....172

Figure 58. EVENT Transient Model Results – Transient Sequence 11.....173

www.manaraa.com

Figure 59. Delayed Neutron Parametric Study Results – Prompt Jump 175

Figure 60. Delayed Neutron Parametric Study Results – Rod Drop.....176

Figure 61. EVENT Delayed Critical Uncertainty Calculation 179

Figure 62. EVENT Transient #1 Verification Uncertainty Calculation 181

Figure 63. 2-D MCNP6 XY Model Illustration 190

Figure 64. EVENT XY Model Illustrations.....194

Figure 65. EVENT RZ Model Region and Mesh Definitions 200

Figure 66. EVENT RZ Model Illustration.....200

Figure 67. Results of Neutron Cross-Section Parametric Study 205

Figure 68. Illustration of UO_2-Polyethylene Cylinder for EVENT Testing ..207

Figure 69. 2-D EVENT 2-D Annular Cylinder k_{eff} Results.....210

Figure 70. 2-D EVENT 2-D Annular Cylinder Reactivity Results.....210

Figure 71. Transient Testing Results for Prompt Jump Case.....212

Figure 72. Transient Testing Results for Prompt Drop Case 213

www.manaraa.com

List of Tables

Table 1. Fuel Plate Specifications for the UNM AGN-201M Reactor [4] 26

Table 2. Control Rod Specifications [4] 29

Table 3. SCALE ENDF/B-VI.1 252-Group Energy Boundaries [34] 45

Table 4. SCALE ENDF/B-VI.1 Broad Group Energy Boundaries 46

Table 5. Core Atom Densities 67

Table 6. Non-Fuel Material Atom Densities 67

Table 7. Control Element Atom Densities 69

Table 8. Prompt Method Calculation Results 89

Table 9. MCNP6 3-D Model Results 93

Table 10. Atom Densities for the Detailed EVENT NETGEN Model 95

Table 11. Detailed EVENT NETGEN Model Results 99

Table 12. Atom Densities for the Simplified EVENT RZ Model 100

Table 13. Simplified EVENT NETGEN Model Rod Worth Results 104

Table 14. Detailed EVENT RZ Model Differential Rod Worth Results 111

www.manaraa.com

Table 15. Atom Densities for the Simplified EVENT RZ Model.....113

Table 16. EVENT Simplified RZ Model Differential Rod Worth Results 114

Table 17. Summary of Integral Rod Worth Estimates.....117

Table 18. Summary of Experimental Delayed Critical Configurations 121

Table 19. EVENT Legrendre Flux Expansion Order Study 125

Table 20. AGN Delayed Critical Configuration EVENT Results 127

Table 21. AGN-201M Thermal Flux Data 129

Table 22. AGN EVENT Flux Calculation Results.....132

Table 23. Summary of Experimental Transient Sequences.....141

Table 24. Delayed Neutron Parameters.....152

Table 25. EVENT RZ Transient Model Reactivity Definitions.....157

Table 26. EVENT NETGEN Transient Model Reactivity Definitions 163

Table 27. Prompt Jump Doubling Time Comparison.....166

Table 28. MCNP6 XY Model Detail and Results 191

Table 29. EVENT XY Model Detail and Results 195

Table 30. Angular Flux Expansion and Scattering Order Comparison Results for the EVENT XY Model 197

Table 31. EVENT RZ Model Detail and Results 201

Table 32. Angular Flux Expansion and Scattering Order Comparison Results for the EVENT RZ Model.....203

Table 33. Transient Testing Reactivity and Control Rod Definitions 209

www.manaraa.com

Chapter 1 – Introduction and Background

1.1 Introduction

The AGN-201M (AGN) reactor at the University of New Mexico (UNM) has been in operation for many years. The reactor was transferred from the Berkeley campus of the University of California in January 1969 and was later upgraded with new controls and instrumentation to allow for operations at a higher power level. The NRC approved UNM AGN operations at a power level of 5 W (thermal) on January 18, 1973 [1]. The AGN was then installed in the UNM Nuclear Engineering Laboratory where it continues to operate today. The AGN is now used for classroom laboratory experiments and for nuclear reactor operator training. Figure 1 illustrates the entire AGN reactor unit and Figure 2 shows the configuration of the fuel plates, the control elements, and the graphite reflector in the core.

www.manaraa.com

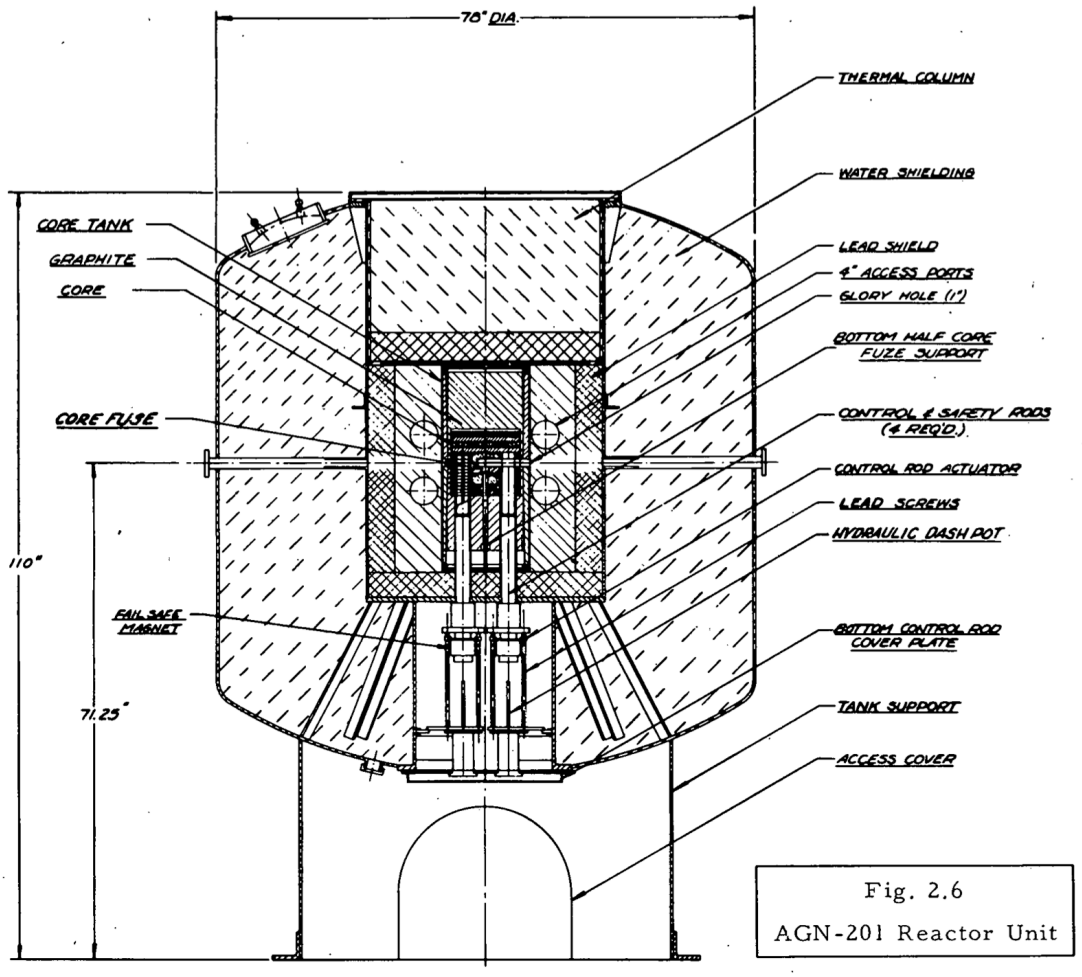

Figure 1. Illustration of the AGN Reactor Unit [2]

www.manaraa.com

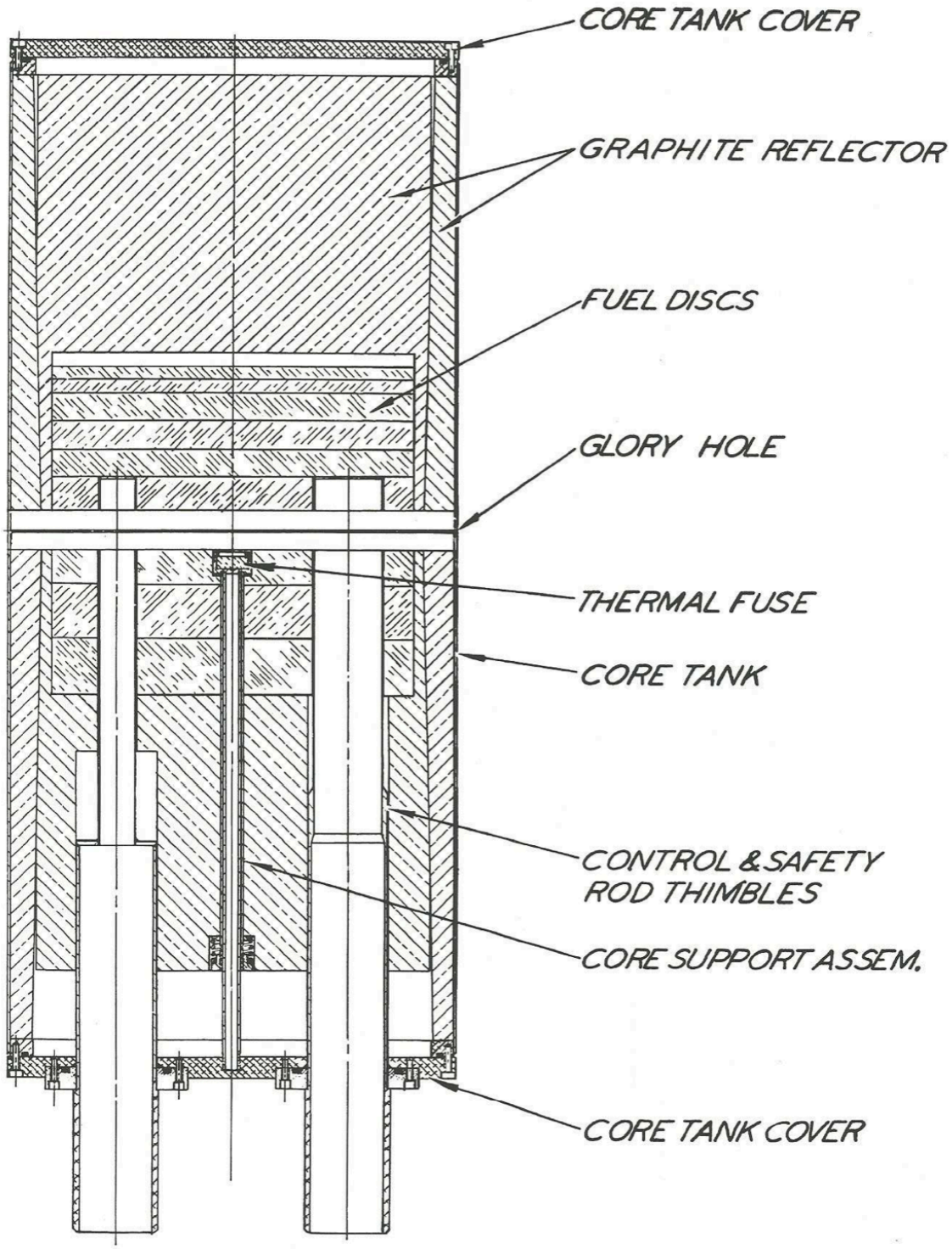

Figure 2. Illustration of the AGN Reactor Core [2]

www.manaraa.com

The AGN reactor was specifically designed for operation on university campuses and it is considered to be one of the safest research reactors currently in use today. Biehl [2] noted the AGN reactor was designed as a low power (0.1 W) nuclear reactor in a compact, self-contained configuration. The core was designed to operate at delayed critical with a minimal quantity of fissile material, about 665 grams of ^{235}U, present in the form of uranium dioxide (UO_2) particles embedded in radiation-stabilized polyethylene. The uranium dioxide fuel is low-enriched uranium with a nominal enrichment of 19.5 ± 0.5 weight percent ^{235}U. The AGN reactor is controlled using two safety rods (SR1 and SR2), one coarse control rod (CCR) and one fine control rod (FCR) which are driven into the core from the bottom of the reactor. The control rods are made of core fuel and are moved inside aluminum tubes present in the bottom half of the AGN core. The core is reflected by reactor-grade graphite, which has good neutron scattering characteristics, albeit less effective than hydrogen, but a lower tendency to absorb neutrons than hydrogen in water. Radiation shielding for the AGN includes a lead shield outside of the graphite reflector for gamma ray shielding and a thick water shield outside of the lead layer to shield the thermal neutrons. These two radiation shields are adequate for AGN reactor operations at the design power of 0.1 W. Additional cement block shielding installed around the UNM AGN reactor unit allow for operations at the licensed power of 5 W. The reactor has four access ports that pass through the outer shielding and into

www.manaraa.com

the graphite reflector. These ports are used to place neutron sources or reactor instrumentation. A glory hole is also present for the introduction of experimental packages during operations or for the placement of neutron sources or other items during operations. Because dose rates are small during approved operations, the AGN can be operated via its control station inside the AGN reactor room without significant risk to students or the reactor operators.

Several AGN-201 research reactors are licensed in the United States at Idaho State University (ISU), Texas A&M University, and UNM. The AGN research reactor at UNM is used for a variety of purposes including undergraduate and graduate research and for training reactor operators. Students routinely perform a variety of experimental measurements to determine neutron multiplication, excess reactivity, reactor period, control rod calibration, importance functions, reactor neutron temperature, neutron flux spatial distribution, and power calibration and detector dead-time.

1.2 Goals of this Work

This work involves using the EVENT code (EVEn parity Neutron Transport) radiation transport code [3] to predict the steady-state and time dependent behavior of the AGN-201M research reactor at the UNM. Previous work [4] used the Monte Carlo neutron transport codes KENO-Va (a module of the SCALE package) [5] and MCNP6 [6] for a complex, three-dimensional representation of the UNM AGN research reactor. The results of these

www.manaraa.com

studies were used as a starting point for AGN model development in EVENT using the GEM pre-processor. An input file for the GEM pre-processor is created to specify the type of problem in EVENT, P_N order, scattering order, nuclear data and material specifications, geometry and finite element mesh definitions, and other options. The GEM pre-processor will then create the necessary input files to execute EVENT. The EVENT model geometry can be viewed by the code user to ensure the desired model configuration is correctly defined in the GEM input file.

A series of experimental measurements were performed for both steady-state and time-dependent AGN configurations. The following experiments were performed for this work:

- Steady-state measurements
    - Delayed critical configurations with the CCR and FCR in variable positions
    - Thermal flux glory hole measurements
    - Integral and differential rod worth measurements
- Time-dependent measurements
    - Positive period measurments
    - Rod drop (prompt drop) measurements

The intent of performing these measurements is to provide experimental data to verify with 2-D and 3-D EVENT models. The EVENT model results will be compared directly to the AGN experimental results and to the results

www.manaraa.com

of previous studies [4]. Data for an operating AGN research reactor at ISU is available [7] as a basis for comparison in addition to the UNM AGN experimental data compiled for this work. The ISU data [7] was used to support EVENT model scoping calculations and complex model development work to test neutron cross-section data, also developed for this work, and to test the various geometry modeling options in GEM. The results of the scoping calculations are not provided for this work but were invaluable with respect to preparing the EVENT calculation methodology.

The detailed 2-D and 3-D EVENT models generated to verify the AGN steady-state configurations were modified for verification of the AGN experimental transients where the neutron population varies as a function of time. The reactor is started in accordance with guidance in the AGN Reactor Operation and Training Manual, [8] which requires the SR1 and SR2 be inserted into the core before the CCR and FCR are inserted in addition to ensuring the glory hole is empty. The AGN configurations considered involve determining a delayed critical state by adjusting the CCR and FCR until the neutron population is not changing with time, i.e., steady-state or time independent configuration. The power level at this state can be close to zero or up to the licensed power of 5 W. AGN operating procedures limit the amount of reactivity that can be added to the standard AGN core to +0.65 percent, which consists of the fixed and removable fuel plates but do not include the four control elements. The four AGN control rods (SR1, SR2, CCR

www.manaraa.com

and FCR) do not add more than +0.25% reactivity to the system, which allows for up to +0.40% maximum excess reactivity that can be inserted into the core for experiments. For the prompt jump or ramp transient, a small amount of excess reactivity is added to the core to achieve a delayed supercritical state. The excess reactivity added to the core results in an exponential rise in the neutron population on a particular reactor period (time required for the neutron population or power to increase by a factor of *e*, 2.7183…). The AGN control system provides information about the doubling time, which is the time required for the neutron population or power to double. For these experiments, the maximum doubling time is approximately 13.5 seconds for all four control rods inserted completely in the AGN core, which is within the realm of human control. Once the desired power level is achieved, the excess reactivity is removed by withdrawing the FCR and/or CCR from the core until a delayed critical configuration is achieved. The other transient considered for this work is a prompt drop or rod drop where the CCR is dropped out of the core from a delayed critical configuration. The reactivity worth of the CCR in addition to characteristics of the delayed neutrons in the system can be examined. The rod drop transient results in rapid reduction in reactor power over a time period of approximately 200 msec as a result of the reactivity worth of the control element removed from the core. Afterward, the reactor power continues to drop exponentially based on the radiological decay

www.manaraa.com

of delayed the neutron precursors present in the fuel. Two EVENT models were developed to verify these transient experiments.

The EVENT calculations require delayed neutron fraction data for use as a neutron source after the transient and the neutron lifetime data. Delayed neutron fraction and neutron lifetime data are provided in the literature [4,9] and can be calculated by performing 2-D transport calculations of the AGN-201M using the SCALE code NEWT [10] or with the Monte-Carlo code MCNP6. A desired outcome of the EVENT calculation methodology is to determine if it can be applied to other transient configurations previously analyzed in the AGN safety basis documentation to demonstrate the safety of certain abnormal conditions during operations. Simple point kinetics calculations are currently used in AGN safety analyses to analyze the worst case transients for the AGN research reactor [11].

1.3 Literature Review

A license renewal application from UNM to the NRC for the AGN provides technical specifications of the reactor during operations [11]. In particular, the coarse and fine control rod calibration curves provide a valuable means to verify EVENT model results, which depends upon the quality of the model geometry, finite element mesh, neutron cross-section data, and code methodology. The curves illustrate the change in system reactivity as a result of inserting or removing each rod into the core. The reactivity worth of the FCR and CCR in the AGN reactor core during operations has been verified

www.manaraa.com

experimentally countless times during routine core operations. This control rod reactivity worth data is used in this work as one measure of the quality of the AGN EVENT models.

High-quality critical benchmark experiments for the International Reactor Physics Experiment Evaluation Project were performed with the AGN-201 at Idaho State University (ISU) [7]. This thesis provides a detailed description of each of the reactor components and includes detailed operating specifications for the AGN-201 at ISU. Numerous experiments are documented by recording the FCR and CCR rod heights with the AGN reactor in a steady-state configuration. In addition, integral rod worth data are also presented. Flux tallies in MCNP were calculated and compared to experimentally determined fast and thermal neutron flux estimates. These experimental results were compared to MCNP calculations documented in the thesis to test the EVENT calculation methodology to determine if the code installation, geometrical configuration, and nuclear data can reasonably estimate the results for the ISU AGN-201. Some of the experimental results for the ISU AGN-201 were used in preliminary calculations with EVENT to test the code package, EVENT AGN models and nuclear data for the experimental verifications.

The ISU AGN-201 also performed some prompt drop (rod drop) measurements where the SR1, SR2, and CCR were each dropped out of the core from a starting power of about 1.5 W. The detector amperage from

www.manaraa.com

Channel 3 was recorded to capture reactor power, prompt drop (rod drop), and delayed neutron decay data. The prompt drop power trace experimental evoluation for the ISU AGN-201 experiments is shown in Figure 3. Similar experiments were performed on the UNM AGN; however, the UNM data also includes a power ramp until the desired power level is reached. The AGN-201 at ISU has some minor differences compared to the UNM AGN. For example, the UNM reactor uses nine stacked fuel plates while the ISU reactor has ten (the tenth location in the UNM reactor is void).

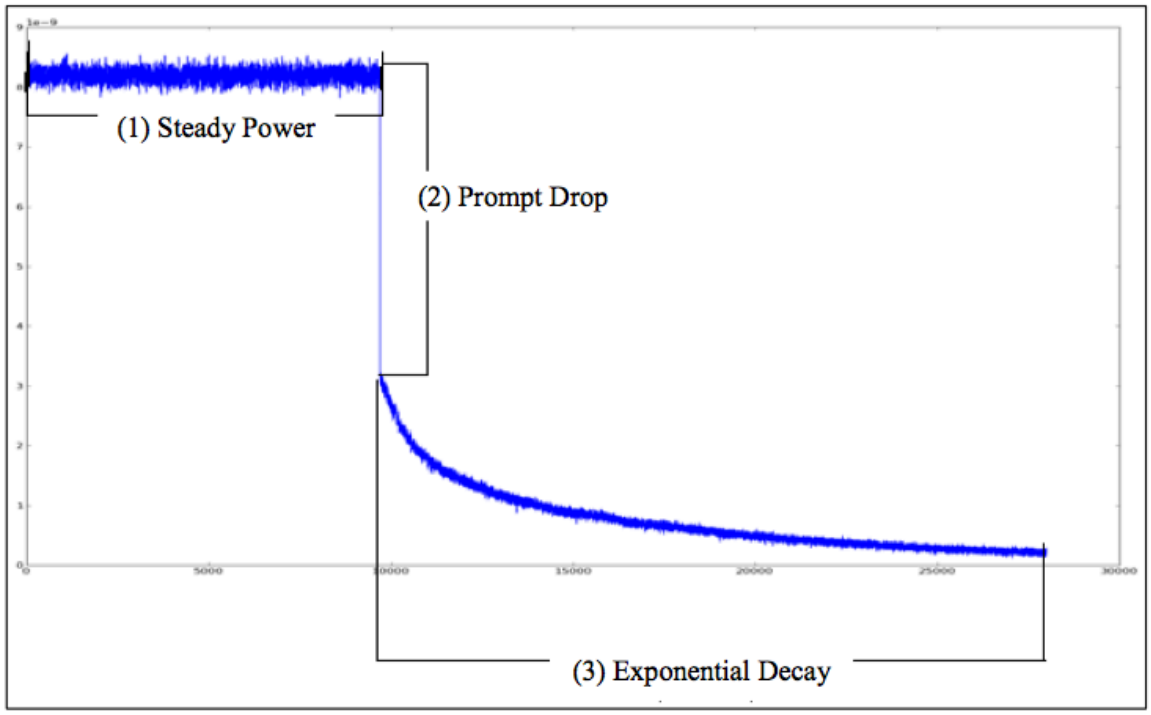

Figure 3. Rod Drop Power Profile for the ISU AGN-201

Years ago, a series of training experiments for the Argonaut and AGN-201 reactors used at Argonne National Laboratory were conducted [9]. The report presents the operating specifications of the AGN-201M. It also presents

www.manaraa.com

information that can be used to test the capabilities of the EVENT code package. For example, the fine control rod calibration curve, the reactivity worth of a variety of reactor components and parameters (safety and coarse control rod reactivity worth, temperature coefficient of reactivity, etc.), the AGN-201M Inhour equation, and flux profile of the horizontal thermal flux at 100 mW power is provided. The training manual also provides experimental data for a variety of experiments, including an approach to critical experiment that provides data on the inverse count rates for the control rods in various positions using a fixed source for comparison to estimate the effective multiplication factor for the system.

An overview of the UNM AGN reactor design, specifications, and inherent safety margin engineered into the reactor is provided in the UNM AGN Safety Analysis Report (SAR) [11]. It also provides a chapter-long discussion related to the hazards that could be experienced during operations via transients and their effect on local dose rates in the vicinity of the reactor. The total excess reactivity of the AGN reactor at the time it was manufactured is approximately 0.5%. The AGN SAR hazards analysis describes a "Nuclear Runaway" hypothetical accident resulting from an instantaneous 2% increase in core reactivity with a reactor period of about 10 milliseconds, i.e., the time required for the neutron population or power level of the reactor to increase by a factor of *e* (2.71828…). The hypothetical excursion would last approximately 200 to 220 milliseconds and result in a

www.manaraa.com

peak power level of about 75 MW at about 140 milliseconds into the pulse. According to the SAR, the scram system for the AGN could take as long as 300 milliseconds to respond, so this accident could not be terminated via a system scram. Other excursions with the reactor involving reactor periods in excess of 30-50 milliseconds, corresponding to an instantaneous reactivity increase of about 1%, can be shut down by scram system action (control rods dropping out of the core). The power rise would result in a core temperature increase of about 150 °C, which should be sufficient to terminate the excursion due to core expansion, i.e., reduction in core density, increasing neutron leakage. The fuel should not melt below 200 °C, so there are no fission product release concerns with the fuel. The core fuse has twice the fuel impregnation density than the core plate fuel and would be at a higher temperature due to the larger fission rate at this location. If the temperature exceeds 200 °C, the fuse will melt and separate the top half of the core from the bottom half by a couple of inches, which is sufficient to terminate the excursion. The analysis methods used for the "Nuclear Runaway" accident are based on solutions to the point kinetics equations with one group of delayed neutrons. Aerojet General Nucleonics performed a similar analysis when the reactors were first manufactured [2]. The solution to the point kinetics equations yields a coupled set of nonlinear differential equations that are solved numerically. This work is used to analyze transient hazard analysis for the AGN SAR and be used to augment the current technical

www.manaraa.com

basis for safety purposes in the future, as well as, to resolve regulatory questions that arise during NRC assessments and licensing reviews.

A study regarding predictions of the dynamic behavior of the High Flux Isotope Reactor (HFIR) at Oak Ridge National Laboratory (ORNL) in response to reactivity-induced perturbations was recently published [12]. A variety of neutron transport codes are used in this study to determine reactivity changes in response to perturbations in the core, e.g., control cylinder movements, hydraulic tube black rabbit injections (in-core experiments), etc. Because the HFIR core runs at 85 MW(t) and the core is small, the core lifetime is short. Thus, fission product burn up must also be considered in the analysis. According to this study, the COMSOL partial differential equation coefficient application mode and 2-D axisymmetric geometry were utilized to solve the three-group neutron diffusion equation for the purpose of studying the power/flux distributions during transients such as a control cylinder ejection transient. Nuclear data was calculated by using the NEWT code within the SCALE 6.0 package and MCNP5. This data and reactor specifications are currently being used to develop a HFIR-specific reactor kinetics and thermal hydraulic transient simulator. This is a challenging problem due to the high flux core that has many fuel plates in an involute geometry and significant axial neutron flux variation that complicates the process of considering fuel burn up in the transient models.

www.manaraa.com

Kimpland [13] describes a computational model for predicting nuclear excursions in aqueous, homogeneous solution systems. The motivation for developing these computer models is the processing of aqueous, homogeneous solutions during the chemical processing of nuclear fuel. Specifically, accidents are credible in these systems based on the criticality accident history that demonstrates prevalence for inadvertent accidents in solution processing systems. The models generated attempt to determine the consequences of such accidents. Both one- and two-region computer models are developed that consider reactivity feedback effects from radiolytic gas generation during an excursion. Further, the multi-region model also considers effects due to the spatial distribution of nuclear energy throughout the system and radial acceleration of the fuel material caused by pressure effects during the excursion. The model results were then compared to actual excursion data from KEWB, CRAC, and SILENE experiments. The computer models appear to accurately predict the magnitude of both the power and pressure pulses as a result of the excursion, in addition to providing information about the spatial distribution of solution parameters such as temperature, pressure, velocity, and density.

A three-dimensional transport-based computer code called TDTORT was developed at the University of Tennessee in the late 1990s [14,15]. This code utilizes a legacy code called TORT, a 3-D discrete ordinates code, to calculate the time-dependent neutron flux shape in the problem geometry during a

www.manaraa.com

transient. The TDTORT uses a calculation methodology and code to solve the 3-D time dependent neutron transport equation with the explicit representation of delayed neutron data for the system of interest. The code uses a discrete ordinance approach for the shape, energy and angular variables and implements an improved quasi-static approach for the time variable in the problem [14]. The improved quasi-static method considers the shape equation being solved for the shape and the result of this solution is used to calculate the point kinetics parameters, e.g., reactivity, the effective delayed neutron fractions, and the neutron generation time, by using their inner product definitions. The point kinetics parameters can then be used to solve the time-dependent amplitude and precursor equations [15]. The benefit of using the improved quasi-static method is that the shape function usually varies slowly in time compared to the amplitude function, which allows larger time steps to be assumed in the calculation to significantly reduce the time required to model a transient. The TDTORT code considers the single step transients, two sequential step transients, a step transient with a subsequent ramp, or a ramp transient configuration. It can also perform a special case where thermal feedback is assumed. The TDTORT code capabilities are successfully tested against some time-dependent benchmarks from Argonne National Laboratory [16].

Additional research and code development was made by Bentley [17] in 1996 with the development of a time-dependent, 3-D Boltzmann Transport

www.manaraa.com

equation with the explicit representation of delayed neutrons, similar to the TDTORT code. This code, TDKENO-M, was developed by enhancing a legacy code called TDKENO and implementing an improved quasi-static methodology into an existing quasi-static framework implemented in TDKENO. The TDKENO code [18] is based on the Monte-Carlo code KENO, which is part of the SCALE package. A quasi-static kinetics framework was developed within KENO to allow it to have a 3-D time dependent capability. The time dependent amplitude function is computed via the deterministic, conventional point-kinetics algorithm. Further, the point-kinetics parameters, reactivity and generation time, and neutron flux shape are computed stochastically during the random walk process of the Monte-Carlo process. This was developed for use as a benchmarking tool for other kinetics codes as well for the modeling of 3-D complex geometrical configurations. At the time TDKENO was developed, it was considered to be intensive and expensive code to use routinely. Improvements made with TDKENO-M increased the efficiency of the solution algorithms in the code.

The Massachusetts Institute of Technology (MIT) research reactor (MITR) is currently undergoing a core conversion effort of its highly enriched uranium (HEU) core to low enriched uranium (LEU) core loaded with fuel material enriched to less than 20 wt. % ^{235}U. Research has been performed to support the conversion efforts to examine the impact to LEU fuel design and overall core performance [19]. This research is similar to the LEU core

www.manaraa.com

conversion efforts for the HFIR research reactor at ORNL [12]. This introduces significant negative reactivity into the core by significantly increasing the concentration of ^{238}U in the core and consequently increasing core neutron absorption. Of course, to maintain reactor performance, the core needs to contain more ^{235}U than before to compensate for the magnitude of the negative reactivity effect of the new fuel type. Analyses have been performed using MCODE that links the Monte-Carlo code MCNP with a point depletion code ORIGEN (fuel burnup) to optimize the LEU fuel and overall reactor design. Further, MCNP and the thermal hydraulics/point kinetics code PARET [20] was also used to model core reactivity coefficients, feedback effects, and step reactivity insertions. The step reactivity insertion analysis is necessary to predict negative core/fuel effects as a result of large transients. The PARET code provides a coupled thermal, hydrodynamic and point kinetics capability. Four core regions can be represented and each region may have a different power level, coolant mass flow rate and hydraulic parameters represented by a single fuel pin or plate with an associated coolant channel.

The EVENT code used for this work does not have the capability to perform transient analysis with the ability to look at feedback effects like other codes; however, EVENT can be used to look at changes in material density as a result of heating or bubble formation, for example, and can incorporate these material characteristics into the transient time steps for

www.manaraa.com

consideration. At the Imperial College of Science, Technology and Medicine in the United Kingdom, the EVENT code has been coupled with other code packages to allow for transient feedback analysis to be performed. This coupled package is called FETCH [21] and is comprised of numerous modules: two transient, three-dimensional finite element modules, the neutron transport code EVENT and the CFD/multiphase code FLUIDITY coupled through an interface module. This code package configuration has been used to analyze a variety of transient configurations and situations, e.g., the criticality behavior of dilute plutonium solutions, [22] an analysis of the criticality accident at Tokaimura, Japan, [23] and the examination of transient criticality in fissile solutions, [24] that consider both neutronic and computational fluid dynamics.

www.manaraa.com

Chapter 2 – Description of the AGN-201M Research Reactor

2.1 AGN-201M General Specifications

The AGN-201M reactor at UNM (Serial Number 112) is a compact and portable nuclear reactor originally designed to operate at a power level of about 0.1 W. Modifications instrumentation and control systems, including the installation of additional personnel shielding, was performed in 1969 to enable reactor operations at a power of 5 W. The core was designed with approximately 656 grams of ^{235}U in the form of uranium dioxide (UO_2) with an enrichment of ~19.5 weight percent ^{235}U [8] At the time of construction, the AGN contained less fissionable material than is required for the operation of any other known reactor, which is one of the unique attributes of this particular reactor type. The UO_2 in the core is embedded throughout approximately 10,900 grams of radiation-stabilized polyethylene moderator

www.manaraa.com

[2]. The ^{235}U concentration within the polyethylene moderator is approximately 0.056 g/cm^3 corresponding to a hydrogen-to-^{235}U (H/X) atomic ratio range of approximately 534, which is comparable to the H/X ratio for other hydrogen-moderated uranium systems with thick reflection.

The core of the reactor has a diameter of approximately 10.08 in. (25.60 cm) and a height of 9.65 in. (24.5 cm), corresponding to a volume of approximately 0.455 ft^3 (12,610 cm^3 or 12.6 liters). A 7.87 in. (20 cm) thick graphite reflector surrounds the uranium-polyethylene. The lead shield surrounding the graphite reflector is 3.94 in. (10 cm) thick, and the water shield surrounding the lead shield is approximately 21.7 in. (55 cm) thick. The overall diameter of the reactor unit is 7 ft. (2.13 m) and the overall height of the reactor unit is 10 ft. (2.05 m). The reactor unit weighs approximately 20,000 lb. (9,090 kg) with the water-shielding present.

The AGN has a glory hole that passes through the entire reactor unit made of aluminum with an outside diameter of 1.0 in (2.54 cm) [8]. The reactor also has four 10 cm diameter (3.94 in.) access ports that pass through the graphite reflector. The AGN also has a thermal column that is used for experimental work with the AGN. The access ports are filled with a combination of graphite, lead, and wood when they are not filled with experiments. The glory hole passes completely through the uranium-polyethylene core, the graphite reflector, and the lead and water shields. This region is used for activation experiments or to allow for access to beams of

www.manaraa.com

radiation outside of the reactor shielding for various experiments. A 2-Curie (Ci) ^{239}Pu-Be source and source drive are mounted to the north end of access port #2 to assist with measuring neutron multiplication measurements during reactor startup. An illustration of the source drive is shown in Figure 4.

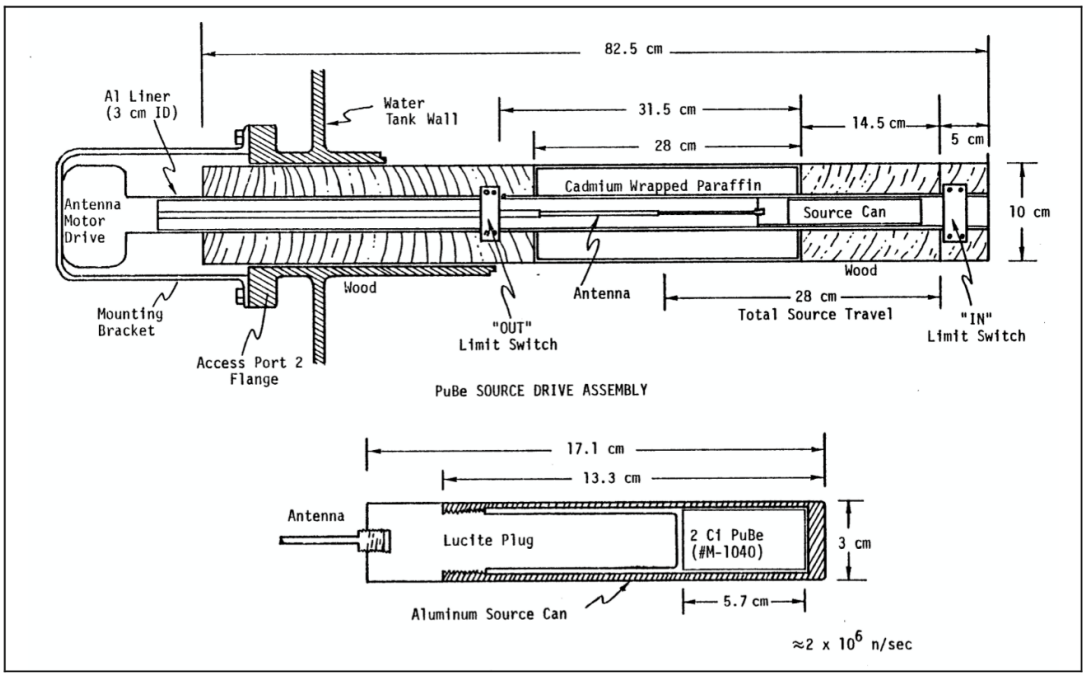

Figure 4. AGN-201M Source Drive Configuration [8]

The AGN reactor is designed with a core fuse that is a polystyrene plug that supports the bottom half of the core (lower three fuel plates). An aluminum rod (0.39 cm diameter) supports the polystyrene plug and is encased in a tube with an inside diameter of 0.5 in. (1.28 cm) and an outside diameter of 0.625 in. (1.588 cm). The core fuse contains a higher fuel loading than the fuel plates (two times the nominal fuel density of 0.061 grams

www.manaraa.com

$^{235}U/cm^3$), so the core fuse will generate more heat than the core fuel plates during operations, in fact the fuse temperature rises about twice as fast as the temperature in the core [8]. A detailed illustration of the AGN core fuse from Reference [7] is shown in Figure 5. If an excursion occurs that results in a fuse temperature greater than 100 °C, the fuse will melt and the lower half of the core will fall downward approximately 5 cm (1.97 in.) as an emergency shutdown mechanism. No polystyrene deformation has been noted in the AGN core fuse at UNM from heat variations during operations [4].

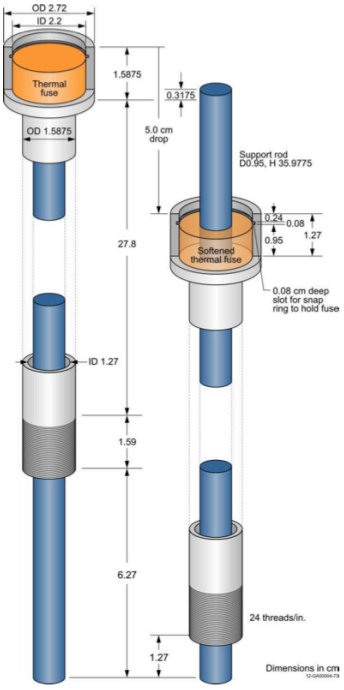

Figure 5. AGN-201 Thermal Fuse [7]

www.manaraa.com

2.2 Core Specifications

2.2.1 Fuel Plates

The nine fuel plates in the UNM AGN reactor are made of polyethylene impregnated with uranium dioxide (UO_2) particles at a fuel density of approximately 0.056 grams $^{235}U/cm^3$. The core fuel plates are designed with the same diameter but with three different axial thicknesses. The fuel is 19.5 ± 0.5 weight percent ^{235}U enriched UO_2 powder embedded in radiation-stabilized polyethylene [8]. The polyethylene present in the core is intended to function as a neutron moderator. The UO_2 particle size is approximately 15 ± 10 μ (0.0015 ± 0.0010 cm) mixed in a polyethylene powder with a particle size of about 100 μ (0.01 cm) [9]. Fissile particle sizes of less than about 100 μ (~0.1 mm) [25] mixed with non-fissile materials, in this case polyethylene, can be treated as a homogeneous mixture rather than a heterogeneous mixture because the individual particle sizes are not sufficient for self-shielding effects to become apparent due to the presence of ^{238}U in the low-enriched fuel. This is important for the AGN core at nominal 19.5 wt. % enrichment because resonance absorption in ^{238}U becomes significant with fissile particle sizes or lumps larger than about 100 μ because of its thickness with respect to the mean free path of the matrix. Thus, the AGN core can be treated as a homogeneous mixture of UO_2 and polyethylene with a uniform concentration of ^{235}U throughout the matrix. Table 1 provides the specifications, i.e., height, diameter, fuel loading, of the nine fuel plates that

www.manaraa.com

make up the AGN core. The two safety rods, the coarse control rod, and the fine control rod enter from the bottom of the core through the four 4-cm thick bottom fuel plates (fuel plate number 20497, 20498, 20499, and 204100) to control the core reactivity.

As described in Table 1, fuel plates 20497, 20498, 20499, and 204100 are each approximately 4.0 cm thick and have holes present to allow for movement of the core support assembly, the CCR, the two safety rods and the FCR. Fuel plates 20499 and 204100 also have hemicylindrical grooves that, when the plates are stacked, form the cylindrical glory hole region where an aluminum tube is present to allow for instrumentation and experiment access to the core. The aluminum glory hole tube is attached to a 0.5-cm thick aluminum baffle plate separating the upper core from the lower core. Fuel plates 204101, 204102, and 204103 are 2-cm thick and are stacked above the 4-cm thick fuel plates. Fuel plates 204104 and 204105 are 1-cm thick and are stacked above the 2-cm thick fuel plates. There is a 1-cm region above 204105 to allow the addition of another fuel plate; however, the UNM AGN does not currently consider fuel in this fuel plate location. All fuel plates have an outside diameter of 25.6 cm (10.01 in.). Figure 6 illustrates the core fuel plate stack of the AGN. The core is contained within a gas-tight aluminum cylindrical tank that is 32.2 cm (12.7 in.) in diameter and 76 cm (29.9 in.) high. Figure 7 provides illustrations of the AGN core control rod locations.

www.manaraa.com

Figures 8 and 9 illustrate the geometry of the various fuel plates that make up the AGN core.

Table 1. Fuel Plate Specifications for the UNM AGN-201M Reactor [4]

Fuel Plate Number	Plate Height (cm)	Plate Diameter (cm)	Total Mass of Fuel (UO_2) in the CH_2 Matrix (g)	^{235}U Mass (g)
20497	4.0	25.6	2,150.0	98.89
20498	4.0	25.6	2,158.5	99.12
20499	4.0	25.6	2,026.5	93.17
204100	4.0	25.6	2,052.0	94.39
204101	2.0	25.6	1,262.5	58.01
204102	2.0	25.6	1,263.5	58.07
204103	2.0	25.6	1,263.0	58.05
204104	1.0	25.6	670.0	30.80
204105	1.0	25.6	648.5	29.79
Fuse	0.9	2.2	5.90	0.44
Fixed Fuel Loading/Density			13,500.4	620.73

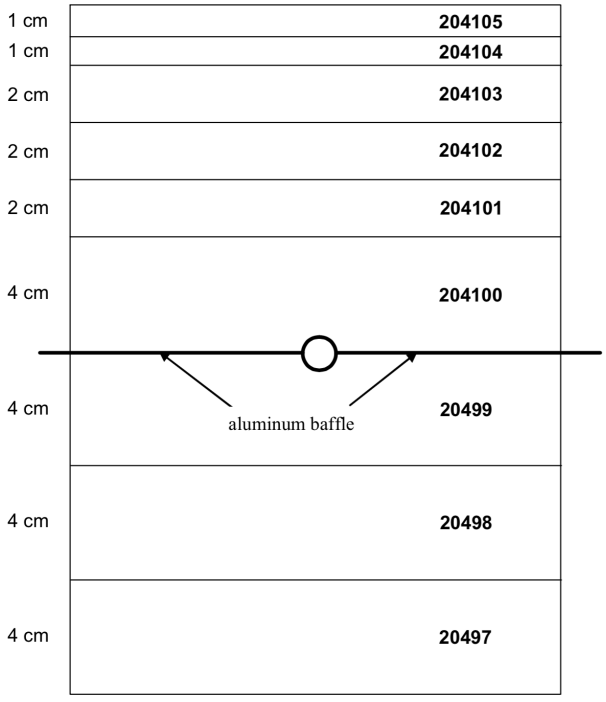

Figure 6. AGN-201M Fuel Plate Stack [8]

www.manaraa.com

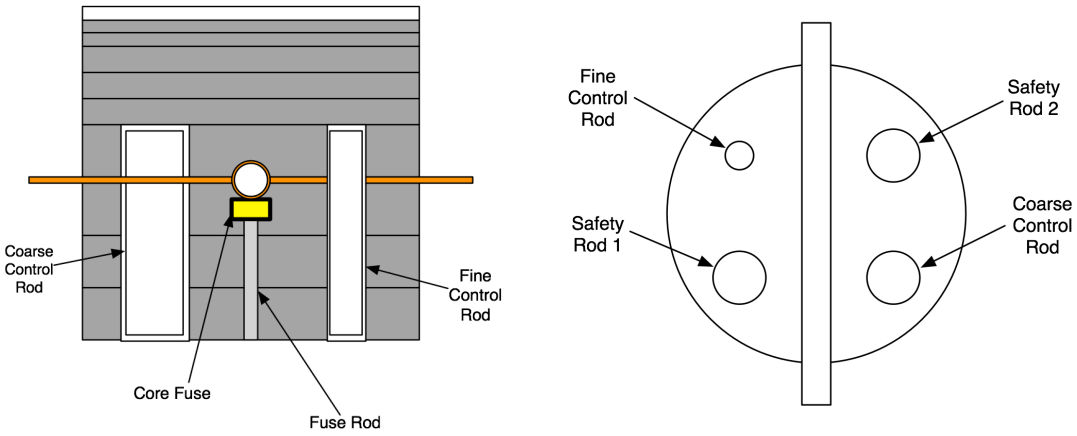

Figure 7. Core Cross Section Illustrations of the Control Rod Locations

Figure 8. Illustration of Fuel Plate Geometry

www.manaraa.com

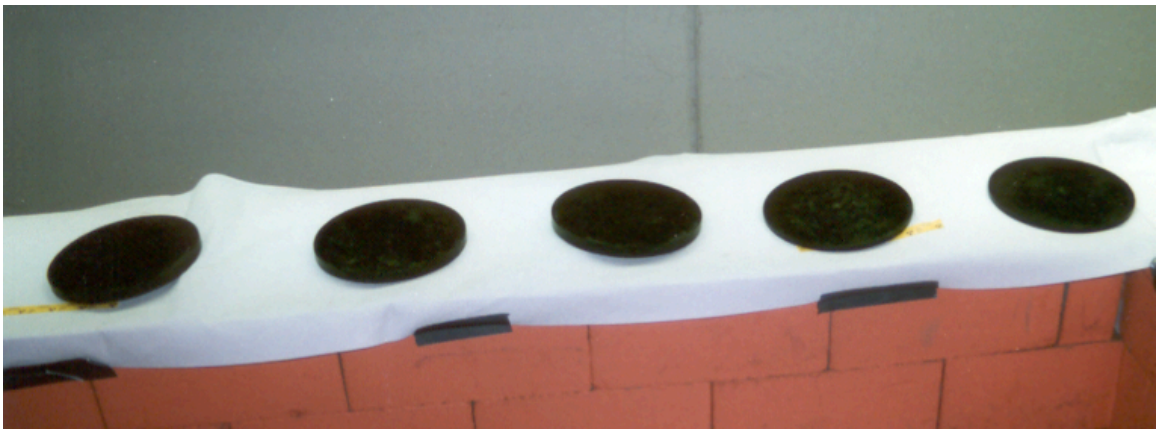

Figure 9. Illustration of the Upper Core Fuel Plate Geometry

2.2.2 Reactor Control

The AGN reactor is controlled by using four control elements. The control elements (SR1, SR2, CCR, and FCR) for the AGN reactor are made of the same fuel material present in the AGN fuel plates, uranium dioxide (UO_2) impregnated polyethylene with a nominal enrichment of 19.5 ± 0.5 wt. % ^{235}U. Table 2 provides the control rod specifications for the AGN reactor. Each of the control rods is doubly encapsulated in two aluminum containers (total thickness is a 0.5-cm) and functions to isolate the control rods from the core region. The control rods have about 16-cm of travel within the control element tubes in the lower AGN core to either insert or remove reactivity from the core. The FCR has a reactivity worth approximately 8¢ when located at the bottom of the core and approximately 28¢ when fully inserted into the core (position of about ~23 cm) [8]. The CCR, SR1, and SR2 are each worth approximately 28¢ when located at the bottom of the core and approximately $1.67 when fully inserted into the core (position of about ~24 cm) [8]. The

www.manaraa.com

safety rods and coarse rod are magnetically coupled to a carriage so that each rod can be dropped without resulting in a reactor scram [8]. These rods fall under gravity with the assistance of compressed springs to increase the speed at which the rods are withdrawn from the core. The fine control rod is used for fine reactivity adjustments. When a scram occurs, rods SR1, SR2, and CCR drop out of the reactor core, but the fine control rod is driven out at a slower rate. The operator is made aware of a reactor scram with a warning light and bell at the reactor console.

Table 2. Control Rod Specifications [4]

Parameter	Safety Rod #1	Safety Rod #2	Coarse Rod	Fine Rod
Outside diameter	4.5 cm	4.5 cm	4.5 cm	2.0 cm
Fuel diameter	4.5 cm	4.5 cm	4.5 cm	4.5 cm
Fuel Loading in Polyethylene	14.5 g ^{235}U	14.5 g ^{235}U	14.5 g ^{235}U	2.71 g ^{235}U
Total Mass	315.77 g	315.53 g	315.58 g	58.95 g
Reactivity Worth	1.25% δk/k	1.25% δk/k	1.25% δk/k	0.28% δk/k
Total Travel Distance	24 cm total 16 cm inside core	24 cm total 16 cm inside core	24 cm total 16 cm inside core	24 cm total 16 cm inside core
Insertion Time	40-50 sec.	40-50 sec.	40-50 sec.† ~80-100 sec.††	40-50 sec.† ~80-100 sec.††
Scram Removal Time	200 msec	200 msec	200 msec	Does not scram – driven out of core when a scram signal is received.

† Normal insertion/withdrawal time at high speed.
†† Normal insertion/withdrawal time at slow speed.

During reactor start-up operations, the control rods are loaded into the core in a particular order: SR1, SR2, CCR and FCR. The CCR and FCR can

www.manaraa.com

be loaded into the core separately, if necessary. The rods are loaded into the core by using a DC motor and lead screws that are attached to the bottom of the control element. The motor speed can be varied (high and low speeds) to either insert or withdraw the control rod from the reactor core during operations. A photograph of the AGN the control rod drive mechanisms and a control element is shown in Figure 10. Figures 11 and 12 show a photograph and an illustration, respectively, of the control rod drive mechanism for the AGN. As previously stated, the control rods add or remove reactivity to the AGN core by changing the quantity of fissile material (^{235}U) mass present in the core. During a scram about 43.5 grams of ^{235}U, corresponding to the ^{235}U in SR1, SR2, and the CCR, can be removed from the core in approximately 200 msec. An additional 2.71 grams of ^{235}U is removed after the FCR withdraws from the core via activation of the DC motor. The control elements represent approximately 7 percent of the ^{235}U mass in the core, corresponding to a total reactivity worth of approximately 4.03% $\delta k/k$ or about 3.75% $\delta k/k$ within 200 msec [8].

www.manaraa.com

Figure 10. Photo of the Control Element Drives and Element

Figure 11. Photograph of the Control Element Drives

www.manaraa.com

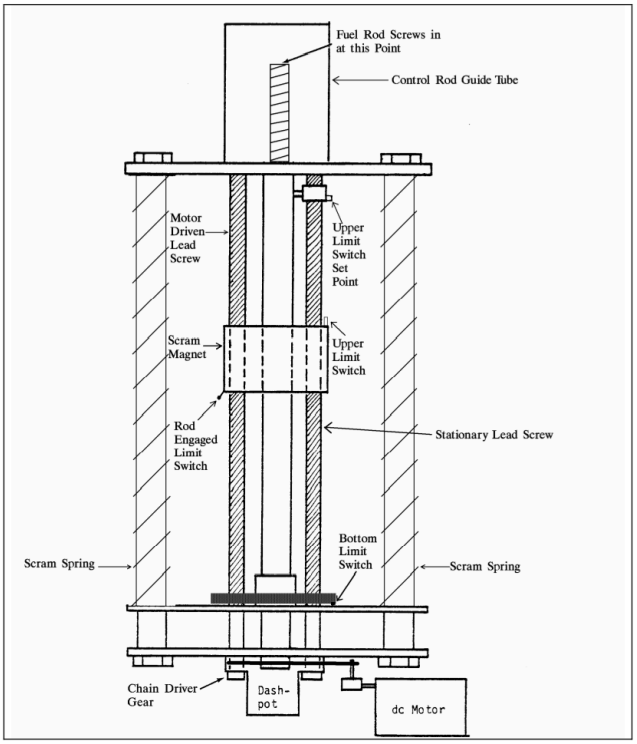

Figure 12. Illustration of the AGN-201M Rod Drive Mechanism [8]

2.2.3 Thermal Fuse and Glory Hole

The thermal fuse has an outside diameter of 2.2 cm (0.87 in.) and a height of 0.9 cm (0.35 in.) [4]. It is made of polystyrene and supports the bottom half of the AGN core. The fuse has a fuel density about twice that of the fuel plates and rests on a 0.39 cm (0.15 in.) diameter aluminum rod. This rod rests in a rod tube with an inside diameter of approximately 1.27 cm (0.5 in.) and an outside diameter of 1.59 cm (0.51 in.). The aluminum rod passes through the center of fuel plates 20497, 20498, and 20499. As previously stated, the thermal fuse melts during a reactor transient that results in the

www.manaraa.com

bottom half of the core falling approximately 5.08 cm (2.0 in.), which terminates the transient.

The glory hole extends through the core, graphite reflector, lead shield, and water tank of the AGN reactor. The glory hole has an inside diameter of 2.37 cm (0.935 in.) with an outside diameter of 2.54 cm (1.0 in.) [4]. The glory hole tube is made of aluminum (density of 2.702 g/cm^3) and penetrates the reactor core through the baffle plate, which separates the upper and lower halves of the AGN core plates.

2.3 Reflector and Shielding Specifications

2.3.1 Graphite Reflector

A 20 cm (7.87 in.) thick graphite reflector with a density of 1.75 g/cm^3 surrounds the AGN core [4]. Scoping calculations with MCNP indicate more than 95% of the fissions in the AGN core are caused by neutrons with energies below 0.625 eV; thus, the polyethylene-UO_2 AGN core is a system dominated by thermal neutrons. Graphite is a good neutron reflector for use with a thermal core because graphite is a poor thermal neutron absorber ($\sigma_a \approx 0.004$ b) compared to other reflectors, such as the hydrogen in water ($\sigma_a \approx 0.322$ b). Thus, the quantity of ^{235}U necessary required for a research reactor such as the AGN is kept to a minimum. The lower portion of the graphite reflector contains holes for the four control elements and core support for the core fuse. The upper core reflector contains four holes for the access ports.

www.manaraa.com

2.3.2 Reactor Shielding

A 10 cm-thick (3.94 in.) lead shield (poured lead blocks) is present in the AGN reactor located outside of the graphite reflector used primarily to shield against gamma radiation emitted during operations [4]. The lead region (density of 10.78 g/cm^3) is enclosed in and supported by a 0.794 cm (0.31 in.) thick steel reactor tank (density of 7.82 g/cm^3) [4]. The next region of the reactor consists of a water shield that is tight fitting around the steel reactor tank. The water tank holds approximately 3,785 liters (1,000 gallons) of water and forms the fast neutron shield. This region has a thickness of 49.54 cm (19.5 in.) and is used to shield neutrons from outside the reactor environment. A removable thermal column tank permits access to the core tank and can be filled with graphite if a thermal column is desired. Additional concrete block shielding is present on the front of the reactor tank and 40 cm (15.7 in.) on the sides and back and is necessary for the AGN to operate at a power level of up to 5 W. There is no additional shielding on the top of the reactor tank.

The AGN reactor power is controlled by inserting or withdrawing the control rods, which contain low enriched uranium dioxide fuel similar in composition to the fuel plates in the core. The reactor core is passively cooled. Any heat generated in the core is dissipated within the core reflector and shielding regions (the lead and water regions).

www.manaraa.com

2.3.3 Instrumentation and Safety Systems

2.3.3.1 Neutron Detectors

Four neutron detectors are used to monitor the neutron flux in the AGN core. Channel 1 is a ^{235}U fission chamber used to monitor the neutron flux during reactor start-up. Channels 2 and 3 consist of boron-lined ionization chambers used to ensure that the reactor power is maintained within reactor limits. The auxiliary channel also is a boron-lined ionization chamber used as an auxiliary monitor for high accuracy reactivity measurements and data acquisition activities. The auxiliary channel allows the reactor operator to record the current measurements every 0.25 seconds and writes the data to a computer file for later use [8].

2.3.3.2 AGN-201M Reactor Safety Interlocks and Radiation Monitoring

There are three safety interlocks included in the reactor instrumentation [8]. The magnet current connected to the control rod drives is deactivated and scrams the reactor if any one of the three safety interlocks is tripped during routine operations. The three safety interlocks involve the shield water level monitor (low water level), shield tank temperature (temperature below 18 °C), and earthquake sensor (excessive vibration). Radiation monitoring equipment is available to the reactor operator during operations to ensure radiation levels in the general lab, at the top of the reactor, at the reactor console and at south side of the reactor is maintained within the acceptable

www.manaraa.com

range during reactor operations to protect staff and students in the vicinity. The instrumentation is calibrated periodically by the Radiation Safety Department of the University [8].

www.manaraa.com

Chapter 3 – Computer Code Descriptions

3.1 Introduction

A variety of computer codes were used for this research in the development of a calculation methodology to analyze experimental steady state and transient configurations on the UNM AGN. This methodology utilized a variety of computer code packages to assist with nuclear data development, steady state computations, and time-dependent computations. The overall calculation methodology was developed iteratively as dictated by the needs of the research. Figure 13 illustrates the calculation methodology for the EVENT steady-state and transient analyses, including the computer codes used to support the methodology.

www.manaraa.com

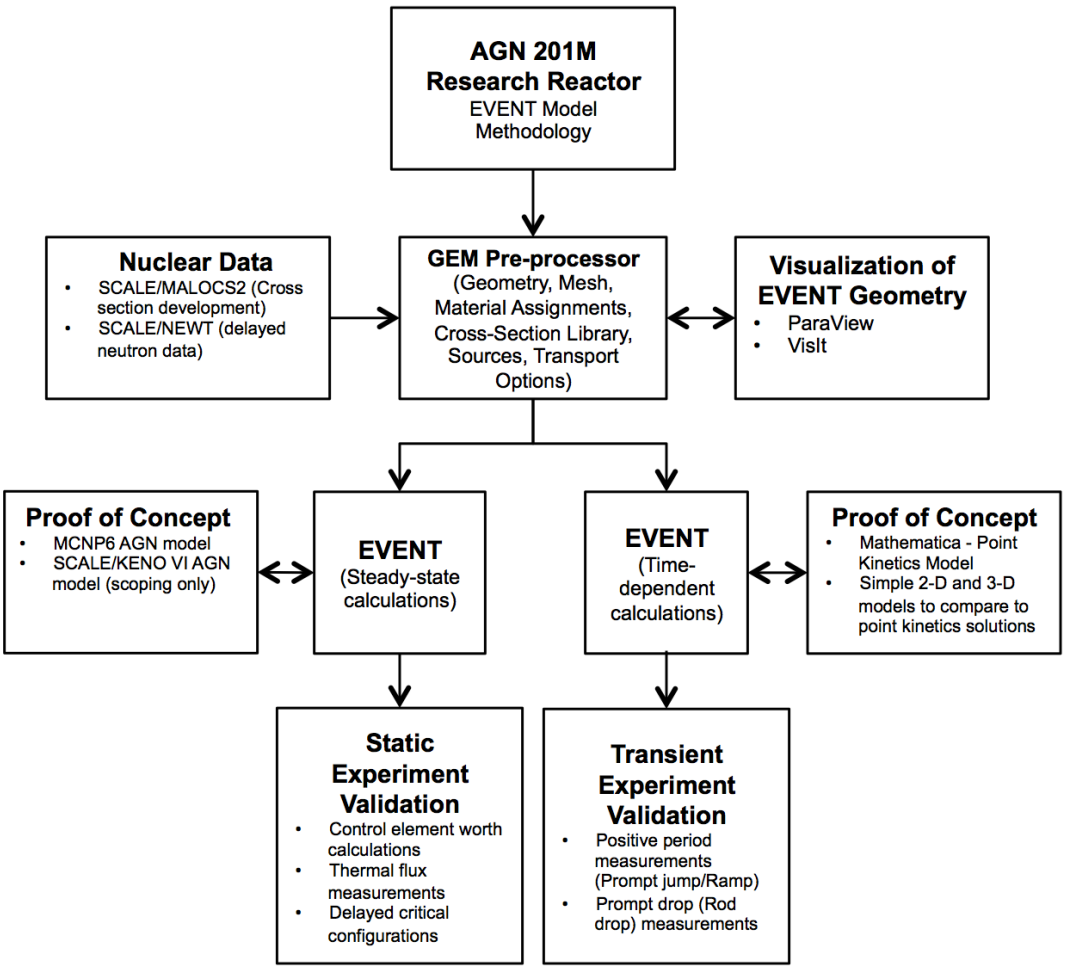

Figure 13. Codes Used to Prepare the AGN Calculation Methodology

3.2 SCALE Code Package

The SCALE (**S**tandardized **C**omputer **A**nalyses for **L**icensing **E**valuation) code package [26] is a comprehensive modeling and simulation suite for nuclear safety analysis and design purposes. The SCALE package consists of a variety of code packages utilized via standardized sequences. For example, a 3-D model was created to support numerous scoping calculations using the SCALE Monte Carlo code KENO-V and utilizes the CSAS5 control sequence that runs the following SCALE codes: BONAMI, NITAWL, XSDRNPM, and

www.manaraa.com

KENO-V. The standardized sequence performs resonance self-shielding calculations of the SCALE cross sections using the Bondarenko method with BONAMI for unresolved resonance processing and using the Nordheim integral method for resolved resonance processing using NITAWL. The WORKER, CENTRM, and PMC modules collapse pointwise continuous energy cross sections using a problem dependent pointwise continuous neutron flux. When complete, the sequence provides a resonance-corrected cross-section library based on the physical charactistics of the problem being analyzed. The resulting cross-section libraries could then be used in the Monte Carlo simulation using KENO-V or the discrete ordinates 1-D code XSDRN. The GEM preprocessor is able to open and access the AMPX formatted cross section file for use with the AGN EVENT models. The SCALE 6.2 beta 3 package is used to generate multigroup cross sections by collapsing the 252-group fine-group library to 8 or fewer neutron groups. The cross-section libraries are based on the ENDF/B-VII.1 library. The collapsed cross sections generated using the SCALE 6.2 utilities use a different cross section library format than was assumed in SCALE 6.1 (AMPX format) and the broad group libraries have to be reformatted to be compatable with GEM and EVENT.

Extensive scoping analysis was performed to test the EVENT code using the KENO V.a and KENO VI [27] Monte-Carlo codes and the 2-D discrete ordinates code NEWT. The NEWT code was used provide results to compare

www.manaraa.com

to EVENT 2-D results, to compute delayed neutron data, and to compute the prompt neutron fission spectrum for both steady-state and transient scoping calculations.

3.2.1 SCALE/KENO-VI AGN Model Development

The Monte Carlo code KENO-VI was extensively used in this work as a basis of comparison as the 2- and 3-D EVENT models of the UNM AGN were developed. A key task to perform both the KENO and EVENT calculations was to develop the case-dependent multigroup cross sections based on modern neutron cross section data. Thus, the CSAS6 control sequence [28] of SCALE was used to provide an automated, problem-dependent, cross section processing followed by calculation of the k_{eff} for the AGN reactor. This control sequence is used to provide resonance-corrected cross-sections in the resolved resonance range via the CENTRM [29] module. The purpose of CENTRM is to compute problem-specific fluxes on a fine energy mesh, which may be used to generate a self-shielded multigroup cross-section library for subsequent analysis using other SCALE modules. For this work, the self-shielded cross-section library for the AGN is then used by the 3-D Monte Carlo criticality transport program KENO-VI to calculate the effective multiplication factor of the AGN for various scoping calculations.

KENO VI calculations were used as a starting point to tally the prompt neutron fission spectrum, $\chi(E)$, using a complex 3-D representation of the AGN reactor. The fission spectrum and neutron flux data from the KENO VI

www.manaraa.com

cases were used to collapse a SCALE fine group library (252-group SCALE library) to a minimal number of groups to improve the efficiency of the complex AGN EVENT models considered later in this work. The KENO-VI calculations performed early in this research supported the development of the case-dependent resonance-corrected neutron cross-section libraries and the complex AGN EVENT models.

3.2.2 Neutron Cross-Section Library Generation

The first step for this work was to generate modern, self-shielded multigroup cross-sections based on the material characteristics of the AGN for use in EVENT. For scoping calculations, the SCALE 6.1.3 package was used with the SCALE modules NEWT [30] and XSDRNPM [31]. These modules were used to collapse multigroup neutron cross sections based on ENDF/B-VII data from 238-groups to 2-, 4-, or 8-groups for scoping studies with 1-D and 2-D AGN models (XSDRN and NEWT, respectively). These scoping calculations were used to gain experience with the AGN EVENT models for the experimental analysis to support this research prior to the development of modern case-dependent neutron cross sections. Older but reliable nuclear data libraries, such as CASK 22-group (ENDF/B-II library) [32] and Hansen-Roach 16-group cross-sections, [33] were used in scoping calculations as needed. Early testing of the GEM and EVENT codes involved CASK 22-group cross-sections, developed primarily for water filled shipping cask-type configurations. Hansen-Roach 16-group cross-sections were also

www.manaraa.com

used for early scoping calculations because of the author's experience with the cross-section library. The Hansen-Roach library was created initially for systems with a fast neutron spectrum but performs well with thermal systems as well. It was developed with 12 fast groups and 4 thermal groups.

The most current version of the SCALE package was desired to ensure the most modern neutron cross section data was used for the EVENT analyses. An AGN model was developed with the KENO VI code based on a KENO-VI model from Wetzel [4] to tally the neutron flux spectrum of the AGN research reactor with the control rods fully inserted into the core. The resulting neutron flux spectrum is shown in Figure 14. Understanding the neutron flux spectrum and the neutron cross sections for the non-fissionable (Figure 15) and fissionable constituents (Figure 16) of the AGN core was used as a starting point for developing case-dependent multigroup cross sections for the AGN steady-state and transient modeling analysis in EVENT.

As the scoping analysis was coming to a close, a development verson of SCALE 6.2 (beta 3) was released [34]. The CSAS1D sequence of SCALE was used, along with the new MALOCS2 utility, to collapse a 252-group fine library into various broad group libraries (2, 3, 4, 6, and 8-neutron energy groups). The 252-group neutron cross-section library, intended to replace the currently available 238-group neutron cross-section library, is based on the ENDF/B-VII.1 library. This fine group library was released in 2011 for testing and is significantly improved over previous Evaluated Nuclear Data

www.manaraa.com

File libraries [35]. Table 3 lists the energy boundaries for the 252-group SCALE 6.2 library and Table 4 lists the energy boundaries for the collapsed broad group energy boundaries. The CSAS1D sequence of SCALE is used for creating the multigroup libraries using the following SCALE utility modules:

- CRAWDAD – produces a continuous energy cross-section library from the 252-group ENDF/B-VII.1 library for use by CENTRM and PMC,
- BONAMI – performs Bondarenko calculations to consider neutron resonance self-shielding effects based on the AGN model definition,
- WORKER – creates an AMPX master working cross-section library for use with subsequent SCALE utility codes,
- CENTRM – uses the continuous energy cross-section library from CRAWDAD and the cell description in the AGN model definition to create a case-dependent pointwise continuous neutron flux spectrum assuming a neutron flux spectrum from a light water reactor, i.e., a thermal neutron system similar to the AGN (Figure 14),
- PMC – uses the case-dependent pointwise continuous neutron flux spectrum created in CENTRM to collapse the pointwise continuous cross sections to a case-dependent set of multigroup cross sections, which includes corrections for resonance self-shielding effects,
- WORKER – creates an AMPX working format library from a master format library with the desired number of neutron groups,

www.manaraa.com

- XSDRN – calculates cell-weighted cross sections based on the specified unit cell in the AGN problem and calculate the k_{eff} for a 1-D system, and
- MALOCS2 – an improved utility code that collapses the 252-group AMPX master cross-section library to the desired number of groups for use with EVENT.

www.manaraa.com

Table 3. SCALE ENDF/B-VI.1 252-Group Energy Boundaries [34]

Group	252 Group Energy Boundaries (eV)	Group	252 Group Energy Boundaries (eV)	Group	252 Group Energy Boundaries (eV)	Group	252 Group Energy Boundaries (eV)	Group	252 Group Energy Boundaries (eV)
1	2.00E+07	51	5.20E+04	101	7.60E+01	151	6.75E+00	202	1.02E+00
2	1.73E+07	52	5.00E+04	102	7.20E+01	152	6.50E+00	203	1.01E+00
3	1.57E+07	53	4.50E+04	103	6.75E+01	153	6.25E+00	204	1.00E+00
4	1.46E+07	54	3.00E+04	104	6.50E+01	154	6.00E+00	205	9.75E-01
5	1.38E+07	55	2.00E+04	105	6.30E+01	155	5.40E+00	206	9.50E-01
6	1.28E+07	56	1.70E+04	106	6.10E+01	156	5.00E+00	207	9.25E-01
7	1.00E+07	57	1.30E+04	107	5.80E+01	157	4.70E+00	208	9.00E-01
8	8.19E+06	58	9.50E+03	108	5.34E+01	158	4.10E+00	209	8.50E-01
9	6.43E+06	59	8.03E+03	109	5.06E+01	159	3.73E+00	210	8.00E-01
10	4.80E+06	60	5.70E+03	110	4.83E+01	160	3.50E+00	211	7.50E-01
11	4.30E+06	61	3.90E+03	111	4.52E+01	161	3.20E+00	212	7.00E-01
12	3.00E+06	62	3.74E+03	112	4.40E+01	162	3.10E+00	213	6.50E-01
13	2.48E+06	63	3.00E+03	113	4.24E+01	163	3.00E+00	214	6.25E-01
14	2.35E+06	64	2.50E+03	114	4.10E+01	164	2.97E+00	215	6.00E-01
15	1.85E+06	65	2.25E+03	115	3.96E+01	165	2.87E+00	216	5.50E-01
16	1.50E+06	66	2.20E+03	116	3.91E+01	166	2.77E+00	217	5.00E-01
17	1.40E+06	67	1.80E+03	117	3.80E+01	167	2.67E+00	218	4.50E-01
18	1.36E+06	68	1.55E+03	118	3.76E+01	168	2.57E+00	219	4.00E-01
19	1.32E+06	69	1.50E+03	119	3.73E+01	169	2.47E+00	220	3.75E-01
20	1.25E+06	70	1.15E+03	120	3.71E+01	170	2.38E+00	221	3.50E-01
21	1.20E+06	71	9.50E+02	121	3.70E+01	171	2.30E+00	222	3.25E-01
22	1.10E+06	72	6.83E+02	122	3.60E+01	172	2.21E+00	223	3.00E-01
23	1.01E+06	73	6.70E+02	123	3.55E+01	173	2.12E+00	224	2.75E-01
24	9.20E+05	74	5.50E+02	124	3.50E+01	174	2.00E+00	225	2.50E-01
25	9.00E+05	75	3.05E+02	125	3.38E+01	175	1.94E+00	226	2.25E-01
26	8.75E+05	76	2.85E+02	126	3.33E+01	176	1.86E+00	227	2.00E-01
27	8.61E+05	77	2.40E+02	127	3.18E+01	177	1.77E+00	228	1.75E-01
28	8.20E+05	78	2.20E+02	128	3.13E+01	178	1.68E+00	229	1.50E-01
29	7.50E+05	79	2.10E+02	129	3.00E+01	179	1.59E+00	230	1.25E-01
30	6.79E+05	80	2.07E+02	130	2.75E+01	180	1.50E+00	231	1.00E-01
31	6.70E+05	81	2.02E+02	131	2.50E+01	181	1.45E+00	232	9.00E-02
32	6.00E+05	82	1.93E+02	132	2.25E+01	182	1.40E+00	233	8.00E-02
33	5.73E+05	83	1.92E+02	133	2.18E+01	183	1.35E+00	234	7.00E-02
34	5.50E+05	84	1.89E+02	134	2.12E+01	184	1.30E+00	235	6.00E-02
35	4.92E+05	85	1.88E+02	135	2.05E+01	185	1.25E+00	236	5.00E-02
36	4.70E+05	86	1.80E+02	136	2.00E+01	186	1.23E+00	237	4.00E-02
37	4.40E+05	87	1.70E+02	137	1.94E+01	187	1.20E+00	238	3.00E-02
38	4.20E+05	88	1.43E+02	138	1.85E+01	188	1.18E+00	239	2.53E-02
39	4.00E+05	89	1.22E+02	139	1.70E+01	189	1.15E+00	240	1.00E-02
40	3.30E+05	90	1.19E+02	140	1.60E+01	190	1.14E+00	241	7.50E-03
41	2.70E+05	91	1.18E+02	141	1.44E+01	191	1.13E+00	242	5.00E-03
42	2.00E+05	92	1.16E+02	142	1.29E+01	192	1.12E+00	243	4.00E-03
43	1.49E+05	93	1.13E+02	143	1.19E+01	193	1.11E+00	244	3.00E-03
44	1.28E+05	94	1.08E+02	144	1.15E+01	194	1.10E+00	245	2.50E-03
45	1.00E+05	95	1.05E+02	145	1.00E+01	195	1.09E+00	246	2.00E-03
46	8.50E+04	96	1.01E+02	146	9.10E+00	196	1.08E+00	247	1.50E-03
47	8.20E+04	97	9.70E+01	147	8.10E+00	197	1.07E+00	248	1.20E-03
48	7.50E+04	98	9.00E+01	148	7.15E+00	198	1.06E+00	249	1.00E-03
49	7.30E+04	99	8.17E+01	149	7.00E+00	199	1.05E+00	250	7.50E-04
50	6.00E+04	100	8.00E+01	150	6.88E+00	200	1.04E+00	251	5.00E-04
						201	1.03E+00	252	1.00E-04

www.manaraa.com

Table 4. SCALE ENDF/B-VI.1 Broad Group Energy Boundaries

Group	8-Group Cross-Section Library	6- Group Cross-Section Library	4- Group Cross-Section Library	3- Group Cross-Section Library	2- Group Cross-Section Library
1	2.00E+07	2.00E+07	2.00E+07	2.00E+07	2.00E+07
2	8.20E+05	1.00E+05	7.50E+04	5.00E+00	6.50E-01
3	2.00E+04	2.00E+04	5.00E+00	6.50E-01	1.00E-05
4	1.05E+02	1.05E+02	6.50E-01	1.00E-05	–
5	5.00E+00	5.00E+00	1.00E-05	–	–
6	6.50E-01	6.50E-01	–	–	–
7	5.00E-02	1.00E-05	–	–	–
8	2.00E-03	–	–	–	–
–	1.00E-05	–	–	–	–

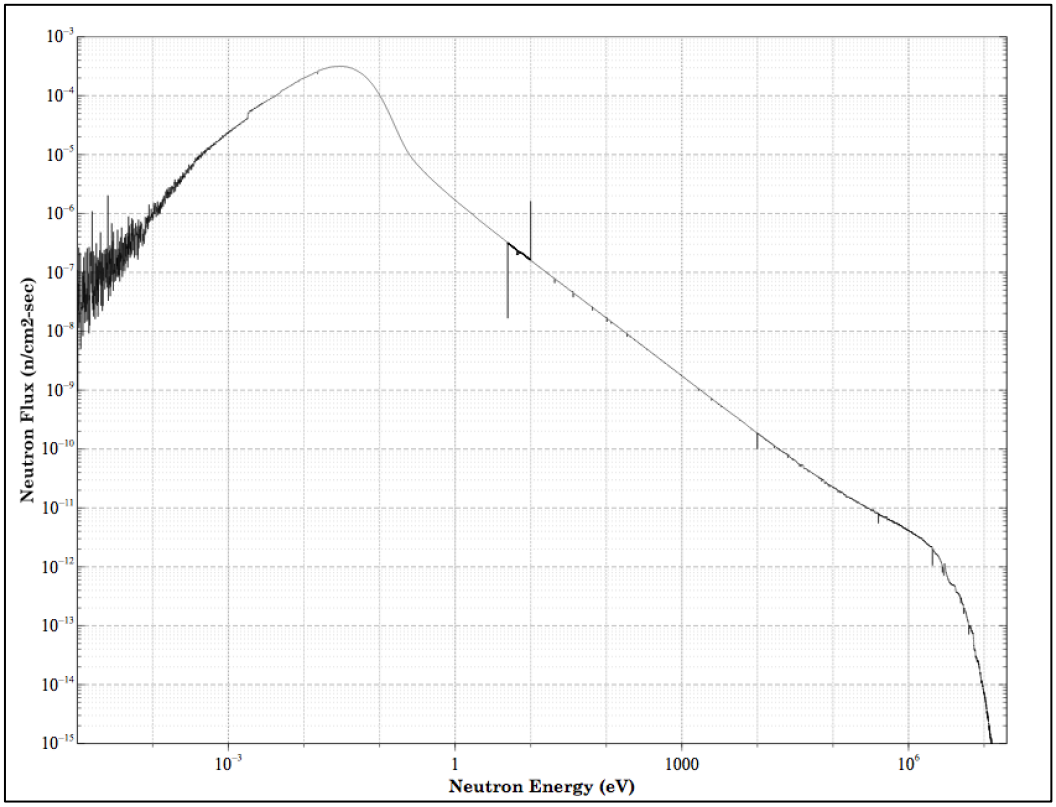

Figure 14. AGN Neutron Flux Spectrum

www.manaraa.com

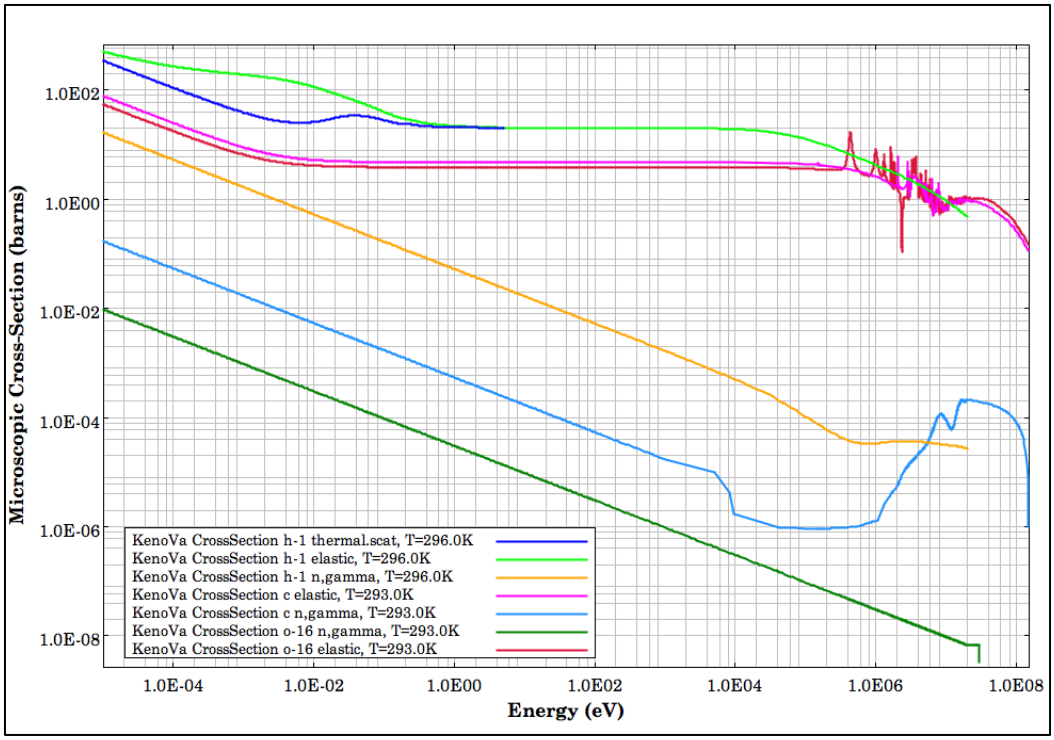

Figure 15. ^{1}H, ^{12}C and ^{16}O Absorption and Scattering Cross Section Plot

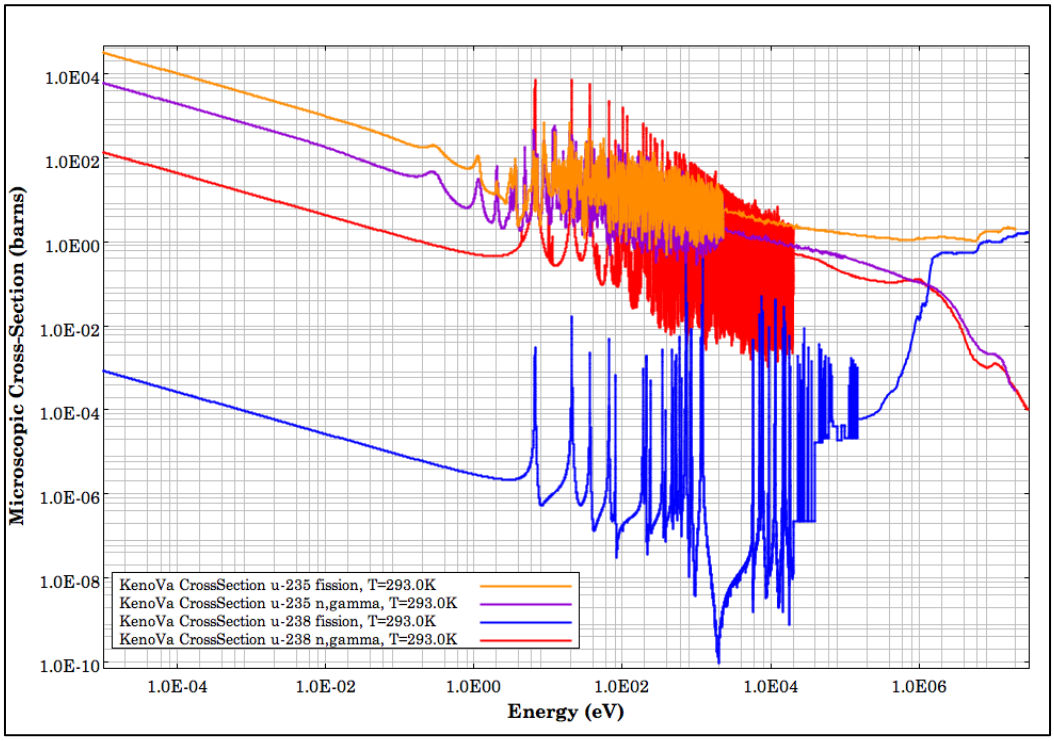

Figure 16. ^{235}U and ^{238}U Absorption and Fission Cross Section Plot

www.manaraa.com

The resulting broad-group libraries (Table 4) were then extensively tested with a variety of 2-D and 3-D AGN configurations in EVENT. The goal of the EVENT testing was to determine an acceptable cross-section library for use with the AGN experimental analysis. A cross section set for this work is a multigroup library with minimal neutron energy groups provides acceptable testing results, i.e., accurate model results and reasonable execution time.

The collapsed multigroup libraries created with SCALE, the 2-, 3-, 4-, 6, and 8-group multigroup neutron cross sections, are all AMPX-formatted libraries that are compatible with EVENT. The broad-group libraries are AGN case-dependent libraries that have been adjusted to account for resonance self-shielding effects due to the significant presence of ^{238}U in the low-enriched AGN core. These case-dependent libraries can be read by GEM using the embedded nuclide identifiers in the assignment of materials and atom densities to the various geometric regions in the AGN model. The use of modern cross-sections, based on the ENDF/B-VII.1 data, provide a solid nuclear data foundation on which to conduct the AGN steady-state and transient analyses. Modern cross section data should compare well to the AGN studies performed by Wetzel [4] that utilize ENDF/B-VI.8 data. Once the the various multigroup cross-section libraries have been tested successfully for steady-state configurations from Wetzel and actual AGN experimental configurations, the library that provides good accuracy with a

www.manaraa.com

minimal number of groups will be used for analysis of the AGN experimental transient configurations.

3.3 MCNP6 Monte Carlo Radiation Transport Code

The MCNP6 [6] is a general-purpose, continuous-energy, generalized-geometry, time-dependent, Monte Carlo radiation-transport code designed to track many particle types over broad ranges of energies. Two types of AGN models, an "X-Y" or infinite-Z model and a 3-D model, were developed with MCNP6 and EVENT. The k_{eff} results from each code were compared to provide some level of confidence in the EVENT results and to ensure the EVENT multigroup cross sections were acceptable before using them for the AGN experimental analysis. The MCNP6 and EVENT model configurations were identical to the extent possible. The two AGN models developed with MCNP6 utilize ENDF/B-VII continuous-energy cross sections, while the AGN models developed in EVENT utilize multigroup cross-sections based on ENDF/B-VII.1 library. The MCNP6 code uses the Monte Carlo method that simulates and tracks individual neutrons in the system and tallies their collision behavior, i.e., absorbed and lost from the system, absorbed and produce additional neutrons via fission, scatter elastically or inelastically off of a nucleus, or leak from the system. EVENT is a deterministic code that considers average neutron behavior in the fissile system. Thus, the MCNP6 code provides an excellent independent computational approach to compare to the EVENT computations.

www.manaraa.com

3.4 GEM Pre-Processor for EVENT

The GEM pre-processor [36] (GEM) is an interactive pre-processor for the radiation transport code EVENT. GEM was developed as a practical tool to generate all the necessary information concerning nodes, constraints, material properties, and other problem characteristics to a radiation transport code, such as EVENT, element-by-element [37]. Created as a convenience to the code user, the GEM pre-processor is a general purpose mesh generator and data preparation code for EVENT that automatically generates the finite-element mesh and input data. The EVENT computations require the use of finite element data to define the geometric configuration for the transport calculation. The GEM input file requires specific information for creating the input specifications for EVENT such as defining:

- The problem geometry in terms of simple geometric objects such as circles, rectangles, and polygons, for example, (GEM can utilize an external code called NETGEN to allow for the generation of constructive solid geometries (CGS) within EVENT for constructing complex geometrical configurations)
- The physical parameters such at the material cross-sections, sources, boundary conditions, and assign these properties to corresponding regions in the geometric model

www.manaraa.com

- The main control parameters for the EVENT run, e.g., eigenvalue problem, number of energy groups in the multigroup cross-sections, X-Y-Z geometry, order of scattering anisotropy, etc.
- The mesh specifications and control parameters

The GEM input file can also define the location of sensors for tallying the scalar flux, for example. GEM can also call EVENT directly and can port data, e.g., neutron flux, directly to a viewing application such as ParaView or VisIt. GEM can also open AMPX-formatted neutron cross-section libraries to view the material types and identification information, which is a useful tool when making material assignments to the regions of the problem geometry.

3.4.1 NETGEN

GEM allows for complex 2- and 3-D geometrical configurations to be constructed with EVENT. The 2-D geometrical configurations are easily reconfigured into a 3-D model by extruding the 2-D place surface axially via the use of axial zone heights. A representative 3-D model of the AGN was created in this way, although it was determined in extensive scoping analysis that the methodology to create a 3-D EVENT model of the AGN was expensive computationally. Thus, another approach was sought to create the AGN 3-D EVENT model. A powerful automatic mesh generation tool called NETGEN [38] may be called by GEM to allow for the generation of complex 3-D geometrical configurations by using CSG, which is similar to the geometric constructs available for use in KENO-VI and in MCNP6. A 3-D

www.manaraa.com

representation of the AGN research reactor was created for this research using the NETGEN mesh generation tool for direct comparison to the Monte-Carlo AGN models.

3.5 EVENT Radiation Transport Code

The primary radiation transport code used for this research is the EVENT [39,40] code. EVENT (**EVE**n parity **N**eutron **T**ransport) code is a general purpose, 3-D code developed for the solution of the Boltzmann transport equation describing the time-dependent and steady-state behavior of neutral particles in complex geometries. EVENT applies the finite element-spherical harmonics radiation transport method [41] to the solution of general radiation transport problems. This combined method provides significant advantages which include full geometric flexibility, reduced angular unknowns, absence of ray effects, and efficient scattering treatment. The problems solved with EVENT can include neutron downscatter or a combination of both neutron upscatter and downscatter. EVENT solves the self-adjoint second order form of the transport equation using a variational finite-element formulation [39]. EVENT is capable of solving multigroup, steady state and time-dependent problems in both forward and adjoint modes with anisotropic scattering. The code can model a variety of geometrical configurations in 1-D (slab, cylindrical, and spherical), 2-D (X-Y and R-Z using finite element meshes), and 3-D (X-Y-Z using finite element meshes).

www.manaraa.com

The EVENT transport code [40] solves the neutral particle transport problem described by Equation 1.

$$\frac{1}{v}\frac{\partial\psi(\vec{r},\vec{\Omega},E,t)}{\partial t}+\Omega\vec{\nabla}\psi(\vec{r},\vec{\Omega},E,t)+\vec{H}\psi(\vec{r},\vec{\Omega},E,t)=S(\vec{r},\vec{\Omega},E,t)$$

Equation 1

where

$\psi(\vec{r},\vec{\Omega},E,t)$ = particle angular flux or intensity,

$S(\vec{r},\vec{\Omega},E,t)$ = a distributed source which depends on the type of problem being solved (time evolution, steady-state fixed-source or steady-state eigenvalue),

$\vec{H}$ = collision operator defined in terms of the total cross-section and differential cross-section by:

$$H\psi(\vec{r},\vec{\Omega},E,t)=\sigma_t(\vec{r},E,t)\psi(\vec{r},\vec{\Omega},E,t)-\int_{4\pi}d\Omega'\,\sigma_s(\vec{r},\vec{\Omega}',E'\rightarrow\vec{\Omega}',E,t)\psi(\vec{r},\vec{\Omega}',E',t)$$

Equation 2

The discretization procedures in EVENT are based on the canonical or parity form of Equation 1 which consists of the coupled pair of first order equations [38]:

$$\frac{1}{v}\frac{\partial\psi^{+}}{\partial t}+C\psi^{+}=S^{+}-\Omega\cdot\vec{\nabla}\psi^{-}$$

Equation 3

and

www.manaraa.com

$$\frac{1}{v}\frac{\partial \psi^{-}}{\partial t} + G\psi^{-} = S^{-} - \Omega \cdot \vec{\nabla}\psi^{+}$$

Equation 4

where

$$\psi^{\pm} = \frac{\psi(\Omega) \pm \psi(-\Omega)}{2}$$

Equation 5

and

$$S^{\pm} = \frac{S(\Omega) \pm S(-\Omega)}{2}$$

Equation 6

The vectors $\vec{C}$ and $\vec{G}$ are the even- and odd-parity components of the angular flux, distributed source and the $\vec{H}$ operator, respectively [38]. The representation of Equation 1 into the even- and odd-parity functions has physical significance. The neutron scalar flux at $\vec{r}$ is represented by the integral of the even-parity angular flux integrated over all solid angles, $\vec{\Omega}$, that governs the neutron reaction rate at $\vec{r}$ as follows: $\int \psi^{+}(\vec{r}, \vec{\Omega}, E, t) d\vec{\Omega}$ [38]. Further, the net neutron current in the direction of $\hat{n}$ at $\vec{r}$ is the product of the odd-parity flux and the dot product of the angular flux and a unit vector in the direction of $\hat{n}$ as follows: $2\int \vec{\Omega} \cdot \hat{n}\phi^{-}(\vec{r}, \vec{\Omega}, E, t) d\vec{\Omega}$ [38].

Three distributed source options are available for use in EVENT. The first is a steady-state eigenvalue problem in which the neutron flux is assumed to

www.manaraa.com

be constant, i.e., time independent, and all extraneous sources, e.g., fixed neutron sources, delayed neutron precursors, etc., are assumed to be zero. The number of neutrons emitted per fission, ν(E) is adjusted so there is a solution to Equation 1 for the following source definition,

$$S(\vec{r},\vec{\Omega},E,t)=\frac{\chi(E)}{4\pi k_{eff}}\int_{4\pi}d\Omega'\psi\left(\vec{r},\vec{\Omega}',E',t\right)\nu(E')\sigma_f(\vec{r},E,t)$$

Equation 7

where the k_{eff} is the eigenvalue for the system providing a measure of whether the system is subcritical or supercritical and by how much [40].

The second source option available in EVENT is for problems involving a steady-state, fixed-source. The source term in these problems are assumed to be constant, i.e., fixed, in time where $S(\vec{r},\vec{\Omega},E,t)=s(\vec{r},\vec{\Omega},E,t)$ [38]. With this source, there is no neutron source contribution from fission. The neutron flux in these problems are assumed to be time independent and correspond to the long-term or equilibrium solution to Equation 1.

The third source option available in EVENT involves a problem where a time-dependent source or initial flux distribution is defined and the evolution of the angular flux is calculated and followed over single or multiple time zones. Each time zone can be used to model a system for a certain duration (modeled with explicit or adaptive time-stepping) that considers different nuclear data, scattering angle, and source strength. For neutrons, the time-dependent distributed source term is defined as follows,

www.manaraa.com

$$S(\vec{r},\vec{\Omega},E,t) = s(\vec{r},\vec{\Omega},E,t) + \frac{\chi(E)}{4\pi}\int dE' \int_{4\pi} d\Omega' \psi\left(\vec{r},\vec{\Omega}',E',t\right)\nu(E')\sigma_f(\vec{r},E',t)$$

Equation 8

where $s(\vec{r},\vec{\Omega},E,t)$ is an extraneous distributed neutron source such as a neutron source from the decay of delayed neutron precursors.

The EVENT code has the ability to consider time-dependent neutron transport problems based on an extension of its second-order or even-parity formulation of the neutron transport equation. The time discretized equations for this method can be solved via the finite element spherical harmonics procedure implemented in EVENT [42]. Within the last 20 years or so, enhanced computer capabilities and increased memory capabilities have allowed the finite element-spherical harmonics radiation transport methodologies to compete with S_N or discrete ordinance methods that solve first-order forms of the neutron transport equation.

This problem is concerned with the solution of neutron transport problems that are described by the linear integro-differential Boltzmann transport equation, previously defined as Equation 1,

$$\frac{1}{v}\frac{\partial\psi(\vec{r},\vec{\Omega},E,t)}{\partial t} + \Omega\vec{\nabla}\psi(\vec{r},\vec{\Omega},E,t) + \vec{H}\psi(\vec{r},\vec{\Omega},E,t) = S(\vec{r},\vec{\Omega},E,t)$$

Equation 9

where the terms in the equation were defined previously.

For neutrons, the distributed time-dependent neutron source is

www.manaraa.com

$$S(\vec{r},\Omega,E,t) = s(\vec{r},\Omega,E,t) +$$

$$\frac{(1-\beta)}{4\pi}\chi_p(E)\int dE'\int \phi(\vec{r},\Omega,E,t)\nu(E')\sigma_f(\vec{r},E',t)d\Omega' + \sum_k \frac{\lambda_k \chi_k^d(E)}{1+\lambda_k \alpha \Delta t_n} C_k^n(\vec{r},E,t)$$

Equation 10

In Equation 10, $s(\vec{r},\Omega,E,t)$ is an extraneous distributed source, the second term is the 'prompt' neutron fission source, i.e., source with no delayed neutron present, and $C_k(\vec{r},t)$ is the delayed neutron precursor concentration for delayed group k which satisifies the relationship for the time rate of change of the delayed neutron precursor concentration:

$$\frac{\delta C_k(\vec{r},t)}{\delta t} = -\lambda_k C_k(\vec{r},t) + \beta_k \int d\Omega' \int_{4\pi} \nu(E')\,\sigma_f(\vec{r},E',t)\phi(\vec{r},\Omega',E',t)dE'$$

Equation 11

where λ_k is the half life of the delayed neutron precursor group k and β_k is the effective delayed neutron fraction for delayed neutron precursor group k. Again, the discretization procedures in EVENT for the finite element-spherical harmonics method are based on the canonical or parity form of Equation 1 are shown in Equations 3 through 6.

The coupled pair of canonical equations, Equations 3 and 4, are discretized to sub-divide the time domain into a sequence of non-overlapping intervals $\Delta t_n = t_{n+1} - t_n$, n=0, 1, 2, …, that are not necessarily of the same length [43]. Further, it is assumed for simplicity that the material properties of the

www.manaraa.com

reactor remain constant during a time interval t_n. This implies the even- and odd-parity flux components, $\vec{C}$ and $\vec{G}$, respectively, which are time-dependent vector quantities, are assumed to remain constant during the time interval, t_n, i.e, $C(t) \equiv C_n$ and $G(t) \equiv G_n$. Thus, the canonical or parity form of Equation 3 and 4 for each time interval are

$$\frac{1}{v}\frac{\psi^+_{n+\alpha} - \psi^+_n}{\alpha \Delta t_n} + C_n \psi^+_{n+\alpha} = S^+_{n+\alpha} - \Omega \cdot \nabla \psi^-_{n+\alpha}$$

Equation 12

and

$$\frac{1}{v}\frac{\psi^-_{n+\alpha} - \psi^-_n}{\alpha \Delta t_n} + {G_n^{-1}}_n \psi^-_{n+\alpha} = S^-_{n+\alpha} - \Omega \cdot \nabla \psi^+_{n+\alpha}$$

Equation 13

where $\psi^+_{n+\alpha} = (1-\alpha)\psi^+_n + \alpha\psi^+_{n+1}$ and $\psi^-_{n+\alpha} = (1-\alpha)\psi^-_n + \alpha\psi^-_{n+1}$ with $\psi^+_n = \psi^+_n(t_n)$, $\psi^-_n = \psi^-_n(t_n)$, etc., and α is an arbitrary parameter in the range of $0 < \alpha < 1$. Reference [40] states that for $\alpha > ½$, the scheme is unconditionally stable. In EVENT, selected values of α result in the use of some well-known schemes for use in the time dependent calculation: (a) Crank-Nicolson ($\alpha = ½$); (b) Galerkin ($\alpha = 2/3$); or (c) Backward-Euler ($\alpha = 1.0$).

Equations 12 and 13 can be combined as follows

www.manaraa.com

$$-\Omega\cdot\nabla G_n\Omega\cdot\nabla\psi_{n+\alpha}+\left(C_n+\frac{1}{\alpha v\Delta t_n}\right)\psi_{n+\alpha}=\$^{+}_{n+\alpha}-\Omega\cdot\nabla G_n\$^{-}_{n+\alpha}$$

Equation 14

where the effective parity sources for this problem are given by

$$\$^{+}_{n+\alpha}=S^{+}_{n+\alpha}+\frac{\psi^{+}_{n}}{\alpha v\Delta t_n}$$

Equation 15

and

$$\$^{-}_{n+\alpha}=S^{-}_{n+\alpha}+\frac{\psi^{-}_{n}}{\alpha v\Delta t_n}$$

Equation 16

The equations for the delayed neutron precursor concentrations are discretized similarly resulting in Equations 17 and 18

$$C_k^{n+1}=\left(1-\frac{\lambda_k\Delta t_n}{1+\lambda_k\alpha\Delta t_n}\right)C_k^{n}+\frac{\beta_k\Delta t_n}{1+\lambda_k\alpha\Delta t_n}\int\nu(E')\sigma_f(E')dE'\int_{\Omega}\psi_{n+\alpha}(\Omega',E')d\Omega'$$

Equation 17

and

www.manaraa.com

$$S^{+}_{n+\alpha}(\vec{r},\Omega,E) = s^{+}_{n+\alpha}(\vec{r},\Omega,E)$$
$$+\left[\frac{(1-\beta)}{4\pi}\chi_p(E)\right.$$
$$\left.+\sum_k \frac{\lambda_k \chi_k^d(E)\beta_k \alpha\Delta t_n}{1+\lambda_k \alpha\Delta t_n}\right]\int dE'\nu(E')\sigma_f(\vec{r},E')\int_{4\pi} d\Omega'\,\psi_{n+\alpha}(\vec{r},\Omega',E',t)$$
$$+\sum_k \frac{\lambda_k \chi_k^d(E)}{1+\lambda_k \alpha\Delta t_n} C_k^n(E)$$

Equation 18

Properly formatted multigroup cross sections, prepared by using the SCALE package, are utilized in EVENT. The reactor materials for the AGN configuration are assigned to the appropriate regions in the reactor model using the GEM pre-processor. GEM can be used to open cross section files and view the cross section material identifier information to determine if the cross section library contains the needed neutron data. Visualization applications are useful to ensure the materials are adequately assigned to the regions of interest.

Spherical harmonics functions are used to approximate the angular dependence on the even-parity flux solutions [40]. The numerical implementation of spherical harmonics functions in EVENT is general and there is no restriction on the order of the angular approximation. The use of

www.manaraa.com

spherical harmonics functions, as implemented in EVENT, eliminate ray effects in the solution. Ray effects in deterministic codes are unphysical oscillations in the scalar flux. They are caused by the inability of a quadrature set in the discrete-ordinates approximation to accurately integrate the angular flux [44].

Each problem is discretized spatially via the use of isoparametric finite elements (having one or more curved sides) to compute the spatial dependence of the angular flux. Ray effects and related phenomena of scalar flux oscillations and instabilities have been shown to be greatly suppressed or eliminated in EVENT which utilize the finite element approach [45]. The use of finite elements allows for the modeling of far more complex geometrical configurations than typical deterministic codes that utilize simpler geometries, e.g., spheres, slabs, cylinders.

The EVENT code has the ability to consider time-dependent neutron transport problems based on an extension of its second-order or even-parity formulation of the neutron transport equation. The time discretized equations for this method can be solved via the finite element spherical harmonics procedure implemented in EVENT [42]. GEM can be used to create a delayed neutron source for a time dependent EVENT problem. Transients in time dependent problems are approximated in EVENT by changing the material properties of the AGN model over a series of time zones or steps, which approximate, for example, the movement of a control

www.manaraa.com

rod or the density of the fissile material in the core during the transient. The EVENT AGN time-dependent models approximate the movement of control rod by varying the volume fraction of fuel in the control elements as a function of time. The reactivity worth associated with the control rod location is defined in various time steps or zones with durations corresponding to the AGN experiments. The neutron population is calculated as a function of time as EVENT steps through the time zones in the problem. In order to estimate the proper delayed neutron precursor concentration when the AGN core at a delayed critical configuration initially, an EVENT eigenvalue problem is executed within the time dependent problem to calculate the neutron flux and delayed neutron precursor concentration when the reactor is initially operating at a critical state prior to the transient. The behavior of the AGN core transients depend upon both the prompt and delayed neutron concentration, so the accuracy of the delayed neutron precursor concentration calculation is important for modeling the transient behavior. The version of EVENT used for this research does not have reactivity feedback capabilities, such as fuel density changes due to heating of bubble formation during the transient.

3.6 Visualization Applications

The development of the calculation models required the use of visualization tools to ensure the EVENT models represent the desired geometrical configuration. MCNP has options to call an interactive plotter

www.manaraa.com

that produces 2-D slices of the model geometry. Commands in GEM can call the ParaView code [46] to view the problem mesh and geometry. Numerous options exist to view the model geometry including the capability to view interior detail of the model geometry. In addition, EVENT is used to calculate the spatial scalar flux and view the resulting flux profiles in ParaView. The VisIt code [47] is an open source interactive, scalable, visualization and analysis tool that was used for this work to view the EVENT model geometry. Both visualization tools used for this work have their advantages and were invaluable during the development of the EVENT models for this work.

3.7 Mathematica

Mathematica is a general computer software system and language intended for mathematical and other applications [48]. *Mathematica* is used to solve the point kinetics equations for one effective delayed neutron group. The NDSOLVE function was used in *Mathematica* to solve the stiff non-linear point kinetics differential equations. The numerical solution to the point kinetics equations is plotted and compared to the analytical solution to the one delayed family approximation to the point kinetics equations. The numerical solution is also compared to a series of simple EVENT AGN models to provide confidence in the EVENT results. The *Mathematica* notebook for the numerical solutions used in the EVENT comparison studies is provided in the Appendix.

www.manaraa.com

Chapter 4 – EVENT Model Development

4.1 Introduction

A variety of computational models were generated to test GEM and EVENT. All EVENT calculations were performed on an Apple Macbook Pro with a 2.4 GHz CPU and 8 GB of RAM. In addition to EVENT testing, the multigroup cross-section libraries generated for the EVENT calculations were also tested to ensure the computational methodology was sufficiently developed for the AGN experimental analysis. The EVENT code provides different geometrical options for modeling the AGN geometry in 2-D and 3-D configurations. The following models were created to test the EVENT code and cross sections:

- an X-Y model (2-D, infinite in the Z-direction),

www.manaraa.com

- an R-Z model (2-D, radius and height rotated around the Z-axis), and
- a NETGEN 3-D model (based on CSG concepts).

These models used for EVENT testing are described and the results are discussed in Appendix A. Based on the results of these testing efforts, a calculation methodology was selected for the experimental analysis. Further, the computational results for each of these geometrical configurations are compared to an independent calculation method. This independent calculation method involves the use of the MCNP6 Monte-carlo based radiation transport code using modern ENDF/B-VII continuous-energy cross sections to compare to the EVENT deterministic methodology that use multigroup cross-sections derived from ENDF/B-VII and ENDF/B-VII.1 nuclear data libraries. The MCNP6 model is essentially identical, to the extent possible, to the EVENT models with respect to the AGN material and geometric characteristics. The Monte Carlo KENO and MCNP calculation results in Wetzel [4] were also used to compare to the EVENT results to gain confidence in the EVENT AGN computation methodology. The testing and comparison studies were useful to determine the most efficient and accurate computation methodology to use with the AGN experimental analysis.

www.manaraa.com

4.2 AGN Reactor Configuration and Materials

This section summarizes the UNM AGN research reactor dimensional configuration as well as the material characteristics used to model the various regions of the reactor. Tables 1 and 2 provide the fuel plate and control element specifications, respectively. These specifications are used to calculate the atom densities for the AGN core (Table 5). Atom densities for the AGN non-fuel components are listed in Table 6, and the atom densities for the AGN control rods are provided in Table 7. As previously discussed, the AGN is a homogeneous thermal reactor containing 19.5% (±0.5%) enriched UO_2 blended with polyethylene and reflected by graphite with a total fissile (^{235}U) loading is 666.9 grams. The UNM AGN research reactor operates at a maximum power of 5 W thermal, although the maximum power level considered for the AGN experimental configurations was 4.06 W. The AGN fuel plates are each 25.6 cm (10.4 in.) in diameter. Figure 6 provides the specifications for the 9 fuel plates in the AGN core. There is a 1-cm (0.39 in.) voided section above fuel plate 204105. The active core height (region of the core containing fuel rods) is approximately 16 cm (6.30 in.), and the total core height is approximately 24 cm (9.5 in.).

www.manaraa.com

Table 5. Core Atom Densities

Fuel Plate Number	N(^{235}U) (at./bn-cm)	N(^{238}U) (at./bn-cm)	N(O) (at./bn-cm)	N(C) (at./bn-cm)	N(H) (at./bn-cm)
20497	1.4766E-04	6.0189E-04	1.4991E-03	3.8288E-02	7.6577E-02
20498	1.4800E-04	6.0326E-04	1.5025E-03	3.8286E-02	7.6571E-02
20499	1.3911E-04	5.6704E-04	1.4123E-03	3.8359E-02	7.6717E-02
204100	1.4093E-04	5.7447E-04	1.4308E-03	3.8344E-02	7.6687E-02
204101	1.4653E-04	5.9726E-04	1.4876E-03	3.8298E-02	7.6596E-02
204102	1.4667E-04	5.9784E-04	1.4890E-03	3.8297E-02	7.6593E-02
204103	1.4663E-04	5.9767E-04	1.4886E-03	3.8297E-02	7.6594E-02
204104	1.5559E-04	6.3420E-04	1.5796E-03	3.8223E-02	7.6447E-02
204105	1.5048E-04	6.1340E-04	1.5278E-03	3.8265E-02	7.6531E-02
Core Fuse	Not Modeled in EVENT				

Table 6. Non-Fuel Material Atom Densities

Reactor Region	Constituent(s)	Atom Density (at./bn-cm)
Control rod tubes, baffle, glory hole tube	^{27}Al	6.0307E-02
Graphite Reflector	^{12}C	8.7815E-02
Lead Shield	^{204}Pb	4.3847E-04
	^{206}Pb	7.5480E-03
	^{207}Pb	6.9216E-03
	^{208}Pb	1.6411E-02
Water Shield	^{1}H	6.6773E-02
	^{16}O	3.3387E-02
Steel	^{12}C	3.9215E-03
	^{54}Fe	4.8804E-03
	^{56}Fe	7.6612E-02
	^{57}Fe	1.7693E-03
	^{58}Fe	2.3546E-04
Air	^{14}N	4.0770E-05
	^{16}O	9.4879E-06

www.manaraa.com

4.3 Control Element Operational Specifications

As discussed in Section 2.2.2, reactivity control of the AGN is through the insertion or the removal of SR1, SR2, the CCR, and the FCR, which are all made of core fuel. The two safety rods have an active length in the core of approximately 16 cm (6.30 in.), have a total travel length of 24 cm (9.45 in.), and a total reactivity worth of approximately 1.25 percent δk/k per rod [8]. The insertion time into the core is 30 to 50 sec. for the full length. The scram removal time is approximately 200 msec. The coarse rod has the same active and total travel length as the safety rods and a total reactivity worth of approximately 1.25 percent δk/k. The insertion time for the coarse rod is 40 to 50 sec., and the scram removal time is approximately 200 msec. The safety and coarse rods are each magnetically coupled to a carriage so that each can be removed from the core without scramming the reactor. This capability is useful for rod drop experiments. The FCR also has a total travel length of 24 cm (9.45 in.) and an active length of 16 cm (6.30 in.) with a total reactivity worth of approximately 0.28 percent δk/k per rod. It can be inserted into the core at either high or low speeds [8]. The FCR can be inserted or removed from the core in 40 to 50 sec at high speed. At low speed, the insertion time takes about two times longer than at high speed. A scram with the AGN de-energizes the electromagnets on SR1, SR2 and the CCR so that they fall under the influence of gravity and the assistance of a compressed spring to a safe position. The FCR will not fall out of the core during a scram but will be

www.manaraa.com

driven out of the core when a scram signal is received. The hazards analysis for the AGN core states a $2 increase in reactivity cannot be terminated by the scram system of the AGN because the reactor dynamics happen too quickly (period is about 10 milliseconds) [49]. However, the scram system can terminate a transient from up to $1 of inserted reactivity. The atom densities for the control elements are summarized in Table 7.

Table 7. Control Element Atom Densities

Control Element	N(U235) (at./bn-cm)	N(U238) (at./bn-cm)	N(O) (at./bn-cm)	N(C) (at./bn-cm)	N(H) (at./bn-cm)
SR1	1.4630E-04	5.9635E-04	1.4853E-03	3.8068E-02	7.6135E-02
SR2	1.4630E-04	5.9635E-04	1.4853E-03	3.8068E-02	7.6135E-02
CCR	1.4630E-04	5.9635E-04	1.4853E-03	3.8068E-02	7.6135E-02
FCR	1.3833E-04	5.6386E-04	1.4044E-03	3.8146E-02	7.6291E-02

4.4 Background for AGN Experimental Analysis

Background information is provided to introduce some key topics before initiating discussion on the EVENT experimental analysis. The steady-state analysis requires the effective multiplication factor be computed for testing the EVENT code and multigroup cross sections. The time-dependent analysis requires the neutron population be calculated by EVENT as a function of time after an experimental transient occurs. The concept of reactivity and system reactivity parameters, e.g., prompt neutron lifetime, effective delayed neutron factor, etc., are introduced in this section for understanding the calculation methodology for the AGN experimental analysis. Lastly, two

www.manaraa.com

techniques are used to estimate the AGN effective delayed neutron fraction to provide confidence in the historical value, 0.0074. This work is performed because the effective delayed neutron fraction is crucial for converting the change in the effective multiplication factor results to system reactivity.

4.4.1 Effective Multiplication Factor

The time-independent neutron diffusion equation can be written as follows for a steady-state configuration [50]:

$$-\boldsymbol{\nabla} \cdot D\boldsymbol{\nabla}\phi + \Sigma_a \phi(\vec{\boldsymbol{r}}) = \nu\Sigma_f \phi(\vec{\boldsymbol{r}})$$

Equation 19

with the boundary condition $\phi(\vec{r}_s) = 0$, meaning the neutron flux at the outer radius, defined by vector $\vec{\boldsymbol{r}}$, vanishes at the boundary. Equation 19 has no general solution because it is rather unlikely that a reactor's core composition and geometrical characteristics combine in such a way to result in an exactly critical configuration, especially on a computer because of the precision involved with the computations. To obtain a solution for Equation 19, an arbitrary parameter, k, is introduced to enable the solution of this equation analytically. This arbitrary parameter can be introduced into the steady-state diffusion equation as shown in Equation 20 to determine a solution for a particular value of k:

$$-\boldsymbol{\nabla} \cdot D\boldsymbol{\nabla}\phi + \Sigma_a \phi(\vec{\boldsymbol{r}}) = \frac{1}{k}\nu\Sigma_f \phi(\vec{\boldsymbol{r}})$$

Equation 20

www.manaraa.com

Thus, a particular core compostion and geometrical configuration results in a solution with a unique value of *k*. If the value of *k* is not equal to unity, the core composition and size can be changed and the calculation is repeated. If the core composition and geometrical configuration in a reactor results in a *k* value of unity, the reactor size and composition represents a critical configuration. This arbitrary parameter, *k*, *or* k_{eff}, is known as the effective multiplication factor or eigenvalue for the reactor.

With respect to the AGN experimental configurations considered in this work, the reactor is in a subcritical, delayed critical or delayed supercritical state. The k_{eff} of a fissile system is a measure of the number of fission neutrons in one generation compared to the number of fission neutrons in the prior generation (Equation 21).

$$k_{eff} = \frac{\text{fission neutrons in a generation}}{\text{fission neutrons in the preceeding generation}}$$

Equation 21

The values of the effective multiplication factor has a physical meaning for nuclear reactors:

- $k_{eff} < 1$ – the system is subcritical, which results in an exponential neutron population reduction from generation to generation.
- $k_{eff} = 1$ – the system is critical or delayed critical, which represents a constant neutron population (steady state or time independent configuration).

www.manaraa.com

- $k_{eff} > 1$ – the system is supercritical, which represents a neutron population which is growing exponentially (time dependent configuration).

The AGN can achieve a delayed supercritical state only. The net reactivity available by loading all the control elements into the reactor core represents a maximum k_{eff} of 1.00185, which represents a supercritical system with delayed neutrons present. Delayed neutrons appear seconds to minutes after the prompt neutrons in the system based on the half life of the delayed neutron precursors present, i.e., fission products, which appear essentially instantaneously after a fission event (~10^{17} sec.). This allows for human control of the reactor by keeping neutron lifetime in the millisecond range. The AGN is not capable of a prompt supercritical excursion as configured, as it has been designed to be inherently safe. However, it is always possible to achieve more reactive configurations by inserting non-reactor fissile material via insertion of the material in the glory hole region of the core. These hypothetical configurations are beyond the scope of this work. The delayed critical window of a nuclear reactor is very small, as illustrated in Figure 17 (not to scale). This window occurs between a k_{eff} of 1.0 and β_{eff} (effective delayed neutron fraction), which is equal to 0.0074 for the AGN-201M reactor. The β_{eff} indicates that the AGN would be delayed supercritical based on the presence of delayed neutrons, which make up less than 1% (0.74%) of the total number of neutrons in the system.

www.manaraa.com

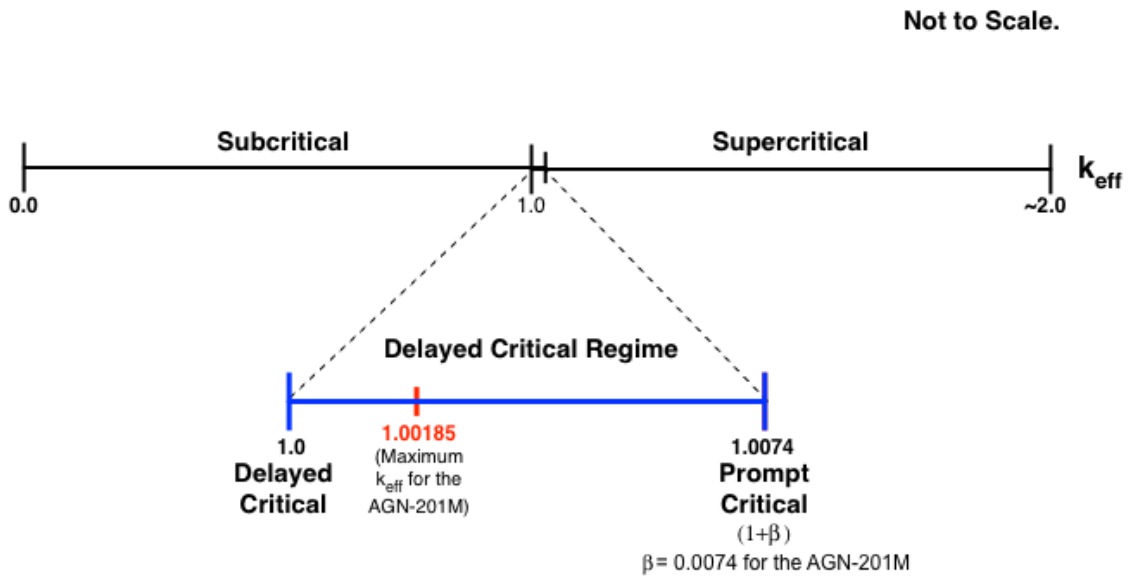

Figure 17. Illustration of the Delayed Critical Window

4.4.2 Definition of Reactivity

A critical nuclear reactor has an effective multiplication factor of unity, which indicates the neutron population is constant as a function of time. Deviations of the k_{eff} from unity, either positive or negative, is known as the excess multiplication factor, which is equal to

$$k_{ex} = k_{eff} - 1.$$

Equation 22

The ratio of the excess multiplication factor in Equation 22 to the effective multiplication factor describes the time dependent change in the effective multiplication factor from a critical configuration where the k_{eff} is unity. The reactivity, then, can be defined by:

www.manaraa.com

$$\rho = \frac{k_{eff} - 1}{k_{eff}}$$

Equation 23

Equation 23 indicates that the reactivity of a critical reactor would result in a reactivity of zero. The units of reactivity can be expressed in terms of the of the ratio of the reactivity to the effective delayed neutron fraction, β_{eff}, which is equal to 0.0074 for the AGN. Units of reactivity in dollars ($) are equal to ρ/β_{eff}. Units of reactivity in cents (¢) is defined as the ratio $\rho/(100*\beta_{eff})$. One dollar (1$) of reactivity is equal to prompt critical and indicates the reactor is critical based on only prompt neutrons in the core. The AGN is not designed to achieve a prompt supercritical state.

Effective multiplication factor calculations are performed to test the EVENT code in 2-D and 3-D configurations. The change in reactivity from two different k_{eff} values can be defined as follows:

$$\rho = \frac{k_{eff} - k_{eff}^{reference}}{k_{eff} \times k_{eff}^{reference}}$$

Equation 24

Of course, the reactivity in dollars can be computed by dividing Equation 24 by the β_{eff}, equal to 0.0074 for the AGN. Equation 24 is used primarily for calculating the reactivity worths corresponding to changes in the control element position in the AGN core.

www.manaraa.com

4.4.3 Point Kinetics Equations

Small adjustments in the reactivity of the reactor result in time-dependent behavior until a new steady-state configuration is achieved. Local perturbations in the angular neutron flux due to control rod movement in a reactor will spread quickly through the core [51]. This is due to the fact that the neutron mean free paths are significantly long and the neutron lifetimes in the core are quite short. Transients from control rod movement will perturb and readjust the flux within a very short period of time. If the k_{eff} of this perturbed configuration increases as a result of the transient, e.g., the FCR or the CCR is moved into the AGN core, the neutron flux level will increase as a function of time. Likewise, if the k_{eff} of the perturbed configuration decreases, e.g., the FCR or the CCR is moved out of the AGN core, the neutron flux level will decrease as a function of time. Time-dependent diffusion or transport theory can be used with significant effort to solve for the solution of the time-dependent neutron flux; however, the point kinetics equations can solve for the magnitude of the neutron flux changes with time. The point kinetics equations are a coupled pair of stiff non-linear differential equations used to predict the change in the average value of the neutron flux and to determine the effect of perturbations in the reactor core [51]. The point kinetics equations with six delayed neutron groups, with no extraneous sources present in the core, are

www.manaraa.com

$$\frac{dn(t)}{dt} = \frac{(\rho - \beta)}{\Lambda} n(t) + \sum_{i=1}^{6} \lambda_i \, C_i(t)$$

Equation 25

$$\frac{dC(t)}{dt} = \frac{\beta_i}{\Lambda} n(t) - \lambda_i C_i \quad (i = 1,2, \ldots ,6)$$

Equation 26

where

$n(t) =$ time dependent neutron population, power, etc.,

$C(t) =$ delayed neutron precursor concentration,

$\rho =$ core reactivity (unitless),

$\beta = \sum_i \beta_i =$ total fraction of fission neutrons which are delayed,

$\Lambda = \frac{1}{k} =$ mean neutron generation time between birth of neutron and subsequent absorption inducing fission,

$\lambda_i =$ decay constant (beta decay) of the *i*-th delayed neutron precursor group, and

$\beta_i =$ fraction of all fission neutrons (both prompt and delayed) emitted per fission that appear from *i*-th delayed neutron precursor group.

The solution to Equation 25 and 26 allow one to estimate the reactor power (neutron population) and delayed neutron precursor concentration as a function of time after a positive or negative change in reactivity occurs. Six delayed neutron groups are assumed (Table 24) for the AGN EVENT

www.manaraa.com

experimental transient analysis. However, EVENT time dependent scoping calculations were performed for a simple cylindrical unreflected LEU-polyethylene mixture, identical to the AGN core, with a cylindrical control rod to compare to the results of the numerical and analytical solution to the simplified point kinetics equations, assuming only one group of delayed neutrons (Appendix A). Assuming one group of delayed neutrons requires the determination of the effective delayed neutron yield fraction, β_i, (Equation 27) and averaged delayed neutron decay constant, λ, (Equation 28).

$$\beta = \sum_{i=1}^{6} \beta_i$$

Equation 27

$$\lambda = \langle \lambda \rangle = \left[\frac{1}{\beta} \sum_{i=1}^{6} \frac{\beta_i}{\lambda_i} \right]^{-1}$$

Equation 28

Using the delayed neutron data from Keepin [58] (Table 24), the effective yield fraction is 0.006524 and the averaged delayed neutron decay constant is 0.40775 for the AGN. The mean generation time, Λ, for the AGN is ~0.0001 seconds [8].

Using these definitions in the point kinetics equations for a single delayed neutron group results in the following simplified form of the point kinetics equations, which are valid for $t \geq 0$ [52].

www.manaraa.com

$$\frac{dn(t)}{dt} = \frac{(\rho - \beta)}{\Lambda} n(t) + \lambda C(t)$$

Equation 29

$$\frac{dC(t)}{dt} = \frac{\beta}{\Lambda} n(t) - \lambda C(t)$$

Equation 30

For the situation where t < 0, the reactor is assumed to be operating at a steady-state configuration, i.e., delayed critical, and the neutron population and the delayed neutron precursor concentration in the reactor is constant, i.e., unchanging with time. This implies $\frac{dn(t)}{dt} = \frac{dC(t)}{dt} = 0$ and the boundary conditions for Equations 29 and 30 are $n(0) = n_0$ and $C(0) = \frac{\beta}{\lambda\Lambda} n_0$. Equations 29 and 30 can be modified as follows seeking exponential solutions of the form $n(t) = n_0 e^{st}$ and $C(t) = C_0 e^{st}$ using Laplace Transforms where n_0, C_0, and s are determined in the solution to Equations 29 and 30. After the transformation, a series of algebraic equations are defined:

$$sn(s) = \frac{(\rho - \beta)}{\Lambda} n(s) + \lambda C(s)$$

Equation 31

$$sC(s) = \frac{\beta}{\Lambda} n(s) - \lambda C(s)$$

Equation 32

Equation 32 can be solved for C, in terms of n, and the result substituted into Equation 31 to obtain the following for $n(s)$:

www.manaraa.com

$$n(s) = \frac{n(s+\lambda) + \lambda C_0}{(s+\lambda)\left(s - \frac{\rho - \beta}{\Lambda}\right) - \frac{\beta\lambda}{\Lambda}}$$

Equation 33

The denominator of Equation 33 is set to zero to determine the poles of the expression. This is needed to determine the inverse transform to obtain a relationship with time dependence. The quadratic formula is now used to determine the roots of the denominator as follows:

$$s = \frac{-(\beta - \rho) + \lambda\Lambda}{2\Lambda}\left(1 \pm \sqrt{1 + \frac{4\lambda\rho\Lambda}{[(\beta - \rho) + \lambda\Lambda]^2}}\right)$$

Equation 34

A couple of simplifications can be made to Equation 34 to simplify the characteristic equation defining the roots for the Equation 33. The first simplification is based on the fact that $\lambda\Lambda \ll (\beta - \rho) \ll 1$. Thus, Equation 34 is simplified to assume the product of the averaged decay constant and the prompt neutron generation time is negligible. Further, another approximation is made, $\sqrt{1+\varepsilon} \approx 1 + \frac{\varepsilon}{2}$, when $\varepsilon \ll 1$. The transformed expression is now defined as follows:

$$n(s) = \frac{n(s+\lambda) + \lambda C_0}{(s - \omega_0)(s - \omega_1)} \approx \frac{n_0\left[\frac{\beta}{\beta - \rho}\right]}{s - \omega_0} - \frac{n_0\left[\frac{\rho}{\beta - \rho}\right]}{s - \omega_1}$$

Equation 35

www.manaraa.com

where $\omega_0 = \frac{-(\beta-\rho)}{\Lambda}$ and $\omega_1 = \frac{\lambda\rho}{(\beta-\rho)}$. Finally, the general solution to the point kinetics equations with one delayed neutron group has the following form:

$$n(t) = n_1 exp[\omega_0 t] + n_2 exp[\omega_1 t]$$

Equation 36

$$C(t) = C_1 exp[\omega_0 t] + C_2 exp[\omega_1 t]$$

Equation 37

and the final solution for both n(t) and C(t) from the general solution in Equation 36 and 37 is provided in Equation 38 and 39, respectively. These equations are known as the one delayed neutron group approximation.

$$n(t) = n_0 \left[\frac{\rho}{(\rho-\beta)} exp\left(\frac{\rho-\beta}{\Lambda} t\right) - \frac{\beta}{(\rho-\beta)} exp\left(-\frac{\lambda\rho}{\rho-\beta} t\right)\right]$$

Equation 38

$$c(t) = n_0 \left[\frac{\rho\beta}{(\rho-\beta)^2} exp\left(\frac{\rho-\beta}{\Lambda} t\right) + \frac{\beta}{\Lambda\lambda} exp\left(-\frac{\lambda\rho}{\rho-\beta} t\right)\right]$$

Equation 39

At $t = 0$, before the reactivity insertion to the critical reactor, the delayed neutron precursor concentration is equal to $C_0 = \frac{\beta n_0}{\Lambda\lambda} \approx 181 n_0$, for the characteristics of the AGN, i.e., thermal reactor, with the reactivity, ρ, equal to zero (representing a critical system). Thus, the population of delayed neutron precursors, hence the latent source of neutrons, is about 181 times greater than the neutron population in a critical reactor [50]. It is the large delayed neutron source in the reactor that controls the time dependent

www.manaraa.com

nature of the neutrons in the system under normal conditions and allows for human control of the system.

As previously discussed, the AGN is designed to operate in subcritical ($\rho < 0$), delayed critical ($\rho = 0$), and delayed supercritical ($0 < \rho < \beta$) reactivity regimes. Examining the value of $n(t)$ (Equation 38) for a subcritical system ($\rho < 0$), the prompt and delayed neutron terms, shown in Figure 18, have negative terms in the exponential that indicate $n(t)$ is declining as a function of time. For a reactor operating at a delayed critical condition ($\rho = 0$), in Equation 38, the prompt neutron term (Figure 18) is zero because the reactivity, ρ, is zero and the delayed neutron term reduces to unity when the reactivity, ρ, is zero and results in a constant delayed neutron population as a function of time, $n(t) = n_0$. For a delayed supercritical configuration ($0 < \rho < \beta$), the neutron population, $n(t)$, increases quickly as the reactivity increases from a subcritical or delayed critical condition to a delayed supercritical condition. If a step increase in reactivity results in a delayed supercritical condition, the prompt neutron term in Equation 38 dominates the neutron population for a short period of time because the delayed neutron population takes some time to react to an instantaneous reactivity perturbation. Once the short lived delayed neutron precursors start to generate neutrons, the delayed neutron term in Equation 38 will start to dominate and $n(t)$ will increase according to $n(t) \approx n_0 \left[\frac{\beta}{(\beta-\rho)} exp\left(\frac{\lambda\rho}{\beta-\rho} t\right)\right]$, where the reactor period is defined as $T = \frac{\rho-\beta}{\lambda\rho}$ (seconds) (Figure 19). The reactor period, i.e., time for the

www.manaraa.com

reactor power or neutron population to increase by a factor of *e*, is equal to the slope of the exponential term in Figure 19.

$$n(t) = n_0 \left[\frac{\rho}{(\rho - \beta)} exp\left(\frac{\rho - \beta}{\Lambda} t \right) - \frac{\beta}{(\rho - \beta)} exp\left(- \frac{\lambda \rho}{\rho - \beta} t \right) \right]$$

Prompt Neutron Term

Delayed Neutron Term

Figure 18. Neutron Population Components in Analytic Solution

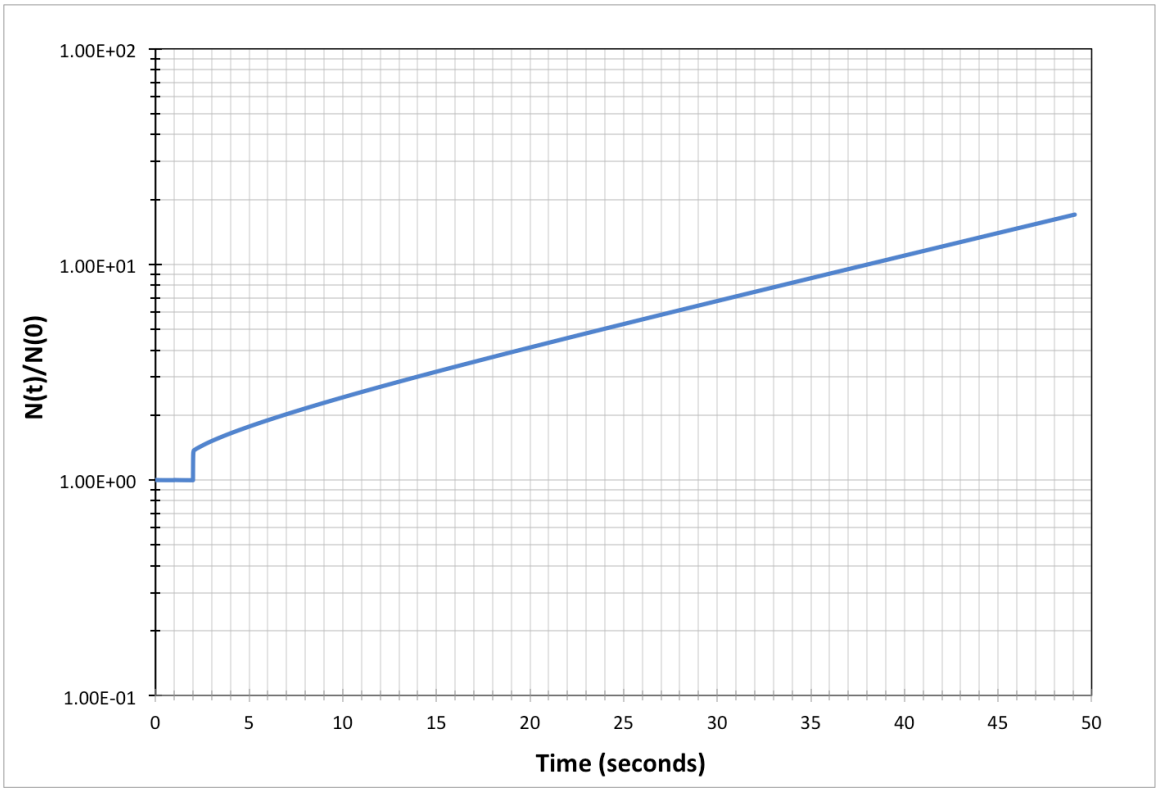

Figure 19. Neutron Population with a Step Increase in Reactivity

www.manaraa.com

4.4.4 Estimation of the Effective Delayed Neutron Fraction

The influence of delayed neutrons on the reactor dynamics can be understood through their impact on the reactor power change rate. In spite of the fact they constitute only a very small fraction of the total number of neutrons generated from fission, they play a dominant role in the fission chain reaction control [53]. The presence of delayed neutrons is fortunate because it allows for human control of a nuclear reactor, which would not be the case if only prompt neutrons, the neutrons born from the fission process, were present in the reactor. The effective delayed neutron fraction, β_{eff}, is an important parameter in reactor physics and an important estimate of the β_{eff} is essential for converting reactivity, measured in dollars, to an absolute reactivity and/or to an absolute k_{eff} [54]. Two methods for estimating the β_{eff} for the AGN for this work are presented in this section:

- The Prompt Method, and
- A Monte Carlo calculation using MCNP6.

The effective delayed neutron fraction is a complicated quantity to compute directly for a complex configuration such as a graphite moderated thermal reactor such as the UNM AGN. In general, the total neutron and delayed neutron production rates, P_t and P_d, respectively, in a reactor are defined as:

www.manaraa.com

$$P_t = \int \nu_t(E)\Sigma_f(\boldsymbol{r},E)\phi(\boldsymbol{r},E,\Omega)dEd\boldsymbol{r}d\Omega$$

Equation 40

$$P_d = \int \nu_d(E)\Sigma_f(\boldsymbol{r},E)\phi(\boldsymbol{r},E,\Omega)dEd\boldsymbol{r}d\Omega$$

Equation 41

Where $\boldsymbol{r}$, E, and Ω are the position, energy, and solid angle of the neutrons (total number of the neutrons is denoted with a t-subscript and delayed neutrons are denoted with a d-subscript), ν is the average number of neutrons released per fission, Σ_f is the macroscopic fission cross section, and ϕ is the neutron flux [53]. The ratio of the delayed neutron production rate (Equation 41) to the total neutron production rate (Equation 40) is equal to the fundamental delayed neutron fraction $\beta_0 = \frac{P_d}{P_t}$. However, this ratio has difficulty considering the effectiveness of the delayed neutrons in a time-dependent reactor with respect to their ability to induce additional fissions in the system. The effectiveness of generating fissions in a reactor is described in neutron transport theory by taking the product of the energy spectrum of the generated neutrons, $\chi(E')$, and the adjoint flux (function), $\psi(\boldsymbol{r},E',\Omega')$, where $\boldsymbol{r}$, E' and Ω' are the position (same neutron position as $\boldsymbol{r}$ in Equation 40 and 41), energy and solid angle of the neutrons generated by the fissions that were induced by the incident neutrons characterized by $\boldsymbol{r}$, E and Ω. Further, the adjoint function, ψ, is defined as the fundamental mode

www.manaraa.com

eigenfunction of the equation adjoint to the time-independent transport equation [53]. The adjoint function, $\psi(\boldsymbol{r}, E', \Omega')$, is needed because it accounts for the significance of a neutron with properties ***r,*** E' and Ω' for producing fission and is proportional to the asymptotic power level resulting from the introduction of a neutron in a critical system at zero power [56]. The term, $\chi(E')$, is needed because the energy with which the neutrons are born has an impact on their effectiveness with inducing fission. Thus, the effective adjoint-weighted neutron production rates for all neutrons, both prompt and delayed, $P_{t,eff}$, and delayed neutrons, $P_{d,eff}$ can be defined as [53]

$$P_{t,eff} = \int \psi(r, E', \Omega')\chi_t(E')\nu_t(E)\Sigma_f(\boldsymbol{r}, E)\phi(\boldsymbol{r}, E, \Omega)d\boldsymbol{r}dEd\Omega\mathrm{d}E'd\Omega'$$

Equation 42

$$P_{d,eff} = \int \psi(r, E', \Omega')\chi_d(E')\nu_d(E)\Sigma_f(\boldsymbol{r}, E)\phi(\boldsymbol{r}, E, \Omega)d\boldsymbol{r}dEd\Omega\mathrm{d}E'd\Omega'$$

Equation 43

Thus, the Keepin definition for the effective delayed neutron fraction, β_{eff}, can be defined by taking the ratio of Equation 42 and 43, $\beta_{eff} = \frac{P_{d,eff}}{P_{t,eff}}$. The value for P can be described as the neutron source in the reactor, i.e., total number of neutrons produced per unit time, whereas the value of P_{eff} is the total number of fissions produced in the reactor by the neutron source, P, in the reactor [53]. Finally, general, traditional, relationship for the effective delayed neutron fraction is written as follows [54]:

www.manaraa.com

$$\beta_{eff} = \frac{\sum_i \sum_m \int \psi \chi_{di}^m \upsilon_{di}^m \Sigma_f'^m \Phi' d\Omega' dE' d\Omega dE d\boldsymbol{r}}{\sum_m \int \psi \chi_t^m \upsilon_t^m \Sigma_f'^m \Phi' d\Omega' dE' d\Omega dE d\boldsymbol{r}}$$

Equation 44

where

$\Omega, E, and\ \boldsymbol{r}$ = angle, energy, and position, respectively,

m = mth isotope,

i = ith delayed neutron group,

$\Phi' = \Phi'(\boldsymbol{r}, \Omega', E')$ = angular flux,

$\psi = \psi(\boldsymbol{r}, \Omega, E)$ = angular adjoint flux,

$\Sigma_f'^m = \Sigma_f'^m(\boldsymbol{r}, E')$ = macroscopic fission cross section,

$\upsilon_t^m = \upsilon_t^m(\boldsymbol{r}, E')$ = average total number of neutrons released per fission,

$\upsilon_{di}^m = \upsilon_{di}^m(\boldsymbol{r}, E')$ = average total number of delayed neutrons for the ith delayed neutron group released per fission,

$\chi_{di}^m = \chi_{di}^m(\boldsymbol{r}, E')$ = normalized spectrum for the ith delayed neutron group, and

$\chi_t^m = \chi_t^m(\boldsymbol{r}, E')$ = normalized total fission neutron spectrum.

4.4.4.1 Prompt Method to Estimate β_{eff}

An approximation known as the Prompt Method can be used to estimate the value of the β_{eff} for a fissile system such as the AGN. Reference [55] is used as the source of the derivation of the approximation. The integral in Equation 42 can be denoted as $\langle \chi_t \nu_t \rangle$ and the integral in Equation 43 as $\langle \chi_d \nu_d \rangle$. The ratio of these expressions, β_{eff}, can be rewritten as follows in

www.manaraa.com

terms of the total neutron production rate and the prompt neutron production rate (denoted with a p-subscript), making use of the fact that integrals are linear and also that $\nu_p = \nu_t - \nu_d$,

$$\beta_{eff} = \frac{\langle \chi_d \nu_d \rangle}{\langle \chi_t \nu_t \rangle} = \frac{\langle \chi_t \nu_t - \chi_d \nu_d \rangle}{\langle \chi_t \nu_t \rangle} = \frac{\langle \chi_t \nu_p - (\chi_d - \chi_t)\nu_d \rangle}{\langle \chi_t \nu_t \rangle} \cong 1 - \frac{\langle \chi_p \nu_p \rangle}{\langle \chi_t \nu_t \rangle}$$

Equation 45

To complete the approximation and eliminate the integrals from Equation 45, Reference [55] states that the term $(\chi_d - \chi_t)\nu_d$ in Equation 45 is two orders of magnitude smaller than the $\chi_t \nu_p$ term due to ν_d being two orders of magnitude smaller than ν_p. Also, for the same reason, the shape of χ is almost equal to the shape of χ_p. By applying these approximations to Equation 45, the following simplification can be made

$$\frac{\langle \chi_p \nu_p \rangle}{\langle \chi_t \nu_t \rangle} = \frac{k_p}{k_t}$$

Equation 46

Substituting the ratio of the effective multiplication factor due to prompt fissions only to the effective multiplication factor due to both prompt and delayed neutrons from Equation 46 into Equation 45 results in an estimate of the β_{eff}:

$$\beta_{eff} \cong 1 - \frac{k_p}{k_t}$$

Equation 47

www.manaraa.com

The MCNP6 Monte-Carlo code [6] was used to calculate values of the k_{eff} for only prompt neutrons, k_p, and for both prompt and delayed neutrons, k_t. The MCNP6 input file created for the AGN experimental analysis for this work was used as a starting point to use the Prompt Method to estimate the β_{eff}. Two input files were required, one for calculating the k_t and another to calculate k_p. The calculation to determine k_t is the default calculation in MCNP6 and utilizes cross section data for the prompt fission spectrum, χ, and the number of neutrons released from fission, ν, for both prompt and delayed neutrons. The calculation to determine k_p involves only utilizing prompt neutron cross section data for χ_p and ν_p. To utilize only prompt neutron data in the MCNP6 calculation, the "TOTNU" card is used with the the "NO" option specified. This will perform the Monte Carlo calculation while ignoring delayed neutron data. The MCNP6 calculations were performed with up to 50 million neutron histories executed, which provided acceptable statistics for a good estimation of the β_{eff}. The calculation results for the Prompt Method for estimating β_{eff} are provided in Table 8. The results show good agreement between the Prompt Method results and the known value of the β_{eff} for the UNM AGN, 0.0074.

www.manaraa.com

Table 8. Prompt Method Calculation Results

Total Number of MCNP6 Neutron Histories	(Prompt and Delayed Neutrons)		(Prompt Neutrons Only)		k_p/k_t	$\beta_{eff} = 1-(k_p/k_t)$
	k_t	σ	k_p	σ		
5.00E+06	1.02035	0.00035	1.01188	0.00034	0.99170	0.00830
6.00E+06	1.02011	0.00032	1.01183	0.00031	0.99188	0.00812
7.00E+06	1.01999	0.00029	1.0119	0.00029	0.99207	0.00793
8.00E+06	1.01996	0.00027	1.01194	0.00027	0.99214	0.00786
9.00E+06	1.01991	0.00026	1.01187	0.00026	0.99212	0.00788
1.20E+07	1.01976	0.00022	1.01212	0.00022	0.99251	0.00749
2.00E+07	1.01945	0.00017	1.01215	0.00017	0.99284	0.00716
3.00E+07	1.01946	0.00014	1.01217	0.00014	0.99285	0.00715
4.00E+07	1.01954	0.00012	1.01214	0.00012	0.99274	0.00726
5.00E+07	1.01961	0.00011	1.01212	0.00011	0.99265	0.00735

4.4.4.2 MCNP6 Calculation to Estimate β_{eff}

For comparison with the Prompt Method, the β_{eff} was estimated directly using MCNP6 and the 3-D AGN model considered for the Prompt Method as well. This is specified in the MCNP6 AGN input file by utilizing the "KOPTS" card with the "KINETICS" and "PRECURSOR" options set to "YES". This will initiate the MCNP6 subroutines dedicated to tracking both prompt and delayed neutrons as part of the Monte Carlo simulation and will calculate the adjoint-weighted point reactor physics parameters [56]. Using these options will also calculate the value for Rossi-alpha, α, the neutron generation time, Λ, effective delayed neutron fraction, β, average delayed neutron emission energy, and delayed neutron decay constants, λ_i, by precursor group, i.

Expanding on the discussion from Section 0, the Monte Carlo simulation attempts to realistically duplicate physical processes. A neutron introduced

www.manaraa.com

into a zero power critical reactor with a particular position, energy, and solid angle will encounter fissile material and induce fissions and generate prompt and delayed neutron precursors. The prompt and delayed neutrons generated are then tracked and will induce further prompt and delayed neutrons and then this process is repeated. For the critical system, on average one neutron is produced for every neutron that leaks out of the system or is absorbed by reactor materials without producing a fission. In a Monte Carlo code, the number of fission neutrons generated in this way will approach a limit, which is given by the iterated fission probability that is proportional to the adjoint function. In the Monte Carlo process, the prompt and delayed neutrons at the start of this process are tracked and the number of induced fissions is tallied by the code package. The tallied information is used to estimate the β_{eff}. The results of the MCNP6 calculation for 50 million neutron histories using the 3-D AGN model is shown in Figure 20 and a comparison of the β_{eff} results from the Prompt Method and the MCNP6 calculations are shown in Figure 21 along with the known value of the β_{eff} for the AGN at UNM. The MCNP6 results also show good agreement with both the known value of β_{eff} for the UNM AGN and the Prompt Method.

www.manaraa.com

the estimated adjoint-weighted point reactor kinetics parameters are:

	estimate	std. dev.	
gen. time	73.79960	0.53274	(usec)
rossi-alpha	-1.00581E-04	2.92444E-06	(/usec)
beta-eff	0.00742	0.00021	

effective delayed neutron fraction, average emission energy, and decay constants by precursor group:

precursor	beta-eff	std. dev.	energy (MeV)	std. dev.	lambda-i (/sec)	std. dev.	half-life (sec)
1	0.00027	0.00004	0.40428	0.00337	0.01334	0.00000	51.97350
2	0.00134	0.00009	0.46984	0.00153	0.03273	0.00000	21.17548
3	0.00138	0.00009	0.44265	0.00151	0.12079	0.00000	5.73831
4	0.00278	0.00013	0.55568	0.00135	0.30291	0.00001	2.28830
5	0.00115	0.00008	0.51750	0.00223	0.85005	0.00003	0.81542
6	0.00049	0.00005	0.54152	0.00377	2.85483	0.00014	0.24280

Figure 20. MCNP6 Kinetic Parameter Results

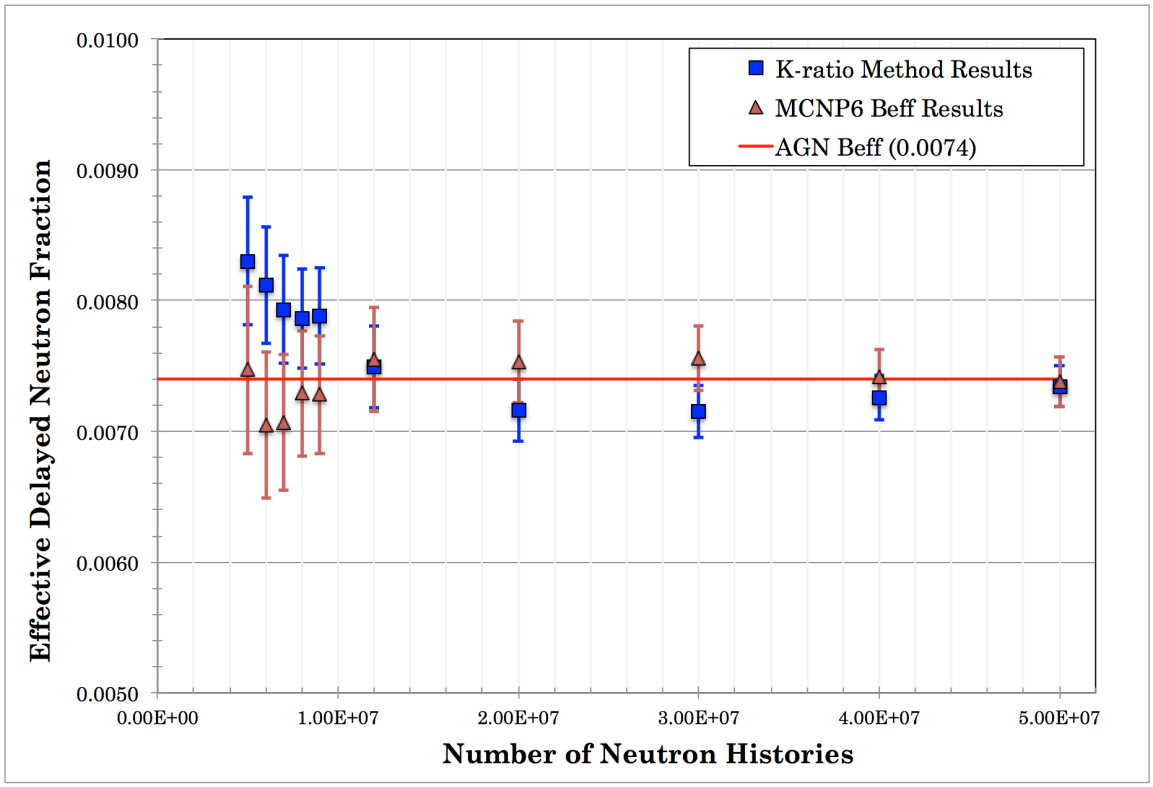

Figure 21. MCNP6 and Prompt Method β_{eff} Results

www.manaraa.com

4.5 EVENT Model Descriptions

4.5.1 MCNP6 AGN Model

An MCNP6 AGN model was developed, based on a similar model by Wetzel [4], to compare to the EVENT 3-D models generated to support this work. The MCNP6 and EVENT 3-D models are nearly identical geometrically and have identical material specifications, i.e., atom densities. The MCNP6 calculations utilized continuous energy neutron cross sections, based on the ENDF/B-VII library.

The MCNP6 AGN model considers significant detail in the core region of the AGN reactor. Each of the core fuel plates is explicitly modeled and each of the control elements, SR1, SR2, CCR and FCR, including the aluminum control rod tubes, is modeled to consider the reactivity worth of the control elements as a function of position in the core. This is also a precursor to the experimental verifications for both the steady-state and time-dependent calculations. Figure 22 shows the AGN MCNP6 model along with the control rods detail in the cutaway view. The MCNP6 results are shown in Table 9 along with the control rod reactivity differential and integral worth results. The MCNP6 mean k_{eff} results for this work and for the Wetzel calculations [4] with the rods fully inserted into the core compare very well, 1.0202 ± 0.0007 and 1.0217 ± 0.0007, respectively. However, each result over-predicts the k_{eff} of the actual AGN with the rods fully inserted into the core, 1.00185. The

www.manaraa.com

cumulative reactivity worth of all the control rods in the core is \$5.43 using a value of β_{eff} of 0.0074.

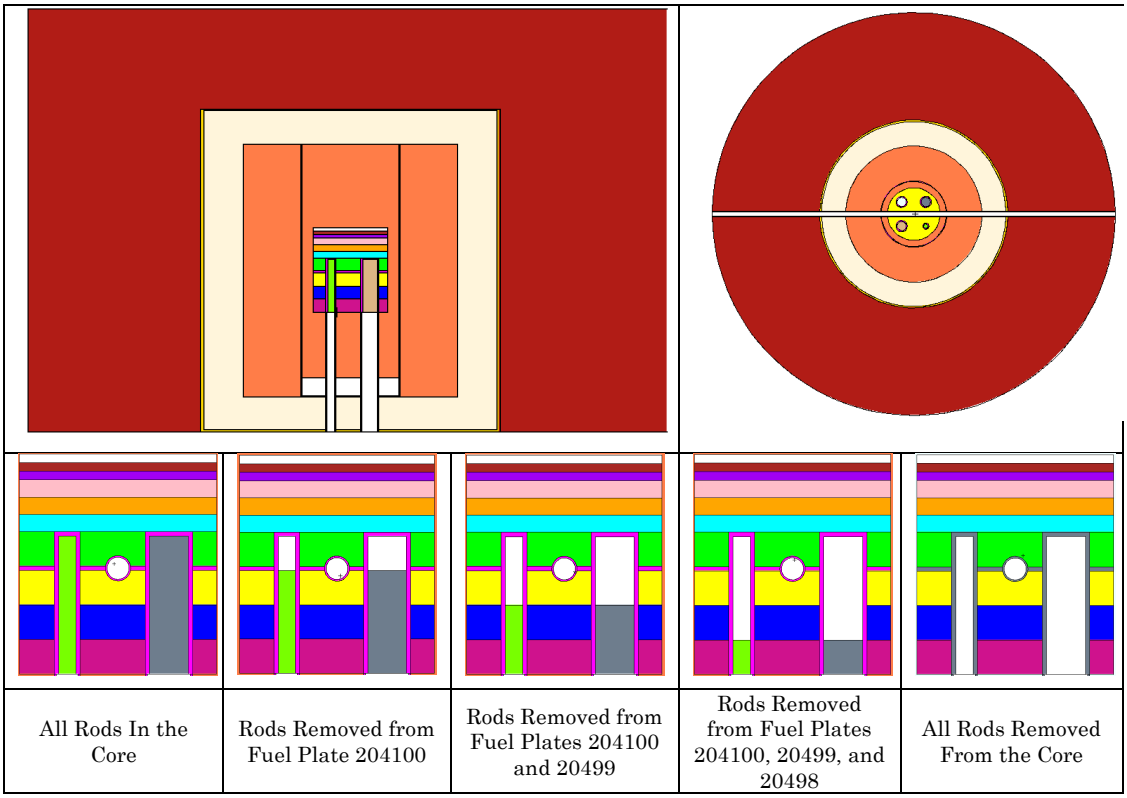

Figure 22. MCNP6 3-D Model for EVENT Model Verification

Table 9. MCNP6 3-D Model Results

Case	Rod Height (cm)	MCNP6 k_{eff} Results (ENDF/B-VII Continuous Energy Cross Sections)	Cumulative Worth
Rods_All_0	0	0.98001 ± 0.0007 0.98380 ± 0.0006*	\$0.00
Rods_All_1a	2	0.98419 ± 0.0007	\$0.56
Rods_All_1b	4	0.98891 ± 0.0007	\$1.20
Rods_All_2a	6	0.99484 ± 0.0006	\$2.00
Rods_All_2b	8	0.99821 ± 0.0007	\$2.46
Rods_All_3a	10	1.00379 ± 0.0007	\$3.20
Rods_All_3b	12	1.00831 ± 0.0007	\$3.83
Rods_All_4a	14	1.01300 ± 0.0007	\$4.46
Rods_All_4b	16	1.02021 ± 0.0007 1.0217 ± 0.0007*	\$5.43

* Results from Wetzel [4]

www.manaraa.com

4.5.2 Detailed EVENT NETGEN Model

A 3-D EVENT model was created for this work using an automatic mesh generation tool called NETGEN [38] that is called by the GEM preprocessor to create the problem geometry and the finite element mesh needed for EVENT. NETGEN can be used in GEM to create and mesh either 2-D or 3-D geometries. Three dimensional geometrical configurations can be specified by constructive solid geometry defined by Eulerian operations, e.g., unions, intersections and complements, from primitives. Primitives used to create the AGN 3-D model included planes, cylinders, and spheres. Thus, very complex arrangements and finite element meshes can be created.

Using NETGEN geometrical options, a simplified 3-D model of the AGN was constructed. The thin regions such as the aluminum shell in the graphite reflector and the carbon steel tank wall between the lead and water shielding were ignored because of their negligible thickness and small thermal neutron flux in these AGN regions. The aluminum control rod tubes and control rod fuel material were homogenized to reduce the model detail. The glory hole tube region was assumed to be aluminum at a much lower effective density. The glory hole and aluminum glory hole tube are arranged vertically to allow for comparison to previous analyses in this work.

This model is defined with the same axial and radial dimensions assumed for the 2-D (XY and RZ) configurations, described in Appendix A. The atom densities for this model are provided in Table 10 for homogenized core regions

www.manaraa.com

(fuel plates 204101-204105) and the homogenized control rods and rod tubes. The atom densities for non-fuel components are provided in Table 6. Again, some model simplifications were made by omitting the aluminum shell separating the inner and outer graphite reflectors and the steel tank shell between the lead and water regions to prevent finite element regions from overlapping with one another. These regions are thin compared to the adjacent regions and the Wetzel report [4] shows the system k_{eff} is not sensitive to the aluminum or carbon steel in these regions. This was also shown in the 2-D EVENT testing analysis in Appendix A. The simplification efforts were made because of the complexity of the 3-D configuration in EVENT.

Table 10. Atom Densities for the Detailed EVENT NETGEN Model

Feature	N(^{235}U) (at./bn-cm)	N(^{238}U) (at./bn-cm)	N(O) (at./bn-cm)	N(C) (at./bn-cm)	N(H) (at./bn-cm)	N(Al) (at./bn-cm)
Core	1.45181-04	5.9178E-04	1.4739E-03	3.8309E-02	7.6618E-02	–
Control Rods	1.1703E-04	4.7705E-04	1.1882E-03	2.5483E-02	5.0967E-02	1.9936E-02

Because of the model complexity, 2-group neutron cross sections, based on the ENDF/B-VII.1 library, were used for these calculations. Vacuum boundary conditions were assumed at the top, bottom and sides of the reactor model. The control rods (SR1, SR2, CCR and FCR) rods were explicitly considered in the model defined as 2 cm axial segments through the four bottom AGN fuel plates and lower portion of the graphite reflector. The

www.manaraa.com

calculations assume the control rod fuel material for each of the rods (SR1, SR2, CCR and FCR) are added to the core in 2 cm increments starting with the rods in a fully-removed position, defined as the top of the fuel rods located at the bottom of the core. This approach is the same configuration considered in the detailed EVENT RZ model and the KENO-VI 3-D model. Figure 23 illustrates a slice of the detailed EVENT NETGEN model geometry showing the vertical glory hole and Figure 24 illustrates a slice of the model geometry showing the core and control element details. The finite element mesh is also illustrated. The model was designed to consider movement of all of the control rods either simultaneously or individually. The control rod positions for the differential calculations are summarized in Figure 25. Differential and integral worth control rod calculations were performed for this study. As before, the integral rod worth calculations were used to compare to the stated worth values from Wetzel [4] and the MCNP6 model. The k_{eff} was calculated for each of these rod positions and the change in reactivity was calculated. The calculated reactivity worth of the 2-cm rod segment was calculated along with the cumulative differential rod worth until the rods were completely inserted into the core. The total reactivity worth (integral worth) being compared is then the total reactivity added to the reactor by inserting the control rods starting from the bottom of the core (~8 cm inserted) and ending at the top of the control rod tube (~24 cm inserted), which is the distance of the active length of the control element. In reality, the AGN operations

www.manaraa.com

manual [8] indicates the FCR is worth approximately 8¢ of reactivity and the CCR and each of the two safety rods, SR1 and SR2, are worth approximately 28¢ of reactivity when located at the bottom of the core. The detailed EVENT NETGEN model results are provided in Table 11. The k_{eff} results show the detailed EVENT NETGEN model is about 2% less than the Wetzel results, probably due to the complexity of the model and the P_N order assumed for the calculations P_{11}. The asymptotic k_{eff} result is obtained with a P_{13} case but the P_9 result is about 99.7% of the converged answer and takes a fifth of the total runtime of the P_{13} calculation. The total integral control element worth for the detailed EVENT NETGEN model is about \$4.79 of reactivity (δk_{eff} of ~0.03546). The mean k_{eff} of the core with the top of the control elements at the bottom of the core is approximately 0.964 and approximately 0.999 with the control elements fully inserted into the core. The Wetzel results from Table 11 indicate the total integral control element worth for the KENO results is about \$5.12 of reactivity (δk_{eff} of ~0.0379), assuming the mean k_{eff} of the core with the top of the control elements at the bottom of the core is approximately 0.9838 and approximately 1.0217 with the control elements fully inserted into the core. The results in Table 11 also provide data from AGN rod worth data [8] to compare to the EVENT results.

www.manaraa.com

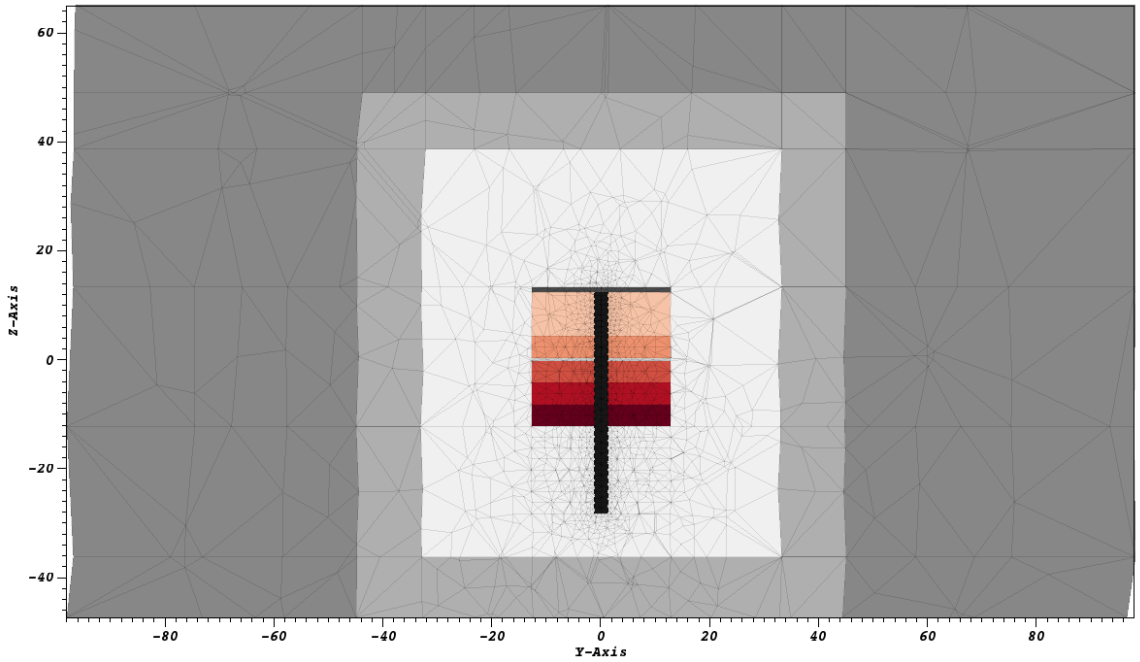

Figure 23. 3-D EVENT NETGEN Model with Vertical Glory Hole

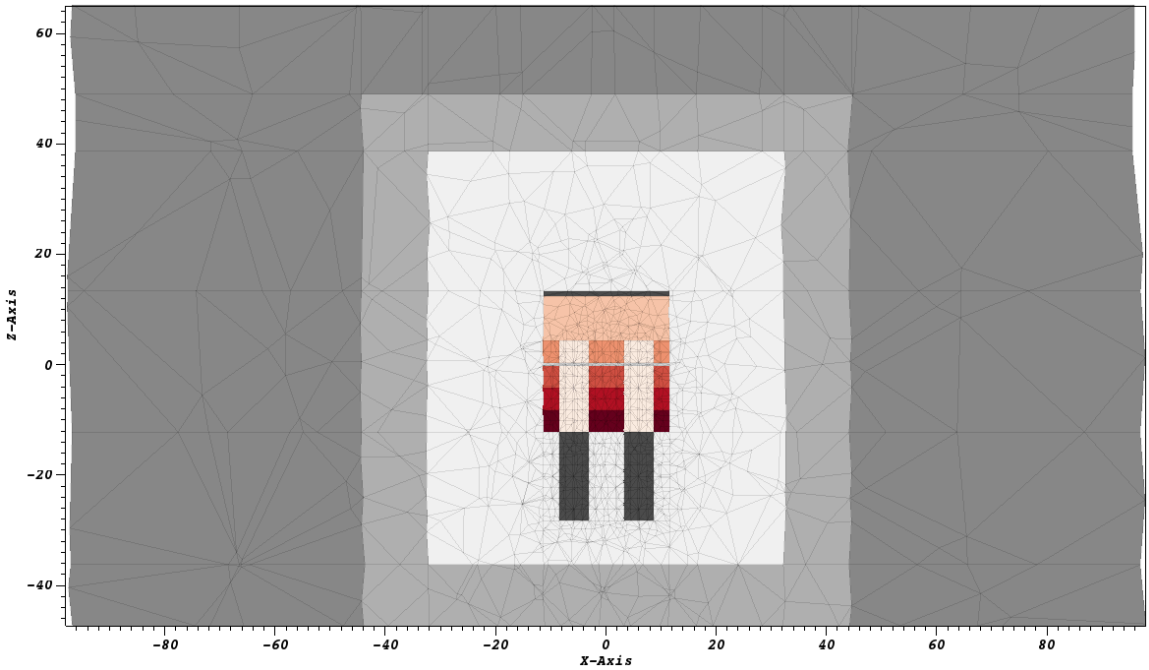

Figure 24. 3-D EVENT NETGEN Model Showing Control Elements

www.manaraa.com

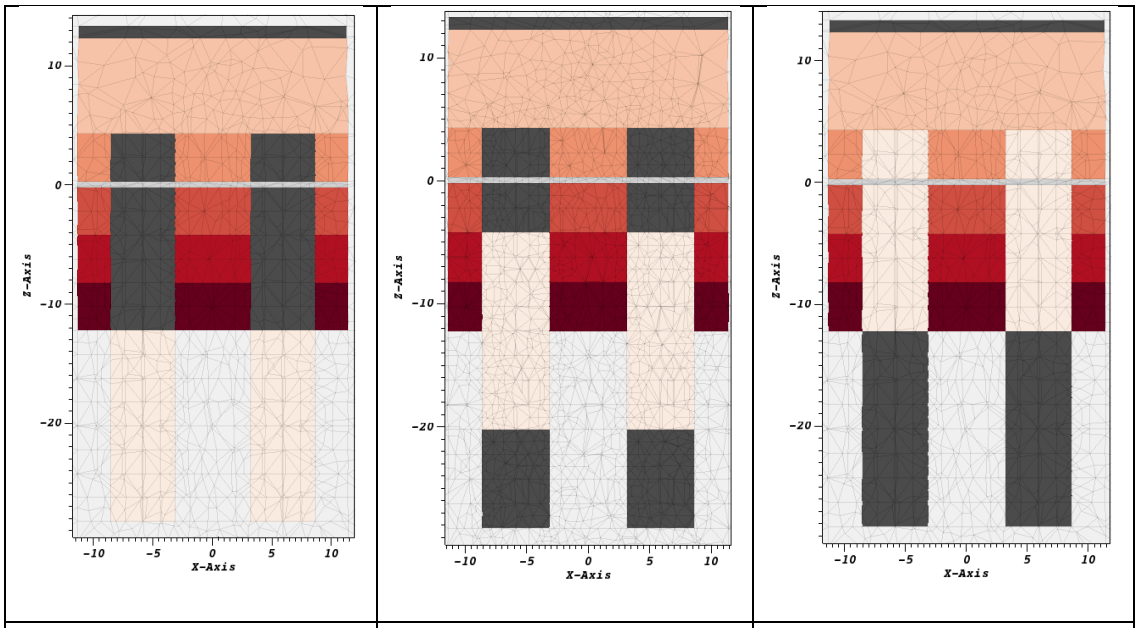

Rods_All_0 (Rods 0% Inserted)	Rods_All_2b (Rods 50% Inserted)	Rods_All_4b (Rods 100% Inserted)

Figure 25. Core Region Illustration of NETGEN Control Rod Position

Table 11. Detailed EVENT NETGEN Model Results

Case	Rod Height (cm)	EVENT NETGEN Model k_{eff} Results	Cumulative Worth	AGN Rod Worth Data [8] ($)
Rods_All_0	0	0.96375 0.9838 ± 0.0006*	–	0.92
Rods_All_1a	2	0.97094	$0.97	1.38
Rods_All_1b	4	0.97535	$1.57	1.84
Rods_All_2a	6	0.97923	$2.09	2.42
Rods_All_2b	8	0.98298	$2.60	3.00
Rods_All_3a	10	0.98662	$3.09	3.58
Rods_All_3b	12	0.99098	$3.68	4.19
Rods_All_4a	14	0.99557	$4.30	4.68
Rods_All_4b	16	0.99921 1.0217 ± 0.0007*	$4.79	5.33

* Results from Wetzel [4]

www.manaraa.com

4.5.3 Simplified EVENT NETGEN Model

Based on scoping studies, the detailed EVENT NETGEN model tested in Section 4.5.2 was simplified to enhance its efficiency for use with the delayed critical and transient experimental analysis. The two safety rods, SR1 and SR2, core were homogenized into the core to decrease the model complexity. This is a reasonable simplification because both safety rods were completely inserted during reactor startup operations and were not moved during the AGN experiments that support this work. The FCR and CCR are present in the model because they are moved during AGN operations to achieve a delayed critical state and to add or remove reactivity from the AGN core. The void regions in the FCR and CCR control elements were removed from the model to minimize computational issues with EVENT considering regions of very low material density, such as air, and the control rod tube under the AGN core in the graphite reflector region was removed from the model, as scoping studies indicated the regions had little impact on the k_{eff} results. The atom densities for the core and the FCR and CCR are summarized in Table 12. The atom densities for the other core constituents are provided in Table 6.

Table 12. Atom Densities for the Simplified EVENT RZ Model

Feature	N(^{235}U) (at./bn-cm)	N(^{238}U) (at./bn-cm)	N(O) (at./bn-cm)	N(C) (at./bn-cm)	N(H) (at./bn-cm)	N(Al) (at./bn-cm)
Core	1.3325E-04	5.4316E-04	1.3528E-03	3.8138E-02	7.6277E-02	2.5291E-03
Control Rods	1.4630E-04	5.9635E-04	1.4853E-03	3.8068E-02	7.6135E-02	–

www.manaraa.com

To approximate fuel element movement in the CCR and FCR, the CCR and FCR tube was modeled as a mixture of fuel and air and the volume fraction of each was changed to represent the distance the fuel was inserted into the core during operations. The volume fraction of an inserted control element is simply defined as a mixture of air and fuel. This simplification is significant because it eliminates the geometrical constructs required to represent the height of the rods in the core. Also, this simplification makes it much easier to make very fine changes in core reactivity, which is a required trait for the time dependent experimental analysis. Scoping calculations confirmed this approach was much more efficient than attempting to model variations in the CCR and FCR heights in the control rod tube. Numerous other enhancements were made to improve the finite element mesh efficiency and the geometrical representations in the model. The model simplification was so significant compared to the more complex NETGEN model considered earlier that a horizontal glory hole could be represented in the model. This allows the model to be used for AGN flux analysis as well because AGN experimental measurements taken in the glory hole region are analyzed in this work. The simplified EVENT NETGEN is illustrated in Figure 26 (X-Y slice) and Figure 27 (Y-Z slice). The k_{eff}, differential worth, and integral worth results for the P_7 EVENT cases are shown in Table 13. The k_{eff} results for the case with the rods fully inserted into the core are slightly greater for the simplified EVENT NETGEN model than for the detailed EVENT NETGEN

www.manaraa.com

model, 0.99921 compared to 1.00139, respectively. The total integral control element worth for the simplified EVENT NETGEN model is about \$2.68 of reactivity (δk_{eff} of ~0.01979). The total rod worth of the FCR is equal to the difference between the reactivity worth at full rod insertion, \$0.38, and the reactivity worth at 8 cm insertation (rod height is located at the bottom of the core), \$0.08 according to the AGN FCR calibration curve [8]. Similarly, the total rod worth of the CCR is equal to the difference between the reactivity worth at full rod insertion, \$1.65, and the reactivity worth at 8 cm insertation, \$0.28 according to the AGN CCR calibration curve [8]. The EVENT results result in an FCR worth of \$0.55 and a CCR worth of \$2.23. The sum of the FCR and CCR rod worths are \$2.68 for the EVENT results are greater than the rod worth values for the AGN FCR and CCR; however, the simplified EVENT NETGEN model only needs to accurately represent changes in reactivity rather than actual worth values based on specific rod positions. The results of this analysis indicate sufficient reactivity worth with the FCR and CCR in the model to consider rod drop configurations with the CCR. Thus, the simplified EVENT NETGEN model will be used for the AGN experimental transient analysis.

www.manaraa.com

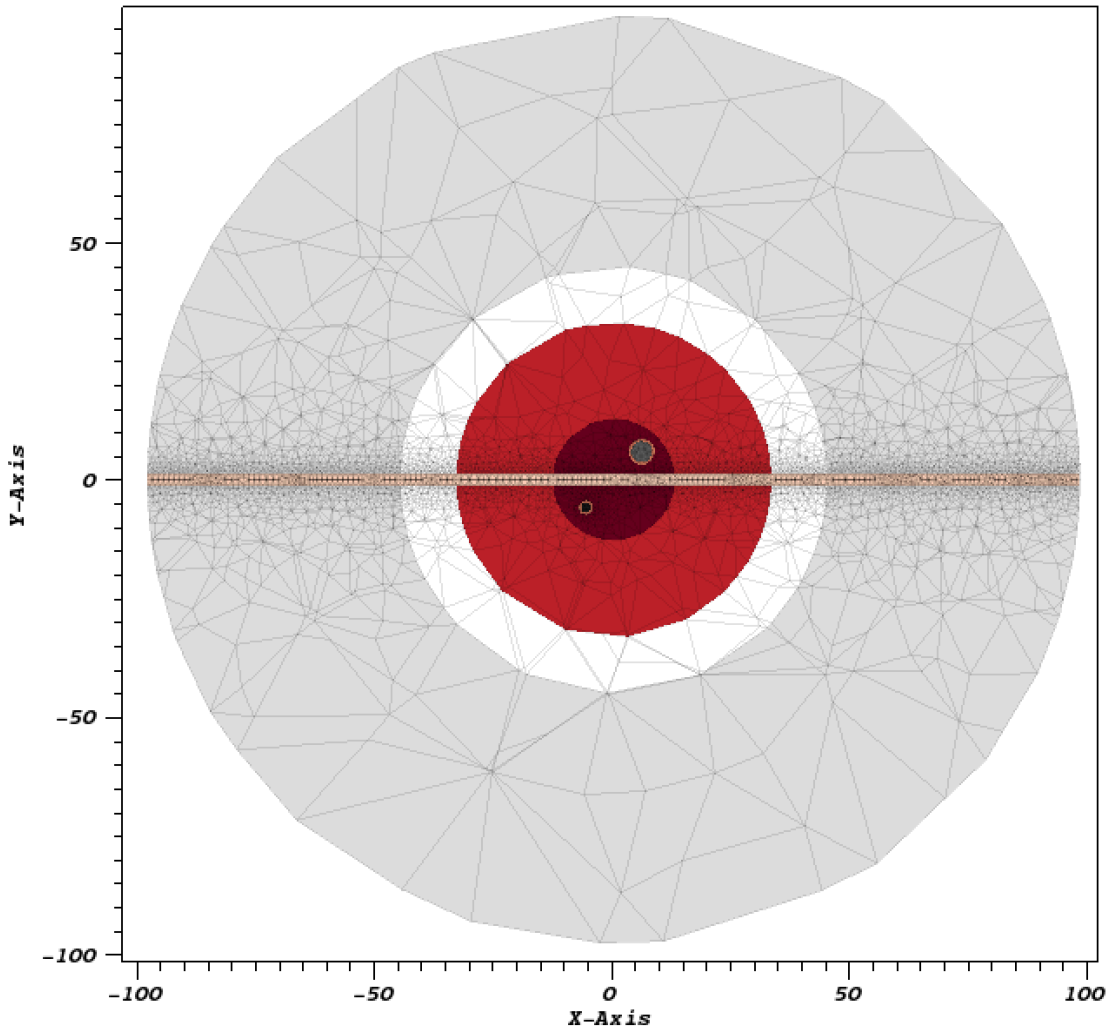

Figure 26. Simplified EVENT NETGEN Model Configuration (XY)

www.manaraa.com

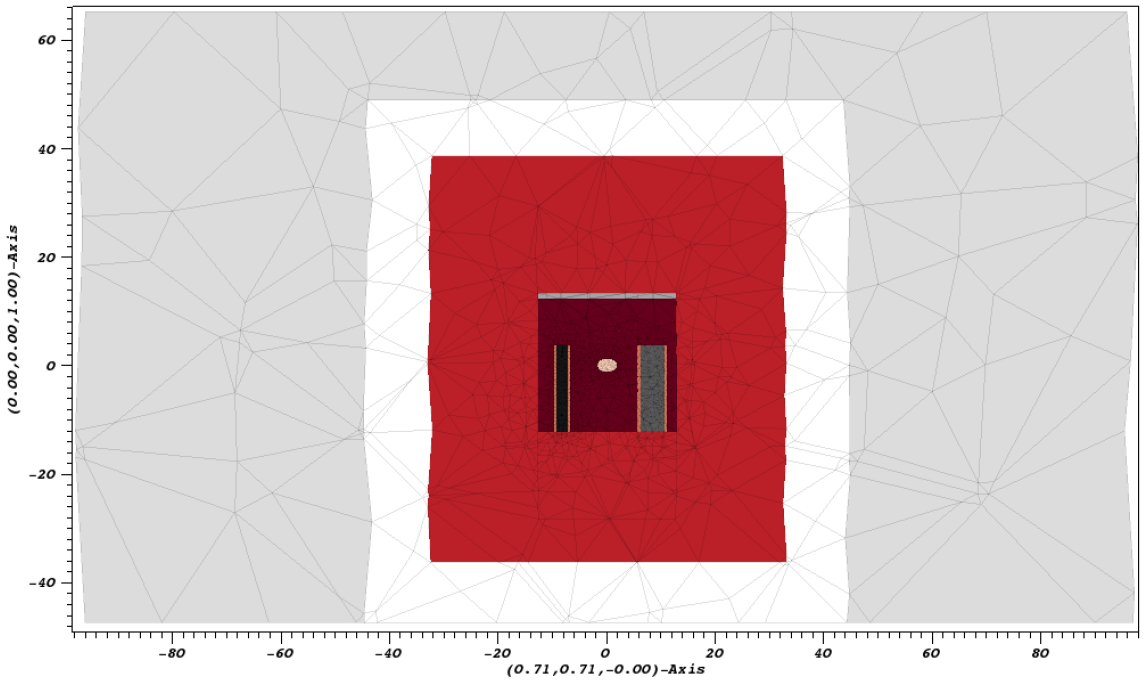

Figure 27. Simplified EVENT NETGEN Model Configuration (YZ)

Table 13. Simplified EVENT NETGEN Model Rod Worth Results

Case	FCR Fuel Volume Fraction	CCR Fuel Volume Fraction	k_{eff}	Cumulative Worth
NG_Rods_HGH0a	0.00	0.00	0.98160	$0.00
NG_Rods_HGH1a	0.25	0.00	0.98337	$0.25
NG_Rods_HGH2a	0.50	0.00	0.98417	$0.36
NG_Rods_HGH3a	0.75	0.00	0.98489	$0.46
NG_Rods_HGH4a	1.00	0.00	0.98556	$0.55
NG_Rods_HGH0b	0.00	0.00	0.98160	$0.00
NG_Rods_HGH1b	0.00	0.25	0.98805	$0.90
NG_Rods_HGH2b	0.00	0.50	0.99165	$1.39
NG_Rods_HGH3b	0.00	0.75	0.99479	$1.83
NG_Rods_HGH4b	0.00	1.00	0.99778	$2.23
NG_Rods_HGH_4ab	1.00	1.00	1.00139	$2.68

www.manaraa.com

4.5.4 Detailed EVENT RZ Model

A detailed EVENT RZ model for the AGN was created to gain experience using the EVENT code package and to compare to the MCNP6 and Wetzel results. Further, the broad multigroup cross sections required additional testing prior to performing AGN experimental analysis. The EVENT RZ model is assembled using a 2-D rectilinear grid to define the core material regions. These grids were refined to define the finite element mesh for the problem. The RZ geometry is ideal to approximate the cylindrical AGN reactor geometry and axial heights of the various cylindrical regions.

The detailed EVENT RZ model is used to calculate the system k_{eff} and reactivity worth of an approximate, annular representation of the AGN control rods. The AGN glory hole and glory hole tube are modeled as air and aluminum regions, respectively, inside the AGN core. The glory hole is oriented vertically instead of horizontally through the reactor to consider its presence in this model. The detailed EVENT RZ model finite element mesh is defined to be consistent with the mean free path for thermal neutrons in the various material regions of the reactor model. The finite element mesh and material regions are defined in Figure 28. The model geometry is defined to be consistent with the KENO VI and MCNP5 models in the Wetzel study [4] and the detailed NETGEN EVENT model. A low density oxygen gas in the center of the glory hole tube was modeled because the nitrogren component in air was not considered when the case-dependent multigroup cross sections

www.manaraa.com

were generated. The aluminum control rod tubes in the first four bottom fuel plates were ignored to simplify the EVENT geometry. The SCALE ENDF/B-VII.1 2-group multigroup cross-section library was used for the P_{11} calculations. The atom densities for the various materials for the RZ model are listed in Table 5 (fuel plates), Table 6 (non-fuel materials), and Table 7 (control rod materials). Vacuum boundary conditions are considered for the top and bottom of the model geometry and outside the water surface (material 15 in Figure 28). The remaining air surface (material 16 in Figure 28) has a reflected boundary condition. Figure 29 illustrates the detailed EVENT RZ model geometry and mesh from ParaView. This calculation involves an eigenvalue calculation for the representative control rod in various positions. Nine separate calculations are performed and involve removing the control rod from the core in 2-cm increments until the rod is completely removed from the core. In such a way, the reactivity worth of the control rod can be calculated by examining the change in the k_{eff} for each rod position as it is being removed from the core. Figure 30 shows an illustration of the annular control rod at various positions in the core for these calculations.

www.manaraa.com

0 - 1.19	1.19 - 1.27	1.27 - 5.13	5.13 - 6.52	6.52 - 12.8	12.8 - 15.85	15.85 - 16.1	16.1 - 33.12	22.12 - 44.93	44.93 - 45.72	45.72 - 98.0	
16	12	13	13	13	13	13	13	13	14	15	-47.29 to -36.25
16	12	11	11	11	11	12	11	13	14	15	-36.25 to -28.25
16	12	11	16	11	11	12	11	13	14	15	-28.25 to -26.25
16	12	11	16	11	11	12	11	13	14	15	-26.25 to -24.25
16	12	11	16	11	11	12	11	13	14	15	-24.25 to -22.25
16	12	11	16	11	11	12	11	13	14	15	-22.25 to -20.25
16	12	11	16	11	11	12	11	13	14	15	-20.25 to -18.25
16	12	11	16	11	11	12	11	13	14	15	-18.25 to -16.25
16	12	11	16	11	11	12	11	13	14	15	-16.25 to -14.25
16	12	11	16	11	11	12	11	13	14	15	-14.25 to -12.25
16	12	1	10	1	11	12	11	13	14	15	-12.25 to -10.25
16	12	1	10	1	11	12	11	13	14	15	-10.25 to -8.25
16	12	2	10	2	11	12	11	13	14	15	-8.25 to -6.25
16	12	2	10	2	11	12	11	13	14	15	-6.25 to -4.25
16	12	3	10	3	11	12	11	13	14	15	-4.25 to -2.25
16	12	3	10	3	11	12	11	13	14	15	-2.25 to -0.25
16	12	12	12	12	11	12	11	13	14	15	-0.25 to 0.25
16	12	4	10	4	11	12	11	13	14	15	0.25 to 2.25
16	12	4	10	4	11	12	11	13	14	15	2.25 to 4.25
16	12	5	5	5	11	12	11	13	14	15	4.25 to 6.25
16	12	6	6	6	11	12	11	13	14	15	6.25 to 8.25
16	12	7	7	7	11	12	11	13	14	15	8.25 to 10.25
16	12	8	8	8	11	12	11	13	14	15	10.25 to 11.25
16	12	9	9	9	11	12	11	13	14	15	11.25 to 12.25
16	12	16	16	16	11	12	11	13	14	15	12.25 to 13.25
16	12	11	11	11	11	12	11	13	14	15	13.25 to 38.567
16	12	13	13	13	13	13	13	13	14	15	38.567 to 48.817
16	12	15	15	15	15	15	15	15	15	15	48.817 to 65.0

1	20497
2	20498
3	20499
4	204100
5	204101
6	204102
7	204103
8	204104
9	204105
10	SR, CCR, FCR
11	graphite
12	aluminum
13	lead
14	steel
15	water
16	air

Figure 28. EVENT RZ Model Region and Mesh Definitions

www.manaraa.com

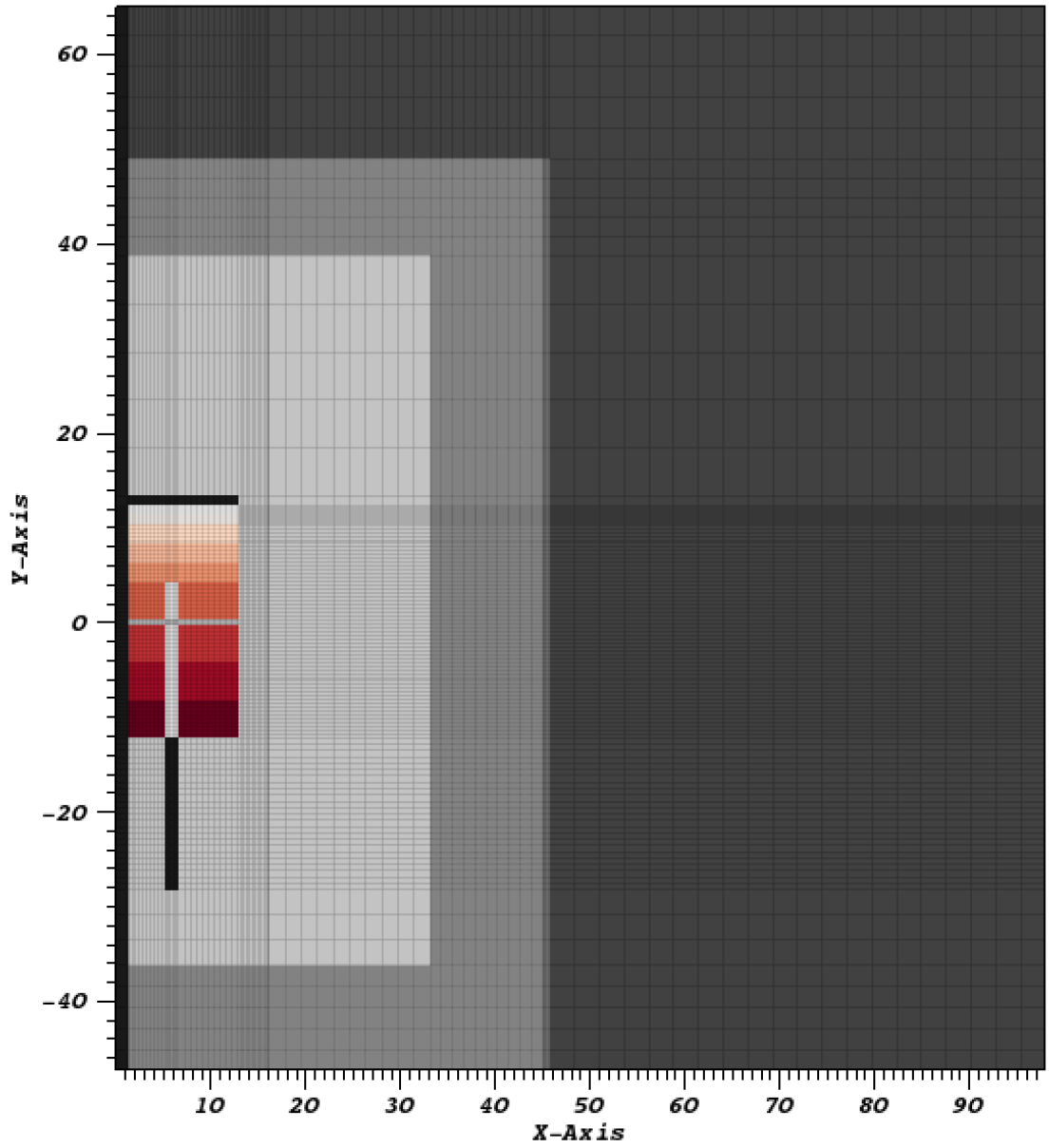

Figure 29. EVENT RZ Model Illustrations

www.manaraa.com

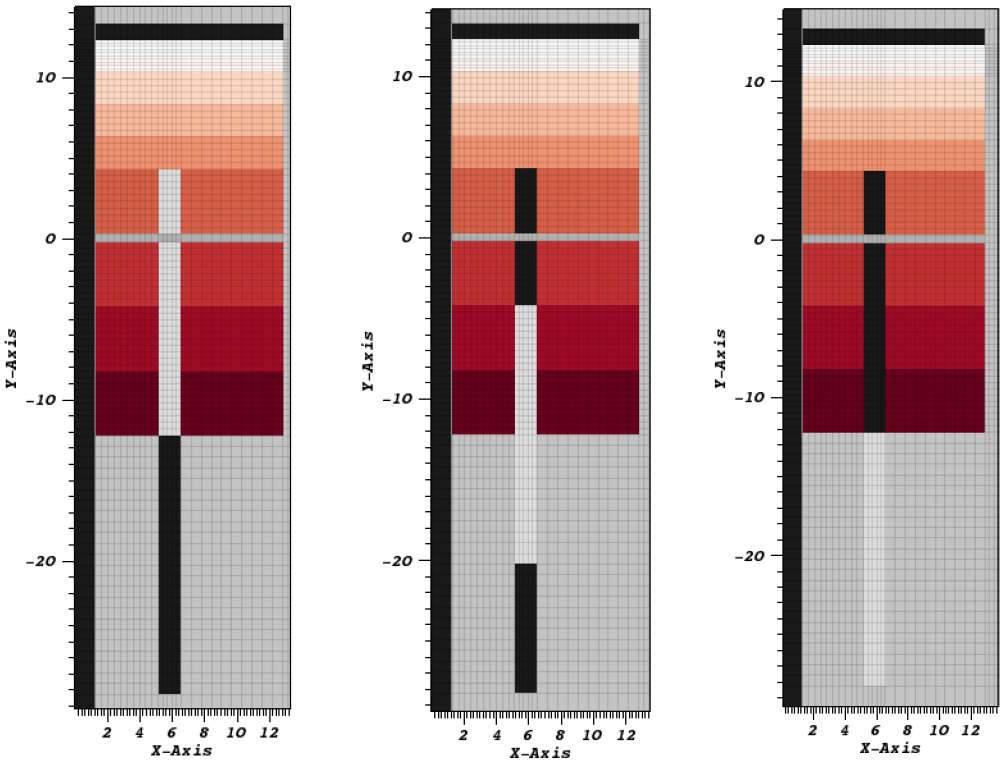

Figure 30. Core Region Illustration of RZ Model Control Rod Position

The EVENT k_{eff} results for this model are provided in Table 14. The k_{eff} results were used to calculate the reactivity worth for each case knowing the beta effective, β_{eff}, for the system is 0.0074 [4]. The EVENT k_{eff} results are larger compared to the maximum k_{eff} for the AGN reactor, 1.00185. This is consistent with the MCNP6, NETGEN, and Wetzel results. The configurations modeled in the RZ model consider the AGN with the annular control rod at various axial positions in the core. Figure 30 shows the movement of the annular control element from a fully-inserted position to a banked position. The AGN control elements are inserted into first four 4-cm thick fuel plates. The model considers the movement of the annular control

www.manaraa.com

element into the first four 4-cm fuel plates in 2 cm steps. The calculated worth comparing the k_{eff} change between case Rods_All_4b and Rods_All_0 is approximately $4.99. Worth estimates by Wetzel [4] were approximately $5.12 for a similar configuration. The total control rod worth for the UNM AGN is approximately $5.33 [8]. The EVENT RZ model results are approximately 2.5% lower than the Wetzel results and about 6.4% below the total AGN control rod worth. The small variation with the EVENT RZ model is likely due to the use of a 2-D deterministic approach and other minor approximations made to simplify the model geometry. This model was developed to test the R-Z geometry modeling capabilities of EVENT in addition to providing a 2-D model to compare to 3-D EVENT models developed for AGN analysis. The use of the 2-group case-dependent cross-section library provides a good combination of calculation accuracy and efficiency.

www.manaraa.com

Table 14. Detailed EVENT RZ Model Differential Rod Worth Results

Case	Rod Position (cm)	k_{eff}	Cumulative Worth ($)	AGN Rod Worth Data [8] ($)
Rods_All_0	0	0.98100 0.9838 ± 0.0006*	0.00	0.92
Rods_All_1a	2	0.98922	1.14	1.38
Rods_All_1b	4	0.99540	1.99	1.84
Rods_All_2a	6	1.00039	2.67	2.42
Rods_All_2b	8	1.00502	3.29	3.00
Rods_All_3a	10	1.00950	3.89	3.58
Rods_All_3b	12	1.01370	4.44	4.19
Rods_All_4a	14	1.01641	4.80	4.68
Rods_All_4b	16	1.01784 1.0217 ± 0.0007*	4.99	5.33

*Results from Wetzel [4].

4.5.5 Simplified EVENT RZ Model

The detailed EVENT RZ model, previously described, was simplified to provide acceptable results while significantly increasing the case efficiency. The previous calculation results demonstrated the capabilities of EVENT in verifying results from previous analyses, such as the MCNP6 or Wetzel results. The purpose of the simplified RZ EVENT model is to enable sufficient fidelity for the transient analysis. The simplifications made include a reduction in the number of material regions in the model, homogenizing the aluminum (from the control rod tube) for the annular fuel rod, and eliminating the control elements below the AGN core. The control elements below the AGN core were initially modeled to consider fuel element movement from inside the core to below the core; however, this was removed from both the EVENT RZ and NETGEN models for the transient analysis

www.manaraa.com

that only need to consider reactivity changes as a result of control element movement. The simplified EVENT RZ model considers the movement of the annular control element by considering the volume fraction of fuel and air within the control element rather than simulating the control rods movement into and out of the core. This simplification made it easier to calculate a reactivity calibration curve for equating the AGN experimental reactivity changes via control rod position changes to EVENT model reactivity for the transient analysis. The model simplifications also eliminated the necessity to model large void regions, i.e., regions of low density such as air, to preclude computational issues within EVENT. To optimize both the precision and efficiency, a P_5 Legrendre expansion and a 2-group multigroup cross-section library based on ENDF/B-VII.1 data were used.

The simplified EVENT RZ model regions and material assignments are shown in Figure 31 and an illustration of the EVENT RZ model is shown in Figure 32. The aluminum of the core baffle is homogenized with a homogenized mixture of the constituents of the core fuel plates. The atom densities for the AGN core regions and annular control element is provided in Table 15. The calculation results for this configuration are provided in Table 16. Several calculations were performed to approximately match the actual AGN total control rod worth of $5.33 to ensure sufficient reactivity was available in the transient analysis for the ramp and rod drop analyses. Even with the significant simplification, the model results are comparable to the

www.manaraa.com

detailed RZ model, except the integral rod worth results for the detailed EVENT RZ model are smaller, \$4.99 for the detailed RZ model as compared to \$5.24 for the simplified model. The control element worth in the simplified EVENT RZ model allows sufficient reactivity worth range to consider control rod movements in the experimental transients.

Table 15. Atom Densities for the Simplified EVENT RZ Model

Feature	N(^{235}U) (at./bn-cm)	N(^{238}U) (at./bn-cm)	N(O) (at./bn-cm)	N(C) (at./bn-cm)	N(H) (at./bn-cm)	N(Al) (at./bn-cm)
Core	1.4418E-04	5.8772E-04	1.4638E-03	3.8078E-02	7.6156E-02	3.3676E-03
Control Rods	1.1703E-04	4.7705E-04	1.1882E-03	2.5483E-02	5.0967E-02	1.9936E-02

0 - 1.19	1.19 - 1.27	1.27 - 5.30	5.30 - 6.30	6.30 - 12.8	12.8 - 15.85	15.85 - 16.1	16.1 - 33.12	33.12 - 44.926	44.926 - 45.72	45.72 - 98.0	
8	4	5	5	5	5	5	5	5	6	7	-47.29 to –36.25
8	4	3	3	3	3	4	3	5	6	7	-36.25 to -28.25
8	4	3	3	3	3	4	3	5	6	7	-28.25 to -14.25
8	4	3	3	3	3	4	3	5	6	7	-14.25 to -12.25
8	4	1	9	1	3	4	3	5	6	7	-12.25 to 3.75
8	4	1	1	1	3	4	3	5	6	7	3.75 to 6.25
8	4	1	1	1	3	4	3	5	6	7	6.25 to 12.25
8	4	8	8	8	3	4	3	5	6	7	12.25 to 13.25
8	4	3	3	3	3	3	3	5	6	7	13.25 to 38.567
8	4	5	5	5	5	5	5	5	6	7	38.567 to 48.817
8	4	7	7	7	7	7	7	7	7	7	48.817 to 65.0

1	Fuel
2	Not used
3	graphite
4	alum
5	lead
6	steel
7	water
8	air
9	SR, CCR, FCR

Figure 31. Simplified EVENT RZ Model for Experimental Analysis

www.manaraa.com

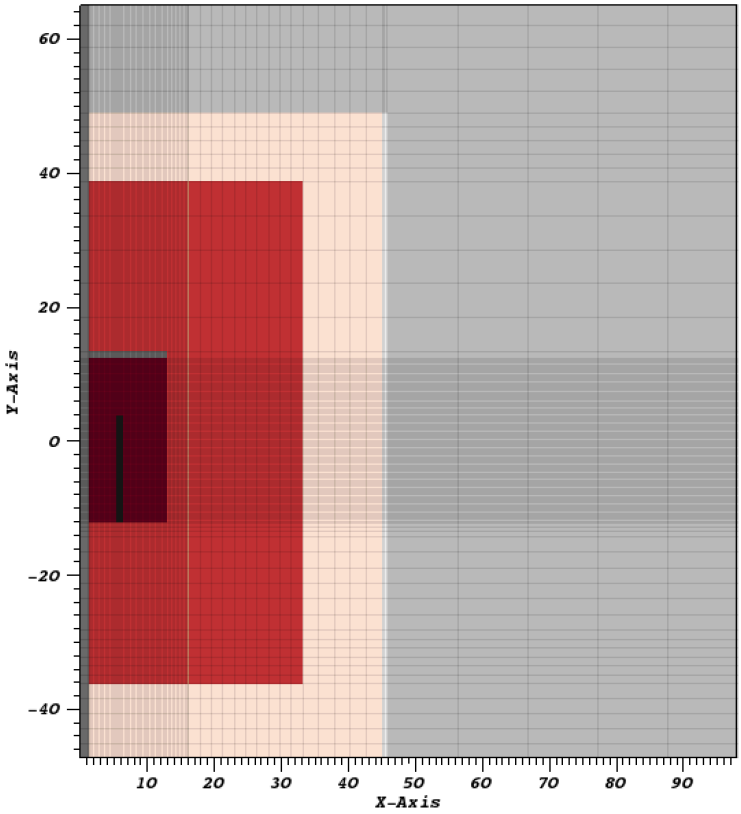

Figure 32. Simplified EVENT RZ Model Configuration

Table 16. EVENT Simplified RZ Model Differential Rod Worth Results

Case	Control Element Fuel Volume Fraction	k_{eff}	Cumulative Worth
RZ_T0	0.000	0.98644	$0.00
RZ_T1	0.125	1.00282	$2.24
RZ_T2	0.250	1.00700	$2.80
RZ_T3	0.375	1.01049	$3.26
RZ_T4	0.500	1.01372	$3.69
RZ_T5	0.625	1.01681	$4.09
RZ_T6	0.750	1.01982	$4.48
RZ_T7	0.875	1.02278	$4.87
RZ_T8	1.000	1.02569	$5.24

www.manaraa.com

4.6 AGN-201M Wetzel Calculations

The specifications for the AGN at UNM were documented in a report by Wetzel [4] in 2007. This report was provided by UNM to assist with EVENT model development for this work. Wetzel [4] compiled a detailed description of the AGN in a delayed critical configuration as a benchmark for the validation of the SCALE and MCNP codes at a nuclear facility in Lynchburg, VA. The SCALE 5.0 package was used for these calculations and infinite homogeneous and multi-region cross-section processing sequences were used to develop the self-shielded, case-dependent cross-sections, based on the SCALE 238-group ENDF/B-VI.8 cross-section set. The eigenvalue results for each cross-section processing sequence (infinite homogeneous medium and multi-region) were then compared to determine which sequence produced better results. A variety of sensitivity analyses were performed on different reactor constituents and conditions, e.g., water shield density, temperature, aluminum density, lead density, etc. The SR1, SR2, CCR and FCR integral rod worth estimates were calculated then compared to stated values for the AGN, based on actual experimental results. In addition to the sensitivity studies, the Wetzel study also calculated SR1, SR2, CCR and FCR integral rod worth estimates for the following configurations:

- All control rods inserted into the core (All_Rods_In),
- Fine control rod out of the core (FCR_Out),
- Coarse control rod out of the core (CCR_Out),
- Safety rod #1 out of the core (SR1_Out),

www.manaraa.com

- Safety rod #2 out of the core (SR2_Out), and
- All control rods out of the core (All_Rods_Out).

The Wetzel results were compared to known rod worth results for the AGN reactor. The results for the integral rod worth calculations show reasonable results with the MCNP6 3-D model and to the stated worth results from Wetzel [4]. The integral worth results for the FCR calculations for the EVENT results ($0.50 and $0.55 for the detailed and simplified EVENT NETGEN cases) do not compare well with the stated worth [8] of the AGN FCR ($0.38); however, the Wetzel and MCNP6 results compare better. According to the UNM Nuclear Engineering Laboratory Director, the quantity of fissile material in the FCR is not known precisely, although it can be estimated from direct reactivity measurements. Table 17 summarizes the calculated integral rod worth estimates from the Wetzel study in addition to compiling the results of the detailed and simplified EVENT RZ and EVENT NETGEN calculations performed previously. Further, Table 17 provides the rod worth data based on the latest set of annual measurement results for each of the control rods [57].

www.manaraa.com

Table 17. Summary of Integral Rod Worth Estimates

Case	AGN UNM Worths[†]	Wetzel Results[††]	MCNP6 Results[§]	Detailed EVENT RZ Results[‡]	Simplified EVENT RZ Results[‡‡]	Detailed EVENT NETGEN Results[††]	Simplified EVENT NETGEN Results[§§]
FCR worth	$0.38	$0.28	$0.33	–	–	$0.50	$0.55
CCR worth	$1.72	$1.60	$1.75	–	–	$1.46	$2.23
SR1 worth	$1.665	$1.63	$1.77	–	–	$1.46	–
SR2 worth	$1.594	$1.55	$1.76	–	–	$1.46	–
Cumulative Rod Worth	$5.359	$5.12	$5.43	$4.99	$5.24	$4.79	$2.68

[†]The AGN UNM control rod worths are measured each year to ensure the control rods and reactor function as intended during operations [57]
[††] 238-group ENDF/B-VI.8 Library
[§] Continuous energy ENDF/B-VII Library
[‡] P_{11} and 2-group ENDF/B-VII.1 Library. All control rods are homogenized in the detailed RZ model. An annular control rod in this model is used to approximate the cumulative reactivity worth for all of the AGN control elements; thus, there is no worth data for the FCR, CCR, SR1 and SR2.
[‡‡] P_5, and 2-group ENDF/B-VII.1 Library. All control rods are homogenized in the detailed RZ model. All control rods are homogenized in the detailed RZ model. An annular control rod in this model is used to approximate the cumulative reactivity worth for all of the AGN control elements; thus, there is no worth data for the FCR, CCR, SR1 and SR2.
[††] P_{11} and 2-group ENDF/B-VII.1 Library
[§§] P_{11} and 2-group ENDF/B-VII.1 Library. The reactivity worth of the FCR and CCR are calculated because they contribute to core reactivity changes. The two safety rods, SR1 and SR2, are loaded into the core at the start of operations and are not considered in the worth calculation.

www.manaraa.com

Chapter 5 – AGN-201M Experimental Verifications

5.1 Description of AGN-201M Experiments

On December 17, 2013, the UNM AGN was used to generate a series of experimental configurations to use for further analysis using the EVENT code. The experimental configurations involved the movement of the CCR and FCR control elements to control the AGN reactivity to produce both delayed critical and transient configurations. Per UNM AGN operating procedure, the two safety rods are always loaded into the core prior to starting up the reactor. These configurations assumed the glory hole was empty and there were no neutron sources present in the core. According to the AGN operations log for these experients, provided in the Appendix, the power level at delayed critical for these experiments was 4.06 W thermal.

www.manaraa.com

The first set of experiments defined a series of delayed critical, i.e., steady state configurations as a result of specific FCR and CCR positions within the rod cans located in the AGN core. For example, to maintain a delayed critical configuration, if the FCR is inserted deeper into the core resulting in a positive reactivity increase, the CCR must be removed to a position commensurate with the magnitude of the reactivity insertion as a result of the FCR position change. The reactor logs in Appendix B indicate the reactor was started at 8:48 am and the FCR and CCR rod locations were changed to introduce a prompt jump with a doubling time of approximately 12.6 sec. (stable period of about 18.2 sec.) until a power level of 4.06 W, at delayed critical, was achieved at about 8:55 am. Over a period of approximately 90 minutes, 24 delayed critical configurations, defined by unique FCR/CCR locations, were conducted until the reactor was shutdown via a manual scram at approximately 10:20 am. In addition to the 24 delayed critical configurations completed in the morning experimental session, twelve additional delayed critical configurations at the same power level were performed in the afternoon experimental session (started at approximately 13:25 pm). The delayed critical configurations considered for the EVENT analysis are listed in Table 18. The EVENT NETGEN model is used for the experimental analysis because the FCR and CCR are explicitly considered in the EVENT model and the model is capable of approximating the unique rod positions in the AGN core.

www.manaraa.com

In addition to the steady-state configurations listed in Table 18, the following sequence of time-dependent reactor operations were performed 11 times over the course of the day:

1. Prompt jump to a stable reactor period for a particular duration to achieve a delayed supercritical configuration until a power level of 4.06 W was obtained.
2. Excess reactivity was removed from the core by removing the FCR and/or the CCR from the AGN core until a delayed critical, i.e., steady-state, configuration was achieved at the desired power level.
3. Prompt drop (rod drop) is performed by removing the CCR from the AGN core. This results in a reduction in reactivity over a time period of approximately 200 msec that is directly proportional to the CCR reactivity present at the time the rod was dropped out of the AGN core.

www.manaraa.com

Table 18. Summary of Experimental Delayed Critical Configurations

DC Case #	Time (hour:min.)	FCR Experimental Position (cm)*	CCR Experimental Position (cm)**	Comment from AGN Operational Data Log Sheet
1	8:55 am	21.37	18.21	Steady power, 4.06 W, Rods Banked
2	8:59 am	22.57	18.00	Steady power
3	9:01 am	23.21	17.90	Steady power
4	9:04 am	23.74	17.80	Steady power
5	9:06 am	24.21	17.70	Steady power
6	9:08 am	24.54	17.67	Steady power, FCR Full-in
7	9:11 am	23.54	17.87	Steady power
8	9:13 am	22.54	18.14	Steady power
9	9:15 am	21.54	18.39	Steady power
10	9:16 am	20.54	18.60	Steady power
11	9:17 am	19.54	18.82	Steady power
12	9:19 am	18.54	19.03	Steady power
13	9:22 am	17.54	19.28	Steady power
14	9:25 am	16.54	19.54	Steady power
15	9:29 am	15.54	19.75	Steady power
16	9:31 am	14.54	20.03	Steady power
17	9:34 am	13.54	20.27	Steady power
18	9:37 am	12.54	20.52	Steady power
19	9:43 am	11.04	20.90	Steady power, CCR Full-in
20	9:49 am	21.55	18.49	Steady power, Rods Banked (Δ = 3.06 cm)
21	9:51 am	21.64	18.48	Steady power, Rods Banked (Δ = 3.16 cm)
22	9:54 am	24.53	17.88	Steady power, FCR Full-in
23	10:00 am	11.15	20.91	Steady power, CCR Full-in
24	10:10 am	11.01	20.44	Steady power, 0.102 W, CCR Full-in
25	10:17 am	21.20	18.04	Steady power, Rods Banked (Δ = 3.16 cm)
26	1:41 pm	10.78	20.16	Steady power
27	1:55 pm	20.28	18.00	Steady power
28	2:08 pm	12.25	19.80	Steady power
29	2:20 pm	12.31	19.90	Steady power
30	2:35 pm	12.50	20.00	Steady power
31	2:47 pm	15.42	19.50	Steady power
32	2:59 pm	17.80	19.00	Steady power
33	3:10 pm	21.50	18.34	Steady power
34	3:20 pm	24.53	17.91	Steady power
35	3:33 pm	11.42	21.02	Steady power
36	3:41 pm	11.48	21.04	Steady power

*FCR – full in: 24.53 cm; full out: 1:09 cm
**CCR – full in: 20.91 cm; full out: 97.93 cm (-2.07 cm)

www.manaraa.com

The transient sequence consists of a prompt jump to the desired power level, a period of operation at delayed critical, and a prompt drop (CCR is withdrawn) with the associated delayed neutron precursor decay tail (Figure 33). This sequence of operations is repeated 11 times with different CCR and FCR positions (Figure 34) to provide unique experimental data for analysis using the simplified EVENT RZ and NETGEN models. Appendix B provides the AGN reactor log sheets for the transient measurements by defining the unique rod positions of the CCR and FCR during the experiment. These rod locations were used to estimate the change in the system reactivity as a result of moving the rod from one position to another. The reactivity change is then compared to a control rod calibration curve developed from the EVENT models to estimate the rod positions for use in the time dependent EVENT analysis. The rod positions in the EVENT models are approximated by defining volume fractions of fuel and air in the control rod tubes in the models, which can then be used to analyze a power ramp or rod drop transient configuration from the experiment.

In April 1996, AGN neutron flux measurements in the glory hole region of the core were conducted at UNM. Because the neutrons in the AGN core are quickly moderated by the polyethylene moderator, the core flux measurements involved a thermal neutron flux. The flux measurements were taken radially from the core centerline to a radius of approximately 40 cm, which extends into the lead shield region of the core present just outside the

www.manaraa.com

graphite reflector region. The EVENT code has the capability to model scalar flux sensors to calculate the scalar flux by integrating the angular flux over all angles at predefined locations in the AGN core. The relative flux is defined as the ratio of the neutron flux at the desired position to the neutron flux at the center of the core. The relative flux for the EVENT model results can then be compared to the thermal neutron flux measurement results.

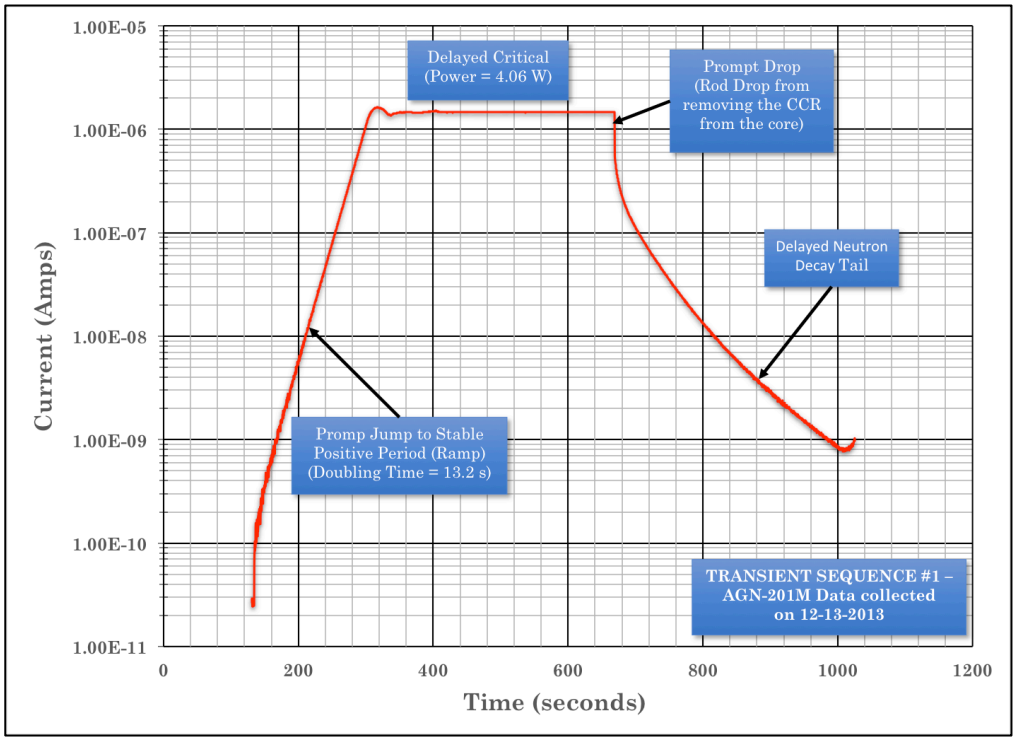

Figure 33. AGN-201M Experimental Data – Transient Sequence #1

www.manaraa.com

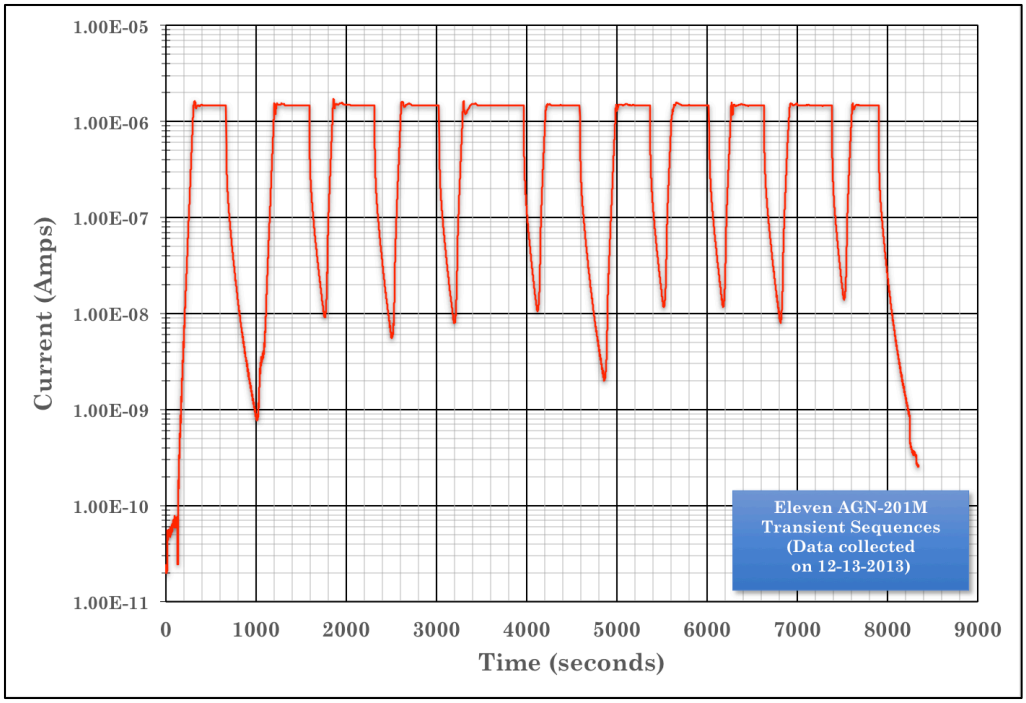

Figure 34. AGN-201M Experimental Transient Data

5.2 AGN Delayed Critical Verifications

The 36 steady state AGN experimental configurations discussed in Section 5.1 were analyzed using the simplified EVENT NETGEN model. This model is used for the delayed critical experimental analysis because the FCR and CCR positions are accurately represented in the AGN model, although the rods are modeled as a volume fraction of fuel and air instead of being modeled as a solid fuel rod at various positions.

Table 18 lists the experimental data and the CCR and FCR positions in the core. The CCR and FCR control rod positions are converted to the volume fraction of fuel and air inside the control rod tubes. These CCR and FCR material card fuel and air volume fraction values are equated to the rod

www.manaraa.com

position to approximate the control element position in the core. This was done largely because EVENT can only perform time-dependent analysis by changes to the material compositions and material region assignments in the core. The fuel and air volume fraction values for each of the 36 steady-state cases are summarized in Table 20.

A Legendre expansion study was performed before the experimental analysis was initiated to determine the P_N order that would provide an adequate result for the delayed critical verifications. The results of the scoping analysis, shown in Table 19, indicates good convergence for most of the cases. Thus, it was decided that each EVENT NETGEN calculation would be performed twice (a P_{11} case and a P_{13} case).

Table 19. EVENT Legrendre Flux Expansion Order Study

EVENT Model Legrendre Flux Expansion Order, P_N	k_{eff}	**Fraction of P_{13} Result (%)**	**Execution Time (sec.)**
P_1	0.95974	95.73	143.76
P_3	0.99436	99.19	189.95
P_5	0.99963	99.71	255.48
P_7	1.00132	99.88	457.75
P_9	1.00201	99.95	694.19
P_{11}	1.00234	99.98	1173.83
P_{13}	1.00251	100.0	1751.17

The 36 simplified EVENT NETGEN results are presented in Table 20 and are shown in Figure 35. These results show excellent agreement with an k_{eff} of unity, which represents a delayed critical or steady-state configuration. As

www.manaraa.com

indicated by the parametric study results in Table 19, the EVENT NETGEN model results slightly overpredict the actual k_{eff} for the experiment, 1.0, by about +0.25% (P_{13} result). The calculational bias is the difference between the k_{eff} result and unity and is either positive or negative. The calculational bias was calculated for each of the 36 delayed critical configurations and then averaged to determine the average bias for the EVENT calculations. For the P_{11} calculations, the average EVENT NETGEN calculation bias in the k_{eff} is -0.0048%. For the P_{13} calculations, the average EVENT NETGEN calculation bias in the k_{eff} is +0.0119%. Thus, the simplified EVENT NETGEN model results closely matches the experimental data for an AGN delayed critical configuration with a small computation bias of much less than 1% in k_{eff}.

www.manaraa.com

Table 20. AGN Delayed Critical Configuration EVENT Results

Case #	FCR Experimental Position and EVENT Representation			CCR Experimental Position and EVENT Representation			k_{eff} (P_{11})	k_{eff} (P_{13})
	Position AGN Exp.	Volume Fraction (fuel)	Volume Fraction (air)	Position AGN Exp.	Volume Fraction (fuel)	Volume Fraction (air)		
1	21.37	0.80188	0.19813	18.21	0.83188	0.16813	0.99990	1.00007
2	22.57	0.87688	0.12313	18.00	0.81875	0.18125	0.99993	1.00010
3	23.21	0.91688	0.08312	17.90	0.81250	0.18750	0.99996	1.00013
4	23.74	0.95000	0.05000	17.80	0.80625	0.19375	0.99997	1.00015
5	24.21	0.97938	0.02062	17.70	0.80000	0.20000	0.99996	1.00016
6	24.54	1.00000	0.00000	17.67	0.79813	0.20188	0.99999	1.00016
7	23.54	0.93750	0.06250	17.87	0.81063	0.18938	0.99998	1.00016
8	22.54	0.87500	0.12500	18.14	0.82750	0.17250	1.00003	1.00020
9	21.54	0.81250	0.18750	18.39	0.84313	0.15688	1.00006	1.00023
10	20.54	0.75000	0.25000	18.60	0.85625	0.14375	1.00006	1.00023
11	19.54	0.68750	0.31250	18.82	0.87000	0.13000	1.00006	1.00023
12	18.54	0.62500	0.37500	19.03	0.88313	0.11688	1.00005	1.00022
13	17.54	0.56250	0.43750	19.28	0.89875	0.10125	1.00007	1.00024
14	16.54	0.50000	0.50000	19.54	0.91500	0.08500	1.00009	1.00026
15	15.54	0.43750	0.56250	19.75	0.92813	0.07187	1.00007	1.00024
16	14.54	0.37500	0.62500	20.03	0.94563	0.05437	1.00010	1.00027
17	13.54	0.31250	0.68750	20.27	0.96063	0.03937	1.00008	1.00025
18	12.54	0.25000	0.75000	20.52	0.97625	0.02375	1.00007	1.00024
19	11.04	0.15625	0.84375	20.90	1.00000	0.00000	1.00002	1.00020
20	21.55	0.81313	0.18688	18.49	0.84938	0.15063	1.00013	1.00031
21	21.64	0.81875	0.18125	18.48	0.84875	0.15125	1.00014	1.00031
22	24.53	0.99938	0.00062	17.88	0.81125	0.18875	1.00015	1.00031
23	11.15	0.16313	0.83688	20.90	1.00000	0.00000	1.00005	1.00022
24	11.01	0.15438	0.84563	20.44	0.97125	0.02875	0.99968	0.99985
25	21.20	0.79125	0.20875	18.04	0.82125	0.17875	0.99975	0.99992
26	10.78	0.14000	0.86000	20.16	0.95375	0.04625	0.99942	0.99959
27	20.28	0.73375	0.26625	18.00	0.81875	0.18125	0.99958	0.99975
28	12.25	0.23188	0.76813	19.80	0.93125	0.06875	0.99948	0.99948
29	12.31	0.23563	0.76438	19.90	0.93750	0.06250	0.99957	0.99974
30	12.50	0.24750	0.75250	20.00	0.94375	0.05625	0.99968	0.99985
31	15.42	0.43000	0.57000	19.50	0.91250	0.08750	0.99987	1.00004
32	17.80	0.57875	0.42125	19.00	0.88125	0.11875	0.99991	1.00008
33	21.50	0.81000	0.19000	18.34	0.84000	0.16000	1.00002	1.00019
34	24.53	0.99938	0.00062	17.91	0.81313	0.18688	1.00017	1.00034
35	11.42	0.18000	0.82000	20.90	1.00000	0.00000	1.00011	1.00028
36	11.48	0.18375	0.81625	20.90	1.00000	0.00000	1.00013	1.00030

www.manaraa.com

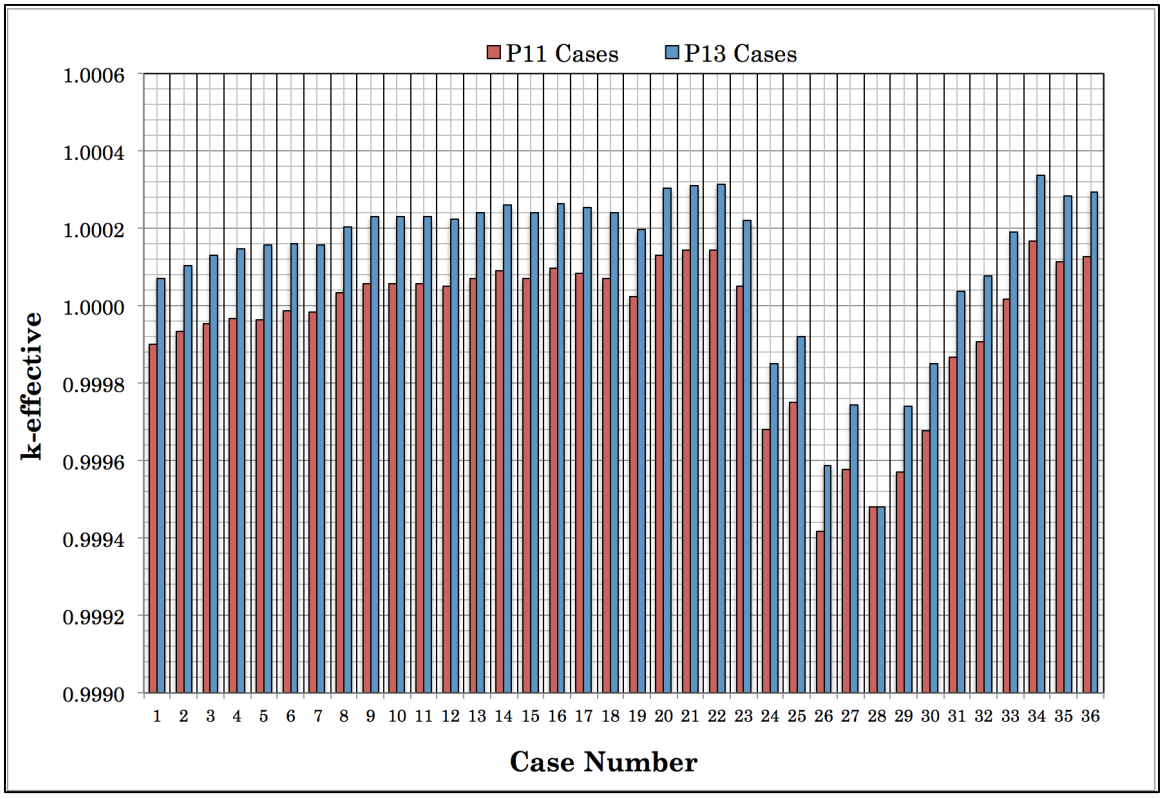

Figure 35. AGN-201M Delayed Critical Analysis Results

5.3 AGN-201M Flux Measurement Analysis

Thermal neutron flux measurements from the UNM AGN in 1996 were analyzed using the simplified EVENT NETGEN and RZ models. During the experiment, the neutron flux of the AGN was measured by inserting small diameter BF_3 or ^3He neutron detectors through the AGN glory hole while the reactor was operating and taking neutron counts at various radii from the center of the AGN core. The EVENT code has the capability for computing the scalar flux as a function of location. The scalar flux is calculated by EVENT by integrating the angular flux over all angles and energies at a particular position in the reactor. The EVENT model requires the location of

www.manaraa.com

the scalar flux calculation to be specified as, in these cases, X-, Y-, and Z-coordinates or R-Z coordinates. Multiple scalar flux sensors are defined in the simplified EVENT NETGEN model along the radial centerline of the glory hole within the AGN core to compute the scalar flux at each location. The calculations assume P_{11} Legendre expansion, which is reasonable based on the P_N order analysis in Table 19. The simplified EVENT NETGEN calculation results are compared to thermal flux experimental results for the AGN at UNM. The experimental data for the thermal flux (relative flux) calculations are listed in Table 21.

Table 21. AGN-201M Thermal Flux Data

AGN Core Radial Location (cm)	April, 1996 AGN Thermal Flux Data (Relative Flux)
0	1
2	1.0103
4	0.9636
6	0.9324
8	0.8578
10	0.7746
12	0.6489
14	0.5348
16	0.4712
18	0.4319
20	0.383
22	0.3353
24	0.296
26	0.2575
28	0.2199
30	0.1842
32	0.1467
34	0.1147
36	0.0933
38	0.0754
40	0.0611

www.manaraa.com

The EVENT flux calculations consider 44 radial sensors inside the glory hole of the simplified EVENT NETGEN model. The ENDF/B-VII.1-based 2-group cross-section library is used for these calculations. The EVENT scalar flux sensors normalize the neutron flux per source neutron, so the detector results can be scaled to the power level of the reactor. The EVENT calculations normalize the flux sensor results for a reactor power level of 4.06 W. For comparison sake, an AGN power level of about 5.0 W corresponds to a thermal flux of about 2.50×10^{8} neutrons/cm^2-sec [2]. The EVENT model scalar flux results show the peak neutron scalar flux at the center of the reactor core is 8.90×10^{8} neutrons/cm^2-sec, which is somewhat larger than expected. The thermal flux calculated with EVENT for a power level of about 4.06 W is 3.40×10^{8} neutrons/cm^2-sec. However, the relative flux, $\phi(r)/\phi(0)$ does approximate the relative experimental flux values well. This could be the result of the P_N order assumed in the calculation or it could involve the precision inherent in the scalar flux sensor response in EVENT. The error in the sensor calculation is not currently provided in the sensor response output results. The EVENT scalar flux results are listed in Table 22 and illustrated in Figure 36.

The relative neutron flux (normalized to the maximum flux value at the core centerline) compares well to the AGN experimental data from the AGN core centerline to a radius of 40 cm, although there are slight deviations in the flux shape in core region, in the outer portion of the graphite reflector,

www.manaraa.com

and lead shield. Simplifications made to the simplified EVENT NETGEN model eliminated the core fuse; however, the horizontal glory hole is considered in the EVENT calculation. The EVENT calculation considers a radial dimension from the core centerline to a radius of 70.0 cm located inside the water tank. The simplified EVENT NETGEN model results show the thermal neutron flux drops more than 36.6% from the core centerline to the outer core radius of 12.8 cm and more than 82.7% from the core centerline to the outer graphite reflector radius of 33.12 cm. However, the experimental AGN flux results show good agreement with the relative flux at ~13.0 cm, the outer boundary of the AGN core and at ~33 cm, the outer boundary of the external graphite reflector. Between the core centerline and the edge of the AGN core, the simplified EVENT NETGEN results tend to underestimate the relative flux but agrees better at the outer portion of the AGN core as well as the graphite reflector. There is no experimental data to compare to outside about 40 cm; however, both the simplified EVENT NETGEN model and experimental results show the relative neutron flux has dropped to about 6.1% for the experimental results and about 1.6% for the total relative neutron flux for the simplified EVENT NETGEN model results. The simplified EVENT NETGEN results indicate the relative neutron flux quickly drops to zero in the lead and water shielded regions of the reactor.

www.manaraa.com

Table 22. AGN EVENT Flux Calculation Results

AGN Model Scalar Flux Detector Location (cm)			Group 1 Neutron Flux (n/cm^2-s)	Relative Neutron Flux	Group 2 Neutron Flux (n/cm^2-s)	Relative Neutron Flux	Total Neutron Flux (n/cm^2-s)	Relative Neutron Flux
x	y	z		$\phi(r)/\phi(0)$		$\phi(r)/\phi(0)$		$\phi(r)/\phi(0)$
0	0	0	5.51E+08	1.00	3.40E+08	1.00	8.90E+08	1.00
1	0	0	5.47E+08	0.99	3.37E+08	0.99	8.84E+08	0.99
2	0	0	5.40E+08	0.98	3.34E+08	0.98	8.74E+08	0.98
3	0	0	5.30E+08	0.96	3.28E+08	0.97	8.59E+08	0.96
4	0	0	5.17E+08	0.94	3.22E+08	0.95	8.38E+08	0.94
5	0	0	5.00E+08	0.91	3.13E+08	0.92	8.13E+08	0.91
6	0	0	4.81E+08	0.87	3.03E+08	0.89	7.85E+08	0.88
7	0	0	4.60E+08	0.84	2.92E+08	0.86	7.52E+08	0.85
8	0	0	4.37E+08	0.79	2.80E+08	0.83	7.17E+08	0.81
9	0	0	4.12E+08	0.75	2.68E+08	0.79	6.79E+08	0.76
10	0	0	3.86E+08	0.70	2.54E+08	0.75	6.40E+08	0.72
11	0	0	3.59E+08	0.65	2.40E+08	0.71	5.99E+08	0.67
12	0	0	3.33E+08	0.60	2.26E+08	0.67	5.59E+08	0.63
12.5	0	0	3.20E+08	0.58	2.19E+08	0.65	5.39E+08	0.61
12.7	0	0	3.15E+08	0.57	2.17E+08	0.64	5.32E+08	0.60
12.8	0	0	3.13E+08	0.57	2.15E+08	0.63	5.28E+08	0.59
12.9	0	0	3.10E+08	0.56	2.14E+08	0.63	5.24E+08	0.59
13	0	0	3.08E+08	0.56	2.12E+08	0.63	5.20E+08	0.58
13.1	0	0	3.05E+08	0.55	2.11E+08	0.62	5.16E+08	0.58
13.2	0	0	3.03E+08	0.55	2.10E+08	0.62	5.12E+08	0.58
13.5	0	0	2.95E+08	0.54	2.06E+08	0.61	5.01E+08	0.56
15	0	0	2.60E+08	0.47	1.87E+08	0.55	4.47E+08	0.50
17.5	0	0	2.11E+08	0.38	1.60E+08	0.47	3.71E+08	0.42
20	0	0	1.73E+08	0.31	1.38E+08	0.41	3.11E+08	0.35
25	0	0	1.17E+08	0.21	1.04E+08	0.31	2.22E+08	0.25
30	0	0	7.88E+07	0.14	7.81E+07	0.23	1.57E+08	0.18
31	0	0	7.26E+07	0.13	7.37E+07	0.22	1.46E+08	0.16
31.3	0	0	6.69E+07	0.12	6.95E+07	0.20	1.36E+08	0.15
32	0	0	6.16E+07	0.11	6.57E+07	0.19	1.27E+08	0.14
32.5	0	0	5.68E+07	0.10	6.21E+07	0.18	1.19E+08	0.13
33	0	0	5.22E+07	0.09	5.88E+07	0.17	1.11E+08	0.12
33.8	0	0	3.37E+07	0.06	4.56E+07	0.13	7.93E+07	0.09
34	0	0	2.08E+07	0.04	3.67E+07	0.11	5.75E+07	0.06
35	0	0	1.23E+07	0.02	2.89E+07	0.09	4.12E+07	0.05

www.manaraa.com

AGN Model Scalar Flux Detector Location (cm)			Group 1 Neutron Flux (n/cm²-s)	Relative Neutron Flux	Group 2 Neutron Flux (n/cm²-s)	Relative Neutron Flux	Total Neutron Flux (n/cm²-s)	Relative Neutron Flux
x	y	z		ϕ(r)/ϕ(0)		ϕ(r)/ϕ(0)		ϕ(r)/ϕ(0)
36.3	0	0	7.47E+06	0.01	2.17E+07	0.06	2.92E+07	0.03
37.5	0	0	4.97E+06	0.01	1.62E+07	0.05	2.11E+07	0.02
38.8	0	0	3.87E+06	0.01	1.27E+07	0.04	1.65E+07	0.02
40	0	0	3.42E+06	0.01	1.05E+07	0.03	1.40E+07	0.02
45	0	0	3.28E+06	0.01	9.32E+06	0.03	1.26E+07	0.01
50	0	0	3.28E+06	0.01	8.61E+06	0.03	1.19E+07	0.01
55	0	0	3.34E+06	0.01	8.05E+06	0.02	1.14E+07	0.01
60	0	0	3.40E+06	0.01	7.37E+06	0.02	1.08E+07	0.01
65	0	0	3.40E+06	0.01	6.20E+06	0.02	9.59E+06	0.01
70	0	0	0.00E+00	0.00	0.00E+00	0.00	0.00E+00	0.00

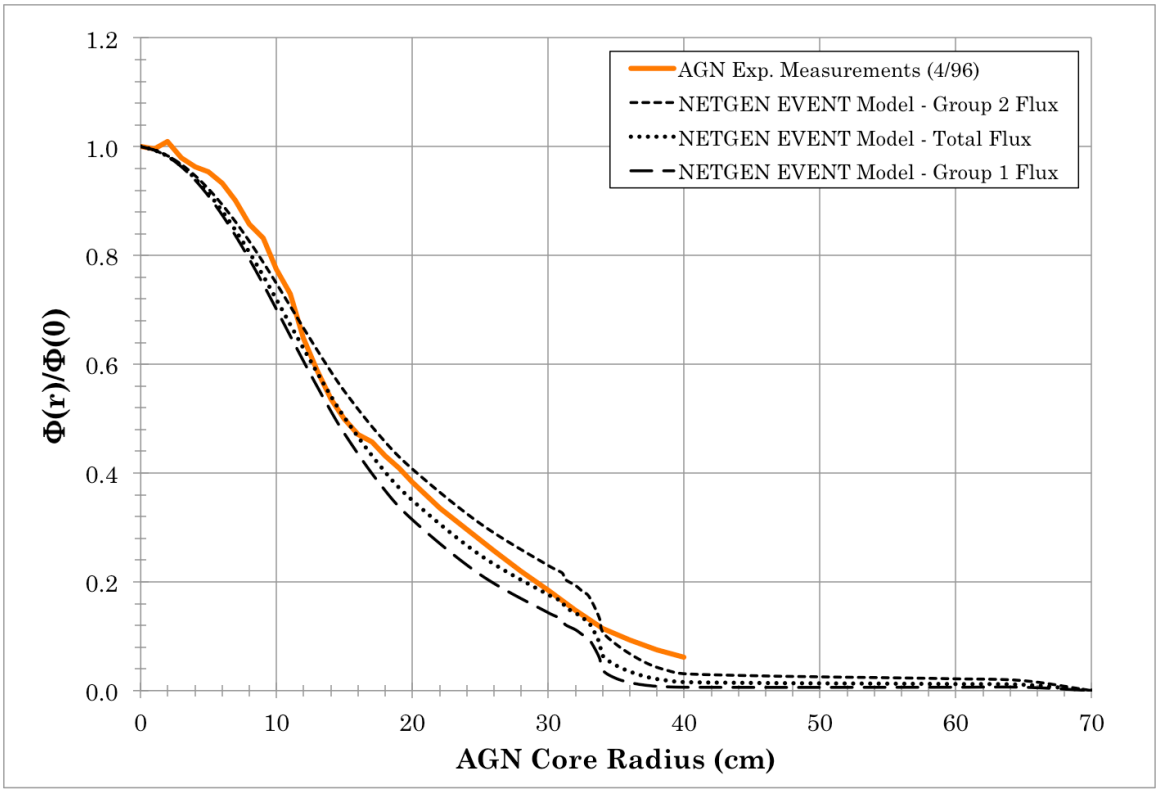

Figure 36. Comparison of EVENT Flux Results with Experiment

www.manaraa.com

5.3.1 Neutron Flux Visualization Calculations

The simplified EVENT RZ and NETGEN models were used to generate illustrations of spatial neutron flux estimates for the AGN. The EVENT calculation stores the angular flux data for each finite element region in the calculation to a binary file. This binary file can be read by ParaView or VisIt and plotted over the problem geometry to graphically view the neutron flux distribution throughout the AGN reactor model geometry. The neutron flux illustrations for the simplified EVENT NETGEN and RZ configurations are shown in Figures 37-39.

The simplified EVENT NETGEN model was used to produce the flux illustrations and calculate the scalar neutron flux. The simplified EVENT NETGEN flux illustration results indicate the total neutron flux (sum of themal and fast contributions) is 1.23×10^{9} neutrons/cm^2-sec and the thermal neutron flux is 5.23×10^{8} neutrons/cm^2-sec. The corresponding simplified EVENT RZ model flux illustrations indicate the total neutron flux is 6.07×10^{8} neutrons/cm^2-sec and thermal neutron flux is 2.58×10^{8} neutrons/cm^2-sec. The simplified EVENT RZ model was used only to calculate the spatial neutron flux illustrations. The flux illustrations show how the neutron flux is concentrated mainly in the core and graphite reflector regions, i.e., there is very little neutron leakage into the lead and water shields. The figures also illustrate how the neutron flux is distributed in the vicinity of the AGN glory hole and how the flux behaves in the regions where the CCR and FCR control

www.manaraa.com

elements are present. The SR1 and SR2 control elements have been homogenized along with the core materials to keep the model as simple as possible and, consequently, are not visible in the figures. The homogenization of SR1 and SR2 in the simplified EVENT NETGEN model for the flux, steady-state and transient configurations was done because SR1 and SR2 are static in the experimental configurations and only the FCR and CCR control elements were moved into and out of the core during the experiments. The visualizations of the AGN neutron flux show some ray effects where anomalies in the shape of the solution of the neutron flux can occur in some regions. This is the case in regions of very low density where the primary material is air, e.g., glory hole and upper fuel plate region. This effect is due to the inability of a particular quadrature set to accurately calculate the scalar flux via integration of the angular flux in EVENT. Typically, increasing the Legendre flux expansion in the calculation can successfully eliminate these effects or the material definitions can be altered to reduce the magnitude of these effects in the EVENT calculation.

www.manaraa.com

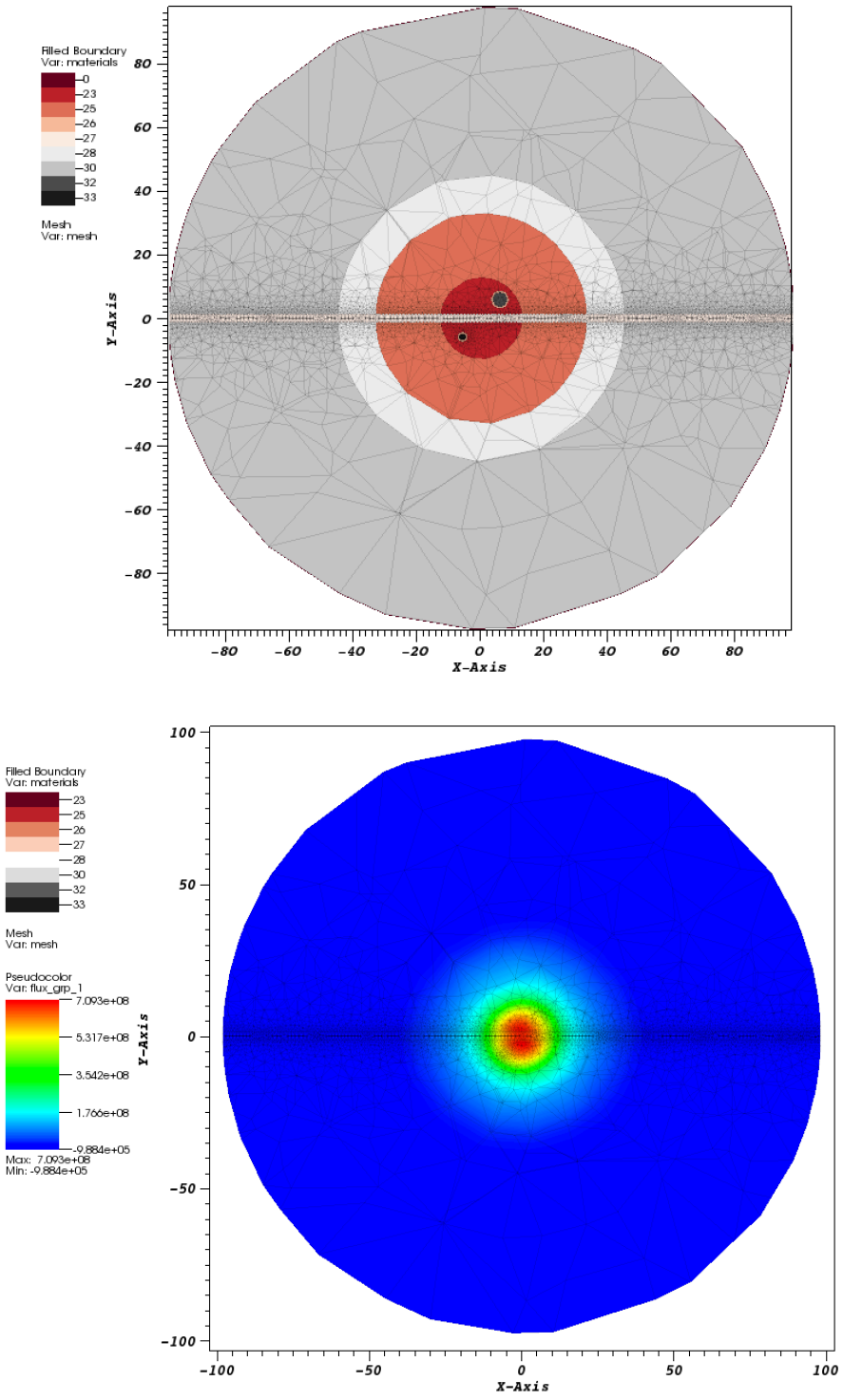

Figure 37. EVENT NETGEN Group 1 Neutron Flux Illustration

www.manaraa.com

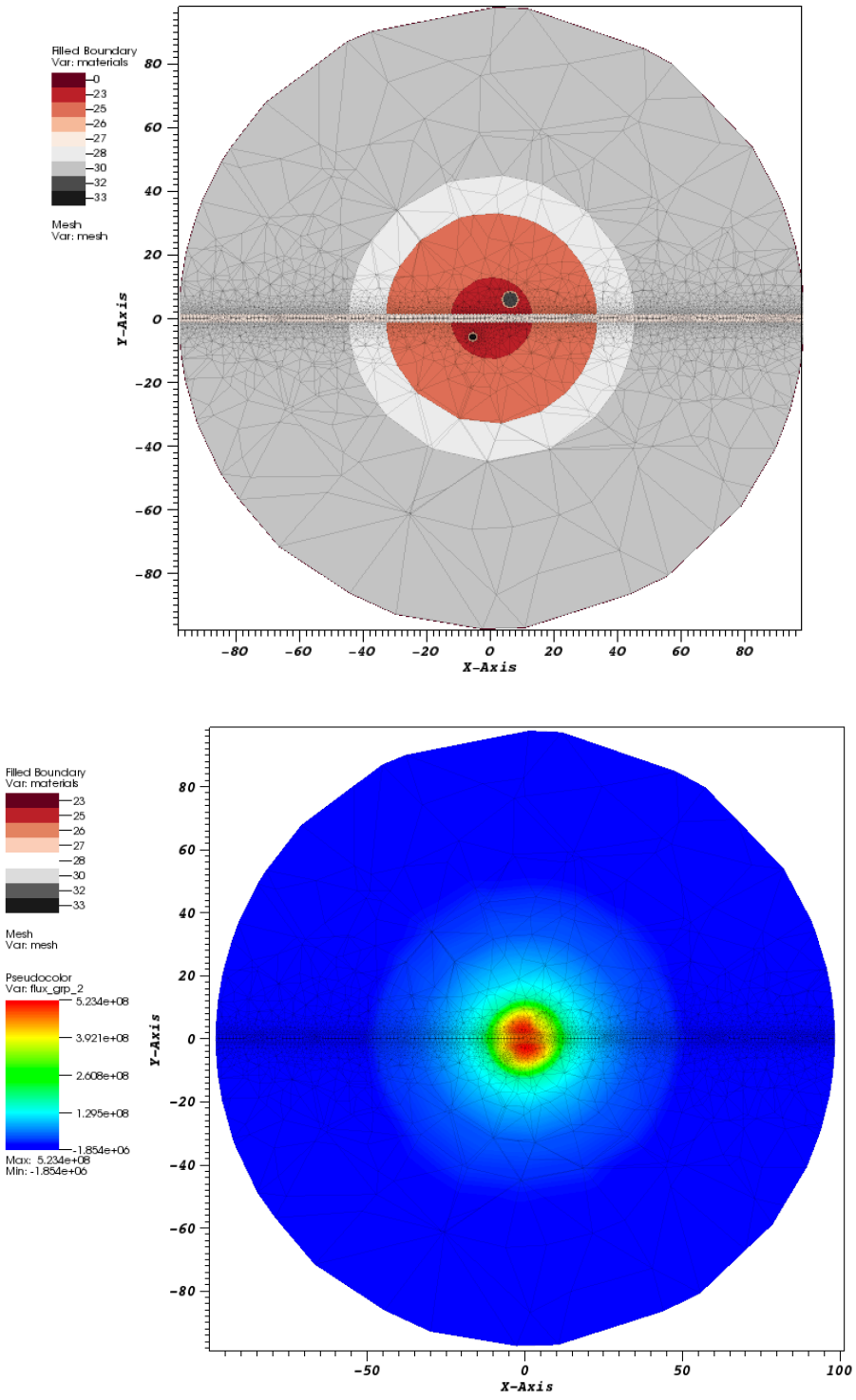

Figure 38. EVENT NETGEN Group 2 Neutron Flux Illustration

www.manaraa.com

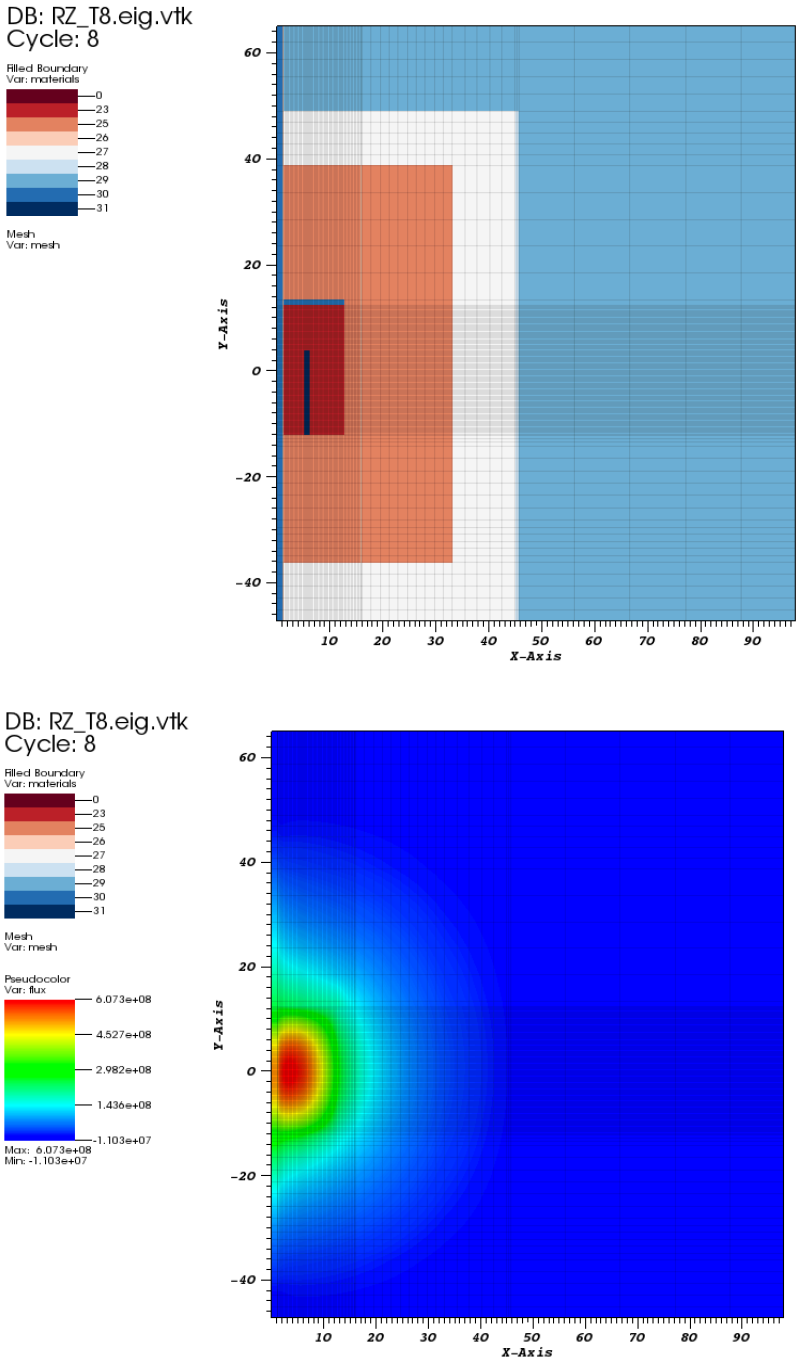

Figure 39. AGN EVENT RZ Neutron Flux Illustrations

www.manaraa.com

5.4 AGN-201M Time Dependent Calculations

5.4.1 Experimental Transient Configurations

The EVENT code was used to create a time-dependent delayed neutron source for use in modeling a variety of AGN experimental transient configurations. The delayed neutron source is based on the behavior of delayed neutron precursors that emit neutrons as a result of beta decay at half-lives of seconds to minutes after the precursors (fission products) are produced. The delayed neutron parameters, e.g., delayed neutron precursor decay constants and delayed neutron fractions, are defined in the simplified EVENT NETGEN and RZ models to generate a time-dependent source.

A total of 11 transient sequences (Figure 34) were performed by adjusting the reactor control elements until a delayed critical configuration was achieved. The AGN operations reactor logs are shown in Appendix B and are summarized in Table 23. This operational data shows the positions of the FCR and CCR control elements in the AGN core during the experiments. The FCR and CCR calibration curves [8] are used to determine the core reactivity changes as a result of rod movements in the core. The reactivity change can then define volume fractions of fuel and air in the AGN control elements for the transient analysis. Figure 33 illustrates the characteristics of the first transient sequence. The transient characteristics indicate three main time periods or sections: 1. Reactivity insertion and power ramp, 2. Reactivity removal to achieve a delayed critical configuration at a larger power level,

www.manaraa.com

and 3. Removal of the CCR from the AGN core to initate a prompt drop transient followed by the radioactive decay of the delayed neutron precursors. After the delayed neutrons have had a few minutes to decay, the next transient is initiated by inserting excess reactivity via the FCR and CCR rods. The rod positions in the core were varied to create unique transient characteristics for use with the EVENT transient analysis.

www.manaraa.com

Table 23. Summary of Experimental Transient Sequences

Transient Sequence #	Time	Channel 3 Reading	FCR* Experimental Position*** (cm)	CCR** Experimental Position*** (cm)	Comment from AGN Operational Data Log Sheet
Startup	1:25 pm	–	–	–	Reactor Restart
1	1:32 pm	–	24.52	20.16	Doubling time (DT) = 13.2 sec. Temperature (T) = 18.3 °C
	1:41 pm	6.8E-08	10.78	20.16	Steady power
	1:41 pm	–	–	–	CCR Dropped
	1:46 pm	–	10.78	97.46	CCR Drive Full Out
2	1:49 pm	–	24.53	20.14	Excess reactivity DT = 13.4 sec.; T = 18.3 °C
	1:55 pm	6.8E-08	20.28	18.00	Steady power
	1:57 pm	–	–	–	CCR Dropped
	1:59 pm	–	20.28	97.50	CCR Drive Full Out
3	2:00 pm	–	24.53	20.14	Excess reactivity DT = 13.3 sec.
	2:08 pm	6.8E-08	12.25	19.80	Steady power
	2:09 pm	–	–	–	CCR Dropped
	2:11 pm	–	12.25	97.42	CCR Drive Full Out
4	2:13 pm	–	24.53	20.23	Excess reactivity DT = 13.2 sec.
	2:20 pm	6.8E-08	12.31	19.90	Steady power
	2:21 pm	–	–	–	CCR Dropped
	2:22 pm	–	12.31	97.46	CCR Drive Full Out
5	2:24 pm	–	24.53	20.30	Excess reactivity DT = 13.5 sec.; T = 18.3 °C
	2:35 pm	6.8E-08	12.50	20.00	Steady power
	2:36 pm	–	–	–	CCR Dropped
	2:38 pm	–	12.50	97.51	CCR Drive Full Out
6	2:40 pm	–	24.53	20.37	Excess reactivity DT = 13.5 sec., T = 18.3 °C
	2:47 pm	6.8E-08	15.42	19.50	Steady power
	2:47 pm	–	–	–	CCR Dropped
	2:51 pm	–	15.42	97.68	CCR Drive Full Out
7	2:53 pm	–	24.53	20.51	Excess reactivity DT = 13.5 sec.; T = 18.3 °C
	2:59 pm	6.8E-08	17.80	19.00	Steady power
	3:02 pm	–	17.80	97.74	CCR Drive Full Out
8	3:10 pm	6.8E-08	21.50	18.34	Steady power
	3:11 pm	–	–	–	CCR Dropped
	3:13 pm	–	21.50	97.95	CCR Drive Full Out
9	3:14 pm	–	24.53	20.79	Excess reactivity DT = 13.4 sec.; T = 18.3 °C
	3:20 pm	6.8E-08	24.53	17.91	Steady power
	3:21 pm	–	–	–	CCR Dropped
	3:23 pm	–	24.53	98.19	CCR Drive Full Out
10	3:25 pm	–	24.53	21.02	Excess reactivity DT = 13.5 sec.; T = 18.3 °C
	3:33 pm	6.8E-08	11.42	21.02	Steady power
	3:33 pm	–	–	–	CCR Dropped
	3:35 pm	–	11.42	98.21	CCR Drive Full Out
11	3:37 pm	–	24.53	21.04	Excess reactivity DT = 13.6 sec.; T = 18.3 °C
	3:41 pm	6.8E-08	11.48	21.04	Steady power
	3:42 pm	–	–	–	SR2 Dropped
Shutdown	3:46 pm	–	–	–	About 10 mW – Seems to flatten out – DT = 55 sec.
	3:48 pm	–	–	–	Manual Scram

*FCR – full in: 24.53 cm; full out: 1:09 cm
**CCR – full in: 20.91 cm; full out: 97.93 cm (-2.07 cm)
***Rod Positions – The rod positions are known to an accuracy of about ±0.5 cm.

www.manaraa.com

The experimental CCR and FCR rod position data listed in Table 23 were used to determine the change in reactivity occurring when the FCR and CCR control elements were moved from one position in the core to another position. The change in rod positions were quantified via comparison with the AGN FCR and CCR calibration curves [8] to determine the net change in system reactivity during the transient sequences. The resulting net change in reactivity caused by moving the FCR or CCR from an initial position to a final position is equated to a reactivity change in the EVENT models to analyze each of the transient sequences. The reactivity changes in the simplified EVENT RZ and NETGEN models are approximated by representing control rod position changes to a changes in the fuel volume fraction in the control element volume in the model. Model reactivity changes as a result of a geometrical control rod movements is not considered in this work because of the model complexity required to represent fine changes in reactivity.

5.4.2 EVENT Time Dependent Calculation Methodology

5.4.2.1 General Discussion

As previously discussed, the EVENT code has the capability to model time-dependent problems and is used for the AGN experimental transient analysis. The GEM pre-processor is used to generate an eigenvalue EVENT input file used to calculate the delayed neutron precursor concentration and neutron flux prior to initiating the transient. The eigenvalue problem

www.manaraa.com

considers the AGN configuration, i.e., control element positions, prior to the initation of a transient. The transient models assume the AGN is operating at delayed critical prior to initiating a transient.

Both the simplified EVENT RZ and NETGEN models were used for the transient sequence analysis calculations. There are significant differences between the two models, especially with respect to the differences in their geometric configuration and complexity. A 3rd order of scattering anisotropy and the diffusion theory approximation, P_1, were used for these calculations. This is reasonable because, assuming a high precision EVENT model, i.e., stringent convergence criteria, the transient analysis only needs to model changes in reactivity, which eliminates the need to model the exact control rod locations in the core. Only an approximate representation of the rods are required to represent precise changes in the system reactivity as a result of experimental control rod movements. Extensive scoping calculations have verified the diffusion theory approximation, P_1, is capable of modeling the transient experiments performed on the AGN. Further, the AGN operates at essentially zero power, so there is no need to consider temperature or other reactivity feedback effects on cross sections, e.g., Doppler broadening effects. Extensive scoping EVENT computations using transport theory (>P_3 Legendre flux expansion), rather than using the diffusion theory approximation, P_1, resulted in issues with respect to the adaptive time step algorithm in EVENT and resulted in EVENT using extremely small time

www.manaraa.com

steps, ~10-12 sec. per time interval. A single P_3 (transport theory) EVENT run would take 6-9 hours to complete compared to <5 min. for a P_1 (diffusion theory) case using adaptive time steps. Typically, these cases would also fail to execute completely. Explicit time steps is an option for using transport theory for the calculation; however, based the results of these scoping studies, the diffusion theory approximation was deemed adequate for this work.

The 2-group multigroup cross-section library, based on ENDF/B-VII.1 data, was used for the time-dependent EVENT analyses based on the excellent results obtained from the steady-state EVENT calculations. Further, the use of 2-group cross sections for these calculations would also increase the efficiency of the EVENT cases rather than using a cross-section library with more energy groups. As shown in Figure 40, the EVENT time dependent model methodology includes two separate GEM input files. One input file corresponds to the eigenvalue computation, the initial delayed neutron precursor concentration, and the neutron flux computations. The second input file corresponds to the time dependent calculation that defines the multiple time zones, control rod reactivity data, delayed neutron source, delayed neutron decay constants and delayed neutron fractions.

www.manaraa.com

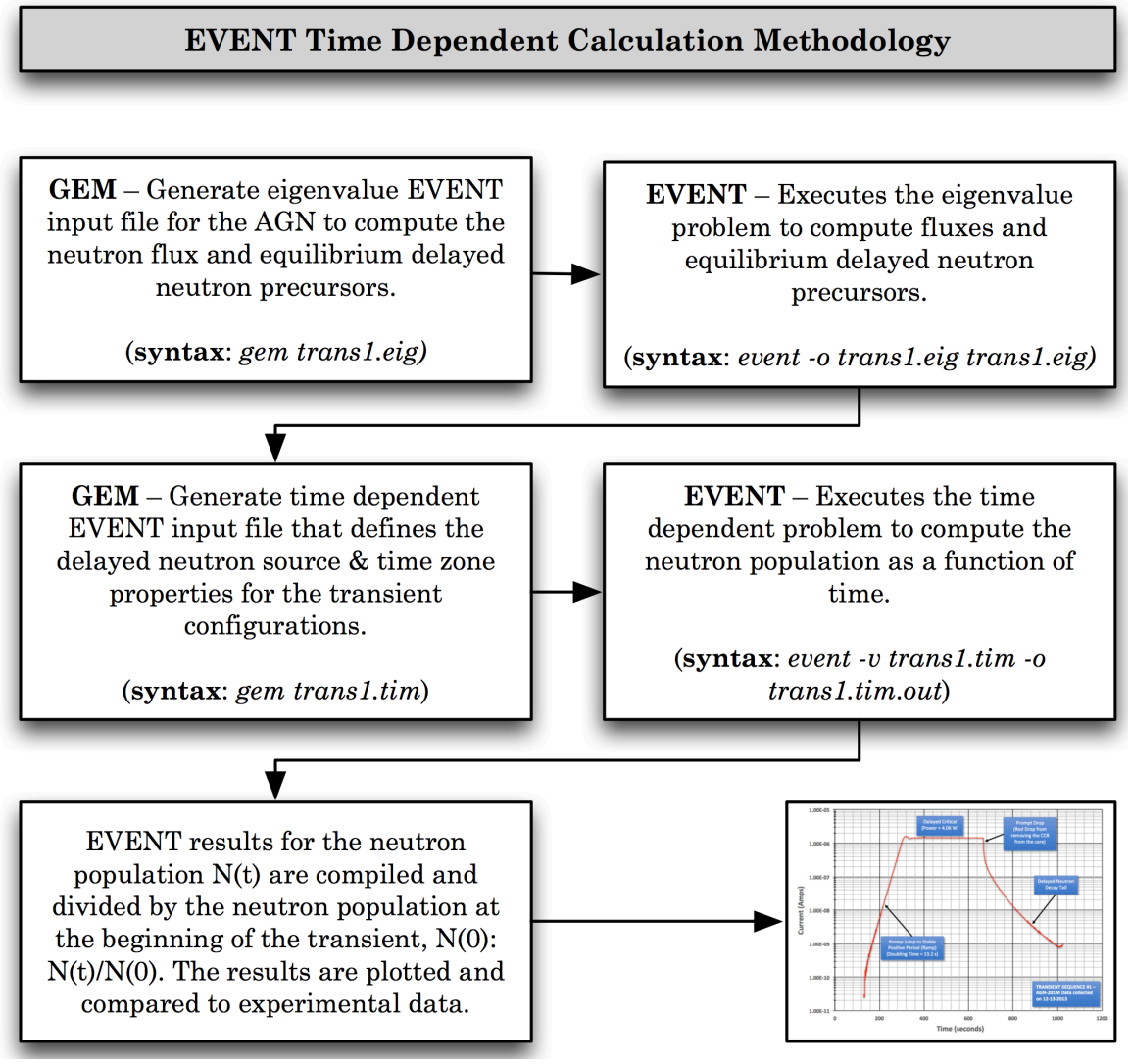

Figure 40. EVENT Time Dependent Calculation Methodology

The volume fractions of the fuel and air must equate the reactivity change data from the actual AGN FCR and CCR rod positions (Table 23) directly to reactivity in the EVENT models. This was done by calculating high precision (P_1) rod calibration curves for each of the simplified EVENT NETGEN and RZ models. The FCR calibration curve from the AGN operational procedure [8] used to quantify changes in reactivity from the FCR rod positions in Table

www.manaraa.com

23 is provided in Figure 41. The equation listed in Figure 41 (Equation 48) provides the relationship between the FCR reactivity and rod position and is defined as

$$y = -2.5479\times10^{-3}x^3 + 1.2192\times10^{-1}x^2 + 1.8978\times10^{-1}x$$

Equation 48

where y is the reactivity (cents) for a particular FCR position in the AGN core, x (cm).

The CCR calibration curve from the AGN operational procedure [8] is used to quantify changes in reactivity from the AGN rod positions in Table 25 is provided in Figure 42. The equation listed in Figure 42 (Equation 49) provides the relationship between the CCR reactivity and rod position and is defined as

$$y = -7.1253\times10^{-03}x^3 + 4.439\times10^{-01}x^2 + 4.2336\times10^{-01}x$$

Equation 49

where y is the reactivity (cents) for a particular CCR position, x (cm).

As shown in Figure 43, the change in reactivity, $\Delta\rho = \rho_2 - \rho_1$, associated with an FCR or a CCR position change, $\Delta x = x_2 - x_1$, is equated directly to the volume fraction of fuel, $\Delta vf = vf_2 - vf_1$, in the FCR and CCR in the EVENT NETGEN model. The difference in the volume fraction of fuel from unity, *1-Δvf*, represents air in the control rod region not filled with fuel.

www.manaraa.com

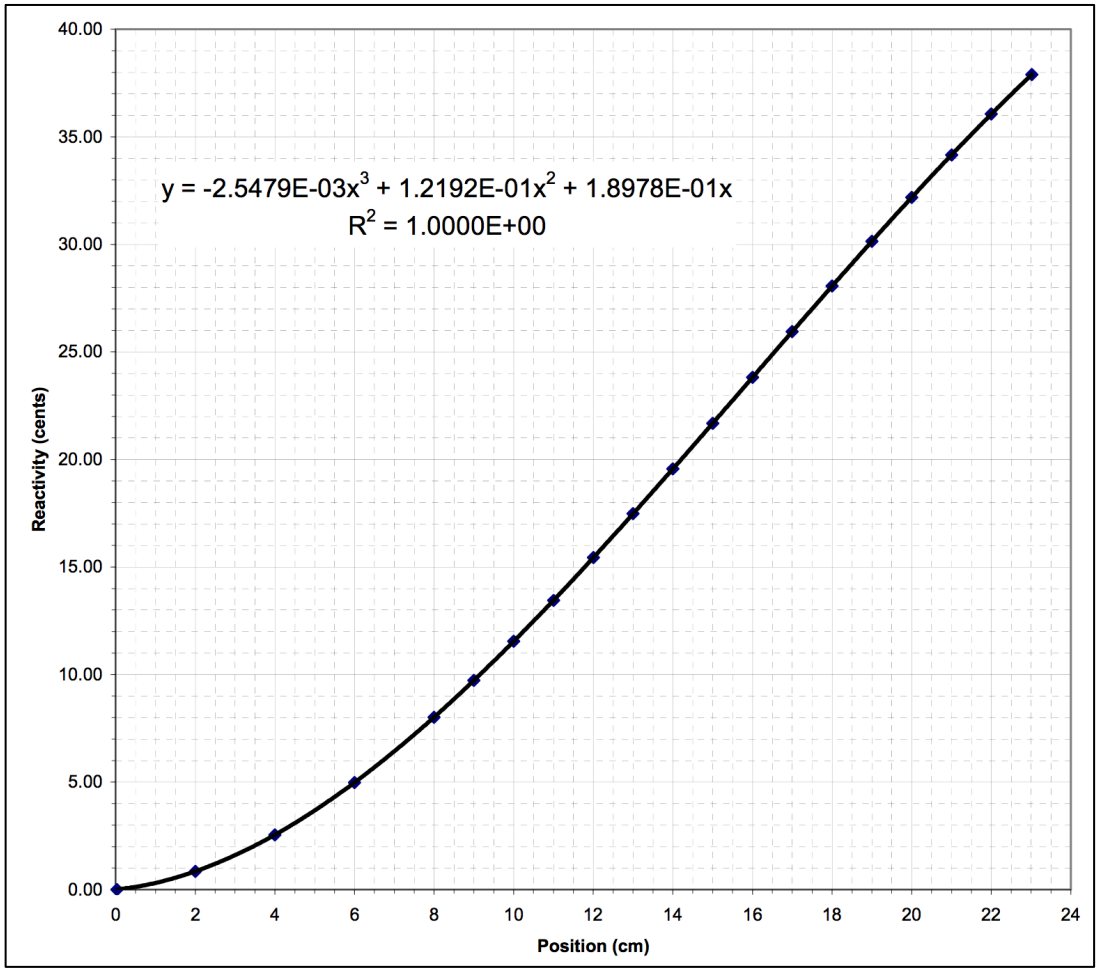

Figure 41. UNM AGN Fine Control Rod Calibration Curve [8]

www.manaraa.com

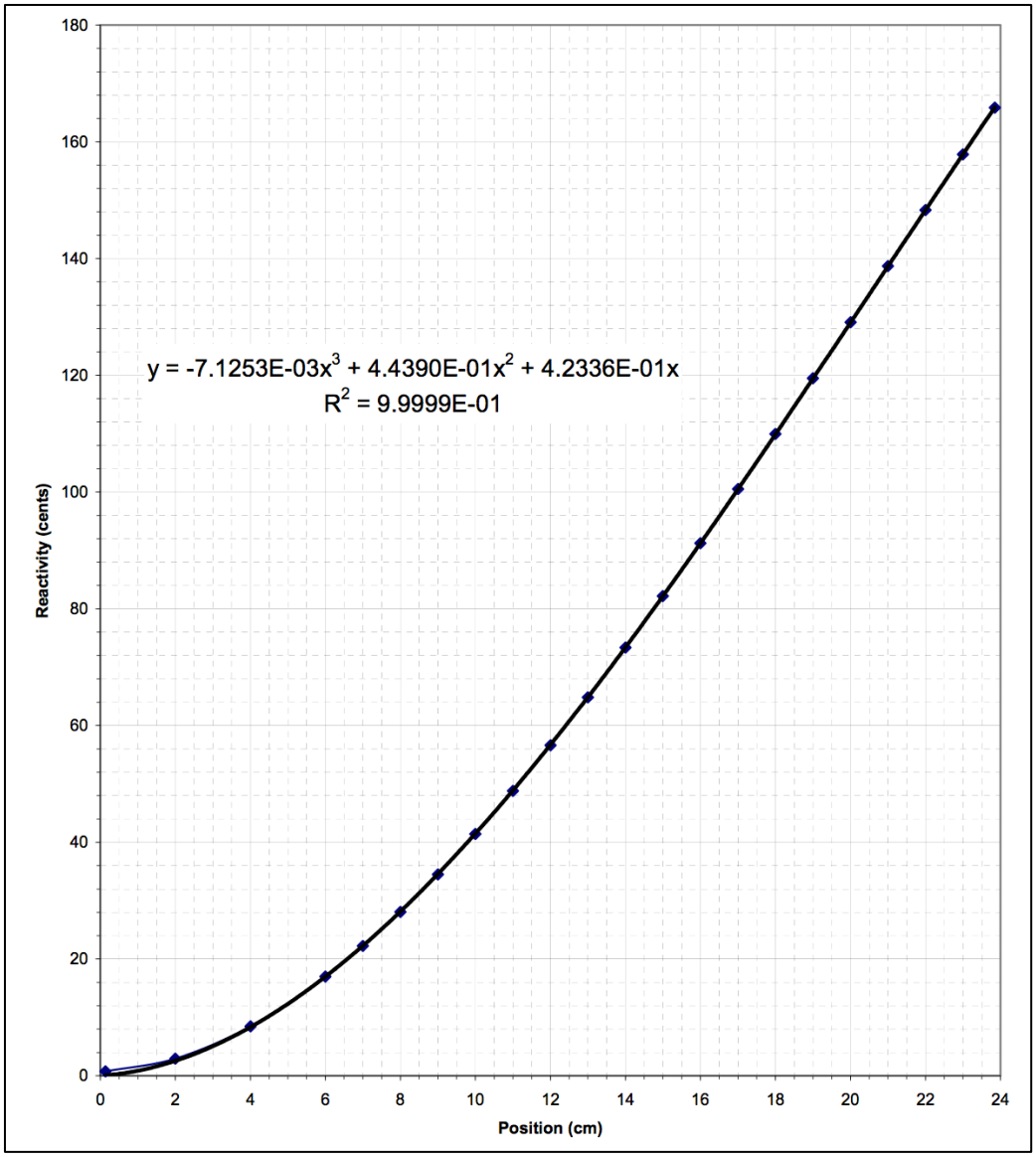

Figure 42. UNM AGN Coarse Control Rod Calibration Curve [8]

www.manaraa.com

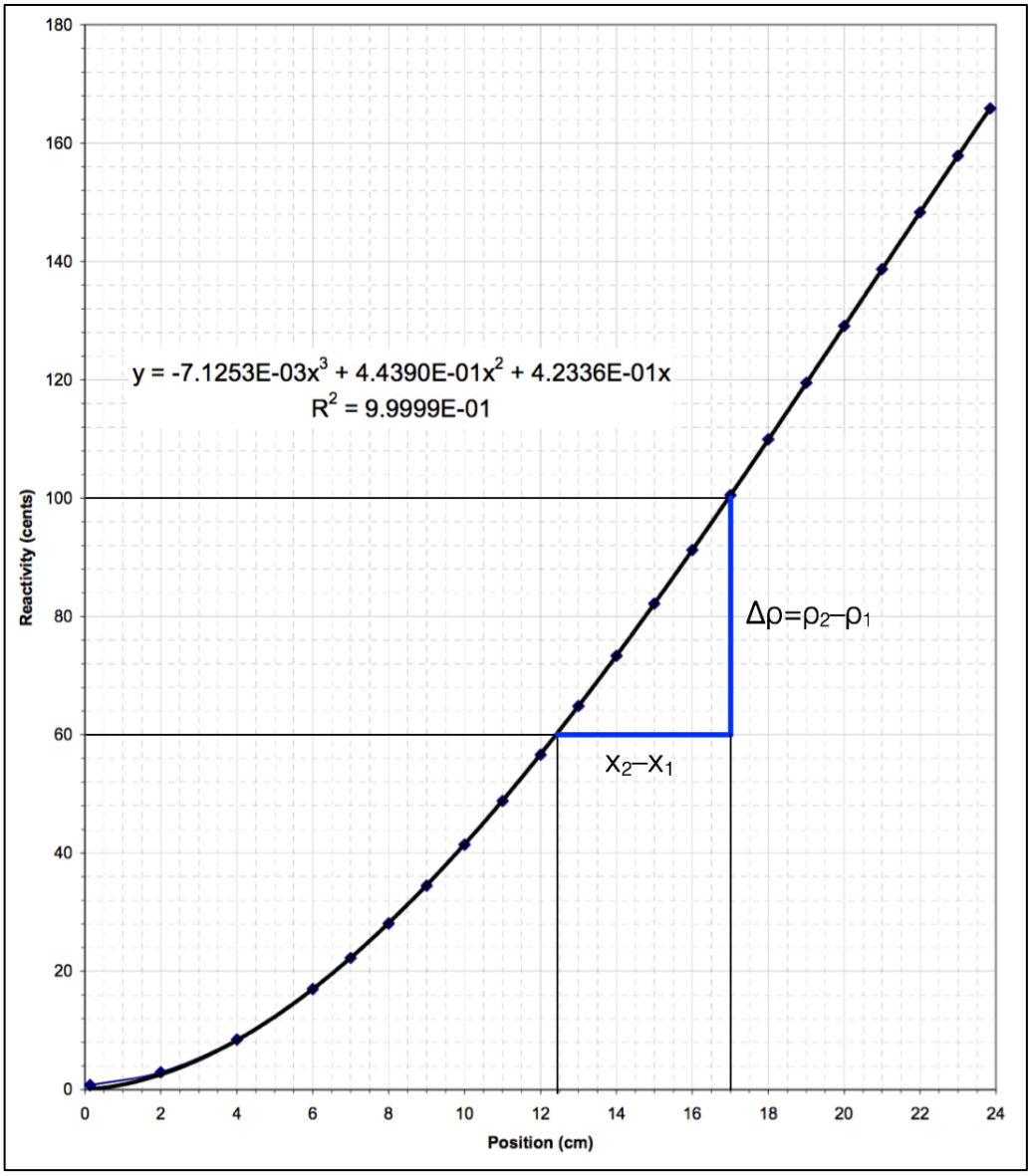

Figure 43. Equating AGN Control Rod Positions to a Reactivity Change

www.manaraa.com

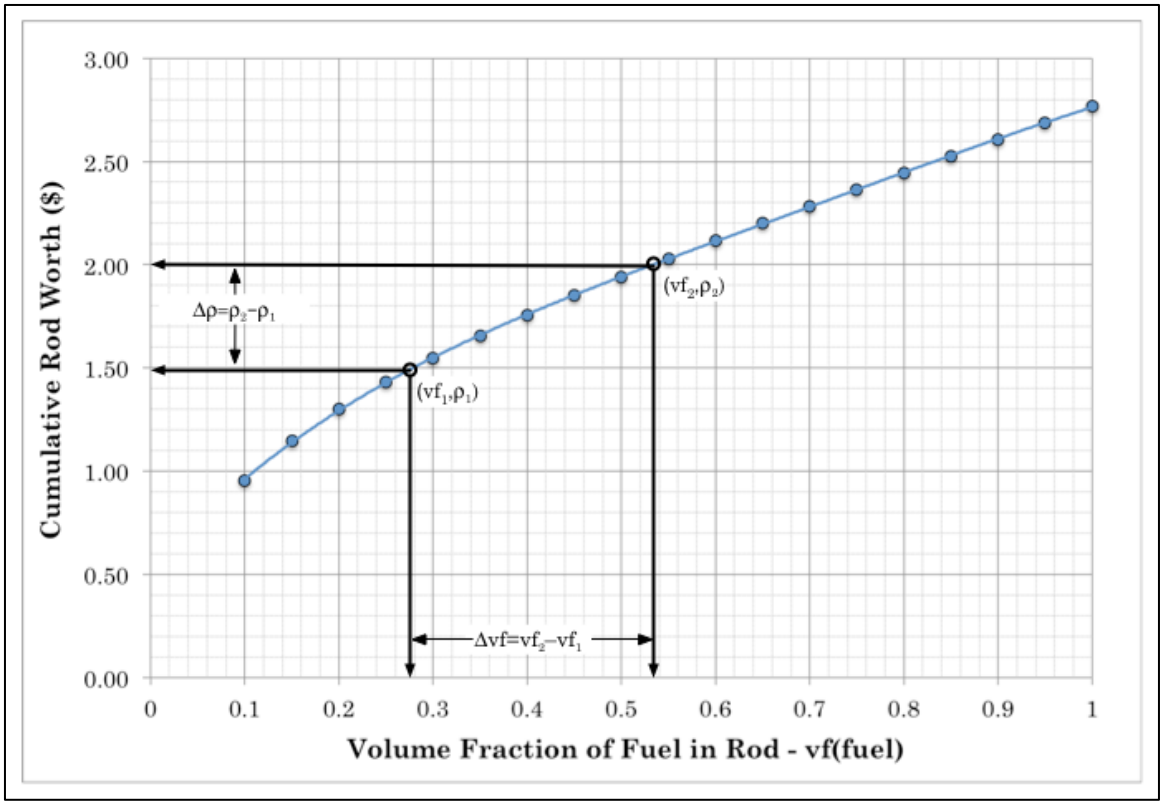

Figure 44. Equating AGN Control Rod Position to Reactivity Change

5.4.2.2 EVENT Model Description

The simplified EVENT NETGEN and RZ models, presented previously, were used for the AGN experimental transient analyses. Each of these models required two GEM and EVENT input files, one input file for an eigenvalue problem and another input file for the time dependent analysis that defines a delayed neutron source and material characteristics for transient time zones. Delayed neutron parameters calculated by Keepin [58] and Brady [59] are provided in Table 24. A comparison of the appropriate delayed neutron parameters from the Keepin and Brady data shows good agreement, although there are small differences in the delayed neutron

www.manaraa.com

fractions for each dataset and some differences between the Keepin and Brady decay constant data in groups 5 and 6. The delayed neutron source defined in GEM, by default, assumed to be the Keepin data. The effective delayed neutron fraction, β_{eff}, for the AGN is 0.0074 [4] and the transient analysis performed in the UNM AGN SAR [11] assumes a β_{eff} of 0.0075. Thus, approximately 0.74% of the neutrons present in the AGN are delayed neutrons while the rest (99.26%) are prompt neutrons. The presence of delayed neutrons in the system allows for operations on time-scales that permit human control of the reactor. The time scale of a nuclear reactor with only prompt neutrons present is too small and the rapid increase in the neutron population precludes the possibility of control except for reactivity feedback effects, i.e., density changes, solution boiling, bubble formation, fuel melting, etc. The delayed neutron data is used in the time-dependent EVENT models to define a volume distributed neutron source for transient analysis. The data have to be entered into both the GEM eigenvalue and GEM time-dependent input files.

www.manaraa.com

Table 24. Delayed Neutron Parameters

Delayed Neutron Group	Keepin [58] for a Thermal ^{235}U System		Brady [59] Data for a Thermal ^{235}U System		MCNP6 Kinetics Parameters (5.0E+07 neutron histories)	
	Decay Constant, λ (sec^{-1})	β_i	Decay Constant, λ (sec^{-1})	β_i	Decay Constant, λ (sec^{-1})	β_i
1	1.241E-02	2.1557E-04	1.241E-02	2.110E-04	1.334E-02	2.70E-04
2	3.054E-02	1.4249E-03	3.050E-02	1.400E-03	3.273E-02	1.34E-03
3	1.1101E-01	1.2760E-03	1.110E-01	1.250E-03	1.121E-01	1.38E-03
4	3.0142E-01	2.5790E-03	3.010E-01	2.530E-03	3.029E-01	2.78E-03
5	1.1482E+00	7.5644E-04	1.130E+00	7.360E-04	8.505E-01	1.15E-03
6	3.03737E+00	2.7208E-04	3.000E+00	2.690E-04	2.855E+00	4.90E-04
Prompt Neutron Lifetime					100 μsec [2]	
β_{eff}					0.0074 [4]	

Each of the transients are defined in EVENT by using a time zone concept. Each time zone corresponds to a transient caused by the movement of the AGN FCR and/or CCR in the core that is represented in the model by material property changes, i.e., fuel volume fraction increases or decreases in the control rod tubes. For example, the first time zone corresponds to a steady-state, i.e., delayed critical configuration, the second time zone corresponds to the rod insertion and subsequent prompt jump to a stable period, the third time zone corresponds to a rod removal step to achieve a steady state configuration at a higher power level, and the fourth, and last, time zone corresponds to the prompt drop (rod drop) where the CCR is quickly removed from the core resulting in a rapid power drop and decay of the delayed neutron precursors present. System reactivity changes due to

www.manaraa.com

control rod movement in the models are represented as a mixture of fuel and air. The sum of the fuel and air volume fractions must equal 1.0.

5.4.3 Transient Modeling with the EVENT RZ Model

The simplified EVENT RZ model is illustrated in Figure 32 and is used for the transient analysis. Two separate EVENT RZ input files are created in GEM for the transient analysis. The first EVENT input is required for an eigenvalue computation to calculate the steady-state neutron flux and delayed neutron precursors. The second EVENT input is required to analyze the transient sequence. The eigenvalue input is also used to generate a high precision annular control rod calibration curve (Figure 45). This curve is used to equate experimental AGN reactivity changes based upon the control rod movements to reactivity changes in the EVENT transient input. As shown in Figure 43, the change in reactivity, $\Delta\rho = \rho_2 - \rho_1$, associated with an FCR or a CCR position change, $\Delta x = x_2 - x_1$, is equated directly to the volume fraction of fuel, $\Delta vf = vf_2 - vf_1$, in the annular control rod in the EVENT RZ model (Figure 44). The difference in the volume fraction of fuel from unity, *1-Δvf*, represents air in the control rod region not filled with fuel. The calibration curve was fitted to a curve using Microsoft Excel and the curve fit equation used to calculate a control rod fuel volume fraction based on the UNM AGN experimental reactivity changes from the control rod movement data. The annular control element calibration curve was fitted to a 4^{th} order polynomial (Equation 50) with a high degree of correlation as follows

www.manaraa.com

$$y = -11.898x^4 + 32.437x^3 - 33.056x^2 + 19.306x - 2.2804$$

Equation 50

where y is the reactivity (dollars) for the annular control rod and x is the fuel volume fraction in the control rod region (unitless). The annular control rod calibration curve for the EVENT RZ model shown in Figure 45 also shows the reactivity data for a P_5 case for comparison purposes. The P_1 calculation clearly illustrates that the diffusion theory approximation provides greater control rod worth values compared to the P_5 case for a particular fuel volume fraction. The P_5 case compares well to the cumulative worth for the AGN control rods; however, the P_1 case can still accurately equate the reactivity changes from the AGN experimental data to EVENT volume fraction data. The P_5 time-dependent EVENT case did not execute successfully in the scoping analysis. Figure 45 also shows only the reactivity data for fuel volume fraction greater than 0.1 were used for the curve fit to simplify the order of polynomial needed for the curve fit.

www.manaraa.com

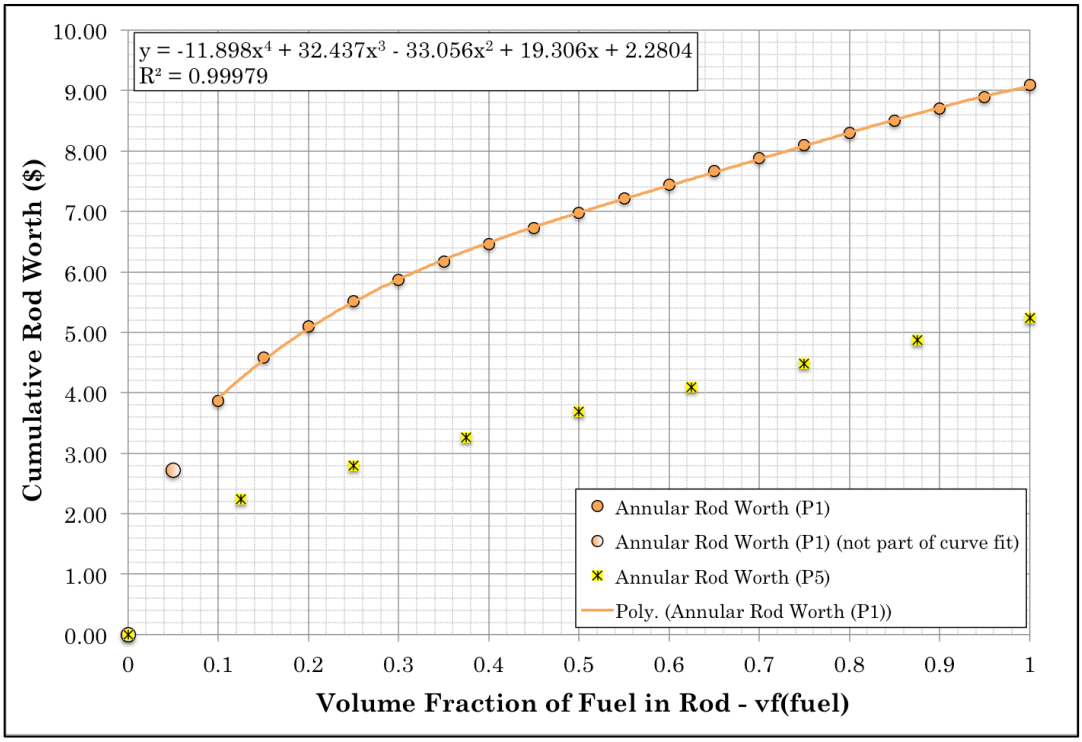

Figure 45. EVENT RZ Annular Control Element Calibration Curve

The eigenvalue GEM input file was created with the annular control rod at an initial position corresponding to a steady-state configuration where, by definition, the reactivity is zero. The time-dependent EVENT GEM input file defines the fuel and air volume fractions for the annular control rod for each transient modeled in a time zone region of the model. Initially, the time-dependent GEM file considers time zone 0 as the steady-state configuration just prior to the first transient. The k_{eff} is normalized in the GEM time-dependent file to ensure the transients are initiated at with the AGN at a delayed critical state. Time zone 1, then defines the control rod fuel and air volume fractions corresponding to the change in reactivity due to the movement of the FCR and CCR in the AGN experiment. The sum of the

www.manaraa.com

reactivity contributions for the FCR and CCR is translated and equated to a reactivity change in the EVENT RZ model. Table 25 provides the following modeling elements for all 11 AGN experimental transient configurations:

- Transient number,
- Transient type,
- Transeint duration in seconds,
- Cumulative transient duration in seconds,
- Annular control rod fuel component volume fraction,
- Annular control rod void component volume fraction, and
- Reactivity worth of the transient in cents of reactivity.

www.manaraa.com

Table 25. EVENT RZ Transient Model Reactivity Definitions

Trans. #	Trans. Type	Transient Duration (sec.)	Cumulative Duration (sec.)	Control Element Fuel Volume Fraction – vf(fuel)	Control Element Fuel Volume Fraction – vf(air)	Reactivity Worth (cents)
1	Ramp	174	174	0.561	0.439	27.67
	DC*	346	520	0.5	0.5	0
	Rod Drop	334	854	0.235	0.765	-160.25
2	Ramp	101	101	0.564	0.436	28.76
	DC	388	489	0.5	0.5	0
	Rod Drop	150	639	0.261	0.739	-139.53
3	Ramp	68	68	0.563	0.437	28.36
	DC	454	522	0.5	0.5	0
	Rod Drop	180	702	0.239	0.761	-156.82
4	Ramp	80	82	0.562	0.438	27.96
	DC	410	492	0.5	0.5	0
	Rod Drop	160	652	0.238	0.762	-157.77
5	Ramp	75	77	0.56	0.44	27.3
	DC	660	737	0.5	0.5	0
	Rod Drop	115	852	0.237	0.763	-158.73
6	Ramp	69	71	0.559	0.441	26.8
	DC	370	441	0.5	0.5	0
	Rod Drop	264	705	0.243	0.757	-153.95
7	Ramp	98	100	0.562	0.438	27.86
	DC	379	479	0.5	0.5	0
	Rod Drop	143	622	0.248	0.752	-149.16
8	Ramp	68	71	0.553	0.447	23.82
	DC	392	463	0.5	0.5	0
	Rod Drop	145	608	0.256	0.744	-142.81
9	Ramp	55	58	0.561	0.439	27.55
	DC	360	418	0.5	0.5	0
	Rod Drop	180	598	0.262	0.738	-138.66
10	Ramp	75	78	0.559	0.441	26.5
	DC	465	543	0.5	0.5	0
	Rod Drop	125	668	0.226	0.774	-168.38
11	Ramp	68	71	0.558	0.442	26.41
	DC	284	355	0.5	0.5	0
	Rod Drop	342	697	0.213	0.787	-180.02

*Delayed Critical

5.4.4 Transient Modeling with the EVENT NETGEN Model

The simplified EVENT NETGEN model from Section 4.5.3 is used to analyze the 11 AGN transient sequences to compare to the EVENT RZ model results. The simplied EVENT NETGEN model is much more complex than the EVENT RZ model as a result of the 3-D geometry. The model has more finite elements and a more complex mesh (Delauney), which requires more execution time to complete the transient sequence calculations. The 2-group

www.manaraa.com

ENDF/B-VII.1 cross section library and Keepin delayed neutron data (Table 24) was used for the analysis. As in the EVENT RZ model, the three components (prompt jump, delayed critical, and prompt drop) of the transient sequence calculations may not match up exactly. This is due to the fine rod movements performed by the reactor operators when the excess reactivity is gradually removed from the core as the desired power level is approached. Experimental uncertainties, e.g., rod height, fissile mass, can also affect how the sequence matches up to the experimental data.

These time-dependent calculations required equating reactivity changes in the experiment to the time dependent model, which involved the generation of both FCR and CCR calibration curves. This was performed by estimating the reactivity changes (Figure 43) due to FCR and CCR rod position changes in the experiments by using the FCR and CCR calibration curves from the UNM AGN operations manual [8]. For example, if the FCR in the AGN core was moved from a core position of 9 cm to a position of 6 cm, the resulting change in reactivity would be worth about -5¢ (0.05β_{eff}) of reactivity (Figure 41). If a transient resulted from a change to both the FCR and the CCR control rod positions, the reactivity values for each rod are directly considered in the FCR and in the CCR reactivity worths for the EVENT NETGEN model.

The methodology for equating AGN control rod position is the same as that considered in Section 5.4.3. The AGN rod position changes in the

www.manaraa.com

experiments were defined by representing the FCR and CCR control rod regions as fuel and air volume fractions. As shown in Figure 43, the change in reactivity, $\Delta\rho = \rho_2 - \rho_1$, associated with an FCR or a CCR position change, $\Delta x = x_2 - x_1$, is equated directly to the volume fraction of fuel, $\Delta vf = vf_2 - vf_1$, in the FCR and CCR in the EVENT NETGEN model. The difference in the volume fraction of fuel from unity, *1-Δvf*, represents air in the control rod region not filled with fuel.

An eigenvalue parametric study was performed with the EVENT NETGEN model to generate control element reactivity calibration curves as a function of fuel volume fraction in the control rod. The NETGEN model required the generation of two calibration curves, one for the FCR and one for the CCR. These EVENT eigenvalue computations were performed using P_1 Legendre flux expansion (diffusion theory approximation) and a rigorous convergence criteria to ensure a precise calibration curve was generated. Equations were fit to the calibration curves for a fuel volume fraction greater than 0.1 (to ensure a simple fit equation) using Microsoft Excel. The fit equations are used to calculate a control rod fuel volume fraction based on the UNM AGN experimental reactivity changes from the control rod movement data. Figure 46 illustrates the EVENT NETGEN FCR calibration curve and Figure 47 shows the CCR calibration curve.

www.manaraa.com

The FCR and CCR calibration curves were fitted to 4th order polynomials (Equation 51) with a high degree of correlation. The FCR fitted curve equation is

$$y = -0.8403x^4 + 2.2845x^3 - 2.3121x^2 + 1.3947x + 0.4702$$

Equation 51

where y is the reactivity (dollars) for the FCR and x is the fuel volume fraction in the model (unitless). The CCR fitted curve equation (Equation 52) is

$$y = -2.4229x^4 + 6.7963x^3 - 7.1463x^2 + 5.0085x + 0.5262$$

Equation 52

where y is the reactivity (dollars) for the CCR and x is the fuel volume fraction in the model (unitless). The curve fit equation for both the FCR and CCR is valid for fuel volume fractions greater than 0.1 to simplify the order of the polynomial for the curve fit. Also, a P_7 case was used to calculate a reactivity data to compare to the P_1 calibration curve. As was shown for the EVENT RZ model, the P_1 case provides greater reactivity results than the P_7 case, although the P_1 case is more than sufficient to model the AGN transients.

www.manaraa.com

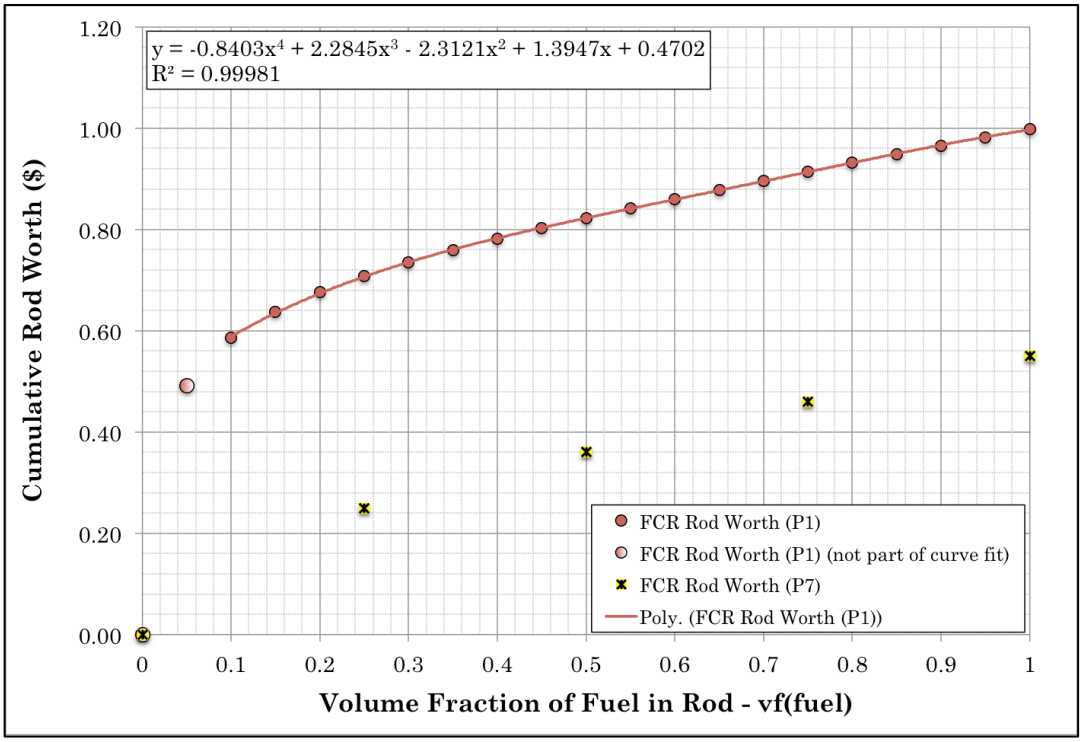

Figure 46. EVENT NETGEN Fine Control Rod Calibration Curve

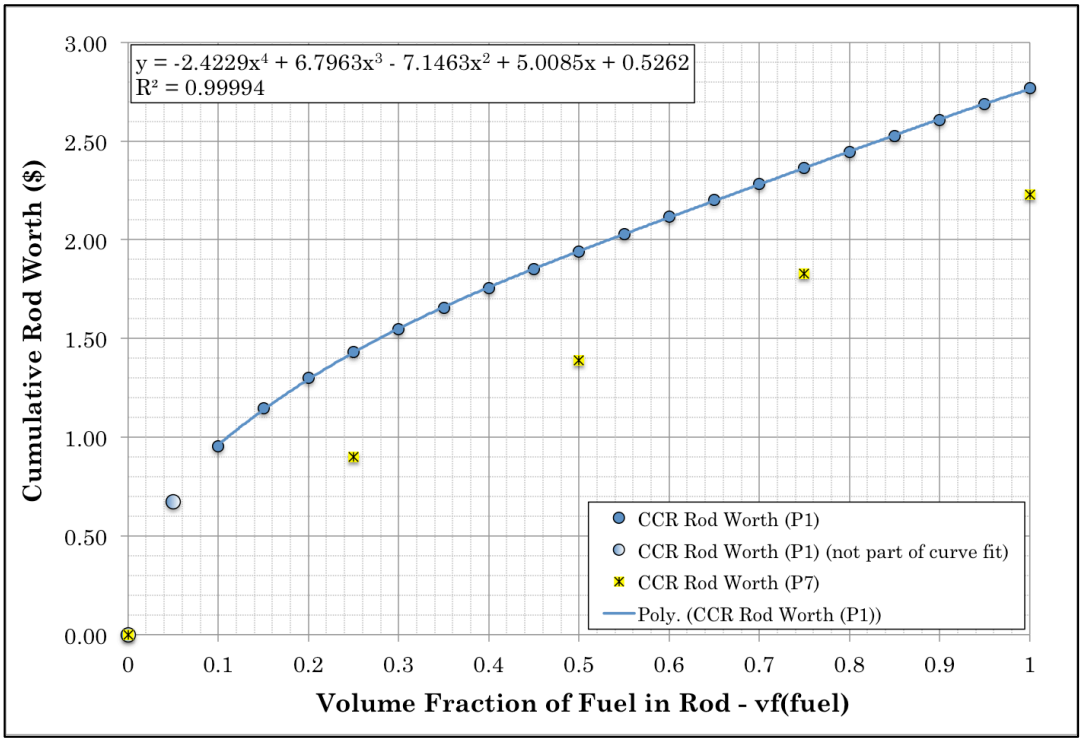

Figure 47. EVENT NETGEN Coarse Control Rod Calibration Curve

www.manaraa.com

The experimental control rod worth data for use with the EVENT NETGEN model is summarized in Table 26 and provides the control rod volume fractions for use in the EVENT NETGEN time-dependent models. Delayed neutron data from Keepin (Table 24) and ENDF/B-VII.1 2-group cross sections were used in these calculations. Table 27 provides the following modeling elements for all eleven AGN experimental transient configurations in the EVENT NETGEN time-dependent model:

- Transient number,
- Transient type,
- Transeint duration in seconds,
- Cumulative transient duration in seconds,
- Annular control rod fuel component volume fraction,
- Annular control rod void component volume fraction, and
- Reactivity worth of the transient in cents of reactivity.

www.manaraa.com

Table 26. EVENT NETGEN Transient Model Reactivity Definitions

Trans. #	Trans. Type	Transient Duration (sec.)	Cumulative Duration (sec.)	Control Element Fuel Volume Fraction – vf(fuel)	Control Element Fuel Volume Fraction – vf(air)	Reactivity Worth (cents)
1	Ramp	175	175	0.852 (FCR)	0.148 (FCR)	27.67 (FCR)
				1.0 (CCR)	0.0 (CCR)	0.0 (CCR)
	DC*	347	522	0.2 (FCR)	0.8 (FCR)	-27.67 (FCR)
				1.0 (CCR)	0.0 (CCR)	0.0 (CCR)
	Rod Drop	334	856	0.2 (FCR)	0.8 (FCR)	0.0 (FCR)
				0.156 (CCR)	0.843 (CCR)	-160.25 (CCR)
2	Ramp	103	103	0.487 (FCR)	0.513 (FCR)	8.23 (FCR)
				0.723 (CCR)	0.277 (CCR)	20.53 (CCR)
	DC	352	455	0.3 (FCR)	0.7 (FCR)	-8.23 (FCR)
				0.6 (CCR)	0.4 (CCR)	-20.53 (CCR)
	Rod Drop	138	593	0.3 (FCR)	0.7 (FCR)	0.0 (FCR)
				0.040 (CCR)	0.960 (CCR)	-139.53 (CCR)
3	Ramp	68	68	0.957 (FCR)	0.043 (FCR)	24.93 (FCR)
				0.721 (CCR)	0.279 (CCR)	3.43 (CCR)
	DC	454	522	0.3 (FCR)	0.7 (FCR)	-24.93 (FCR)
				0.7 (CCR)	0.3 (CCR)	-3.43 (CCR)
	Rod Drop	180	702	0.3 (FCR)	0.7 (FCR)	0.0 (FCR)
				0.039 (CCR)	0.961 (CCR)	-156.82 (CCR)
4	Ramp	75	75	0.953 (FCR)	0.047 (FCR)	24.82 (FCR)
				0.719 (CCR)	0.281 (CCR)	3.14 (CCR)
	DC	247	322	0.3 (FCR)	0.7 (FCR)	-24.82 (FCR)
				0.7 (CCR)	0.3 (CCR)	-3.14 (CCR)
	Rod Drop	170	492	0.3 (FCR)	0.7 (FCR)	0.0 (FCR)
				0.037 (CCR)	0.963 (CCR)	-157.77 (CCR)
5	Ramp	74	74	0.941 (FCR)	0.059 (FCR)	24.45 (FCR)
				0.817 (CCR)	0.183 (CCR)	2.85 (CCR)
	DC	670	744	0.3 (FCR)	0.7 (FCR)	-24.45 (FCR)
				0.8 (CCR)	0.2 (CCR)	-2.85 (CCR)
	Rod Drop	143	887	0.3 (FCR)	0.7 (FCR)	0.0 (FCR)
				0.074 (CCR)	0.926 (CCR)	-158.72 (CCR)
6	Ramp	69	69	0.769 (FCR)	0.231 (FCR)	18.51 (FCR)
				0.850 (CCR)	0.150 (CCR)	8.29 (CCR)
	DC	367	436	0.3 (FCR)	0.7 (FCR)	-18.51 (FCR)
				0.8 (CCR)	0.2 (CCR)	-8.29 (CCR)
	Rod Drop	264	700	0.3 (FCR)	0.7 (FCR)	0.0 (FCR)
				0.086 (CCR)	0.914 (CCR)	-153.95 (CCR)
7	Ramp	98	98	0.630 (FCR)	0.370 (FCR)	13.47 (FCR)
				0.888 (CCR)	0.112 (CCR)	14.41 (CCR)
	DC	372	470	0.3 (FCR)	0.7 (FCR)	-13.47 (FCR)
				0.8 (CCR)	0.2 (CCR)	-14.41 (CCR)
	Rod Drop	143	615	0.3 (FCR)	0.7 (FCR)	0.0 (FCR)
				0.098 (CCR)	0.902 (CCR)	-149.16 (CCR)
8	Ramp	67	67	0.423 (FCR)	0.577 (FCR)	5.72 (FCR)
				0.911 (CCR)	0.089 (CCR)	18.11 (CCR)
	DC	395	462	0.3 (FCR)	0.7 (FCR)	-5.72 (FCR)
				0.8 (CCR)	0.2 (CCR)	-18.11 (CCR)
	Rod Drop	145	607	0.3 (FCR)	0.7 (FCR)	0.0 (FCR)
				0.115 (CCR)	0.885 (CCR)	-142.81 (CCR)
9	Ramp	55	55	0.3 (FCR)	0.7 (FCR)	0.0 (FCR)
				0.973 (CCR)	0.027 (CCR)	27.55 (CCR)
	DC	362	417	0.3 (FCR)	0.7 (FCR)	0.0 (FCR)
				0.8 (CCR)	0.2 (CCR)	-27.55 (CCR)
	Rod Drop	183	600	0.3 (FCR)	0.7 (FCR)	0.0 (FCR)
				0.127 (CCR)	0.873 (CCR)	-138.66 (CCR)

www.manaraa.com

Trans. #	Trans. Type	Transient Duration (sec.)	Cumulative Duration (sec.)	Control Element Fuel Volume Fraction – vf(fuel)	Control Element Fuel Volume Fraction – vf(air)	Reactivity Worth (cents)
10	Ramp	75	75	0.819 (FCR)	0.181 (FCR)	26.50 (FCR)
				0.8 (CCR)	0.2 (CCR)	0.0 (CCR)
	DC	465	540	0.2 (FCR)	0.8 (FCR)	-26.50 (FCR)
				0.8 (CCR)	0.2 (CCR)	0.0 (CCR)
	Rod Drop	125	665	0.3 (FCR)	0.7 (FCR)	0.0 (FCR)
				0.051 (CCR)	0.949 (CCR)	-168.38 (CCR)
11	Ramp	60	60	0.817 (FCR)	0.183 (FCR)	26.41 (FCR)
				0.8 (CCR)	0.2 (CCR)	0.0 (CCR)
	DC	284	344	0.072 (FCR)	0.928 (FCR)	-11.45 (FCR)
				0.8 (CCR)	0.2 (CCR)	0.0 (CCR)
	Rod Drop	347	691	0.072 (FCR)	0.928 (FCR)	0.0 (FCR)
				0.050 (CCR)	0.950 (CCR)	-168.57 (CCR)

*Delayed Critical

5.4.5 Transient Sequence Results

The results of the simplified EVENT RZ and NETGEN model analysis for the eleven transient sequences are shown in Figures 48-58. Each figure includes the simplified EVENT RZ and NETGEN model results plotted with the AGN experimental data for the transient sequences. The figures illustrate the neutron population as a function of time, N(t), relative to the initial neutron population, N(0), (N[t]/N[0]) over the duration of the transient sequence.

Overall, there is good agreement between the EVENT RZ and NETGEN results and the UNM AGN experimental time-dependent experiments conducted for this work. As previously stated, the individual portions of the transient sequence (prompt jump/ramp, delayed critical, and the rod drop/delayed neutron decay as shown in Figure 33) were modeled in a single EVENT model. Small, ad hoc, time zone adjustments are made at the transition from the prompt jump to delayed critical configuration to ensure

www.manaraa.com

the relative neutron population matched up with the experimental data at the start of the rod drop transient. These ad hoc adjustments would not have been necessary had the models only considered each major transient section (prompt jump, steady-state, and prompt drop) separately.

The results for the prompt jump portion of the transient sequence match up well with experimental data considering the neutron population changes exponentially with time. The transient results show there are some small deviations in the slope in transient sequence 1, 4, and 8; however, these deviations are very small and do not significantly impact the results. The other prompt jump results show a slope value that line up well with the slope of the experimental data. Doubling time data from the reactor log sheets was compiled to compare to the calculation results. The EVENT RZ and NETGEN calculation results were plotted on a linear scale to fit the data to an exponential equation. The slope of this equation, the reactor period (T, with units of seconds) can be used to calculate the doubling time, DT, by calculating the following quantity, $DT = T \cdot ln(2)$. The doubling time information for the EVENT results and AGN experiments are summarized in Table 27. Most of the doubling time results from the calculations compare within about 10% of the experimental data. The doubling time for several prompt jump transients vary from experimental data more than 10% but are all within 16%. In general, the EVENT NETGEN doubling time results compare better to the experimental data than the EVENT RZ results. The

www.manaraa.com

doubling time uncertainty is not known and the curve fits used to calculate the curve fit slope data has good but not excellent regression results.

Table 27. Prompt Jump Doubling Time Comparison

Transient #	EVENT RZ Transient Models			EVENT NETGEN Transient Models		
	Calculation Doubling Time (sec.)	Experimental Doubling Time (sec.)	% Diff	Calculation Doubling Time (sec.)	Experimental Doubling Time (sec.)	% Diff
1	13.2	13.2	0.2%	14.1	13.2	6.5%
2	11.8	13.4	-11.6%	13.4	13.4	-0.1%
3	11.2	13.3	-15.8%	12.0	13.3	-9.7%
4	12.1	13.2	-8.0%	12.0	13.2	-8.7%
5	12.4	13.5	-8.2%	13.0	13.5	-3.5%
6	12.4	13.5	-8.3%	12.7	13.5	-5.8%
7	12.4	14.2	-12.5%	12.5	14.2	-11.7%
8	14.3	–*	–	15.0	–*	–
9	11.4	13.4	-15.2%	11.7	13.4	-12.3%
10	13.3	13.5	-1.6%	13.3	13.5	-1.5%
11	12.6	13.6	-7.2%	12.5	13.6	-8.0%

* Data not available

The delayed critical results are acceptable because each transient configuration modeled was able to compare to the AGN experimental data with respect to the relative neutron population. The rod drop results also compare quite well to the experimental data. As the transient result plots indicate, the rod drop results compare quite well to the experimental results for each of the transients. Poor rod drop results would indicate there were problems matching up changes in reactivity in the experiments to the simplified EVENT RZ and NETGEN models; however, this is not the case. The results clearly show the changes in reactivity from rod movement changes in the experiments have been represented well in the EVENT models. Otherwise, there would be significant deviation in the delayed

www.manaraa.com

neutron decay plot results. Close examination of the simplified EVENT RZ and NETGEN results for the delayed neutron decay tails for each of the transient configurations show excellent agreement with the experimental data. The EVENT results consider the radiological decay of the 6 delayed neutron groups after the rod drop until the end of the transient configuration. The delayed neutron data from Keepin (Table 24) for the EVENT computations was sufficiently accurate to compare well to the experimental data for all 11 AGN transient sequences. The NETGEN results agree very well to the RZ results even with the significant differences in modeling complexity, 2-D vs. 3-D, and control element representation (single, annular control rod for the RZ model and the FCR and CCR control rods considered in the NETGEN model).

www.manaraa.com

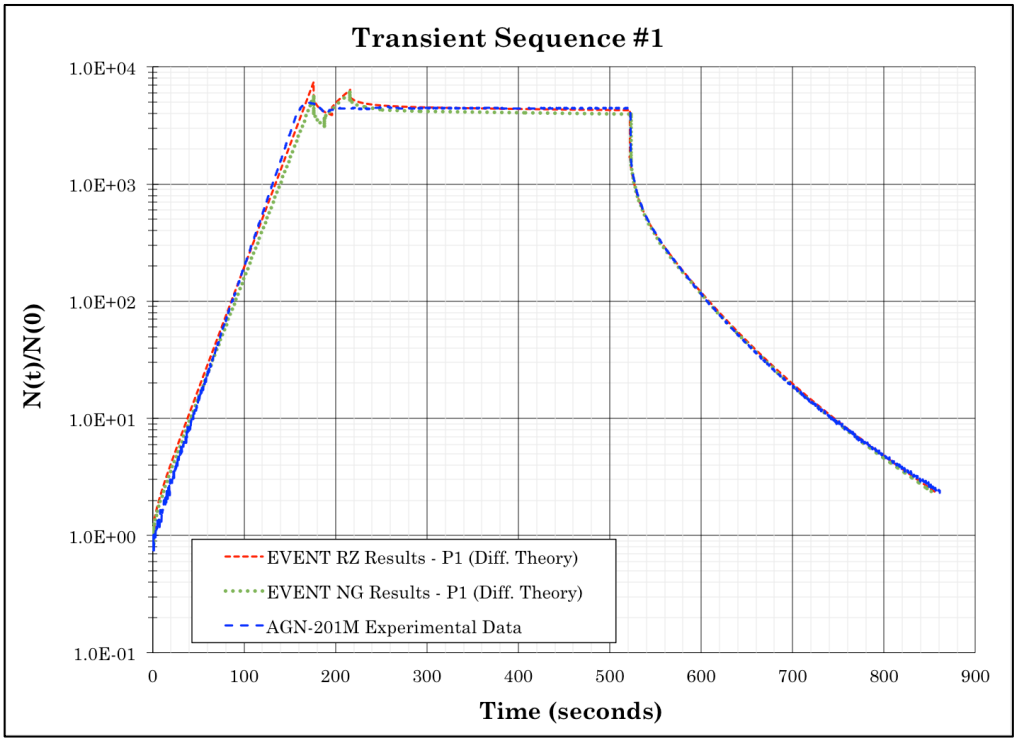

Figure 48. EVENT Transient Model Results – Transient Sequence 1

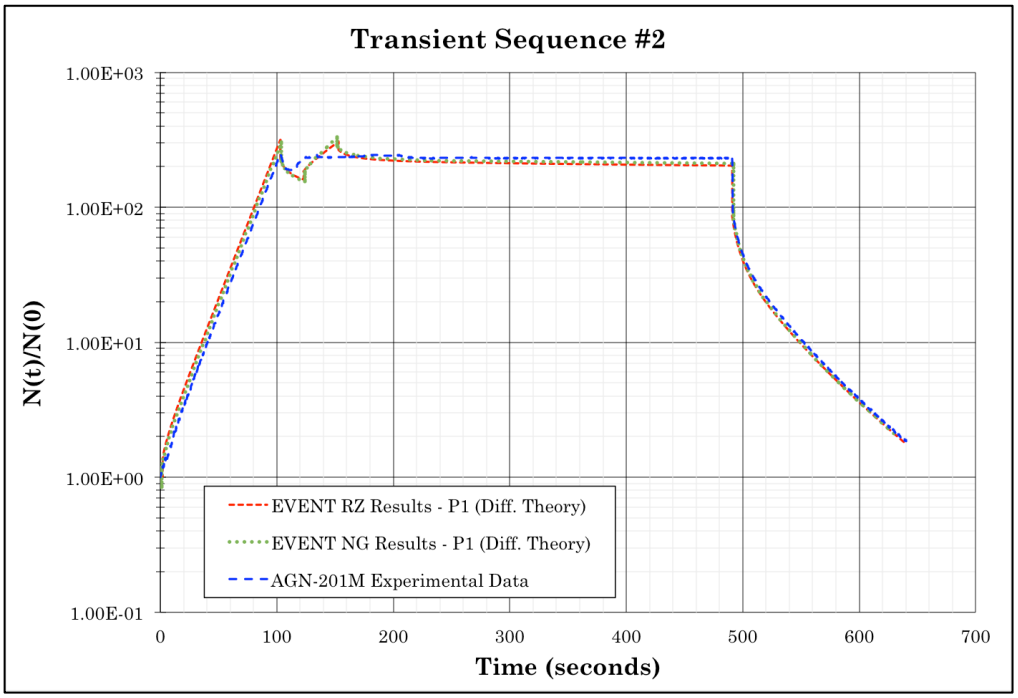

Figure 49. EVENT Transient Model Results – Transient Sequence 2

www.manaraa.com

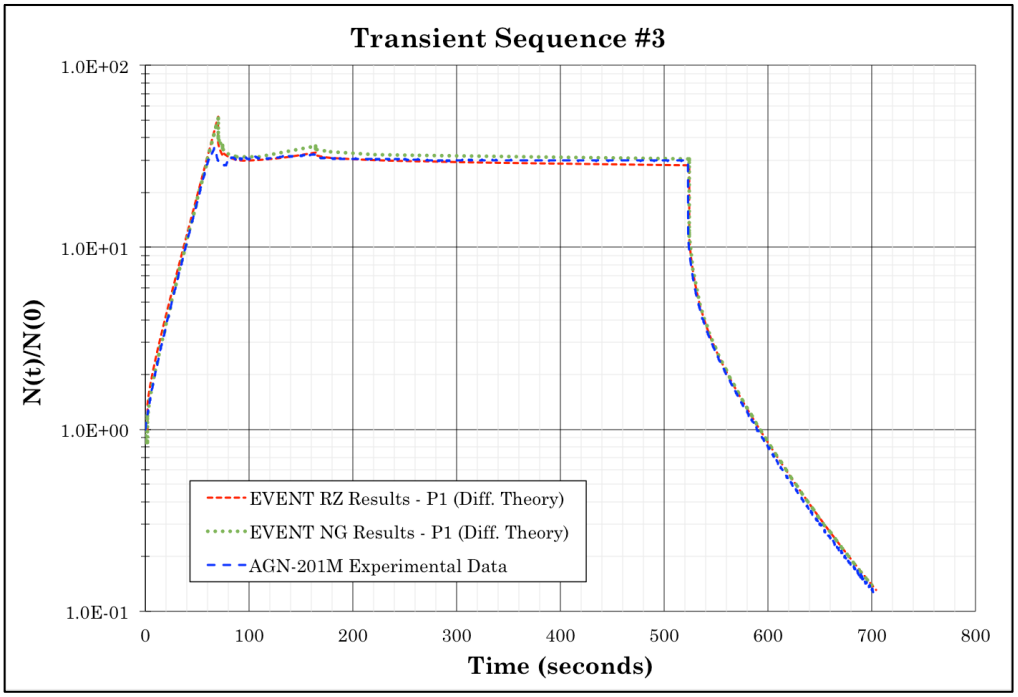

Figure 50. EVENT Transient Model Results – Transient Sequence 3

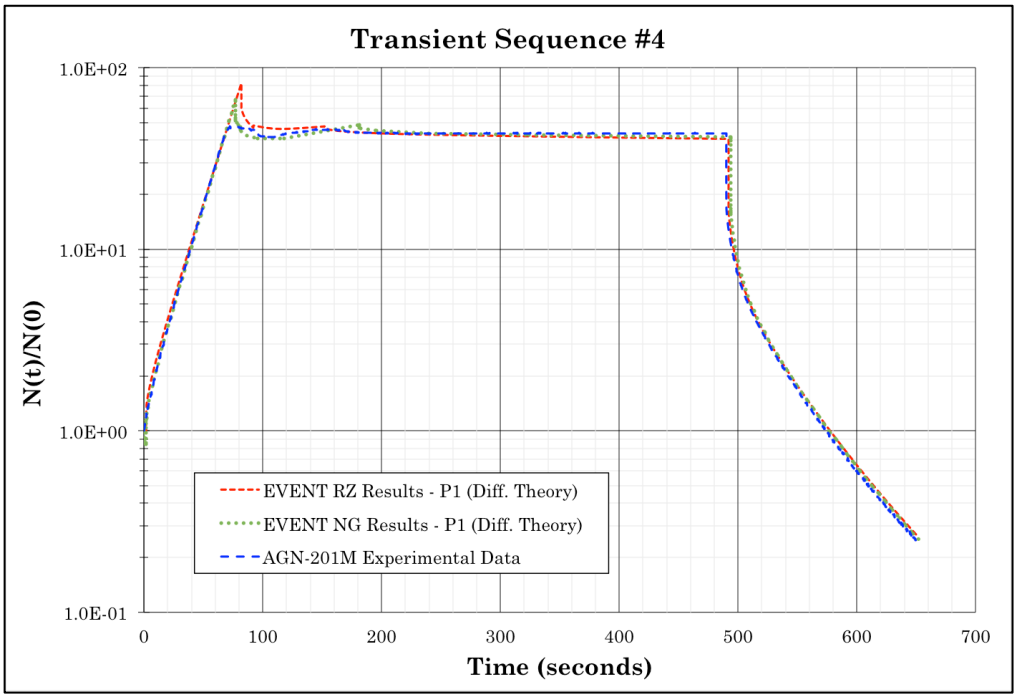

Figure 51. EVENT Transient Model Results – Transient Sequence 4

www.manaraa.com

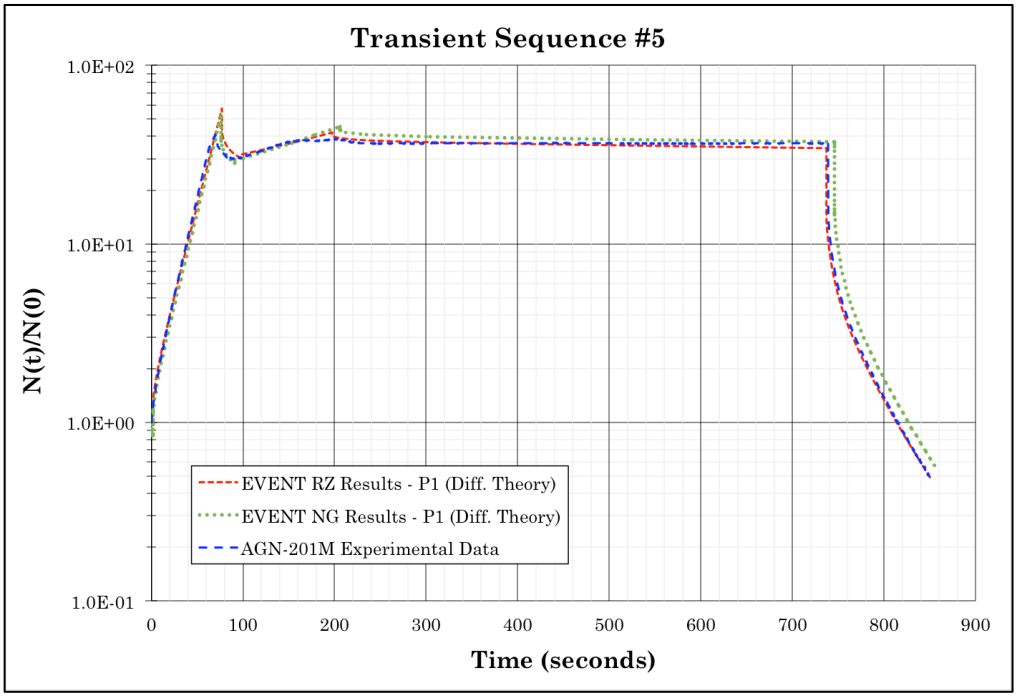

Figure 52. EVENT Transient Model Results – Transient Sequence 5

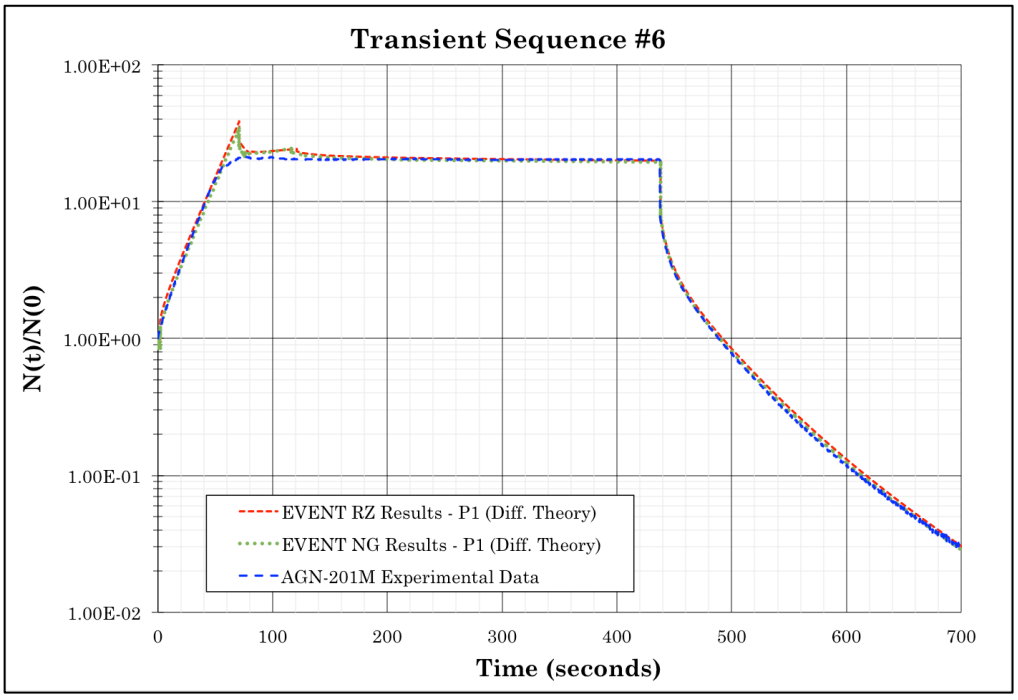

Figure 53. EVENT Transient Model Results – Transient Sequence 6

www.manaraa.com

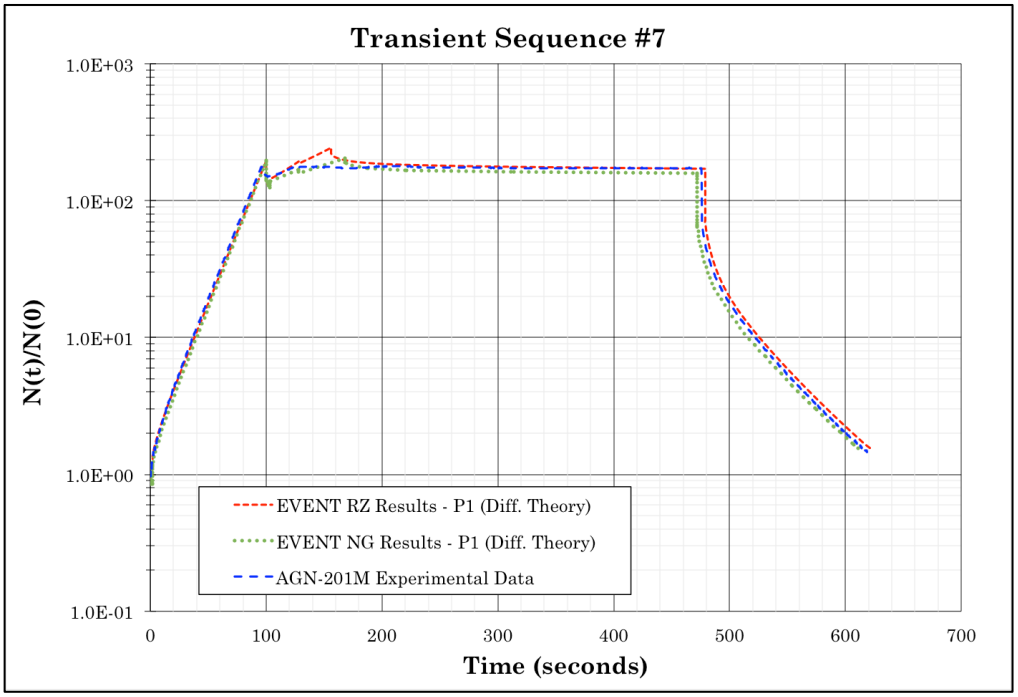

Figure 54. EVENT Transient Model Results – Transient Sequence 7

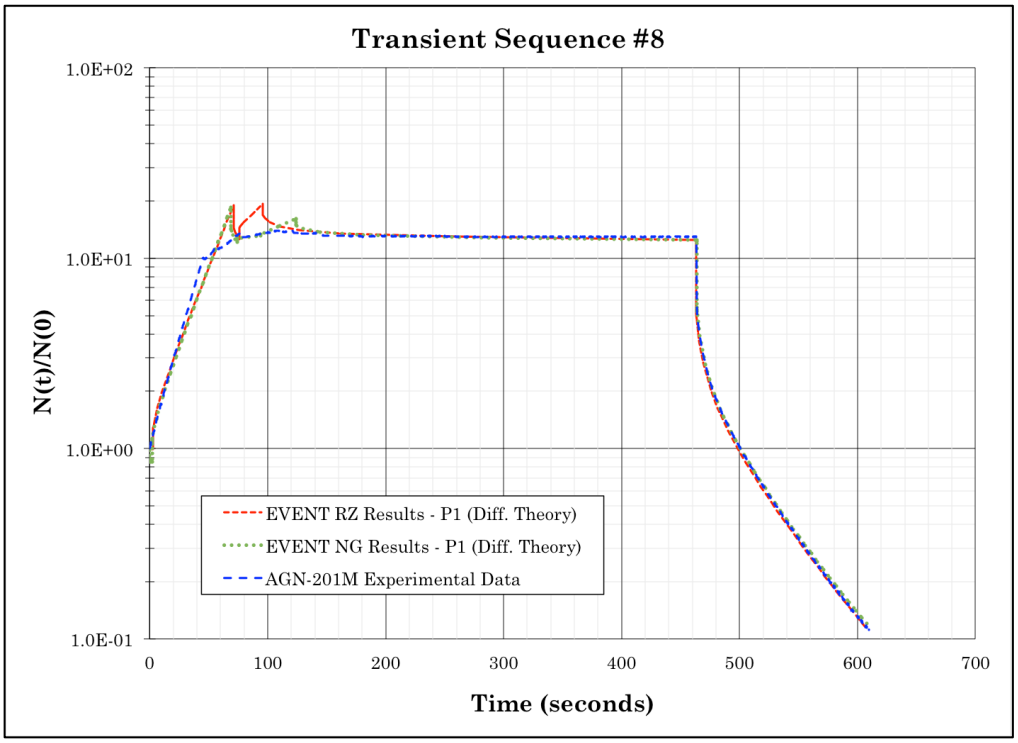

Figure 55. EVENT Transient Model Results – Transient Sequence 8

www.manaraa.com

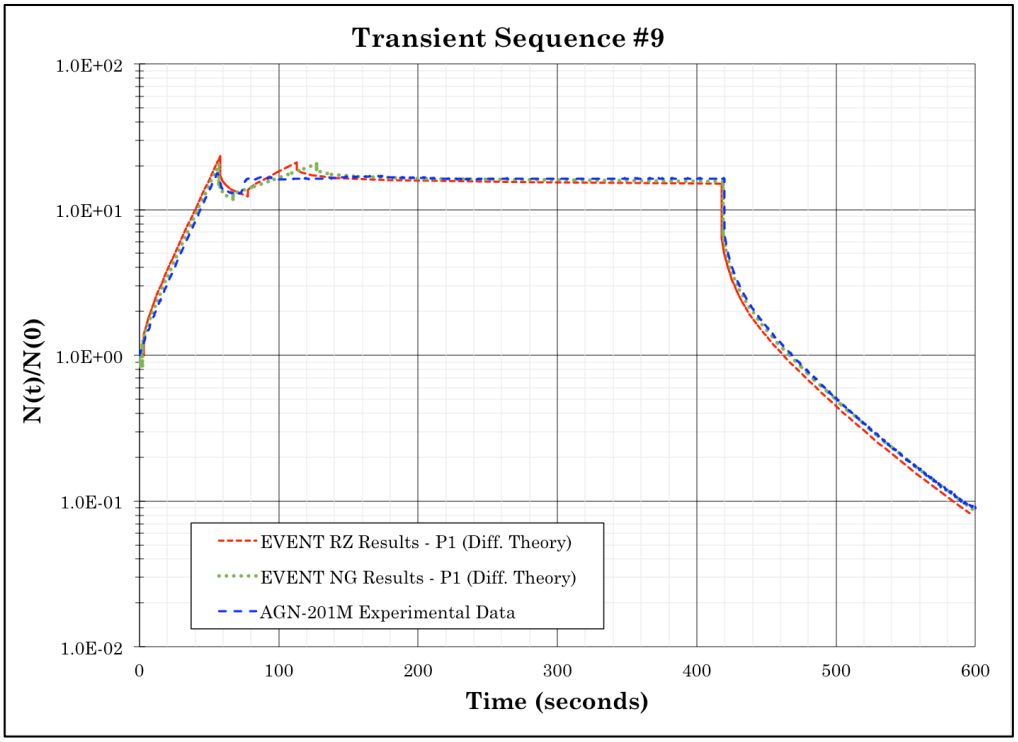

Figure 56. EVENT Transient Model Results – Transient Sequence 9

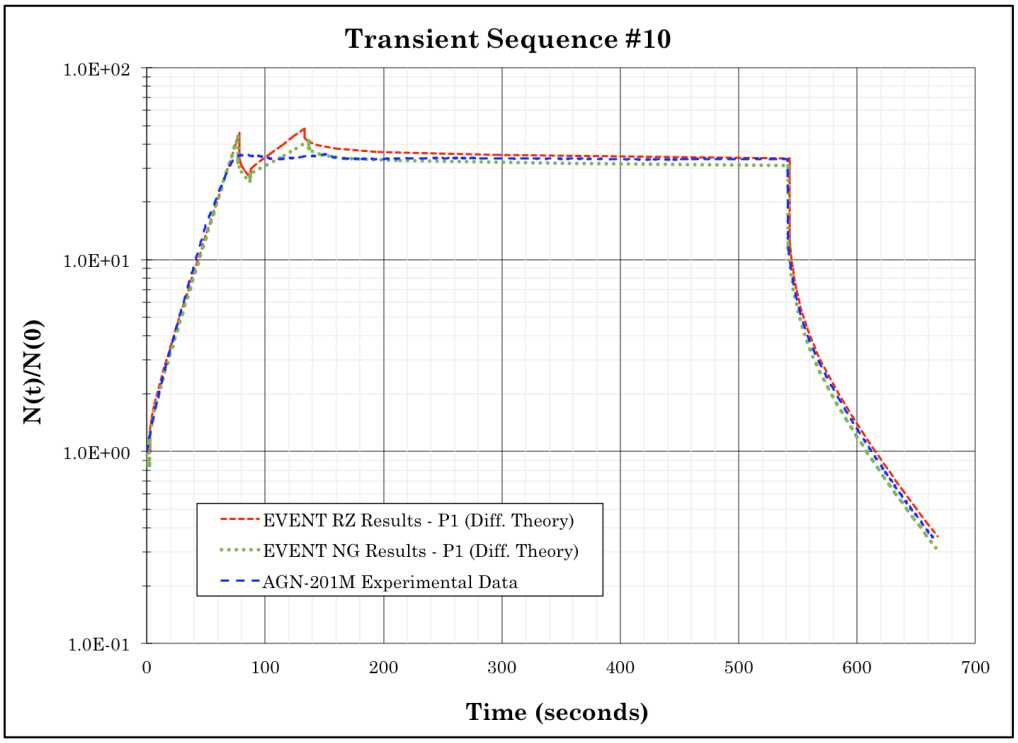

Figure 57. EVENT Transient Model Results – Transient Sequence 10

www.manaraa.com

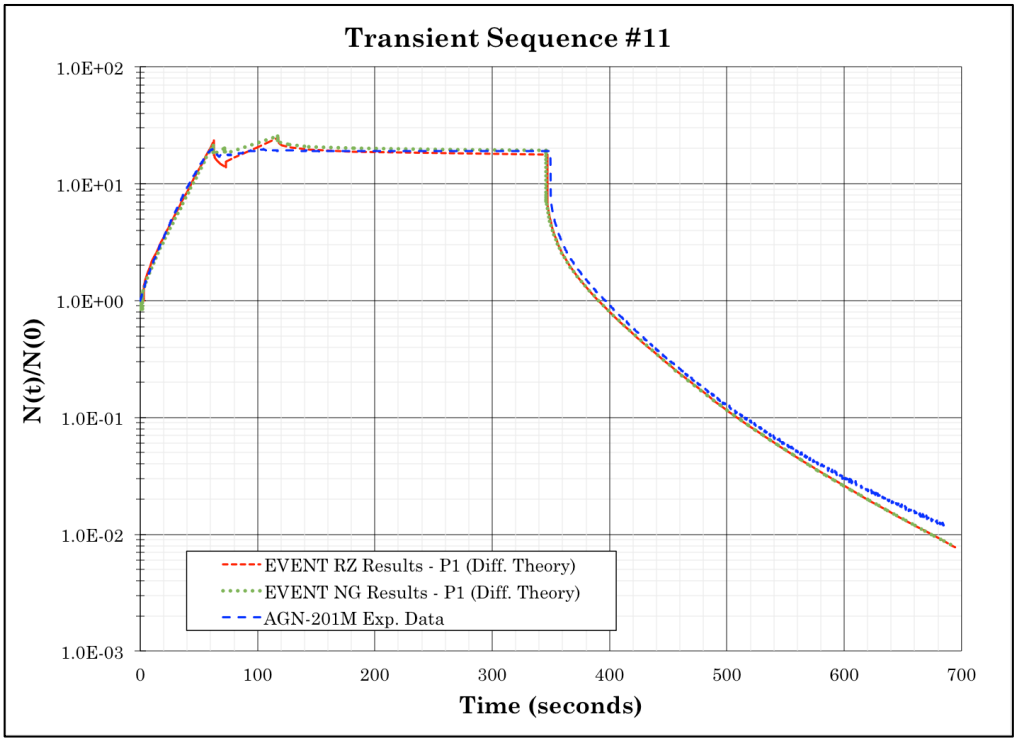

Figure 58. EVENT Transient Model Results – Transient Sequence 11

5.4.5.1 EVENT RZ Model Delayed Neutron Parametric Study

The effect of the delayed neutrons in the AGN experiments is most clearly seen in the power ramps and the rod drop measurments. The EVENT RZ model illustrated differences with using delayed neutron data from the literature (Keepin and Brady data from Table 24) and results from 3-D AGN Monte Carlo-based MCNP6 calculations (Table 9). The results of this parametric study are shown in Figure 59. There is good agreement between the three sets of delayed neutron data; however, the MCNP6 data does not compare as well as the Brady and Keepin delayed neutron data. The significant effect noted in Figure 59 is the slight increase in neutron population (prompt jump due to the prompt neutrons) in the ramp phase of

www.manaraa.com

the transient, which results in the steady-state and prompt drop phases to be somewhat misaligned. Furthermore, the quality of the comparison depends upon where the actual experimental transient begins. Because the same EVENT RZ model was used for all three sets of delayed neutron data, the only conclusion that can be drawn is the behavior in the delayed neutrons during the prompt jump phase of the first transient resulted in a higher neutron population at the end of the first transient time zone, as a result of the exponential behavior of the system when it is operated in a delayed supercritical state. Figure 60 illustrates the results of the first AGN rod drop experimental measurement conducted after the prompt jump measurement shown in Figure 59. There is excellent agreement between the rod drop transient experimental data and the transient calculations using delayed neutron data from the literature.

www.manaraa.com

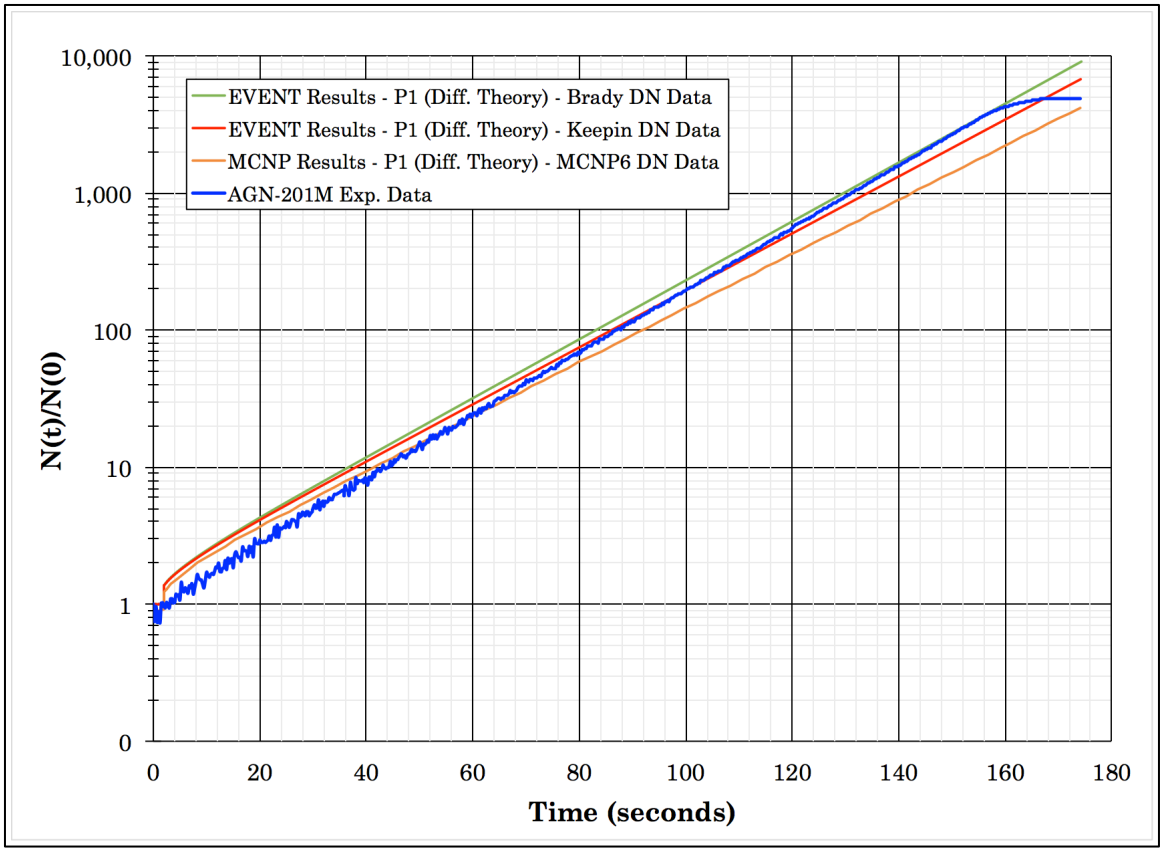

Figure 59. Delayed Neutron Parametric Study Results – Prompt Jump

www.manaraa.com

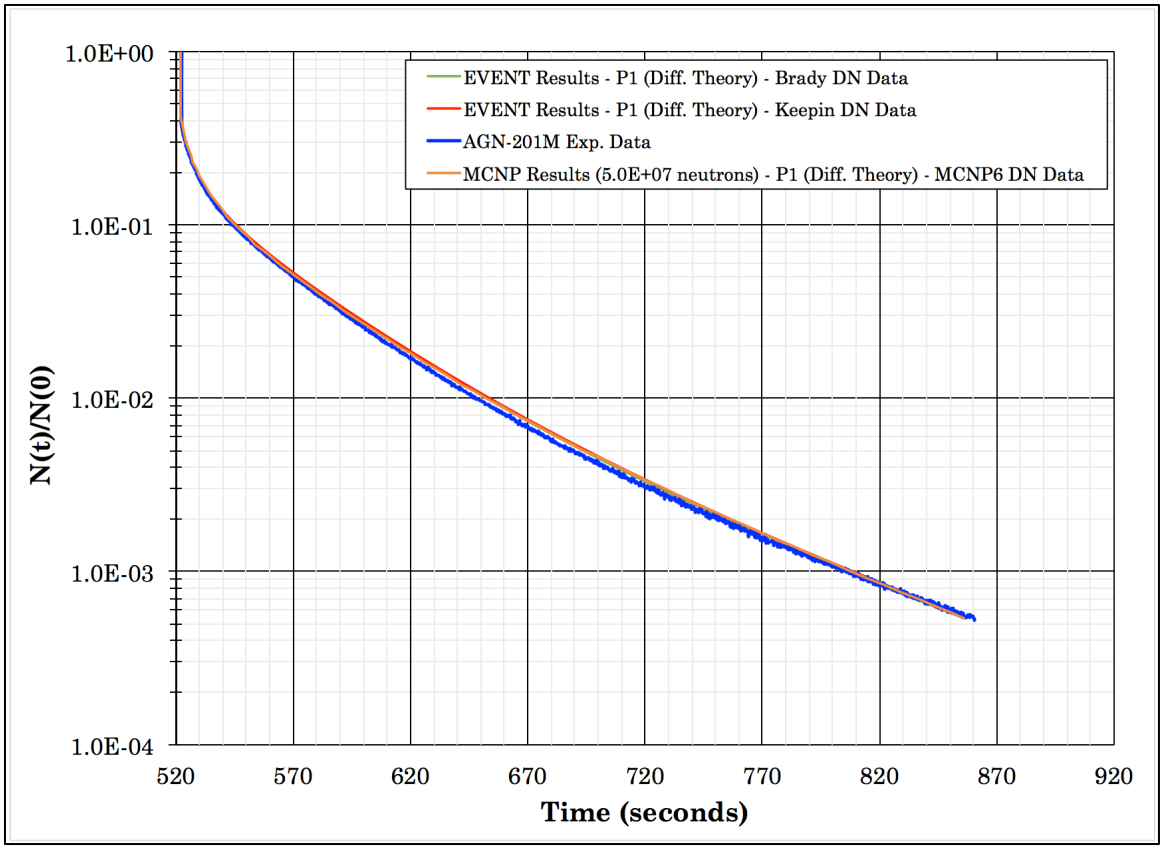

Figure 60. Delayed Neutron Parametric Study Results – Rod Drop

5.4.6 Material Sensitivities and Experimental Uncertainties

Wetzel [4] documented a thorough assessment of material sensitivities for the UNM AGN. The material and dimensional UNM AGN specifications were referenced from Wetzel [4] to initiate the EVENT AGN model development. The sensitivity assessment utilized an AGN model developed in SCALE utilizing multigroup cross sections (238 energy groups) with the KENO Monte-Carlo neutron transport code. There are many uncertainties that impact the operational capabilities of the research reactor configuration. Wetzel provides uncertainty estimates for the following reactor materials to

www.manaraa.com

determine the sensitivity of the k_{eff} to small changes in the material characteristics:

- ^{235}U enrichment
- ^{235}U and ^{238}U mass
- Polyethylene moderator mass, hydrogen in polyethylene density, carbon in polyethylene density
- Graphite reflector density
- Lead shield density
- Aluminum density
- Steel density
- Water shield density
- Temperature variations

The uncertainty in the nominal enrichment was known to about ±0.5 wt. % ^{235}U and can be used to estimate the ^{235}U mass uncertainty (^{235}U mass can vary from 649.83 g to 684.03 g). Small, uniform changes in material density and small changes in the reactor temperature are assumed and modeled in KENO V.a to determine the impact to the k_{eff}. According to Wetzel, there is no uncertainty data for the polyethylene (including ^{1}H and ^{12}C in polyethylene), graphite, lead, aluminum, steel, and water for the AGN [4]. Small, credible, temperature variations can be modeled by adjusting the neutron cross sections for Doppler broadening effects over the credible changes in core temperatures based on ambient temperature, the reactor

www.manaraa.com

power level and the duration of operation. The sensitivity results [4] indicate the system k_{eff} is most sensitive to small changes in the mass of ^{235}U and polyethylene in the AGN core and the graphite reflector. This makes sense considering how important both the fissile and moderator mass are for this thermal research reactor and considering the fissile material and polyethylene moderator are imtimately mixed together in the fuel plates. The sensitivity of the k_{eff} on graphite density changes is also reasonable considering dependence of the core on the graphite to achieve criticality with such a small mass of ^{235}U. Wetzel estimates that the total material uncertainty on the reactor materials is about 0.0025 δk. Wetzel also considers geometric uncertainties as a result of uncertainties in diameter thickness and gaps between components, i.e., warping from use, manufacturer defects or inconsistencies. The uncertainty data used to determine the geometric uncertainty are estimated based on expert judgement and ultimately results in a high estimate for the total geometric uncertainty, 0.020 δk. This value is excessive based on the fact that the reactor is limited to 0.0019 δk excess reactivity and the reactor does achieve criticality [4].

A large number of rod height measurements were generated for the steady-state and transient experiments performed on the AGN in 2013. The AGN reactor supervisor provided a rod height uncertainty of approximately ±0.5 cm [60] to consider when performing the delayed critical and transient analyses in EVENT. To examine the impact of the rod height uncertainty,

www.manaraa.com

two sets of computations were performed with the core rod heights varied ±0.5 cm:

1. EVENT NETGEN model of delayed critical case 1 and 3 (chosen arbitrarily), and
2. EVENT RZ model for transient sequence 1 was modified to consider a change in the height of the annular control rod.

The impact of the rod height uncertainty on the k_{eff} using the EVENT NETGEN model is illustrated in Figure 61. Figure 61 shows a linear relationship between the rod height uncertainty and k_{eff} for both delayed critical case #1 and #3. The effect of ±0.5 cm uncertainty in rod height is 0.0004 δk for case #1 and 0.0003 δk for case #3, which is a rather small impact to the system k_{eff}.

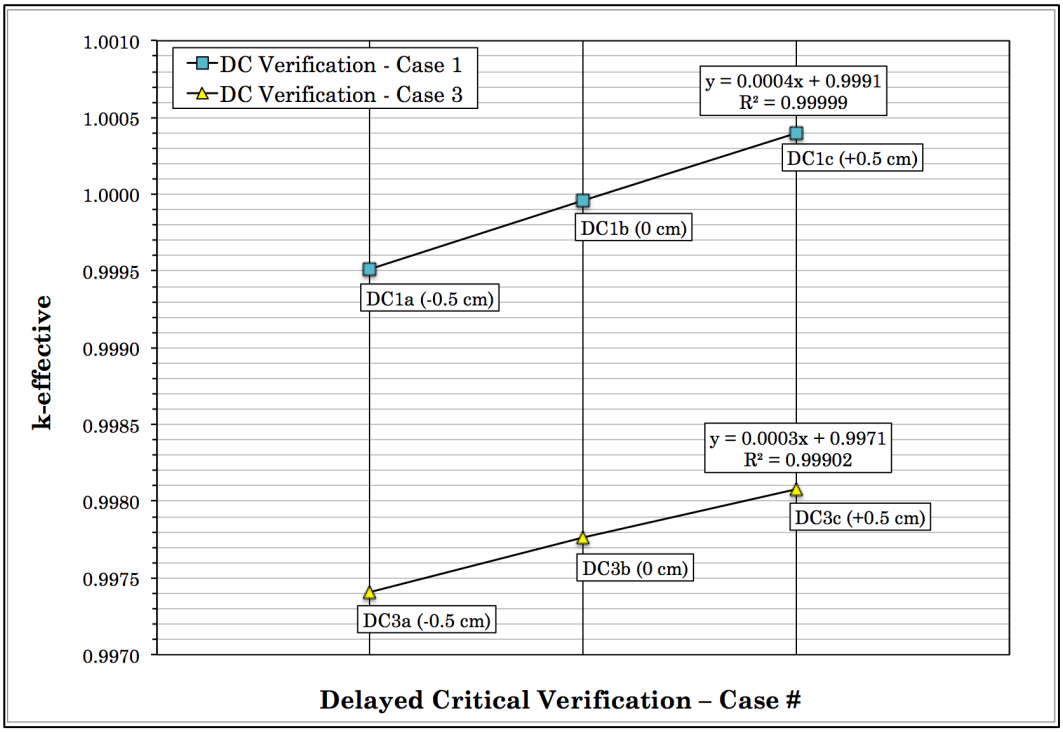

Figure 61. EVENT Delayed Critical Uncertainty Calculation

www.manaraa.com

The impact of the rod height uncertainty to the neutron population in an EVENT RZ transient case is depicted in Figure 62. The figure illustrates the change in the neutron population for a prompt jump transient for the nominal case, a prompt jump transient with an additional +0.5 cm of rod insertion and a prompt jump transient with -0.5 cm less rod insertion than expected. Because the neutron population increases exponentially, the effect of the rod height uncertainty on the transient is time dependent in nature, meaning the impact to the system increases as a function of time. The prompt jump, or power ramp, for transient sequence 1 is almost 170 seconds long. The effect of the uncertainty is small early in the transient and larger at 170 seconds, $3000N_o$ (3000 times the initial neutron population in the core) for -0.5 cm and $8000N_o$ for +0.5 cm with the value at 0 cm is about $4000N_o$. This effect does account for some variation in the reactor power level for the EVENT results compared to the AGN experimental transient after long transient durations.

www.manaraa.com

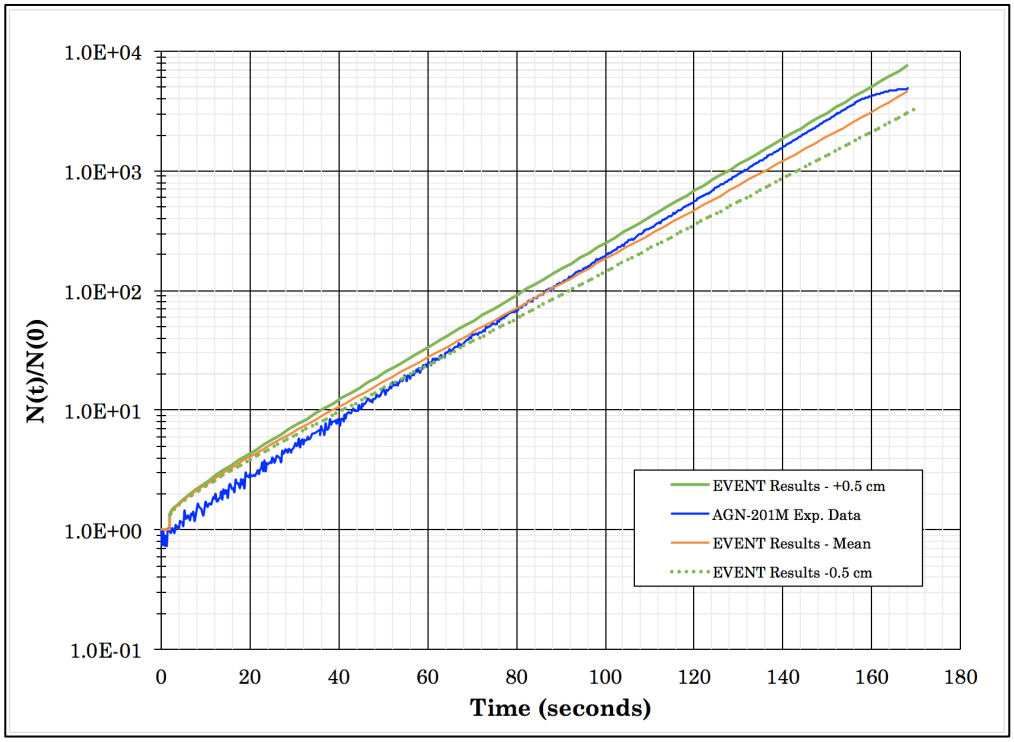

Figure 62. EVENT Transient #1 Verification Uncertainty Calculation

www.manaraa.com

Chapter 6 – Conclusions

The steady-state and time-dependent EVENT AGN analyses compare well with experimental AGN data. Extensive scoping analysis permitted the testing of different types of cross-libraries, old and modern. Modern multigroup neutron cross-section libraries based on the ENDF/B-VI.1 library were generated using a development version of the SCALE package to use as the nuclear data for these experimental verifications. Complex 2-D and 3-D EVENT models were created for this work and compared to results obtained from comparable Monte Carlo calculations with MCNP6. This allowed the author to develop confidence in the GEM pre-processor, the EVENT code, and the modern cross-section data. Detailed EVENT RZ and NETGEN models were created for the comparison to results by Wetzel[4] and as a starting point to develop simplified EVENT RZ and NETGEN models for use with the AGN steady-state and transient experimental analysis. The steady-state models consider high P_N order while the time dependent models consider the

www.manaraa.com

diffusion theory approximation, P_1, and high calculational precision. The delayed critical experimental verifications compared well to calculations performed by Wetzel and delayed critical experimental data from the UNM AGN research reactor in December 2013. A average computational bias of -0.0048% for the P_{11} cases and +0.0119% for the P_{13} cases resulted from the delayed critical experimental analysis, which indicates the EVENT models are effective for modeling the UNM AGN.

The experience generated with the steady-state analysis was used to develop the transient calculation methodology that involved equating the reactivity changes from experimental control rod movements directly to the control element reactivity worths in the simplified EVENT RZ and NETGEN models. This was done by using the simplified EVENT RZ and NETGEN models to develop a set of highly precise FCR and CCR calibration curves. This methodology was applied to the eleven AGN experimental transient sequences. The transient characteristics indicate three main time periods or sections: 1. reactivity insertion and power ramp, 2. reactivity removal to achieve a delayed critical configuration at a larger power level, and 3. rapid removal of the CCR from the core to initate a prompt drop transient proceeded by an exponential drop in reactor power due to the radioactive decay of the delayed neutron precursors present. The results of the time-dependent analyses show the EVENT code package can model AGN core

www.manaraa.com

reactivity changes extremely well, even using P_1 Legendre flux expansion (diffusion theory approximation) and using two geometrical configurations.

Sensitivity and uncertainty conclusions from Wetzel [4] for the UNM AGN demonstrated some sensitivity of the k_{eff} to small changes in the ^{235}U and polyethylene mass, and the density of the graphite reflector. Wetzel also estimated the dimensional uncertainties for the AGN based on expert judgement; however, the propagation of the dimensional and gap uncertainties resulted in a nonsensical total uncertainty estimate. The AGN experimental measurements relied significantly on rod height measurements to determine the system reactivity. Busch [60] estimated a rod height uncertainty of about ±0.5 cm for these measurements. An uncertainty analysis performed on with EVENT models for delayed critical and prompt jump configurations concluded the k_{eff} is affected slightly, but not significantly, by the ±0.5 cm rod height uncertainty. The EVENT transient case concluded that there were very small effects noted with the neutron population at the beginning of a transient that increased as the duration of the transient increased.

The EVENT radiation transport code has proven to be an excellent tool for AGN research reactor analysis. More experiments are recommended to provide additional data for more rigorous analyses using the EVENT code. It is recommended these analyses consider AGN geometric and material

www.manaraa.com

uncertainties to allow for more complex analyses to be peformed on the AGN research reactor.

6.1 Future Work

The version of EVENT used for these calculations did not consider reactivity feedback effects. It would be useful for EVENT to have the capability to be coupled to another code package to consider reactivity feedback effects from density changes from heating and cooling effects in fissile solids and bubble formation in fissile solutions, for example. For a reactor like the AGN, feedback effects due to core heating during operation are very subtle but would be interesting to implement for teaching purposes and for understanding the reactor design and possible enhancements and upgrades.

Improving EVENT to allow the efficient use of transport theory with adaptive time steps for transient analysis rather than using only diffusion theory would be a benefit for more complex transients than was considered in this work. Diffusion theory was more than sufficient for the power ramp and rod drop configurations performed for this work; however, the use of transport theory could be of benefit for other reactors that utilize conditions that challenge diffusion theory, such as strongly absorbing regions, i.e., control rods containing poisions instead of fuel.

Also included as future work is to develop a single version of GEM and EVENT for distribution to the Radiation Safety Information Computation

www.manaraa.com

Center at Oak Ridge National Laboratory. This will allow for a great deal of user feedback to the code developer for future enhancements. It would also be beneficial for end-users to have a comprehensive manual for both the GEM pre-processor and the EVENT radiation transport code that contains example problems, as well as a Primer for use with developing multigroup cross sections. This research identified a significant number of EVENT code errors that were fixed by the developer in parallel with this research.

The logical path forward from the AGN EVENT analyses is to consider publishing a reactor physics benchmark experiment or a series of experiments in the UNM AGN, complete with accurate material and geometric uncertainty data. The experimental data would be valuable for more precise modeling of the UNM AGN reactor configuration, along with generating case-dependent cross sections using the latest raw ENDF/B neutron data libraries. Analysis at this level would require an EVENT package with more robust quality control, a much faster computer system, the use of transport theory rather than the diffusion theory approximation, and the utilization of multigroup cross-section libraries with many more energy groups.

www.manaraa.com

Appendix A – EVENT 2-D Model Testing

A.1 MCNP6 XY Model

A 2-D model was generated using Monte-Carlo code MCNP6 by taking a "slice" of the AGN core at the core centerline to produce a simple model of concentric circular regions for use to test the EVENT package capabilities for this work. Because MCNP6 is a 3-D Monte-Carlo radiation transport code, a 2-D model can be generated by creating a model representing the core "slice" along the XY plane with a finite height. The top and bottom of the finite 3-D model can be modeled with mirror boundary conditions that approximate a 2-D XY model of infinite extent in the Z-direction.

A.1.1 Model Specifications and Results

The AGN geometric specifications for this model are the same as those for Wetzel [4]. A homogeneous core composition was assumed for the 2-D XY

www.manaraa.com

calculations and the atom densities for this core configuration are listed in Table 5. The glory hole in the AGN is horizontally arranged in the actual reactor core; however, a vertical glory hole was assumed throughout this work to simplify modeling efforts. The inside radius of the glory hole is 1.27 cm and the aluminum glory hole tube has an outside radius of 1.47 cm. The core fuse is not modeled here as it simplifies the modeling effort with the subsequent deterministic EVENT calculations.

Table 6 provides the atom densities for the AGN structure, graphite neutron reflector and shielding materials. To construct the MCNP6 XY model, a representation of the AGN reactor was assembled into different computational cases to determine the change in the k_{eff} between each significant section of the AGN reactor:

- **AGN_2D_a** – UO_2 and Polyethylene core with a vertical representation of the glory hole and the aluminum glory hole tube,
- **AGN_2D_b** – The AGN_2D_a geometry with a portion of the graphite reflector,
- **AGN_2D_c** – The AGN_2D_b geometry with the aluminum core shell outside of the graphite,
- **AGN_2D_d** – The AGN_2D_c geometry with the outer graphite reflector outside of the aluminum shell material,
- **AGN_2D_e** – The AGN_2D_d geometry with the lead gamma shield outside the outer graphite reflector material,
- **AGN_2D_f** – The AGN_2D_e geometry with a carbon steel water tank shell outside the lead gamma shield, and

www.manaraa.com

- **AGN_2D_g** – The AGN_2D_f geometry with the water shielding outside the carbon steel water tank shell material.

The MCNP6 AGN XY model geometry for this analysis is illustrated in Figure 63. The case, composition, dimensions, model illustrations, and the MCNP6 k_{eff} result for these cases are listed in Table 27. The MCNP6 models approximate an infinite configuration by assuming mirror boundary conditions in the positive and negative Z-directions. The outer cylindrical surface of the AGN configuration assumes vacuum boundary conditions. The MCNP6 ENDF/B-VII continuous energy cross-section library was used for the calculations and does not require adjustment for resonance self-shielding effects. The MCNP6 calculations assumed 600 generations and 2,500 neutrons per generation with 50 generations skipped. The k_{eff} results are also provided in Table 27. In addition to the k_{eff} results, the percent difference in k_{eff} between the particular case and the initial case, AGN_2D_a, is provided to show the change in k_{eff} due to adding an additional region onto the core model. The results show there is little change in k_{eff} with additional neutron reflector materials beyond the outer graphite reflector. Adding the graphite reflector to the AGN core results in a 21.33% increase in the bare core k_{eff} result (sum of percent change in k_{eff} for configurations AGN_2D_b through AGN_2D_d). The results also show there are only minor contributions of the lead (2.45%) and water reflectors (0.31%) to the core k_{eff} at their locations in the AGN reactor. The unique design of the AGN core allows for very efficient

www.manaraa.com

neutron moderation in the core and effective scattering of thermal neutrons in the graphite reflector back into the core fuel.

The Monte-Carlo-based MCNP6 calculations summarized here are compared to subsequent EVENT calculations that consider an identical geometric configuration. The purpose of these initial calculations is to gain experience with the generating modern cross-section libraries for EVENT and to understand the modeling and computational capabilities of finite element spherical harmonics code EVENT compared to a Monte Carlo-based code package.

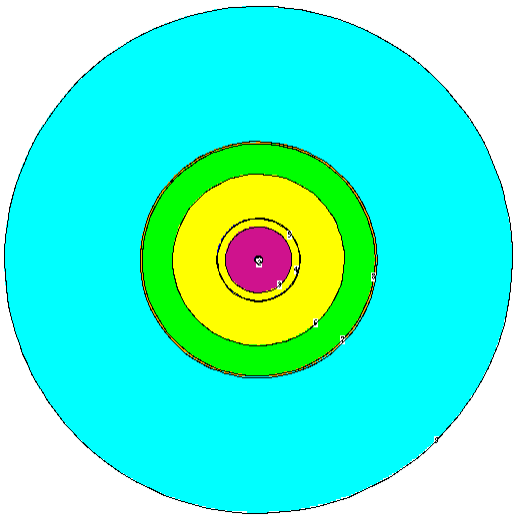

Figure 63. 2-D MCNP6 XY Model Illustration

www.manaraa.com

Table 28. MCNP6 XY Model Detail and Results

Case Name	Composition	Radius (Thickness)	Model Illustration (Mirror Boundary Conditions in ±Z Direction, Vacuum Boundary Conditions on the Outer Surface)	Results	
				k_{eff}	Sigma
				(% Difference from AGN_2D_a Case)	
AGN_2D_a	Air	1.1875 cm (1.1875 cm)	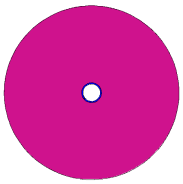	0.98592	0.00071
	Aluminum	1.27 cm (0.0825 cm)			
	Homogeneous Fuel	12.80 cm (11.53 cm)		0.00%	
AGN_2D_b	AGN_2D_a + Graphite	15.85 cm (3.05 cm)	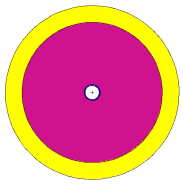	1.05747	0.00069
				7.26%	
AGN_2D_c	AGN_2D_b + Aluminum	16.10 cm (0.25 cm)	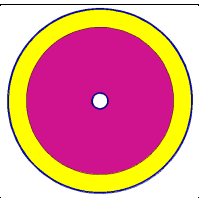	1.05817	0.00070
				0.07%	
AGN_2D_d	AGN_2D_c + Graphite	33.12 cm (17.02 cm)	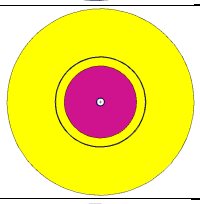	1.20701	0.00061
				14.07%	
AGN_2D_e	AGN_2D_d + Lead	44.926 cm (11.806 cm)	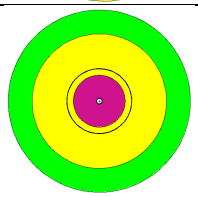	1.23659	0.00057
				2.45%	
AGN_2D_f	AGN_2D_e + Carbon Steel	45.72 cm (0.794 cm)	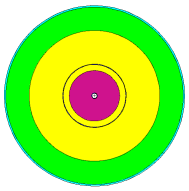	1.23898	0.00055
				0.19%	
AGN_2D_g	AGN_2D_g + Water	98.00 cm (52.28 cm)	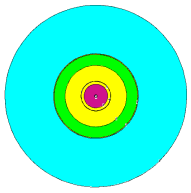	1.24276	0.00059
				0.31%	

www.manaraa.com

A.2 EVENT XY Model

An EVENT XY model was developed to test the capabilities of EVENT using this geometry option in the code. The XY model allows for the AGN to be represented with a cylindrical geometry with infinite height. Further, because the configuration is modeled as a 2-D system (two coordinates, X and Y) the problem executes quickly and efficiently in EVENT. This EVENT model is essentially identical to the MCNP6 model generated in the last section, except for those characteristics relevant to the deterministic EVENT code and more modern neutron cross sections based on the ENDF/B-VII.1 library.

A.2.1 Model Specifications and Results

The XY EVENT model consists of concentric circles of various radii that consider the regions of the core as was done for the MCNP6 model previously. In EVENT, an XY model is constructed by defining primitives such as points and circles for this case. The center of the core was defined as the origin for the problem, in this case (0,0). A series of concentric circles were then specified by defining a radius and the region material to represent the glory hole (1.27 cm, air), glory hole tube (1.47 cm, aluminum), core (12.8 cm, UO_2-polyethylene), inside graphite reflector (15.85 cm, graphite), aluminum shell (16.1 cm, aluminum), outer graphite reflector (33.12 cm, graphite), lead shield (45.72 cm, lead), carbon steel tank wall (45.72 cm, carbon steel), and the water shield (98.0 cm, water). The various geometric regions represented

www.manaraa.com

by the concentric circles are then assigned material properties and a finite element mesh for the problem. In this case, a fine Delaunay finite element mesh was assumed for the EVENT calculations which is an unstructured mesh type used to fit the mesh to irregular geometries such as curved surfaces (cylinders, circles, etc.). For these test cases, multigroup cross-sections were generated from the 238-group ENDF/B-VII library by collapsing the fine library to 8 energy groups. This ENDF/B-VII 8-group working library was used for this calculation. Figure 64 illustrates the EVENT XY AGN model and the Delaunay mesh detail. The dimensions assumed the AGN regions with the calculation results are provided in Table 28. The results are similar to MCNP6 model results for the same configuration, although the MCNP6 results are about 1-2% greater than the EVENT XY results, which is probably due to the difference between the MCNP6 and EVENT calculation methodologies (Monte Carlo-based compared to deterministic) and the use of continuous energy cross-sections. The k_{eff} for the AGN core is approximately 0.98 (case AGN_2D_a). The addition of the first graphite layer (case AGN_2D_c) results in a 8.98% increase in the k_{eff} and the addition of the thin aluminum shell and second graphite layer results in an increase in the k_{eff} of 13.28% for a total change in about 22.26% (~1% greater than the corresponding MCNP6 result). The lead and water regions of the core have a small overall effect on the k_{eff} of the AGN. An example input file for the EVENT XY model can be found in the Appendix C.

www.manaraa.com

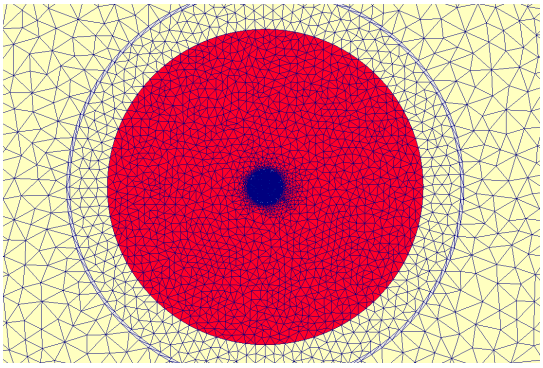	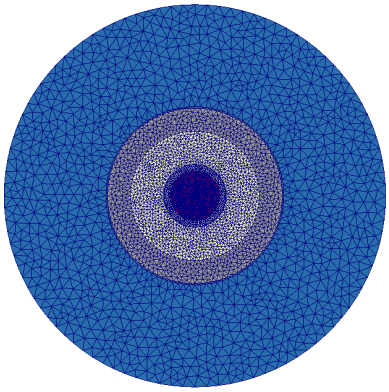
Illustration in ParaView of the center of the glory hole center, aluminum glory hole tube, and fuel. The Delaunay mesh is also shown.	Illustration of the entire AGN-201M EVENT XY model as generated by ParaView.

Figure 64. EVENT XY Model Illustrations

www.manaraa.com

Table 29. EVENT XY Model Detail and Results

Case Name	Composition	Radius (Thickness)	Model Illustration (Mirror Boundary Conditions in ±Z Direction, Vacuum Boundary Conditions on the Outer Surface)	Results k_{eff} (% Difference from AGN_2D_a Case)
AGN_2D_a	Air	1.1875 cm (1.1875 cm)	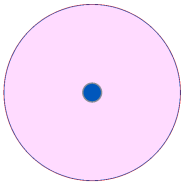	0.97696
	Aluminum	1.27 cm (0.0825 cm)		
	Homogeneous Fuel	12.80 cm (11.53 cm)		0.00%
AGN_2D_b	AGN_2D_a + Graphite	15.85 cm (3.05 cm)	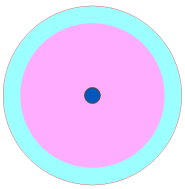	1.06472
				8.98%
AGN_2D_c	AGN_2D_b + Aluminum	16.10 cm (0.25 cm)	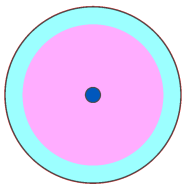	1.06661
				0.18%
AGN_2D_d	AGN_2D_c + Graphite	33.12 cm (17.02 cm)	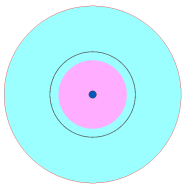	1.20829
				13.28%
AGN_2D_e	AGN_2D_d + Lead	44.926 cm (11.806 cm)	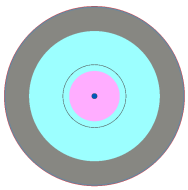	1.23689
				2.37%
AGN_2D_f	AGN_2D_e + Carbon Steel	45.72 cm (0.794 cm)	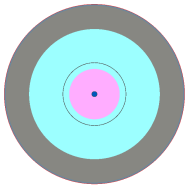	1.23924
				0.19%
AGN_2D_g	AGN_2D_g + Water	98.00 cm (52.28 cm)	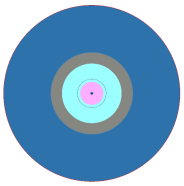	1.24606
				0.55%

www.manaraa.com

A.2.2 Angular Flux Expansion and Order of Scattering Anisotropy for EVENT XY Model

The EVENT code is a deterministic spherical harmonics code capable of using the finite element method and treating anisotropic scattering rigorously. The spherical harmonics angular flux expansion order and order of scattering anisotropy are both specified by the user for each EVENT run. Since the P_N equations solved by EVENT are very complicated, adverse issues regarding the solution can arise for some geometrical configurations. For this work, it is desired to determine the proper discretization method to ensure the EVENT computations are sufficiently converged for the results to match the actual k_{eff}. A parametric study was performed with variations of both the angular flux expansion and the order of scattering anisotropy to determine an optimal combination, i.e., the case with calculation accuracy of about 0.1% and the lowest execution time. The execution time in EVENT for the configuration was also included because more rigorous treatment for the angular flux expansion is offset by additional runtime, i.e., inefficiency, with little added benefit to the result of the calculation. The optimal combination was then used for the calculations for these configurations. The results of this parametric study are summarized in Table 29 and show P_5 angular flux expansion and a 3rd order of scattering anisotropy produces both an accurate result and an efficient calculation. These options will be used for the EVENT XY cases unless otherwise stated.

www.manaraa.com

Table 30. Angular Flux Expansion and Scattering Order Comparison Results for the EVENT XY Model

	P_1 Angular Flux Expansion	P_3 Angular Flux Expansion	P_5 Angular Flux Expansion	P_9 Angular Flux Expansion
0th Order Scattering Anisotropy	[1,0]	[3,0]	[5,0]	[9,0]
k_{eff}	1.29586	1.30211	1.30227	1.30230
% Diff. from [9,9] Result	3.9926%	4.4935%	4.5068%	4.5092%
Time to Execute	30.44 sec.	49.02 sec.	114.23 sec.	414.41 sec.
1st Order Scattering Anisotropy	[1,1]	[3,1]	[5,1]	[9,1]
k_{eff}	1.23629	1.24473	1.24497	1.24503
% Diff. from [9,9] Result	-0.7881%	-0.1108%	-0.0920%	-0.0866%
Time to Execute	15.02 sec.	46.69 sec.	87.46 sec.	316.14 sec.
3rd Order Scattering Anisotropy	[1,3]	[3,3]	**[5,3]**	[9,3]
k_{eff}	1.23629	1.24595	**1.24606**	1.24611
% Diff. from [9,9] Result	-0.7881%	-0.0129%	**-0.0043%**	-0.0003%
Time to Execute	15.15 sec.	47.50 sec.	**90.50 sec.**	254.63 sec.
5th Order Scattering Anisotropy	[1,5]	[3,5]	[5,5]	[9,5]
k_{eff}	1.23629	1.24595	1.24605	1.24611
% Diff. from [9,9] Result	-0.7881%	-0.0129%	-1.5235%	-0.0047%
Time to Execute	15.06 sec.	47.09 sec.	116.43 sec.	223.46 sec.
9th Order Scattering Anisotropy	[1,9]	[3,9]	[5,9]	[9,9]
k_{eff}	1.23629	1.24595	1.24605	1.24611
% Diff. from [9,9] Result	-0.7881%	-0.0129%	-0.0047%	0.0000%
Time to Execute	15.13 sec.	47.33 sec.	126.64 sec.	237.48 sec.

www.manaraa.com

A.3 EVENT RZ Model

An RZ EVENT model was developed to test the capabilities of EVENT using this geometry option in the code. The RZ model allows for the AGN to be represented with a cylindrical geometry with finite height. Because this particular EVENT RZ model is intended to approximate an infinite system (±Z directions), the top and bottom surfaces in the model consider mirror boundary conditions. Further, because the configuration is modeled as a 2-D system (two coordinates, a radius and dimensions in the Z-direction), the problem executes quickly and efficiently in EVENT. The RZ EVENT model assumes a rectilinear mesh that is defined manually in the GEM input file (Figure 65). This RZ model approximates a 3-D AGN configuration. The glory hole and glory hole tube are modeled vertically instead of horizontally to simplify modeling efforts. Scoping calculations indicate the glory hole simplification has a negligible effect on the system k_{eff}. The control rod tubes are not represented in this RZ model but must be approximated in subsequent calculations for the experimental verifications that consider the presence of the control elements in the core. The core fuse is not considered in the model.

A.3.1 Model Specifications and Results

The AGN specifications for the RZ model are the same as those for the AGN MCNP6 XY and EVENT XY models with respect to the radii for the individual regions of the reactor. Figure 65 illustrates the AGN model

www.manaraa.com

dimensions (radii and Z-dimension), the finite element mesh, and region material definitions and Figure 66 illustrates the EVENT RZ model for this calculation. The mesh size is subdivided further for the actual calculation to correspond to the approximate mean free path of a neutron in the material of interest. For these test cases and similar to the XY EVENT calculations, the ENDF/B-VII 8-group working library was used for this calculation. The atom densities for the homogenous fuel mixture are listed in Table 5 and the atom densities for the non-fuel materials are listed in Table 6.

The EVENT RZ model results (Table 30) are similar to MCNP6 model results for the same configuration, although the MCNP6 results are about 1-2% greater than the EVENT RZ results, which is probably due to the differences between the MCNP6 and EVENT calculation methodologies (Monte Carlo-based compared to deterministic) and the use of continuous energy cross-sections. The k_{eff} for the AGN core is approximately 0.98 (case AGN_2D_a). The addition of the first graphite layer (case AGN_2D_c) results in a 5.34% increase in the k_{eff} and the addition of the thin aluminum shell and second graphite layer results in an increase in the k_{eff} of 11.79% (total change of 17.13%, similar to the EVENT XY result). As the MCNP6 and EVENT XY calculations also show, the lead and water regions of the core have little effect on the k_{eff} of the AGN overall. There is good comparison between the EVENT XY, RZ and MCNP6 results for the 2-D calculations.

www.manaraa.com

0 - 1.27	1.27 - 1.47	1.47 - 4.9474	12.8 - 15.85	15.85 - 16.1	16.1 - 33.12	33.12 - 44.926	44.926 - 45.72	45.72 - 98.0	
16	12	1	11	12	11	13	14	15	-12.25 to -10.25
16	12	1	11	12	11	13	14	15	-10.25 to -8.25
16	12	1	11	12	11	13	14	15	-8.25 to -6.25
16	12	1	11	12	11	13	14	15	-6.25 to -4.25
16	12	1	11	12	11	13	14	15	-4.25 to -2.25
16	12	1	11	12	11	13	14	15	-2.25 to 0.25
16	12	1	11	12	11	13	14	15	0.25 to 2.25
16	12	1	11	12	11	13	14	15	2.25 to 4.25
16	12	1	11	12	11	13	14	15	4.25 to 6.25
16	12	1	11	12	11	13	14	15	6.25 to 8.25
16	12	1	11	12	11	13	14	15	8.25 to 10.25
16	12	1	11	12	11	13	14	15	10.25 to 12.25

Legend

1	FUEL
11	GRAPHITE
12	ALUMINUM
13	LEAD
14	STEEL
15	WATER
16	AIR

The top and bottom surfaces consider mirror boundary conditions which make the model infinite in extent.

Figure 65. EVENT RZ Model Region and Mesh Definitions

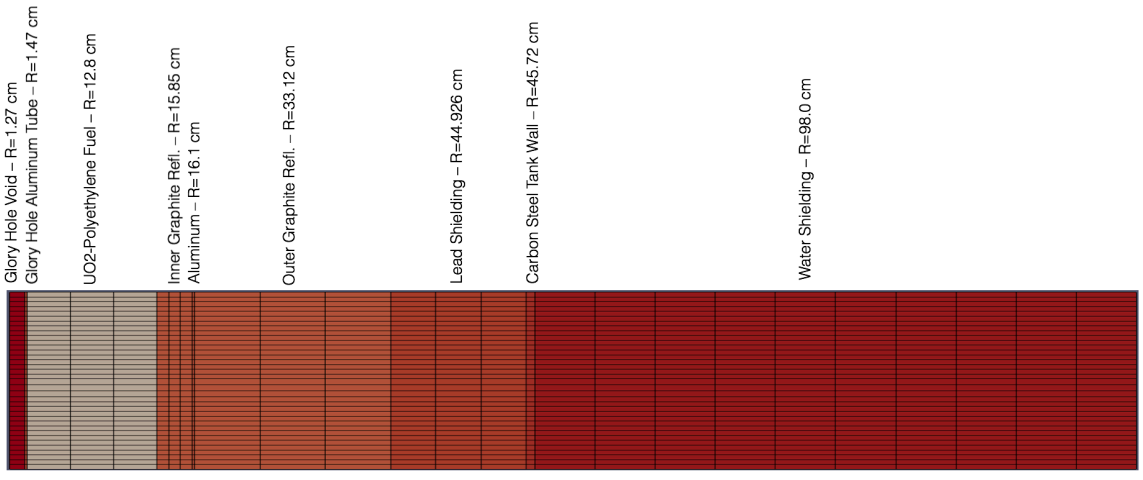

Figure 66. EVENT RZ Model Illustration

www.manaraa.com

Table 31. EVENT RZ Model Detail and Results

Case Name	Composition	Radius (Thickness)	Model Illustration (Mirror Boundary Conditions in ±Z Direction, Vacuum Boundary Conditions on the Outer Surface)	Results k-eff (% Diff. from AGN_2D_a Case)
AGN_2D_a	Air	1.1875 cm (1.1875 cm)	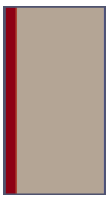	1.03178
	Aluminum	1.27 cm (0.0825 cm)		
	Homogeneous Fuel	12.80 cm (11.53 cm)		0.00%
AGN_2D_b	AGN_2D_a + Graphite	15.85 cm (3.05 cm)	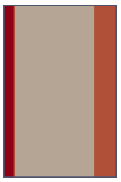	1.08692
				5.34%
AGN_2D_c	AGN_2D_b + Aluminum	16.10 cm (0.25 cm)	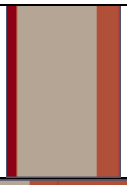	1.08827
				0.12%
AGN_2D_d	AGN_2D_c + Graphite	33.12 cm (17.02 cm)	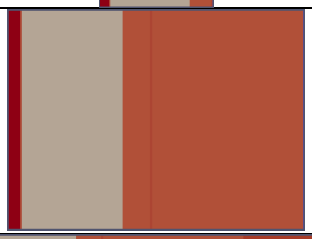	1.21655
				11.79%
AGN_2D_e	AGN_2D_d + Lead	44.926 cm (11.806 cm)	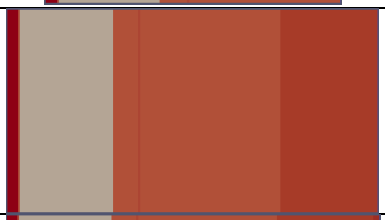	1.24356
				2.22%
AGN_2D_f	AGN_2D_e + Carbon Steel	45.72 cm (0.794 cm)	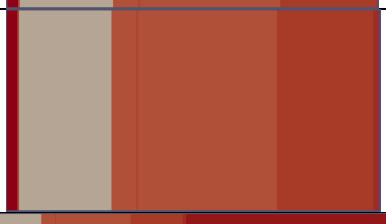	1.24606
				0.20%
AGN_2D_g	AGN_2D_g + Water	98.00 cm (52.28 cm)	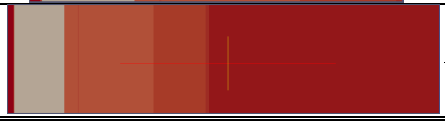	1.25596
				0.79%

www.manaraa.com

A.3.2 Angular Flux Expansion and Order of Scattering Anisotropy for EVENT RZ Model

As was discussed in Section A.2.2 for the XY EVENT cases, a parametric study was performed with variations of both the angular flux expansion and the order of scattering anisotropy to determine the optimal combination for the RZ EVENT model as well. The results of this parametric study are summarized in Table 31 and show P_5 angular flux expansion and a 3rd order of scattering anisotropy produces both an accurate k_{eff} result and an efficient calculation, using the same criteria as the XY parametric study summarized in Table 29. These options will be used for the EVENT RZ computations for this work unless otherwise stated.

www.manaraa.com

Table 32. Angular Flux Expansion and Scattering Order Comparison Results for the EVENT RZ Model

	P_1 Angular Flux Expansion	**P_3 Angular Flux Expansion**	**P_5 Angular Flux Expansion**	**P_9 Angular Flux Expansion**
0th Order Scattering Anisotropy	[1,0]	[3,0]	[5,0]	[9,0]
k_{eff}	1.33394	1.33568	1.33570	1.33571
% Diff. from [9,9] Result	6.2079%	6.3458%	6.3477%	6.3484%
Time to Execute	5.75 sec.	44.45 sec.	150.75 sec.	451.39 sec.
1st Order Scattering Anisotropy	[1,1]	[3,1]	[5,1]	[9,1]
k_{eff}	1.25230	1.25557	1.25561	1.25563
% Diff. from [9,9] Result	-0.2927%	-0.0322%	-0.0289%	-0.0277%
Time to Execute	4.33 sec.	33.69 sec.	81.01 sec.	294.16 sec.
3rd Order Scattering Anisotropy	[1,3]	[3,3]	**[5,3]**	[9,3]
k_{eff}	1.25230	1.25592	**1.25596**	1.25598
% Diff. from [9,9] Result	-0.2927%	-0.0046%	**-0.0012%**	0.0000%
Time to Execute	4.34 sec.	33.46 sec.	**66.74 sec.**	295.03 sec.
5th Order Scattering Anisotropy	[1,5]	[3,5]	[5,5]	[9,5]
k_{eff}	1.25230	1.25596	1.25596	1.25598
% Diff. from [9,9] Result	-0.2927%	-0.0012%	-0.0011%	0.0000%
Time to Execute	4.31 sec.	69.41 sec.	76.54 sec.	263.76 sec.
9th Order Scattering Anisotropy	[1,9]	[3,9]	[5,9]	[9,9]
k_{eff}	1.25230	1.25592	1.25596	1.25598
% Diff. from [9,9] Result	-0.2927%	-0.0046%	-0.0011%	0.0000%
Time to Execute	4.28 sec.	32.14 sec.	90.20 sec.	261.31 sec.

www.manaraa.com

A.3.3 Cross-Section Parametric Study with EVENT RZ Model

The methodology for generating case-dependent or working neutron cross-section libraries, discussed in Section 3.2.2, describes how the broad group libraries, particularly the 2-, 4-, and 8-group case-dependent cross-section libraries, were created for this work by collapsing a fine 252-group or 238-group library from the ENDF/B-VII.1 and ENDF/B-VII libraries, respectively. The final working library has also been adjusted to account for resonance self-shielding effects due to the significant presence of ^{238}U in the AGN core fuel. After this work was initiated, a beta version of SCALE 6.2 was released that included the new ENDF/B-VII.1 neutron cross-section libraries. The SCALE 252-group master library was created from raw point-wise data from the ENDF/B-VII.1 library. Using the methodology described previously, a suite of collapsed multigroup working libraries were created with a different number of neutron energy groups: 2-, 3-, 4-, 6-, and 8-group cross-sections. These new, collapsed neutron cross-sections are tested in this section by using the EVENT RZ model with the optimized P_N and scattering order results determined previously, 5 and 3, respectively. Figure 67 shows the results of performing the same calculation for the EVENT RZ model with a different set of neutron cross-sections. The results for the MCNP6 calculations, cases AGN_2D_a through AGN_2D_g, using continuous-energy (CE) neutron cross-sections are also plotted alongside the EVENT RZ results for comparison purposes.

www.manaraa.com

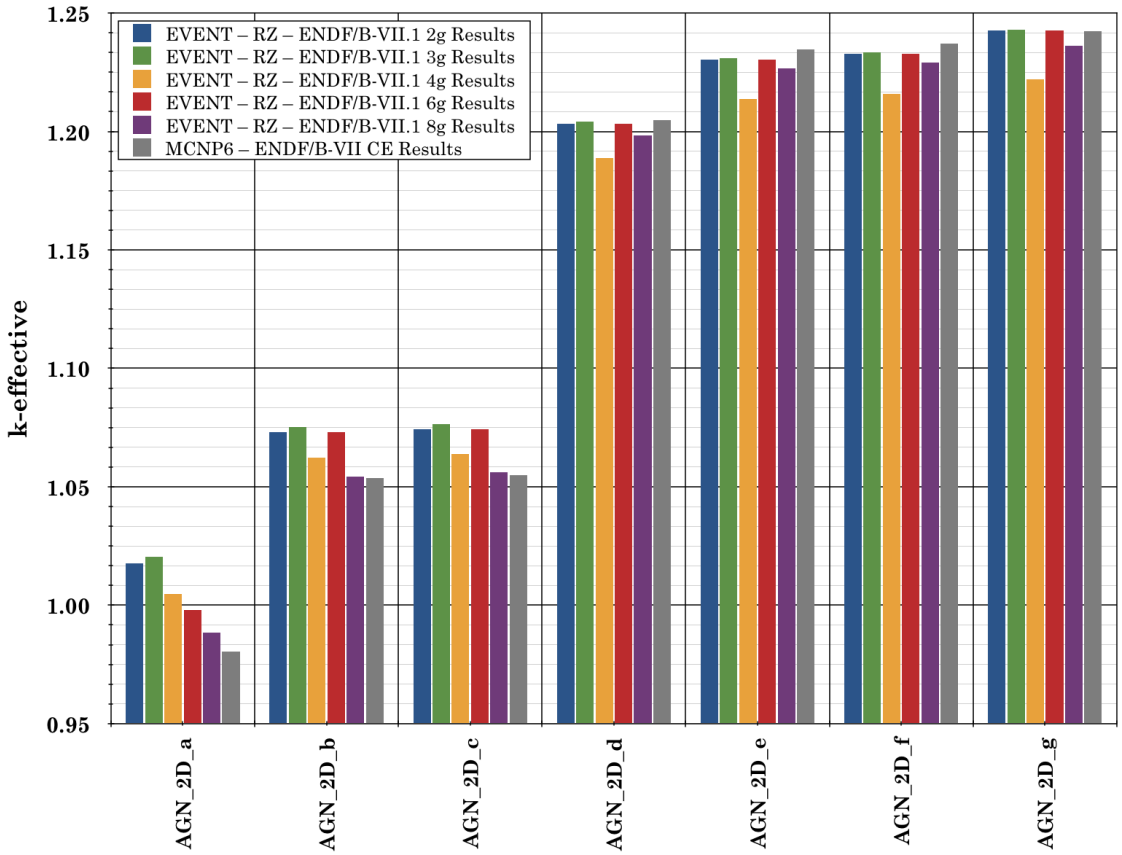

Figure 67. Results of Neutron Cross-Section Parametric Study

The results show the 2-, 3-, 6-, and 8-group working cross-section libraries (ENDF/B-VII.1 library) provide k_{eff} results several percent greater than the ENDF/B-VII CE MCNP6 case for AGN_2D_a through AGN_2D_c. The k_{eff} results for the AGN_2D_d through AGN_2D_g cases show better agreement (within a couple percent) for all multigroup libraries compared to the MCNP6 cases. The ENDF/B-VII.1 4-group working library results in k_{eff} results approximately 2% smaller than the other cases, and the ENDF/B-VII.1 8-group working library results in k_{eff} results about ~1% smaller than the other cases. The results from the AGN_2D_g calculations indicate the computation

www.manaraa.com

with the 8-group library takes more than five times longer than the same case using the 2-group library, assuming a P_5 computation with a scattering order of 3 for both problems. The 2-group result provides similar eigenvalue results with a significant reduction in EVENT execution time. For the AGN experimental analysis, the steady-state and time-dependent EVENT calculations for this work, scoping calculations have shown more efficient EVENT results with the 2-group working library compared to the 4-group (or greater) number of energy groups, especially for P_3 computations compared to P_1 (diffusion theory) results (hours versus minutes). Because the AGN is a thermal homogeneous research reactor, the 2-group library compared well to the other libraries. Scoping calculations also indicate the 2-group library works well for 3-D EVENT models and provides for very efficient computations. Thus, the SCALE 2-group library based on the latest ENDF/B-VII.1 cross-sections will be used for the subsequent EVENT 3-D model testing work.

A.4 EVENT Time Dependent Calculation Testing

The analytical solution to the point kinetics equations with one delayed family, shown in Equation 25 and Equation 26, are used to compare a point kinetics equations approximation to the results for a simple EVENT time dependent problem. The EVENT case was also compared to a numerical solution to the point kinetics equations with one delayed neutron group using the NDSOLVE function in *Mathematica*. The AGN values for the mean

www.manaraa.com

neutron lifetime, Λ, (0.0001 sec.) and the effective delayed neutron yield fraction, β, (0.006524) the averaged delayed neutron decay constant, λ, (0.4078 sec^{-1}) and reactivity, ρ, (Table 32) are substituted into Equation 38 and Microsoft Excel is used to plot the results as a function of time.

The configuration considered is a 2-D annulus with an outer diameter of 25.0 cm and an inner diameter of 4.0 cm (Figure 68). The annulus contains a fissile material and moderator mixture identical to that of the AGN core, LEU (19.5 wt. % enriched ^{235}U core) mixed uniformly with polyethylene moderator.

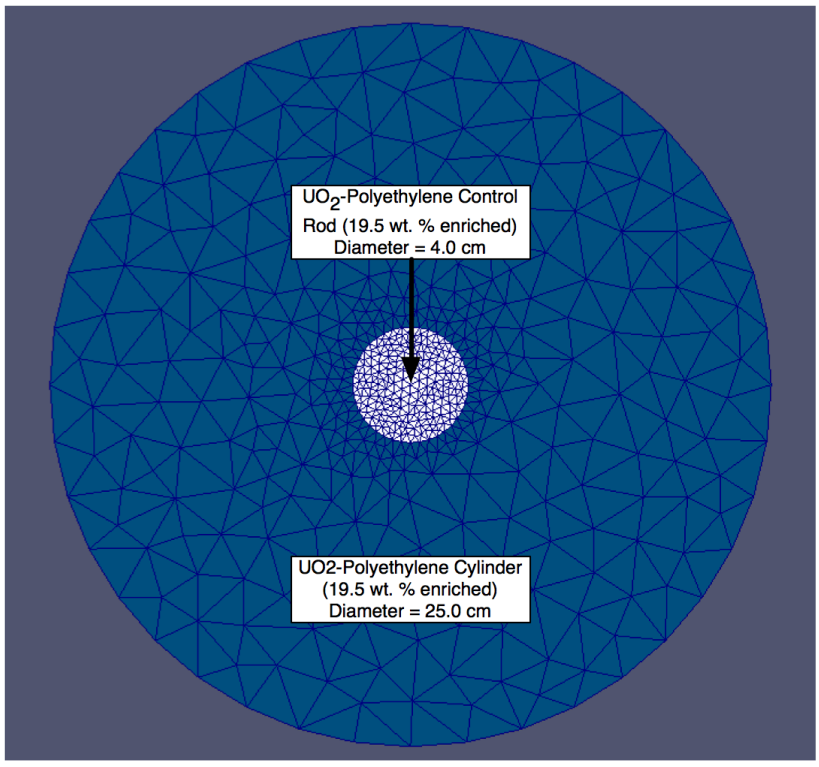

Figure 68. Illustration of UO_2-Polyethylene Cylinder for EVENT Testing

www.manaraa.com

Atom density composition data for this model is provided in Table 5.

Scoping calculations were performed with the 4-group ENDF/B-VII.1 cross-sections and the EVENT computations compared to the analytical and numerical solutions were done with the 2-group library (also based on the ENDF/B-VII.1 library). Of course, the EVENT model considered only one group of delayed neutrons as the delayed neutron source for the problem. The reactivity of the EVENT model was controlled with a single, cylindrical control rod present inside the core annulus. Specifically, the volume fraction of fuel in a fuel/air mixture was changed to simulate insertion of the rod into the core. Thus, a removed control rod would have a fuel volume fraction of zero and an inserted control rod would have a fuel volume fraction of 1.0. The EVENT input file is listed in Appendix C. Based on the k_{eff} results for the control rod volume fraction parametric study, the reactivity, ρ, can be calculated using the definition of reactivity, defined previously. The ratio $n(t)/n(0)$ is calculated to compare to EVENT results and represents the multiplication of the neutron population in the reactor as a function of time compared to the neutron population at the start of the reactivity change, i.e., $t = 0$. The k_{eff} results are shown in Figure 69 and reactivity (rod calibration curve) results are illustrated in Figure 70 for this simple 2-D EVENT configuration.

The reactivity values from the EVENT calibration curve (curve fit) were used to examine the effect of a transient worth for a prompt jump in reactivity from a delayed critical configuration as a result of introducing

www.manaraa.com

reactivity through a control rod insertion. During actual AGN operations, excess reactivity is introduced into the AGN from a delayed critical state by inserting all the control rods, except for the fine control rod, fully into the core. Thus, the reactivity change from a delayed critical state (ρ=0) to an arbitrary maximum k_{eff} of 1.0025 (ρ=0.00253) is then modeled by determining the control rod fuel volume fraction from the reactivity curve fit equation. The resulting volume fraction is defined in EVENT and the reactivity value is used in the numerical and analytical models to examine the resulting prompt jump transient. This procedure was repeated for a prompt drop case where the rod was removed from the core, i.e., fuel volume fraction reduced, while the core was initially in a delayed critical state. The core reactivity and fuel/air volume fraction values (vf[fuel] and vf[air]) are shown in Table 32.

Table 33. Transient Testing Reactivity and Control Rod Definitions

Raw Data – Correlate USLUG Reactivity to POINT KINETICS Reactivity			**EVENT XY TRANSIENT MODEL Control Rod Definitions**				
Transient	k_{eff}	ρ	Time	vf(core)	vf(air)	k_{eff}	Reactivity
1 - ramp	1.0025	0.00253	0	0.67944	0.32056	1.00000	0
			> 0	0.76655	0.23345	1.00250	0.00253
2 - drop	0.98337	-0.01680	0	0.67944	0.32056	1.00000	0
			> 0	0.10000	0.90000	0.98337	-0.01680

www.manaraa.com

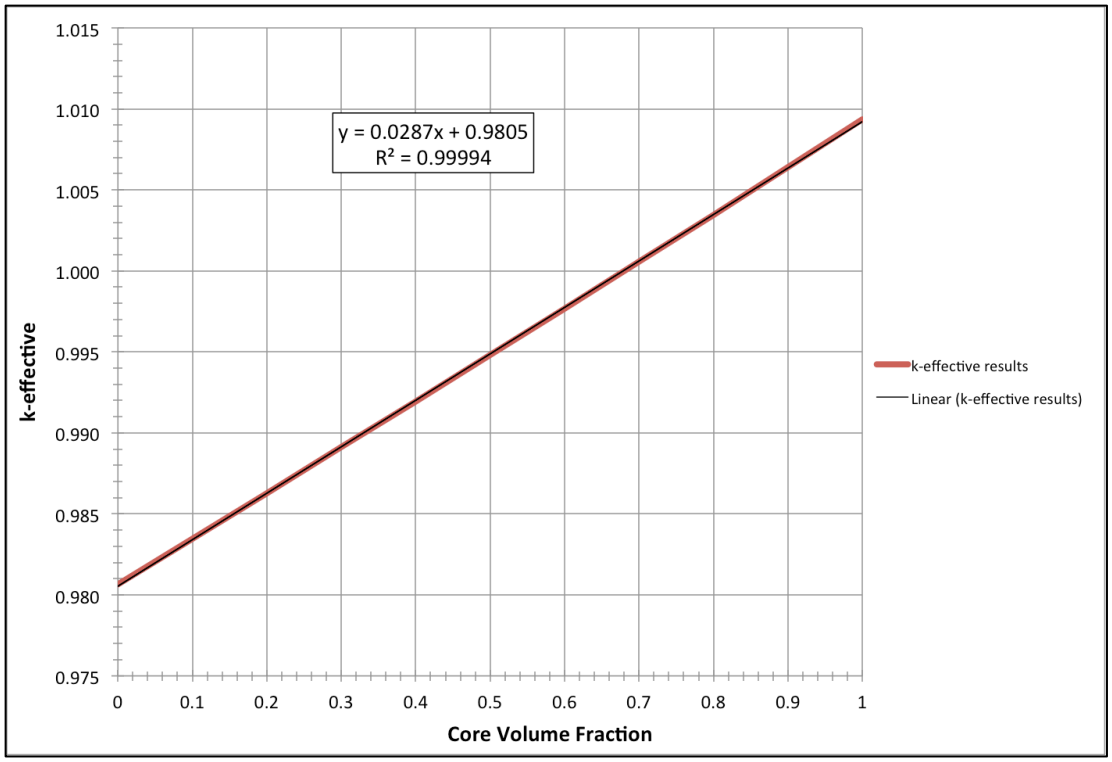

Figure 69. 2-D EVENT 2-D Annular Cylinder k_{eff} Results

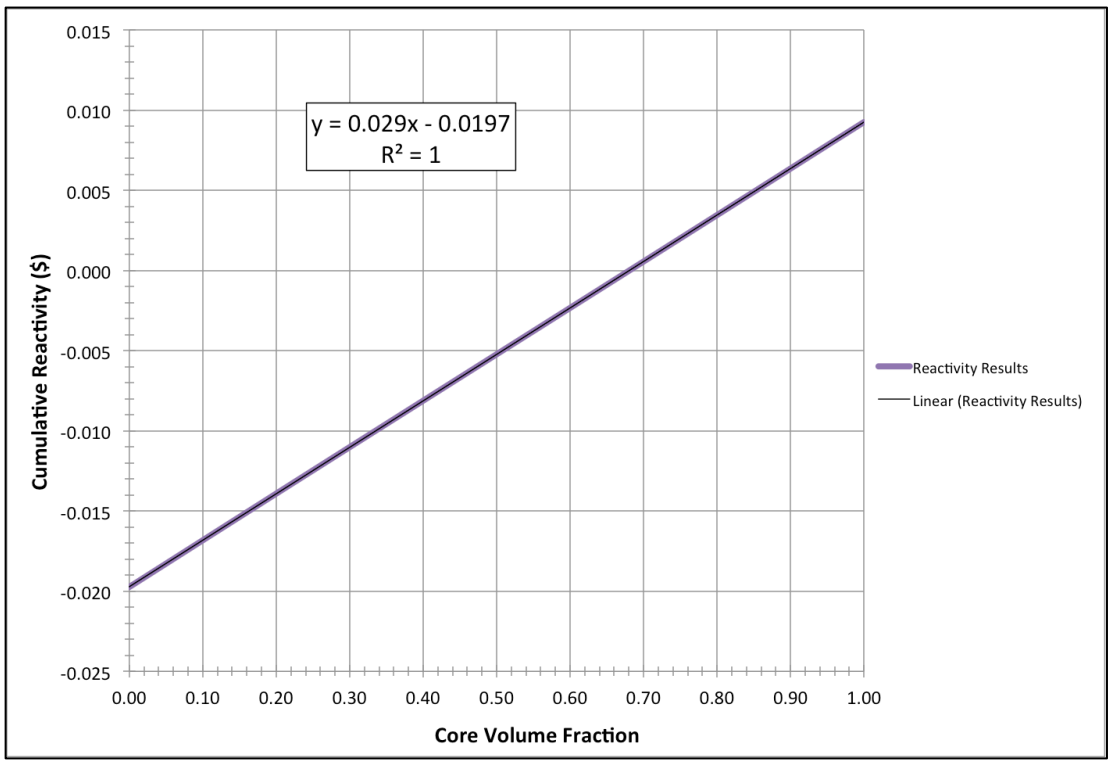

Figure 70. 2-D EVENT 2-D Annular Cylinder Reactivity Results

www.manaraa.com

The transient testing results for the prompt jump case is shown in Figure 71 and the results for the prompt drop case is shown in Figure 72. The results for the prompt jump case compare well to both the numerical and analytical computations. The one delayed group approximation analytical calculation and the numerical solution using the NDSOLVE function in *Mathematica* agree well over the range of interest, in this case between zero and 1.0 second. There are some differences in the agreement between EVENT and the approximation results between 0 and 0.05 seconds after the transient is initiated. This region is related to the presence of prompt neutrons in the system during the transient that are dampened quickly after the transient begins. This difference is likely due to increased rigor of the EVENT calculation compared to the ODG approximation results. EVENT considers the 2-D geometry, material cross-section data, and delayed neutron source explicitly in the calculation, whereas the ODG approximation considers uniform reactivity changes in the core region. The consistent slope of the EVENT, ODG Approx., and ODG NSOLVE curve implies the delayed neutron treatment in EVENT is reasonable.

www.manaraa.com

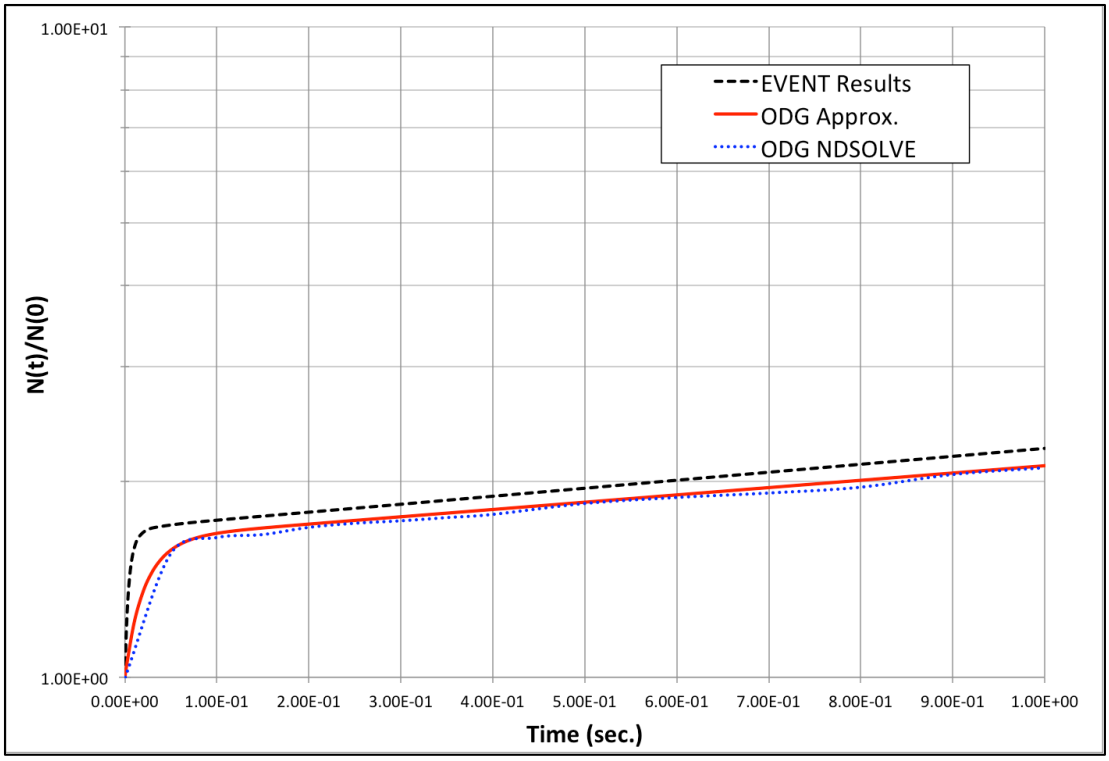

Figure 71. Transient Testing Results for Prompt Jump Case

The prompt drop results show reasonable agreement as well between the three representations. There is a small inconsistency between the three calculations during the prompt drop phase of the calculations where the presence of prompt neutrons are important. The EVENT results slightly underpredict the reactivity worth of the control rod in this region, although the curve slopes are similar in the region up to about 0.03 seconds. The three models seem to represent the dampening of the prompt neutrons after this point and the importance of the delayed neutrons showing the delayed neutron decay tail in the range considered. Overall, the EVENT results appear to confirm predictions using the point kinetics approximation for one delayed neutron group. These calculations provide some level of confidence

www.manaraa.com

that the EVENT results could reasonably predict transient behavior in the AGN due to the movement of the CCR and FCR in the core. These computations also proved invaluable for defining the calculation methodology for the subsequent AGN EVENT experimental transient analysis.

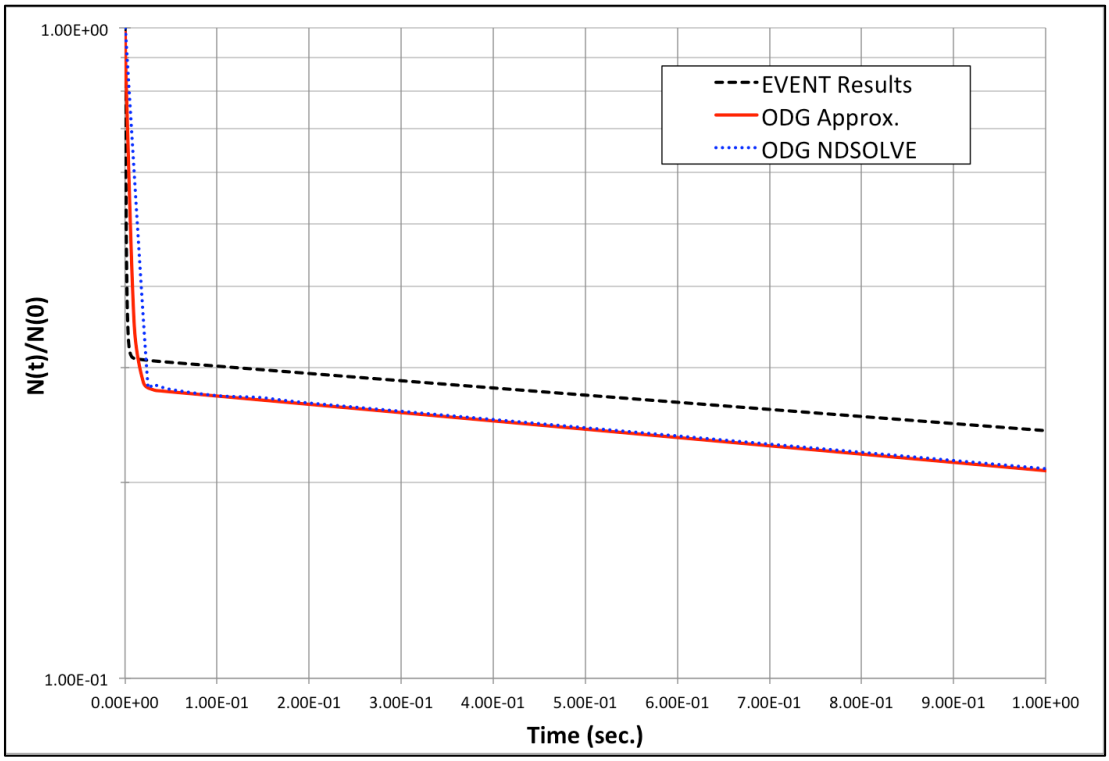

Figure 72. Transient Testing Results for Prompt Drop Case

www.manaraa.com

Appendix B – AGN Reactor Experiment Logs

www.manaraa.com

Appendix III B

THE UNIVERSITY OF NEW MEXICO
AGN-201M REACTOR OPERATIONS LOG

Page 1/____
Date 12/17/13

OPERATIONAL INFORMATION:

OPERATOR R. Busch **SUPERVISOR** R. Busch

AUTHORIZED EXPERIMENTS Rod Measurements - OP Requal **RFU#** 559

AUTHORIZED CHANGES (loading, instruments, etc.): ~~None~~ RB Back Side Glory Hole Shielding Removed

DATE LAST MONTHLY 12/2/13 **GLORY HOLE LOADING** As Noted in Log

WATER TEMP. 18.2°C **REMARKS** None

SUPERVISOR'S APPROVAL N/A
(SIGNATURE REQUIRED FOR NEW EXPERIMENTS)

PRECRITICAL START-UP CHECK-OUT

a. *Nearby personnel informed* ✓

b. *Radiation monitors operational* ✓

c. *Radiation Survey OK* ✓

d. Reactor Inspection:
- *Thermal column secured* ✓
- *Manhole cover secured* ✓
- *Shield doors in place* ✓
- *Check for water leaks* ✓
- *Stair gate locked ,access alarm works* ✓
- *Cadmium in Glory Hole* ✓

e. TURN ON CONTROL PANEL POWER
DO NOT CONTINUE UNLESS BELL RINGS!

f. *Data Display on.* ✓

g. *Source drive operational* ✓

h. NIM bin & HVPS (1-2-3-4) on 6 ✓

i. Channel one instrument check:
- *Counts per minute* 222
- *Detector high voltage* 250 VDC
- *Amplifier gain:* Fine 7.0, Coarse 4
- *Discriminator Level* 0.6
- *Automatic H V removal okay* ✓
- *Compare to previous conditions* ✓

j. Channel two instrument check:
- *Detector high voltage* 600 VDC
- *Low level INTERLOCK OK* ✓
- *High level SCRAM OK* ✓
- *Calibrate check @ $1x10^{-11}$* ✓
- *Calibrate check @ $5x10^{-7}$* ✓

k. Channel three instrument check:
- *Detector high voltage* 600 VDC
- *High level SCRAM OK* ✓
- *Calibrate check @ $1x10^{-11}$* ✓
- *Calibrate check @ $5x10^{-7}$* ✓

l. Magnet current check:
- *Magnet current level* 70 ma
- *Low current trip operational* ✓

m. *Interlocks cleared* ✓

n. *Manual SCRAM operational* ✓
(fully insert SR1 and then scram)

o. *Data Display operational* ✓

Precritical Start-up check-out completed ✓

Reactor Supervisor Robert Busch

www.manaraa.com

Time of startup 8:40

Elapsed time meter 36:05 hours

Cd removed from Glory Hole ✓

Console radiation level 0.015 mR/hr

Control Rod Lower Limit Positions:

Fine rod 1.09 cm

Coarse rod 97.93 (-2.07) cm

Instrument Readings		
Channel	All Rods OUT	Safety Rods IN
1	316 CPM	526 CPM
2	2.5×10^{-11} Amps	2.5×10^{-11} Amps
3	2.5×10^{-12} Amps	5×10^{-12} Amps
4	4.2×10^{-11} Amps	1.05×10^{-10} Amps
Previous Meter Readings Noted ___		

Critical Readings

Time of day 8:54	Channel two 8×10^{-8} Amps	Reactor Top 100 mR/hr
Elapsed time 36:19 Hours	Channel three 6.8×10^{-8} Amps	Reactor Console 1.1 mR/hr
Power Level 4.06 Watts	Aux. Channel 1.46×10^{-6} Amps	Check Pt. 3 22 mR/hr

OPERATIONAL DATA:

Time	Channel 3 Reading	Fine Rod Position	Coarse Rod Position	Comments (loading changes, power level, changes, scrams
8:48	—	—	—	Source Removed
8:49	—	24.53	20.73	Excess ρ $T_{1/2}$=12.6 sec. T=18.2°C
8:55	6.8×10^{-8}	21.37	18.21	Steady Power 4.06 W Rods Banked (ΔX = 3.16 cm)
8:59	6.8×10^{-8}	22.57	18.00	Steady Power
9:01	6.8×10^{-8}	23.21	17.90	Steady Power

REACTOR SHUTDOWN:

Scram method MANUAL

Time of day 15:49

Elapsed time 40:07

All rods down ✓

Startup source inserted ✓

Cadmium inserted in Glory Hole ✓

Data Display off ✓

Console power off ✓

Portable radiation monitors off ___

Reactor Assistant

Licensed Reactor Operator Robert D Busch

Authorized Operator

Reactor Supervisor Robert D Busch

www.manaraa.com

Page 3/5
Date 12/17/13

OPERATIONAL DATA:

Time	Channel 3 Reading	Fine Rod Position	Coarse Rod Position	Comments (loading changes, power level, changes, scrams)
9:04	6.8×10^{-8}	23.74	17.80	Steady Power
9:06	6.8×10^{-8}	24.21	17.70	Steady Power
9:08	6.8×10^{-8}	24.54	17.67	Steady Power - FCR Full IN
9:11	6.8×10^{-8}	23.54	17.87	Steady Power
9:13	6.8×10^{-8}	22.54	18.14	Steady Power
9:15	6.8×10^{-8}	21.54	18.39	Steady Power
9:16	6.8×10^{-8}	20.54	18.60	Steady Power
9:17	6.8×10^{-8}	19.54	18.82	Steady Power
9:19	6.8×10^{-8}	18.54	19.03	Steady Power
9:22	6.8×10^{-8}	17.54	19.28	Steady Power
9:25	6.8×10^{-8}	16.54	19.54	Steady Power
9:29	6.8×10^{-8}	15.54	19.75	Steady Power
9:31	6.8×10^{-8}	14.54	20.03	Steady Power
9:34	6.8×10^{-8}	13.54	20.27	Steady Power
9:37	6.8×10^{-8}	12.54	20.52	Steady Power
9:43	6.8×10^{-8}	11.04	20.90	Steady Power - CCR Full IN
9:49	6.8×10^{-8}	21.55	18.49	Steady Power Rods Banked (Δ = 3.04cm)
9:51	6.8×10^{-8}	21.64	18.48	Steady Power Rods Banked (Δ = 3.16 cm)
9:54	6.8×10^{-8}	24.53	17.88	Steady Power - FCR Full IN
10:00	6.8×10^{-8}	11.15	20.91	Steady Power - CCR Full IN
10:10	1.5×10^{-9}	11.01	20.44	Steady Power 0.102 W CCR Full IN.
10:15	—	24.53	20.44	Exceeds Reactivity $T_{1/2}$ = 13.2 sec
10:17	6.8×10^{-9}	21.20	18.04	Steady Power Rods Banked (Δ = 3.16 cm)
10:19	—	01.65	97.55	Manual Scram

www.manaraa.com

OPERATIONAL DATA:

Time	Channel 3 Reading	Fine Rod Position	Coarse Rod Position	Comments (loading changes, power level, changes, scrams)
13:25	—	—	—	Reactor Restart
13:32	—	24.52	20.16	Doubling Time $T_{1/2}$ = 13.2sec. T=18.3°C
13:41	$6.8X10^{-8}$	10.78	20.16	Steady Power
13:41	—	—	—	Coarse Rod Dropped
13:46	—	10.78	97.46	CR Drive Full Out
13:49	—	24.53	20.14	Excess ρ $T_{1/2}$ = 13.4 sec. T=18.3°C
13:55	$6.8X10^{-8}$	20.28	18.00	Steady Power
13:57	—	—	—	Coarse Rod Dropped
13:59	—	20.28	97.50	CR Drive Full Out
14:00	—	24.53	20.16	Excess ρ $T_{1/2}$ = 13.3
14:08	$6.8X10^{-8}$	12.25	19.80	Steady Power
14:09	—	—	—	Coarse Rod Dropped
14:11	—	12.25	97.42	CR Drive Full Out
14:13	—	24.53	20.23	Excess ρ $T_{1/2}$ = 13.2 sec
14:20	$6.8X10^{-8}$	12.31	19.90	Steady Power
14:21	—	—	—	Coarse Rod Dropped
14:22	—	12.31	97.46	CR Drive Full Out
14:24	—	24.53	20.30	Excess ρ $T_{1/2}$ = 13.5 sec T=18.3°C
14:35	$6.8X10^{-8}$	12.50	20.00	Steady Power
14:36	—	—	—	Coarse Rod Dropped
14:38	—	12.50	97.51	CR Drive Full Out
14:40	—	24.53	20.37	Excess ρ $T_{1/2}$ = 13.5 sec. T=18.3°C
14:47	$6.8X10^{-8}$	15.42	19.50	Steady Power
14:47	—	—	—	Coarse Rod Dropped
14:51	—	15.42	97.68	CR Drive Full Out
14:53	—	24.53	20.51	Excess ρ $T_{1/2}$ = 14.2 sec T=18.3°C

www.manaraa.com

Page 5/5
Date 12/17/13

OPERATIONAL DATA:

Time	Channel 3 Reading	Fine Rod Position	Coarse Rod Position	Comments (loading changes, power level, changes, scrams)
14:59	6.8×10^{-8}	17.80	19.00	Steady Power
15:02	—	17.80	97.74	CR Drive Full Out
15:10	6.8×10^{-8}	21.50	18.34	Steady Power
15:11	—	—	—	Coarse Rod Dropped
15:13	—	21.50	97.95	CR Drive Full Out
15:14	—	24.53	20.79	Excess ρ $T_{1/2} = 13.4$ sec $T = 18.3°C$
15:20	6.8×10^{-8}	24.53	17.91	Steady Power
15:21	—	—	—	Coarse Rod Dropped
15:23	—	24.53	98.19	CR Drive Full Out
15:25	—	24.53	21.02	Excess ρ $T_{1/2} = 13.5$ sec $T = 18.3°C$
15:33	6.8×10^{-8}	11.42	21.02	Steady Power
15:33	—	—	—	Coarse Rod Dropped
15:35	—	11.42	98.21	CR Drive Full Out
15:37	—	24.53	21.04	Excess ρ $T_{1/2} = 13.6$ sec $T = 18.3°C$
15:41	6.8×10^{-8}	11.48	21.04	Steady Power
15:42	—	—	—	Safety Rod 2 Dropped
15:46	—	—	—	About 10 mW seems to flatten out from $T_{1/2} = 55$ sec
15:48	—	—	—	Manual Scram
		No Further Entries		

www.manaraa.com

Appendix C – Model Input Files

C.1 Introduction

This appendix provides listings of the input files generated to support this work. Input files are provided for the generation of the nuclear data, effective delayed neutron fraction determination, 2-D model for cross section testing using MCNP6 and EVENT, and 3-D models for cross section testing and experimental verification analysis. Also included are the *Mathematica* notebook listing of the numerical solution of the point kinetics equations to support EVENT transient testing and delayed neutron analysis.

C.2 SCALE Models

C.2.1 Generation of the Multigroup Cross Sections

The following input file was used to generate case dependent multigroup cross sections for the AGN-201M research reactor using the CSAS1D

www.manaraa.com

sequence of SCALE (version 6.2, beta 3) and ENDF/B-VII.1 cross section data. The resonance self-shielding calculation was performed using CENTRM and the cross section collapsing was perormed by MALOCS2. The KENO-VI input file following the self-shielding calculation and the cross section collapse is used to test the new broad group library with an detailed AGN model to ensure the cross sections were prepared correctly.

```
=shell
ln -sf /projects/scale/scale_dev_data/scale.rev03.xn252v7.1  ft88f001
end

=csas1d  parm=centrm
PWR Cell fuel=600K, clad=600K, Mod=600K
ft88f001
read composition
 uo2         5 den=10.936 0.029985 291
                                  92235 19.5
                                  92238 80.5   end
 polyethylene 5 den=0.92 0.97661 291   end
 al          15 1 291   end
 al          25 1 291   end
 al          35 1 291   end
 graphite    16 den=1.75 1 291   end
 graphite    26 den=1.75 1 291   end
 pb          17 0.95 291   end
 h2o         18 den=0.9985 1 291   end
 carbonsteel 19 1 291   end
end composition

read celldata
multiregion cylindrical left_bdy=reflected right_bdy=white end
 15 0.5
  0 0.635
 25 0.794
  5 12.8
 16 15.85
 35 16.1
 26 33.12
 17 44.926
 19 45.72
 18 55.291
  end zone
 centrmdata ixprt=1 demin=0.0001 npxs=6 nmf6=0 iup=20  end centrmdata
 moredata nsensx=61 fwr=62
     eps=1.0-6 ptc=1.0-7 szf=.25 isn=32 icm=100
 end moredata
end celldata
end
=malocs2
  sig=yes valid=yes max=3
  fine=ft88f001 broad=xn8v7.1.mnew  problem=ft61f001 flux=ft62f001
  numn=252 numg=0 neu= 27r1 27r2 40r3 61r4 57r5 23r6 10r7 7r8
  eps=0.01  end
end

=shell
  cp -f xn8v7.1.mnew  ${RTNDIR}/
  cp -f xn8v7.1.mnew doug_agn
end

=csas6 parm=(centrm)
agn-201m detailed model
doug_agn
read composition
 uo2         1 den=10.936 0.030283 291
                                  92235 19.5
                                  92238 80.5   end
 polyethylene 1 den=0.92 0.98497 291   end
 uo2         2 den=10.936 0.030354 291
                                  92235 19.5
                                  92238 80.5   end
 polyethylene 2 den=0.92 0.98945 291   end
 uo2         3 den=10.936 0.029914 291
```


www.manaraa.com

```
                                  92235 19.5
                                  92238 80.5   end
 polyethylene 3 den=0.92 0.97352 291   end
 uo2          4 den=10.936 0.0301 291
                                  92235 19.5
                                  92238 80.5   end
 polyethylene 4 den=0.92 0.9789 291   end
 uo2          5 den=10.936 0.029985 291
                                  92235 19.5
                                  92238 80.5   end
 polyethylene 5 den=0.92 0.97661 291   end
 uo2          6 den=10.936 0.030016 291
                                  92235 19.5
                                  92238 80.5   end
 polyethylene 6 den=0.92 0.9773 291   end
 uo2          7 den=10.936 0.030005 291
                                  92235 19.5
                                  92238 80.5   end
 polyethylene 7 den=0.92 0.97689 291   end
 uo2          8 den=10.936 0.03184 291
                                  92235 19.5
                                  92238 80.5   end
 polyethylene 8 den=0.92 1.03639 291   end
 uo2          9 den=10.936 0.030796 291
                                  92235 19.5
                                  92238 80.5   end
 polyethylene 9 den=0.92 1.0034 291   end
 uo2          10 den=10.936 0.04519 291
                                  92235 19.5
                                  92238 80.5   end
 polyethylene 10 den=0.92 0.78221 291   end
 uo2          11 den=10.936 0.030341 291
                                  92235 19.5
                                  92238 80.5   end
 polyethylene 11 den=0.92 0.98814 291   end
 uo2          12 den=10.936 0.03032 291
                                  92235 19.5
                                  92238 80.5   end
 polyethylene 12 den=0.92 0.98736 291   end
 uo2          13 den=10.936 0.030341 291
                                  92235 19.5
                                  92238 80.5   end
 polyethylene 13 den=0.92 0.98733 291   end
 uo2          14 den=10.936 0.028688 291
                                  92235 19.5
                                  92238 80.5   end
 polyethylene 14 den=0.92 0.93374 291   end
 al           15 1 291   end
 graphite     16 den=1.75 1 291   end
 pb           17 0.95 291   end
 h2o          18 den=0.9985 1 291   end
 carbonsteel 19 1 291   end
end composition
read celldata
    infhommedium  1  end
    infhommedium  2  end
    infhommedium  3  end
    infhommedium  4  end
    infhommedium  5  end
    infhommedium  6  end
    infhommedium  7  end
    infhommedium  8  end
    infhommedium  9  end
    infhommedium  10  end
    infhommedium  11  end
    infhommedium  12  end
    infhommedium  13  end
    infhommedium  14  end
    infhommedium  15  end
    infhommedium  16  end
    infhommedium  17  end
    infhommedium  18  end
    infhommedium  19  end
    centrmdata iup=10 id1=0  ipbt=1  ixprt=1  end centrmdata
end celldata
read parameter
 gen=50
 npg=10000
 nsk=10
 htm=yes
 flx=yes
end parameter
read geometry
unit 1
com="disk 20497 "
 cylinder 5      0.5        4        0
 cylinder 6    0.635        4        0
 cylinder 7    0.794        4        0
 cylinder 10     12.8         4        0
 hole 11   origin  x=-5.87 y=5.87 z=0
 hole 12   origin  x=5.87 y=-5.87 z=0
 hole 13   origin  x=5.87 y=5.87 z=0
 hole 14   origin  x=-5.87 y=-5.87 z=0
 cylinder 20    15.85         4        0
 cylinder 30     16.1         4        0
```


www.manaraa.com

```
 cylinder 40    33.12        4        0
 cylinder 50   44.926        4        0
 cylinder 60    45.72        4        0
 cylinder 70       98        4        0
 cuboid 80       98      -98       98      -98        4        0
 media 15 1 5           vol= 3.13607E+00
 media 0 1 6 -5         vol= 1.91919E+00
 media 15 1 7 -6        vol= 2.84350E+00
 media 1 1 10 -7        vol= 1.73237E+03
 media 16 1 20 -10      vol= 1.09474E+03
 media 15 1 30 -20      vol= 1.00048E+02
 media 16 1 40 -30      vol= 1.04951E+04
 media 17 1 50 -40      vol= 1.15435E+04
 media 19 1 60 -50      vol= 9.01616E+02
 media 18 1 70 -60      vol= 9.41321E+04
 media 0 1 80 -70       vol= 3.28761E+04
 boundary 80
unit 2
com="disk 20498 "
 cylinder 5      0.5        4        0
 cylinder 6    0.635        4        0
 cylinder 7    0.794        4        0
 cylinder 10     12.8        4        0
 hole 11   origin  x=-5.87 y=5.87 z=0
 hole 12   origin  x=5.87 y=-5.87 z=0
 hole 13   origin  x=5.87 y=5.87 z=0
 hole 14   origin  x=-5.87 y=-5.87 z=0
 cylinder 20    15.85        4        0
 cylinder 30     16.1        4        0
 cylinder 40    33.12        4        0
 cylinder 50   44.926        4        0
 cylinder 60    45.72        4        0
 cylinder 70       98        4        0
 cuboid 80       98      -98       98      -98        4        0
 media 15 1 5         vol= 3.15359E+00
 media 0 1 6 -5       vol= 1.92991E+00
 media 15 1 7 -6      vol= 2.85938E+00
 media 2 1 10 -7      vol= 1.74205E+03
 media 16 1 20 -10    vol= 1.10086E+03
 media 15 1 30 -20    vol= 1.00607E+02
 media 16 1 40 -30    vol= 1.05537E+04
 media 17 1 50 -40    vol= 1.16080E+04
 media 19 1 60 -50    vol= 9.06653E+02
 media 18 1 70 -60    vol= 9.46580E+04
 media 0 1 80 -70     vol= 3.30597E+04
 boundary 80
unit 3
com="disk 20499 "
 xcylinder 5     1.27       98      -98   origin  x=0 y=0 z=4.25
 xcylinder 6     1.47       98      -98   origin  x=0 y=0 z=4.25
 cylinder 10     12.8        4        0
 hole 11   origin  x=-5.87 y=5.87 z=0
 hole 12   origin  x=5.87 y=-5.87 z=0
 hole 13   origin  x=5.87 y=5.87 z=0
 hole 14   origin  x=-5.87 y=-5.87 z=0
 hole 81   origin  x=0 y=0 z=1.05
 hole 82
 cylinder 20    15.85        4        0
 cylinder 30     16.1        4        0
 cylinder 40    33.12        4        0
 cylinder 50   44.926        4        0
 cylinder 60    45.72        4        0
 cylinder 70       98        4        0
 cuboid 80       98      -98       98      -98        4        0
 media 0 1 5 10          vol= 4.92464E+01
 media 15 1 6 -5 10      vol= 1.95132E+01
 media 3 1 10 -6         vol= 1.66996E+03
 media 0 1 5 20 -10      vol= 1.17591E+01
 media 15 1 6 -5 20 -10  vol= 4.67128E+00
 media 16 1 20 -10 -6    vol= 1.08443E+03
 media 0 1 5 30 -20      vol= 9.58382E-01
 media 15 1 6 -5 30 -20  vol= 3.81896E-01
 media 15 1 30 -20 -6    vol= 9.92671E+01
 media 0 1 40 -30 5      vol= 6.55758E+01
 media 15 1 40 -30 6 -5  vol= 2.60321E+01
 media 16 1 40 -30 -6    vol= 1.04621E+04
 media 0 1 50 -40 5      vol= 4.54798E+01
 media 15 1 50 -40 6 -5  vol= 1.80472E+01
 media 17 1 50 -40 -6    vol= 1.15445E+04
 media 0 1 60 -50 5      vol= 3.04052E+00
 media 15 1 60 -50 6 -5  vol= 1.21325E+00
 media 19 1 60 -50 -6    vol= 9.02400E+02
 media 0 1 70 -60 5      vol= 2.01368E+02
 media 15 1 70 -60 6 -5  vol= 7.99112E+01
 media 18 1 70 -60 -6    vol= 9.43767E+04
 media 0 1 80 -70        vol= 3.30597E+04
 boundary 80
unit 4
com="disk 204100 "
 xcylinder 5     1.27       98      -98   origin  x=0 y=0 z=-0.25
 xcylinder 6     1.47       98      -98   origin  x=0 y=0 z=-0.25
 cylinder 10     12.8        4        0
 hole 15   origin  x=-5.87 y=5.87 z=0
 hole 16   origin  x=5.87 y=-5.87 z=0
 hole 17   origin  x=5.87 y=5.87 z=0
```


www.manaraa.com

```
 hole 18   origin  x=-5.87 y=-5.87 z=0
 cylinder 20    15.85        4        0
 cylinder 30     16.1        4        0
 cylinder 40    33.12        4        0
 cylinder 50   44.926        4        0
 cylinder 60    45.72        4        0
 cylinder 70       98        4        0
 cuboid 80       98      -98       98      -98        4        0
 media 0 1 5 10          vol= 4.87191E+01
 media 15 1 6 -5 10      vol= 1.94214E+01
 media 4 1 10 -6         vol= 1.68185E+03
 media 0 1 5 20 -10      vol= 1.16331E+01
 media 15 1 6 -5 20 -10  vol= 4.64922E+00
 media 16 1 20 -10 -6    vol= 1.08458E+03
 media 0 1 5 30 -20      vol= 9.48095E-01
 media 15 1 6 -5 30 -20  vol= 3.80064E-01
 media 15 1 30 -20 -6    vol= 9.92792E+01
 media 0 1 40 -30 5      vol= 6.48732E+01
 media 15 1 40 -30 6 -5  vol= 2.59092E+01
 media 16 1 40 -30 -6    vol= 1.04629E+04
 media 0 1 50 -40 5      vol= 4.49925E+01
 media 15 1 50 -40 6 -5  vol= 1.79620E+01
 media 17 1 50 -40 -6    vol= 1.15451E+04
 media 0 1 60 -50 5      vol= 3.00794E+00
 media 15 1 60 -50 6 -5  vol= 1.20746E+00
 media 19 1 60 -50 -6    vol= 9.02438E+02
 media 0 1 70 -60 5      vol= 1.99210E+02
 media 15 1 70 -60 6 -5  vol= 7.95342E+01
 media 18 1 70 -60 -6    vol= 9.43792E+04
 media 0 1 80 -70        vol= 3.30597E+04
 boundary 80
unit 5
com="disk 204101 "
 cylinder 10     12.8        2        0
 cylinder 20    15.85        2        0
 cylinder 30     16.1        2        0
 cylinder 40    33.12        2        0
 cylinder 50   44.926        2        0
 cylinder 60    45.72        2        0
 cylinder 70       98        2        0
 cuboid 80       98      -98       98      -98        2        0
 media 5 1 10        vol= 1.02058E+03
 media 16 1 20 -10   vol= 5.44314E+02
 media 15 1 30 -20   vol= 4.97448E+01
 media 16 1 40 -30   vol= 5.21823E+03
 media 17 1 50 -40   vol= 5.73952E+03
 media 19 1 60 -50   vol= 4.48290E+02
 media 18 1 70 -60   vol= 4.68031E+04
 media 0 1 80 -70    vol= 1.63462E+04
 boundary 80
unit 6
com="disk 204102 "
 cylinder 10     12.8        2        0
 cylinder 20    15.85        2        0
 cylinder 30     16.1        2        0
 cylinder 40    33.12        2        0
 cylinder 50   44.926        2        0
 cylinder 60    45.72        2        0
 cylinder 70       98        2        0
 cuboid 80       98      -98       98      -98        2        0
 media 5 1 10        vol= 1.03204E+03
 media 16 1 20 -10   vol= 5.50430E+02
 media 15 1 30 -20   vol= 5.03037E+01
 media 16 1 40 -30   vol= 5.27687E+03
 media 17 1 50 -40   vol= 5.80401E+03
 media 19 1 60 -50   vol= 4.53327E+02
 media 18 1 70 -60   vol= 4.73290E+04
 media 0 1 80 -70    vol= 1.65299E+04
 boundary 80
unit 7
com="disk 204103 "
 cylinder 10     12.8        2        0
 cylinder 20    15.85        2        0
 cylinder 30     16.1        2        0
 cylinder 40    33.12        2        0
 cylinder 50   44.926        2        0
 cylinder 60    45.72        2        0
 cylinder 70       98        2        0
 cuboid 80       98      -98       98      -98        2        0
 media 7 1 10        vol= 1.03204E+03
 media 16 1 20 -10   vol= 5.50430E+02
 media 15 1 30 -20   vol= 5.03037E+01
 media 16 1 40 -30   vol= 5.27687E+03
 media 17 1 50 -40   vol= 5.80401E+03
 media 19 1 60 -50   vol= 4.53327E+02
 media 18 1 70 -60   vol= 4.73290E+04
 media 0 1 80 -70    vol= 1.65299E+04
 boundary 80
unit 8
com="disk 204104 "
 cylinder 10     12.8        1        0
 cylinder 20    15.85        1        0
 cylinder 30     16.1        1        0
 cylinder 40    33.12        1        0
 cylinder 50   44.926        1        0
```


www.manaraa.com

```
 cylinder 60    45.72        1        0
 cylinder 70       98        1        0
 cuboid 80       98      -98       98      -98        1        0
 media 8 1 10       vol= 5.16021E+02
 media 16 1 20 -10  vol= 2.75215E+02
 media 15 1 30 -20  vol= 2.51519E+01
 media 16 1 40 -30  vol= 2.63843E+03
 media 17 1 50 -40  vol= 2.90201E+03
 media 19 1 60 -50  vol= 2.26663E+02
 media 18 1 70 -60  vol= 2.36645E+04
 media 0 1 80 -70   vol= 8.26493E+03
 boundary 80
unit 9
com="disk 204105 "
 cylinder 10     12.8        1        0
 cylinder 15     12.8        2        0
 cylinder 20    15.85        2        0
 cylinder 30     16.1        2        0
 cylinder 40    33.12        2        0
 cylinder 50   44.926        2        0
 cylinder 60    45.72        2        0
 cylinder 70       98        2        0
 cuboid 80       98      -98       98      -98        2        0
 media 9 1 10       vol= 5.16021E+02
 media 0 1 15 -10   vol= 5.16021E+02
 media 16 1 20 -15  vol= 5.50430E+02
 media 15 1 30 -20  vol= 5.03037E+01
 media 16 1 40 -30  vol= 5.27687E+03
 media 17 1 50 -40  vol= 5.80401E+03
 media 19 1 60 -50  vol= 4.53327E+02
 media 18 1 70 -60  vol= 4.73290E+04
 media 0 1 80 -70   vol= 1.65299E+04
 boundary 80
unit 11
com="sr1 full in disk "
 cylinder 10     2.25        4        0
 cylinder 20      2.5        4        0
 cylinder 30     2.75        4        0
 media 11 1 10      vol= 1.91001E+02
 media 15 1 20 -10  vol= 4.47669E+01
 media 15 1 30 -20  vol= 4.94631E+01
 boundary 30
unit 12
com="sr2 full in disk "
 cylinder 10     2.25        4        0
 cylinder 20      2.5        4        0
 cylinder 30     2.75        4        0
 media 12 1 10      vol= 1.91001E+02
 media 15 1 20 -10  vol= 4.47669E+01
 media 15 1 30 -20  vol= 4.94631E+01
 boundary 30
unit 13
com="ccr full in disk "
 cylinder 10     2.25        4        0
 cylinder 20      2.5        4        0
 cylinder 30     2.75        4        0
 media 13 1 10      vol= 1.91001E+02
 media 15 1 20 -10  vol= 4.47669E+01
 media 15 1 30 -20  vol= 4.94631E+01
 boundary 30
unit 14
com="fcr full in disk "
 cylinder 10        1        4        0
 cylinder 20     1.25        4        0
 cylinder 30      1.5        4        0
 media 14 1 10      vol= 3.77437E+01
 media 15 1 20 -10  vol= 2.12062E+01
 media 15 1 30 -20  vol= 2.59046E+01
 boundary 30
unit 15
com="sr1 with cap "
 cylinder 10     2.25      3.5        0
 cylinder 20      2.5     3.75        0
 cylinder 30     2.75        4        0
 media 11 1 10      vol= 5.56347E+01
 media 15 1 20 -10  vol= 1.78513E+01
 media 15 1 30 -20  vol= 2.17673E+01
 boundary 30
unit 16
com="sr2 with cap "
 cylinder 10     2.25      3.5        0
 cylinder 20      2.5     3.75        0
 cylinder 30     2.75        4        0
 media 12 1 10      vol= 5.56347E+01
 media 15 1 20 -10  vol= 1.78513E+01
 media 15 1 30 -20  vol= 2.17673E+01
 boundary 30
unit 17
com="ccr with cap "
 cylinder 10     2.25      3.5        0
 cylinder 20      2.5     3.75        0
 cylinder 30     2.75        4        0
 media 13 1 10      vol= 5.56347E+01
 media 15 1 20 -10  vol= 1.78513E+01
 media 15 1 30 -20  vol= 2.17673E+01
```


www.manaraa.com

```
 boundary 30
unit 18
com="fcr with cap "
 cylinder 10        1      3.5        0
 cylinder 20     1.25     3.75        0
 cylinder 30      1.5        4        0
 media 14 1 10       vol= 1.09940E+01
 media 15 1 20 -10  vol= 7.37999E+00
 media 15 1 30 -20  vol= 9.96331E+00
 boundary 30
unit 24
com="sr1 0.5 cm section "
 cylinder 10     2.25      0.5        0
 cylinder 20      2.5      0.5        0
 cylinder 30     2.75      0.5        0
 media 11 1 10       vol= 7.79594E+00
 media 15 1 20 -10   vol= 1.82722E+00
 media 15 1 30 -20   vol= 2.01890E+00
 boundary 30
unit 25
com="sr2 0.5 cm section "
 cylinder 10     2.25      0.5        0
 cylinder 20      2.5      0.5        0
 cylinder 30     2.75      0.5        0
 media 12 1 10       vol= 7.79594E+00
 media 15 1 20 -10  vol= 1.82722E+00
 media 15 1 30 -20  vol= 2.01890E+00
 boundary 30
unit 26
com="ccr 0.5 cm section "
 cylinder 10     2.25      0.5        0
 cylinder 20      2.5      0.5        0
 cylinder 30     2.75      0.5        0
 media 13 1 10       vol= 7.79594E+00
 media 15 1 20 -10   vol= 1.82722E+00
 media 15 1 30 -20   vol= 2.01890E+00
 boundary 30
unit 27
com="fcr 0.5 cm section "
 cylinder 10        1      0.5        0
 cylinder 20     1.25      0.5        0
 cylinder 30      1.5      0.5        0
 media 14 1 10       vol= 1.54056E+00
 media 15 1 20 -10  vol= 8.65558E-01
 media 15 1 30 -20  vol= 1.05733E+00
 boundary 30
unit 31
com="top reflector "
 cylinder 10    15.85   25.317        0
 cylinder 20     16.1   25.567        0
 cylinder 30    33.12   25.567        0
 cylinder 40   44.926   35.567        0
 cylinder 50    45.72    36.36        0
 cylinder 60    45.72       65        0
 cylinder 70       98       65        0
 cuboid 80       98      -98       98      -98       65        0
 media 16 1 10       vol= 1.99743E+04
 media 15 1 20 -10   vol= 8.34506E+02
 media 16 1 30 -20   vol= 6.72507E+04
 media 17 1 40 -30   vol= 1.37396E+05
 media 19 1 50 -40   vol= 1.33058E+04
 media 18 1 60 -50   vol= 1.86825E+05
 media 18 1 70 -60   vol= 1.52978E+06
 media 0 1 80 -70    vol= 5.34282E+05
 boundary 80
unit 32
com="bottom reflector "
 cylinder 10      0.5     25.5      5.5
 cylinder 20    0.635     25.5      5.5
 cylinder 30    0.794     25.5      5.5
 cylinder 40    15.85     25.5      5.5
 hole 34   origin  x=-5.87 y=5.87 z=0
 hole 34   origin  x=5.87 y=-5.87 z=0
 hole 34   origin  x=5.87 y=5.87 z=0
 hole 35   origin  x=-5.87 y=-5.87 z=0
 cylinder 50    15.85     25.5     0.25
 hole 41   origin  x=-5.87 y=5.87 z=0
 hole 41   origin  x=5.87 y=-5.87 z=0
 hole 41   origin  x=5.87 y=5.87 z=0
 hole 42   origin  x=-5.87 y=-5.87 z=0
 hole 40
 cylinder 60     16.1     25.5        0
 cylinder 70    33.12     25.5        0
 cylinder 80   44.926     25.5      -10
 hole 36   origin  x=-5.87 y=5.87 z=-10
 hole 36   origin  x=5.87 y=-5.87 z=-10
 hole 36   origin  x=5.87 y=5.87 z=-10
 hole 37   origin  x=-5.87 y=-5.87 z=-10
 cylinder 90    45.72     25.5   -10.79
 hole 38   origin  x=-5.87 y=5.87 z=-10.79
 hole 38   origin  x=5.87 y=-5.87 z=-10.79
 hole 38   origin  x=5.87 y=5.87 z=-10.79
 hole 39   origin  x=-5.87 y=-5.87 z=-10.79
 cylinder 100       98     25.5   -10.79
 cuboid 110       98      -98       98      -98     25.5   -10.79
```


www.manaraa.com

```
 media 15 1 10          vol= 1.57329E+01
 media 0 1 20 -10       vol= 9.62810E+00
 media 15 1 30 -20      vol= 1.42652E+01
 media 16 1 40 -30      vol= 1.41829E+04
 media 0 1 50 -40       vol= 3.71157E+03
 media 15 1 60 -50      vol= 8.50971E+02
 media 16 1 70 -60      vol= 6.71335E+04
 media 17 1 80 -70      vol= 1.36483E+05
 media 19 1 90 -80      vol= 1.30883E+04
 media 18 1 100 -90     vol= 8.56655E+05
 media 0 1 110 -100     vol= 2.99191E+05
 boundary 110
 unit 333
   com="baffle plate void "
    cuboid   10       98      -98     1.27    -1.27      0.5        0
    media    0 1 10     vol= 2.44002E+02
    boundary 10
 unit 33
  com="baffle plate "
   hole 333   origin  x=0 y=0 z=0
   cylinder 20     12.8      0.5        0
   hole 24   origin  x=-5.87 y=5.87 z=0
   hole 25   origin  x=5.87 y=-5.87 z=0
   hole 26   origin  x=5.87 y=5.87 z=0
   hole 27   origin  x=-5.87 y=-5.87 z=0
   cylinder 30    33.05      0.5        0
   cylinder 40   44.926      0.5        0
   cylinder 50    45.72      0.5        0
   cylinder 60       98      0.5        0
   cuboid 70       98      -98       98      -98      0.5        0
   media 15 1 20      vol= 1.82068E+02
   media 16 1 30 -20  vol= 1.37916E+03
   media 17 1 40 -30  vol= 1.39631E+03
   media 19 1 50 -40  vol= 1.08843E+02
   media 18 1 60 -50  vol= 1.14391E+04
   media 0 1 70 -60   vol= 4.04063E+03
   boundary 70
unit 34
com="sr1, sr2, ccr in reflector "
 cylinder 10      2.5    25.25      5.5
 cylinder 20     2.75     25.5      5.5
 media 0 1 10        vol= 1.16397E+03
 media 15 1 20 -10   vol= 2.61659E+02
 boundary 20
unit 35
com="fine control rod in reflector "
 cylinder 10     1.25    25.25      5.5
 cylinder 20      1.5     25.5      5.5
 media 0 1 10       vol= 9.70103E+01
 media 15 1 20 -10  vol= 4.43613E+01
 boundary 20
unit 36
com="sr1, sr2, ccr in lead "
 cylinder 10      2.5       10        0
 cylinder 20     2.75       10        0
 media 0 1 10      vol= 5.89200E+02
 media 15 1 20 -10 vol= 1.23612E+02
 boundary 20
unit 37
com="fine control rod in lead "
 cylinder 10     1.25       10        0
 cylinder 20      1.5       10        0
 media 0 1 10       vol= 4.91067E+01
 media 15 1 20 -10  vol= 2.15791E+01
 boundary 20
unit 38
com="sr1, sr2, ccr in steel "
 cylinder 10      2.5     0.79        0
 cylinder 20     2.75     0.79        0
 media 0 1 10       vol= 4.59287E+01
 media 15 1 20 -10  vol= 9.63568E+00
 boundary 20
unit 39
com="fine control rod in steel "
 cylinder 10     1.25     0.79        0
 cylinder 20      1.5     0.79        0
 media 0 1 10       vol= 3.82791E+00
 media 15 1 20 -10  vol= 1.68212E+00
 boundary 20
unit 40
com="fuse rod in void "
 cylinder 10      0.5      5.5     0.25
 cylinder 20    0.635      5.5     0.25
 cylinder 30    0.794      5.5     0.25
 media 15 1 10      vol= 4.11719E+00
 media 0 1 20 -10   vol= 2.51960E+00
 media 15 1 30 -20  vol= 3.73309E+00
 boundary 30
unit 41
com="sr1, sr2, ccr in void "
 cylinder 10      2.5      5.5     0.25
 cylinder 20     2.75      5.5     0.25
 media 0 1 10       vol= 3.08379E+02
 media 15 1 20 -10  vol= 6.46967E+01
 boundary 20
```


www.manaraa.com

```
unit 42
com="fine control rod in void "
 cylinder 10     1.25      5.5     0.25
 cylinder 20      1.5      5.5     0.25
 media 0 1 10       vol= 2.57017E+01
 media 15 1 20 -10  vol= 1.12942E+01
 boundary 20
unit 43
com="fuse rod in lead "
 cylinder 10      0.5       10        0
 cylinder 20    0.635       10        0
 cylinder 30    0.794       10        0
 media 15 1 10       vol= 7.85398163397448
 media 0 1 20 -10    vol= 4.81370534346296
 media 15 1 30 -20   vol= 7.13804408414791
 boundary 30
unit 81
com="fuse cup "
 cylinder 10      1.1   1.5875   0.3175
 cylinder 20     1.36   1.5875   0.3175
 cylinder 30     1.36   1.5875        0
 media 10 1 10       vol= 4.82939E+00
 media 0 1 20 -10    vol= 2.54836E+00
 media 15 1 30 -20   vol= 1.81208E+00
 boundary 30
unit 82
com="rod under fuse cup "
 cylinder 10      0.5     1.05        0
 cylinder 20    0.635     1.05        0
 cylinder 30    0.794     1.05        0
 media 15 1 10       vol= 8.23438E-01
 media 0 1 20 -10    vol= 5.03921E-01
 media 15 1 30 -20   vol= 7.46617E-01
 boundary 30
global unit 100
 cuboid 10       98      -98       98      -98  126.6075        0
 array 1 10  place 1 1 1 0 0 10.79
 boundary 10
end geometry
read array
ara=1 nux=1 nuy=1 nuz=12 typ=square
 fill
   32
    1
    2
    3
   33
    4
    5
    6
    7
    8
    9
   31  end fill
end array
end data
end

=shell
  cp -f ft04f001  ${RTNDIR}/xn8v7.1.wnew
end
```

C.3 MCNP6 Models

C.3.1 MCNP XY Model and 3-D Model

Two MCNP6 input files were generated to test the EVENT 2-D and 3-D model results using a Monte Carlo methodology. The 2-D and 3-D models were generated to be essentially identical to the 2-D and 3-D EVENT models; however, the MCNP6 models assumed ENDF/B-VII continuous-energy cross

www.manaraa.com

sections instead of the SCALE-generated ENDF/B-VII.1 multigroup cross-section libraries. The MCNP6 package has neutron cross sections based on ENDF/B-VII cross sections, which allows for some comparison between ENDF/B-VII and ENDF/B-VII.1 cross sections.

www.manaraa.com

C.3.2 MCNP6 XY AGN Model Input File

```
AGN-201M Detailed Model : UNM
c
c   Model by L. Wetzel, BWXT
c   Modified for 2D "X-Y" Infinite Z by Doug Bowen, 2014
c
1   0            -1                          u=1 imp:n=1      $ glory hole void
2  15  -2.702    +1 -2                       u=1 imp:n=1      $ glory hole tube - Al
3   1  -1.2373   +2 -3                       u=1 imp:n=1      $ 20497 fuel plate
4  16  -1.7500   +3 -4                       u=1 imp:n=1
5  15  -2.702    +4 -5                       u=1 imp:n=1
6  16  -1.7500   +5 -6                       u=1 imp:n=1
7  17  -10.7770  +6 -7                       u=1 imp:n=1
8  19  -7.82120  +7 -8                       u=1 imp:n=1
9  18  -0.99848  +8                          u=1 imp:n=1
50  0            -9 +20 -21          fill=1      imp:n=1
101 0            #50                         imp:n=0

c
1  cz 1.1875                 $ vertical glory hole void
2  cz 1.27                   $ glory hole aluminum tube
3  cz 12.8                   $ outside of the fuel/inside of graphite
4  cz 15.85                  $ outside of graphite/inside of aluminum barrier
5  cz 16.1                   $ outside of aluminum barrier/inside of graphite
6  cz 33.12                  $ outside of graphite/inside of lead
7  cz 44.926                 $ outside of lead/inside of steel
8  cz 45.72                  $ outside of steel/inside of water
9  cz 98                     $ outside of water
c
c  Planes
c
*20 pz 0.0
*21 pz 12.0

mode n
kcode 2500 1 50 600
ksrc   4   4  4
      -4   4  4
       4  -4  4
      -4  -4  4
       4   4  8
      -4   4  8
       4  -4  8
      -4  -4  8
m1     1001  -0.10522 6000  -0.62713  8016  -0.03178 92235  -0.04600
      92238  -0.18988
mt1    poly
m15   13027  -1.00000
m16    6000  -1.00000
mt16   grph
m17   82000  -1.00000
m18    1001  -0.11190  8016  -0.88811
mt18   lwtr
m19    6000  -0.01000 26000  -0.99000
print
```

C.3.3 MCNP6 3-D AGN Model Input File

```
AGN-201M Detailed Model : UNM
c
c   Model by L. Wetzel, BWXT
c   Modified for AGN-201M EVENT Model Comparions, D. Bowen, 2014
c
1   1  -1.2373   -4   13 16 19 22      -42 41  u=1 imp:n=1               $ 20497
2   2  -1.2422   -4   13 16 19 22      -43 42  u=1 imp:n=1               $ 20498
3   3  -1.2228   -4 13 16 19 22 26 -44 43      u=1 imp:n=1               $ 20499
4  15  -2.702    -4   13 16 19 22 26   -45 44  u=1 imp:n=1               $ baffle plate
5   4  -1.2298   -4   13 16 19 22 26   -46 45  u=1 imp:n=1               $ 204100
6   5  -1.2264   -4                    -47 46  u=1 imp:n=1               $ 204101
7   6  -1.2264   -4                    -48 47  u=1 imp:n=1               $ 204102
8   7  -1.2274   -4                    -49 48  u=1 imp:n=1               $ 204103
9   8  -1.3017   -4                    -50 49  u=1 imp:n=1               $ 204104
10  9  -1.2599   -4                    -51 50  u=1 imp:n=1               $ 204105
11  0            -4                    -52 51  u=1 imp:n=1               $ void above fuel
12  0            -11 -53  27                   u=1 imp:n=1               $ SR1 void above fuel
121 11  -1.2809  -11  41 -27                   u=1 imp:n=1               $ SR1 fuel
13 15  -2.7020   -13 -46 41 #12 #121           u=1 imp:n=1               $ -
14 12  -1.2800   -14 -53 41                    u=1 imp:n=1               $ SR2
15 15  -2.7020   -16 -46 41 #14                u=1 imp:n=1               $
16 13  -1.2801   -17 -53 41                    u=1 imp:n=1               $ CCR
17 15  -2.7020   -19 -46 41 #16                u=1 imp:n=1               $
18 14  -1.2106   -20 -53 41                    u=1 imp:n=1               $ FCR
19 15  -2.7020   -22 -46 41 #18                u=1 imp:n=1               $
22  0            -25 -10                       u=1 imp:n=1               $ glory hole
23 15  -2.7020   -26  25 -10                   u=1 imp:n=1               $
24 16  -1.7500   (-5 4 -52 41 26):(-5 -60 52):(-5 -41 59 13 16 19 22)
                                               u=1 imp:n=1               $ graph in can
```


www.manaraa.com

```
25  0            -5 -59 58 13 16 19 22         u=1 imp:n=1               $ void below
29  0            -12 -41 65                    u=1 imp:n=1               $ SR1 below core
30 15  -2.7020   -13 12 -41 65                  u=1 imp:n=1               $ -
31  0            -15 -41 65                    u=1 imp:n=1               $ SR2 below core
32 15  -2.7020   -16 15 -41 65                  u=1 imp:n=1               $ -
33  0            -18 -41 65                    u=1 imp:n=1               $ CCR below core
34 15  -2.7020   -19 18 -41 65                  u=1 imp:n=1               $ -
35  0            -21 -41 65                    u=1 imp:n=1               $ FCR below core
36 15  -2.7020   -22 21 -41 65                  u=1 imp:n=1               $ -
37 15  -2.7020   (-6 5 -60 58 26):(-6 -62 60):(-6 -58 61 13 16 19 22)
                                               u=1 imp:n=1               $ Al barrier
38 16  -1.7500   (-7 6 -62 61 26)               u=1 imp:n=1               $ graphite outside
39 17 -10.7770   (-8 7 -62 61 26):(-8 -64 62):(-8 -61 63 13 16 19 22)
                                               u=1 imp:n=1               $ Pb Shield
40 19 -7.82120   (-9 8 -64 63 26):(-9 -66 64):(-9 -63 65 13 16 19 22)
                                               u=1 imp:n=1               $ Steel Vessel
41 18 -0.99848   (-10 9 -66 65 26):(-10 -67 66)
                                               u=1 imp:n=1               $ Water
c
c
99  0             10:67:-65                    u=1 imp:n=1
100 0            -999       fill=1                imp:n=1
101 0            +999                             imp:n=0

4  cz 12.8                    $ outside of the fuel/inside of graphite
5  cz 15.85                   $ outside of graphite/inside of aluminum barrier
6  cz 16.1                    $ outside of aluminum barrier/inside of graphite
7  cz 33.12                   $ outside of graphite/inside of lead
8  cz 44.926                  $ outside of lead/inside of steel
9  cz 45.72                   $ outside of steel/inside of water
10 cz 98                      $ outside of water
11 c/z 5.869 5.869 2.25       $ inside of SR1
12 c/z 5.869 5.869 2.5        $ outside of clad
13 c/z 5.869 5.869 2.75       $ outside of aluminum in rod path
14 c/z -5.869 5.869 2.25      $ inside of SR2
15 c/z -5.869 5.869 2.5       $ outside of clad
16 c/z -5.869 5.869 2.75      $ outside of aluminum in rod path
17 c/z -5.869 -5.869 2.25     $ inside of CCR
18 c/z -5.869 -5.869 2.5      $ outside of clad
19 c/z -5.869 -5.869 2.75     $ outside of aluminum in rod path
20 c/z 5.869 -5.869 1.0       $ inside of FCR
21 c/z 5.869 -5.869 1.25      $ outside of clad
22 c/z 5.869 -5.869 1.50      $ outside of aluminum in rod path
25 c/x 0.0   12.25  1.27      $ inside of glory hole
26 c/x 0.0   12.25  1.47      $ outside of glory hole
27 pz 8.0                     $ height of fuel in rod
c
c  Planes
c
41 pz 0.0                     $ bottom of 20497
42 pz 4.0                     $ bottom of 20498
43 pz 8.0                     $ bottom of 20499
44 pz 12.0                    $ bottom of baffle plate
45 pz 12.5                    $ bottom of 204100
46 pz 16.5                    $ bottom of 204101
47 pz 18.5                    $ bottom of 204102
48 pz 20.5                    $ bottom of 204103
49 pz 22.5                    $ bottom of 204104
50 pz 23.5                    $ bottom of 204105
51 pz 24.5                    $ bottom of void above core
52 pz 25.5                    $ top of void above core
53 pz 16.0                    $ bottom of cap on rods
54 pz 16.25                   $ top of cap on rods
58 pz -25.25                  $ bottom of void inside barrier
59 pz -20                     $ bottom of  graphite below core inside barrier
60 pz 50.817                  $ top of graphite inside barrier
61 pz -25.5                   $ bottom of aluminum barrier
62 pz 51.067                  $ top of aluminum barrier
63 pz -35.5                   $ bottom of lead
64 pz 61.067                  $ top of lead
65 pz -36.293                 $ bottom of steel
66 pz 61.680                  $ top of steel
67 pz 91.86                   $ top of water
c extra
999 so  200

mode n
kcode 2500 1 50 550
ksrc   0  0  3
       0  0  6
       0  0  9
       0  0 12
       0  0 15
       0  0 18
       0  0 21
       0  0 24
m1     1001  -0.10522 6000  -0.62713  8016  -0.03178 92235  -0.04600
      92238  -0.18988
mt1    poly
m2     1001  -0.10529 6000  -0.62749  8016  -0.03173 92235  -0.04592
      92238  -0.18957
mt2    poly
m3     1001  -0.10529 6000  -0.62749  8016  -0.03173 92235  -0.04592
      92238  -0.18957
mt3    poly
```


www.manaraa.com

```
m4     1001  -0.10524 6000  -0.62711  8016  -0.03178 92235  -0.04600
      92238  -0.18990
mt4    poly
m5     1001  -0.10526 6000  -0.62735  8016  -0.03175 92235  -0.04595
      92238  -0.18969
mt5    poly
m6     1001  -0.10525 6000  -0.62730  8016  -0.03175 92235  -0.04596
      92238  -0.18974
mt6    poly
m7     1001  -0.10524 6000  -0.62729  8016  -0.03175 92235  -0.04596
      92238  -0.18974
mt7    poly
m8     1001  -0.10524 6000  -0.62725  8016  -0.03176 92235  -0.04597
      92238  -0.18978
mt8    poly
m9     1001  -0.10527 6000  -0.62742  8016  -0.03174 92235  -0.04594
      92238  -0.18964
mt9    poly
m10    1001  -0.08518 6000  -0.50768  8016  -0.04834 92235  -0.06997
      92238  -0.28884
mt10   poly
m11    1001  -0.10526 6000  -0.62734  8016  -0.03175 92235  -0.04595
      92238  -0.18970
mt11   poly
m12    1001  -0.10526 6000  -0.62733  8016  -0.03175 92235  -0.04596
      92238  -0.18971
mt12   poly
m13    1001  -0.10524 6000  -0.62721  8016  -0.03177 92235  -0.04598
      92238  -0.18981
mt13   poly
m14    1001  -0.10524 6000  -0.62724  8016  -0.03176 92235  -0.04597
      92238  -0.18978
mt14   poly
m15   13027  -1.00000
m16    6000  -1.00000
mt16   grph
m17   82000  -1.00000
m18    1001  -0.11190  8016  -0.88811
mt18   lwtr
m19    6000  -0.01000 26000  -0.99000
print
```

C.4 EVENT XY and RZ Models

A single EVENT XY model and three EVENT RZ models were generated for this work. The EVENT XY model was used to test the multigroup neutron cross sections generated for the AGN experiment verification analysis. The EVENT RZ models were generated to perform the following:

- Detailed eigenvalue model for verification of delayed critical configurations,
- Simplified eigenvalue model for transient testing and and AGN experimental transient analysis, and
- Simplified eigenvalue and time-dependent models for AGN transient analysis.

www.manaraa.com

C.4.1 Detailed EVENT XY Model

```
Title: AGN Infinite Z model

@
@ - AGN Infinite Z model
@

@
@ - define main problem parameters
@

problem radiation         @ radiation problem
geometry xy               @ 2D xy geometry
case eigenvalue           @ Keff determination
angle   5                @ Pn angular flux expansion
scatter 3                 @ order of scattering anisotropy
groups  8                 @ # energy group problem
upscatter yes             @  upscattering from energy groups
solution pcg5             @ solution scheme
monitor eigenvalue        @ monitor the Keff
iter  25 100 5.0e-04 5.0e-04 100 1.0e-07 100 @ iteration parameters

@
@ - define geometry
@

@
@ - define points
@

pnt p1  0.0  0.0

@
@ - define circles
@

circle   c1   p1   1.27     50
circle   c2   p1   1.47     50
circle   c3   p1   12.8     50
circle   c4   p1   15.85    50
circle   c5   p1   16.10    50
circle   c6   p1   33.12    50
circle   c7   p1  44.926    50
circle   c8   p1   45.72    50
circle   c9   p1   98.00    50

@
@ - define regions
@

region r1 c1
region r2 c2 c1
region r3 c3 c2
region r4 c4 c3
region r5 c5 c4
region r6 c6 c5
region r7 c7 c6
region r8 c8 c7
region r9 c9 c8

@
@ - define boundary conditions
@

boundary vacuum c9

@
@ - define library
@

@library scale work agn8g_08-01-2014.03
@library scale work doug_2g_wlib.old
@library scale work doug_4g_wlib.old
@library scale work doug_8g_wlib.old
library scale work scale_8g_wlib.old

@
@ - spectrum
@

@spectrum 9.09220E-01 9.07802E-02 0 0 0 0 0 0
spectrum 0.906693 0.093307 4.64109E-9 4.64109E-11 4.33366E-13 0 0 0
@spectrum 9.99617E-1 3.83467E-4 1.16856E-11 0
@spectrum 1.000E+00 1.47703E-13

@
@ - define material xs table ( iht, ihs, ihm )
@
```


www.manaraa.com

```
xstab 7 8 15

@
@ - Define Isotopes
@

material u-235    1092235
material u-238    1092238
material o1       1008016
material h1       1001901
material ca1      1006000
material ca2     16006312
material pb204   17082204
material pb206   17082206
material pb207   17082207
material pb208   17082208
material o2      18008016
material h2      18001001
@material o3       5008016
@material n        5007014
material alum    15013027
material ca3     19006000
material fe54    19026054
material fe56    19026056
material fe57    19026057
material fe58    19026058

@
@ - mixing instructions
@
@ Uranium-Polyethylene Core - density 1.2409 g/cm3
@ Material 1
mix core
mix core u-235       1.40281E-04
mix core u-238       5.71806E-04
mix core ca1         3.83490E-02
mix core h1          7.66981E-02
mix core o1          1.42418E-03

@ Graphite - density 1.2801 g/cc - 11
mix graph
mix graph ca2        8.78149E-02

@ Aluminum - density 2.702 g/cc - 12
mix al
mix al   alum        6.03073E-02

@ Lead - density 10.777 g/cc - 13
mix lead
mix lead   pb204     4.38482E-04
mix lead   pb206     7.54815E-03
mix lead   pb207     6.92175E-03
mix lead   pb208     1.64118E-02

@ Steel - density 7.82120 g/cc - 14
mix steel
mix steel  ca3       3.92153E-03
mix steel  fe54      4.88044E-03
mix steel  fe56      7.66124E-02
mix steel  fe57      1.76931E-03
mix steel  fe58      2.35463E-04

@ Water - density 0.99848 g/cc - 15
mix water
mix water  h2        6.67731E-02
mix water  o2        3.33866E-02

@ Air - 16
mix air
mix air    h2         4.07700E-05
mix air    o2        9.48790E-06

@
@ - define averaging regions
@

average 1 r1
average 2 r2
average 3 r3
average 4 r4
average 5 r5
average 6 r6
average 7 r7
average 8 r8
average 9 r9

@
@ - assign sources and material properties to regions
@

property r1 air
property r2 al
property r3 core
property r4 graph
property r5 al
```


www.manaraa.com

```
property r6 graph
property r7 lead
property r8 steel
property r9 water

@
@ - generate mesh
@

mesh r1 delaunay
mesh r2 delaunay
mesh r3 delaunay
mesh r4 delaunay
mesh r5 delaunay
mesh r6 delaunay
mesh r7 delaunay
mesh r8 delaunay
mesh r9 delaunay

fill

@
@ - plotting device
@
@dev x11

@
@ - output data to default file
@
paraview
data

@
@ - stop the gem run
@

stop
```

C.4.2 Detailed EVENT RZ Model

```
title AGN-201 full model, total spectrum

@
@ define main problem parameters
@

problem   radiation        @ Radiation problem
case      eigenvalue       @ Keff determination
geometry  rz               @ 2D RZ geometry
angle     11                @ angular flux expansion
scatter   3                @ Order of scattering anisotropy
groups    2                @ Number of energy groups for the problem
upscatter yes              @ upscattering from energy groups
monitor   eigenvalue       @ Monitor the Keff
iter  25 100 5.0e-05 5.0e-05 100 1.0e-08 100   @ Iteration Parameters

@
@ - define library
@

library scale work xn2v7.1.wlib.old
@library scale work scale_8g_wlib.old
@
@ - spectrum
@

@spectrum 0.906693 0.093307 4.64109E-9 4.64109E-11 4.33366E-13 0 0 0
@spectrum 9.99617E-1 3.83467E-4 1.16856E-11 0
spectrum 1 0

@
@ - define material xs table ( iht, ihs, ihm )
@

xstab 7 8 15

@
@ - Define Isotopes
@

material u-235a    1092235
material u-238a    1092238
material o1a       1008016
material h1a       1001901
material ca1a      1006000
material u-235b    2092235
material u-238b    2092238
material o1b       2008016
material h1b       2001901
material ca1b      2006000
material u-235c    3092235
```


www.manaraa.com

```
material u-238c    3092238
material o1c       3008016
material h1c       3001901
material ca1c      3006000
material u-235d    4092235
material u-238d    4092238
material o1d       4008016
material h1d       4001901
material ca1d      4006000
material u-235e    5092235
material u-238e    5092238
material o1e       5008016
material h1e       5001901
material ca1e      5006000
material u-235f    6092235
material u-238f    6092238
material o1f       6008016
material h1f       6001901
material ca1f      6006000
material u-235g    7092235
material u-238g    7092238
material o1g       7008016
material h1g       7001901
material ca1g      7006000
material u-235h    8092235
material u-238h    8092238
material o1h       8008016
material h1h       8001901
material ca1h      8006000
material u-235i    9092235
material u-238i    9092238
material o1i       9008016
material h1i       9001901
material ca1i      9006000
material u-235j   10092235
material u-238j   10092238
material o1j      10008016
material h1j      10001901
material ca1j     10006000
material u-235k   11092235
material u-238k   11092238
material o1k      11008016
material h1k      11001901
material ca1k     11006000
material u-235l   12092235
material u-238l   12092238
material o1l      12008016
material h1l      12001901
material ca1l     12006000
material u-235m   13092235
material u-238m   13092238
material o1m      13008016
material h1m      13001901
material ca1m     13006000
material ca2     16006312
material pb204   17082204
material pb206   17082206
material pb207   17082207
material pb208   17082208
material o2      18008016
material h2      18001001
@material o3       5008016
@material n        5007014
material alum    15013027
material ca3     19006000
material fe54    19026054
material fe56    19026056
material fe57    19026057
material fe58    19026058

@
@ - mixing instructions
@

@ Uranium-Polyethylene Core -1
mix c497
mix c497 u-235a       1.4536E-04
mix c497 u-238a       5.9251E-04
mix c497 ca1a         3.8307E-02
mix c497 h1a          7.6615E-02
mix c497 o1a          1.4757E-03
@ Uranium-Polyethylene Core - 2
mix c498
mix c498 u-235b       1.4570E-04
mix c498 u-238b       5.9389E-04
mix c498 ca1b         3.8305E-02
mix c498 h1b          7.6609E-02
mix c498 o1b          1.4792E-03
@ Uranium-Polyethylene Core - 3
mix c499
mix c499 u-235c       1.4224E-04
mix c499 u-238c       5.7978E-04
mix c499 ca1c         3.8333E-02
mix c499 h1c          7.6666E-02
mix c499 o1c          1.4440E-03
```


www.manaraa.com

```
@ Uranium-Polyethylene Core - 4
mix c4100
mix c4100 u-235d       1.4410E-04
mix c4100 u-238d       5.8737E-04
mix c4100 ca1d         3.8318E-02
mix c4100 h1d          7.6635E-02
mix c4100 o1d          1.4629E-03
@ Uranium-Polyethylene Core - 5
mix c4101
mix c4101 u-235e       1.4458E-04
mix c4101 u-238e       5.8934E-04
mix c4101 ca1e         3.8314E-02
mix c4101 h1e          7.6627E-02
mix c4101 o1e          1.4678E-03
@ Uranium-Polyethylene Core - 6
mix c4102
mix c4102 u-235f       1.4473E-04
mix c4102 u-238f       5.8995E-04
mix c4102 ca1f         3.8313E-02
mix c4102 h1f          7.6625E-02
mix c4102 o1f          1.4694E-03
@ Uranium-Polyethylene Core - 7
mix c4103
mix c4103 u-235g       1.4468E-04
mix c4103 u-238g       5.8975E-04
mix c4103 ca1g         3.8313E-02
mix c4103 h1g          7.6626E-02
mix c4103 o1g          1.4689E-03
@ Uranium-Polyethylene Core - 8
mix c4104
mix c4104 u-235h       1.5353E-04
mix c4104 u-238h       6.2581E-04
mix c4104 ca1h         3.8240E-02
mix c4104 h1h          7.6481E-02
mix c4104 o1h          1.5587E-03
@ Uranium-Polyethylene Core - 9
mix c4105
mix c4105 u-235i       1.4850E-04
mix c4105 u-238i       6.0529E-04
mix c4105 ca1i         3.8282E-02
mix c4105 h1i          7.6563E-02
mix c4105 o1i          1.5076E-03
@ Uranium-Polyethylene Elements - 10
mix sr1
mix sr1 u-235j         1.463033E-04
mix sr1 u-238j         5.963529E-04
mix sr1 ca1j           3.806768E-02
mix sr1 h1j            7.613536E-02
mix sr1 o1j            1.485312E-03
@ Graphite - density 1.2801 g/cc - 11
mix graph
mix graph ca2        8.78149E-02

@ Aluminum - density 2.702 g/cc - 12
mix al
mix al   alum        6.03073E-02

@ Lead - density 10.777 g/cc - 13
mix pb
mix pb   pb204     4.38482E-04
mix pb   pb206     7.54815E-03
mix pb   pb207     6.92175E-03
mix pb   pb208     1.64118E-02

@ Steel - density 7.82120 g/cc - 14
mix steel
mix steel  ca3       3.92153E-03
mix steel  fe54      4.88044E-03
mix steel  fe56      7.66124E-02
mix steel  fe57      1.76931E-03
mix steel  fe58      2.35463E-04

@ Water - density 0.99848 g/cc - 15
mix water
mix water  h2        6.67731E-02
mix water  o2        3.33866E-02

@ Air - 16
@mix air
@mix air    alum         1E-06
mix air
@mix air    h2         4.07700E-05
mix air    o2         1E-6

@
@ define the geometry
@

define grid

  xcoord  0.0 1.1875 1.27 5.133363 6.522186 12.8 15.85 16.1 33.12 44.926 45.72 98.0
@  xcoord  0.0 1.1875 1.27 4.68790049 6.849373037 12.8 15.85 16.1 33.12 44.926 45.72 98.0

  xint       2    3    15       5          15   15     4   15    15     2     10
```


www.manaraa.com

```
  ycoord  -47.29 -36.25 -28.25 -26.25 -24.25 -22.25 -20.25 ^
          -18.25 -16.25 -14.25 -12.25 -10.25 -8.25 -6.25 -4.25 -2.25 -0.25 0.25 ^
                        2.25 4.25 6.25 8.25 10.25 11.25 12.25 13.25 38.567 48.817 65.0

  yint          9      9      9       9     9       9     9 ^
                9      9      9       9     9     9   9   9    2   9 ^
              9   9   9   9    9    9     2    9      9      9

@
@    full core model
@

  material  16 12 13 13 13 13 13 13 13 14 15 ^   / -47.29 to -36.25
            16 12 11 11 11 11 12 11 13 14 15 ^   / -36.25 to -28.25
            16 12 11 16 11 11 12 11 13 14 15 ^   / -28.25 to -26.25
            16 12 11 16 11 11 12 11 13 14 15 ^   / -26.25 to -24.25
            16 12 11 16 11 11 12 11 13 14 15 ^   / -24.25 to -22.25
            16 12 11 16 11 11 12 11 13 14 15 ^   / -22.25 to -20.25
            16 12 11 16 11 11 12 11 13 14 15 ^   / -20.25 to -18.25
            16 12 11 16 11 11 12 11 13 14 15 ^   / -18.25 to -16.25
            16 12 11 16 11 11 12 11 13 14 15 ^   / -16.25 to -14.25
            16 12 11 16 11 11 12 11 13 14 15 ^   / -14.25 to -12.25
            16 12  1 10  1 11 12 11 13 14 15 ^   / -12.25 to -10.25
            16 12  1 10  1 11 12 11 13 14 15 ^   / -10.25 to -8.25
            16 12  2 10  2 11 12 11 13 14 15 ^   / -8.25 to -6.25
            16 12  2 10  2 11 12 11 13 14 15 ^   / -6.25 to -4.25
            16 12  3 10  3 11 12 11 13 14 15 ^   / -4.25 to -2.25
            16 12  3 10  3 11 12 11 13 14 15 ^   / -2.25 to -0.25
            16 12 12 12 12 11 12 11 13 14 15 ^   / -0.25 to  0.25
            16 12  4 10  4 11 12 11 13 14 15 ^   /  0.25 to 2.25
            16 12  4 10  4 11 12 11 13 14 15 ^   /  2.25 to 4.25
            16 12  5  5  5 11 12 11 13 14 15 ^   /  4.25 to 6.25
            16 12  6  6  6 11 12 11 13 14 15 ^   /  6.25 to 8.25
            16 12  7  7  7 11 12 11 13 14 15 ^   /  8.25 to 10.25
            16 12  8  8  8 11 12 11 13 14 15 ^   /  10.25 to 11.25
            16 12  9  9  9 11 12 11 13 14 15 ^   /  11.25 to 12.25
            16 12 16 16 16 11 12 11 13 14 15 ^   /  12.25 to 13.25
            16 12 11 11 11 11 12 11 13 14 15 ^   /  13.25 to 38.567
            16 12 13 13 13 13 13 13 13 14 15 ^   /  38.567 to 48.817
            16 12 15 15 15 15 15 15 15 15 15 ^   /  48.817 to 65.0

  average   16 12 13 13 13 13 13 13 13 14 15 ^   / -47.29 to -36.25
            16 12 11 11 11 11 12 11 13 14 15 ^   / -36.25 to -28.25
            16 12 11 16 11 11 12 11 13 14 15 ^   / -28.25 to -26.25
            16 12 11 16 11 11 12 11 13 14 15 ^   / -26.25 to -24.25
            16 12 11 16 11 11 12 11 13 14 15 ^   / -24.25 to -22.25
            16 12 11 16 11 11 12 11 13 14 15 ^   / -22.25 to -20.25
            16 12 11 16 11 11 12 11 13 14 15 ^   / -20.25 to -18.25
            16 12 11 16 11 11 12 11 13 14 15 ^   / -18.25 to -16.25
            16 12 11 16 11 11 12 11 13 14 15 ^   / -16.25 to -14.25
            16 12 11 16 11 11 12 11 13 14 15 ^   / -14.25 to -12.25
            16 12  1 10  1 11 12 11 13 14 15 ^   / -12.25 to -10.25
            16 12  1 10  1 11 12 11 13 14 15 ^   / -10.25 to -8.25
            16 12  2 10  2 11 12 11 13 14 15 ^   / -8.25 to -6.25
            16 12  2 10  2 11 12 11 13 14 15 ^   / -6.25 to -4.25
            16 12  3 10  3 11 12 11 13 14 15 ^   / -4.25 to -2.25
            16 12  3 10  3 11 12 11 13 14 15 ^   / -2.25 to -0.25
            16 12 12 12 12 11 12 11 13 14 15 ^   / -0.25 to  0.25
            16 12  4 10  4 11 12 11 13 14 15 ^   /  0.25 to 2.25
            16 12  4 10  4 11 12 11 13 14 15 ^   /  2.25 to 4.25
            16 12  5  5  5 11 12 11 13 14 15 ^   /  4.25 to 6.25
            16 12  6  6  6 11 12 11 13 14 15 ^   /  6.25 to 8.25
            16 12  7  7  7 11 12 11 13 14 15 ^   /  8.25 to 10.25
            16 12  8  8  8 11 12 11 13 14 15 ^   /  10.25 to 11.25
            16 12  9  9  9 11 12 11 13 14 15 ^   /  11.25 to 12.25
            16 12 16 16 16 11 12 11 13 14 15 ^   /  12.25 to 13.25
            16 12 11 11 11 11 12 11 13 14 15 ^   /  13.25 to 38.567
            16 12 13 13 13 13 13 13 13 14 15 ^   /  38.567 to 48.817
            16 12 15 15 15 15 15 15 15 15 15 ^   /  48.817 to 65.0

end grid

@
@ - define boundary conditions
@

bounds on

boundary reflect west
boundary vacuum south east north

fill

@run

data

paraview

stop
```


www.manaraa.com

C.4.3 Simplified EVENT RZ Model

```
title AGN-201 full model, total spectrum

@
@ define main problem parameters
@

problem   radiation        @ Radiation problem
case      eigenvalue       @ Keff determination
geometry  rz               @ 2D RZ geometry
angle     5                @ angular flux expansion
scatter   3                @ Order of scattering anisotropy
groups    2                @ Number of energy groups for the problem
upscatter yes              @ upscattering from energy groups
monitor   eigenvalue       @ Monitor the Keff
iter 100 100 1.0e-05 1.0e-04 300 1.0e-9 300   @ Iteration Parameters
dump 99999

normalize power 4.06 total

@opposite flux

@
@ - define library
@

library scale work xn2v7.1.wlib.old

@
@ - spectrum
@

@spectrum 0.906693 0.093307 4.64109E-9 4.64109E-11 4.33366E-13 0 0 0
@spectrum 9.99617E-1 3.83467E-4 1.16856E-11 0
spectrum 1.0 0

@
@ - define material xs table ( iht, ihs, ihm )
@

xstab 7 8 15

@
@ - Define Isotopes
@

material u-235a    1092235
material u-238a    1092238
material o1a       1008016
material h1a       1001901
material ca1a      1006000
material u-235j   10092235
material u-238j   10092238
material o1j      10008016
material h1j      10001901
material ca1j     10006000
material ca2     16006312
material pb204   17082204
material pb206   17082206
material pb207   17082207
material pb208   17082208
material o2      18008016
material h2      18001001
@material o3       5008016
@material n        5007014
material alum    15013027
material ca3     19006000
material fe54    19026054
material fe56    19026056
material fe57    19026057
material fe58    19026058

@
@ - mixing instructions
@

@ Uranium-Polyethylene Core - homo - 1
mix c4105
mix c4105 u-235a       1.441848E-04
mix c4105 u-238a       5.877176E-04
mix c4105 ca1a         3.807824E-02
mix c4105 h1a          7.615649E-02
mix c4105 o1a          1.463805E-03
mix c4105 alum         3.367565E-03
@ Uranium-Polyethylene Elements - 2
mix sr1
mix sr1 u-235j         1.170347E-04
mix sr1 u-238j         4.770500E-04
mix sr1 ca1j           2.548332E-02
mix sr1 h1j            5.096665E-02
mix sr1 o1j            1.188169E-03
```


www.manaraa.com

```
mix sr1 alum           1.993627E-02

@ Graphite - density 1.2801 g/cc - 3
mix graph
mix graph ca2        8.78149E-02

@ Aluminum - density 2.702 g/cc - 4
mix al
mix al   alum        6.03073E-02

@ Lead - density 10.777 g/cc - 5
mix pb
mix pb   pb204     4.38482E-04
mix pb   pb206     7.54815E-03
mix pb   pb207     6.92175E-03
mix pb   pb208     1.64118E-02

@ Steel - density 7.82120 g/cc - 6
mix steel
mix steel  ca3       3.92153E-03
mix steel  fe54      4.88044E-03
mix steel  fe56      7.66124E-02
mix steel  fe57      1.76931E-03
mix steel  fe58      2.35463E-04

@ Water - density 0.99848 g/cc - 7
mix water
mix water  h2        6.67731E-02
mix water  o2        3.33866E-02

@ Air - 8
mix air
mix air    o2         9.48790E-06
@mix air    n         4.07700E-05
@mix air    o3        9.48790E-06

@ Zone 1 - 9

  mix hole1
  mix hole1 air  0.0
  mix hole1 sr1  1.0

@
@ define the geometry
@

define grid

xcoord  0.0 1.1875 1.27 5.3 6.30 12.8 15.85 16.1 33.12 44.926 45.72 98.0

  xint       1    2     15        5        25   10     2   10    5      2     5

  ycoord  -47.29 -36.25 -28.25 -14.25 -12.25 3.75 6.25 12.25 13.25 38.567 48.817 65.0

  yint          5      6      6       3     65   10   25    1     5      5      5

@
@    full core model
@

  material    8  4  5  5  5  5  5  5  5  6  7 ^   / -47.29 to -36.25
              8  4  3  3  3  3  4  3  5  6  7 ^   / -36.25 to -28.25
              8  4  3  3  3  3  4  3  5  6  7 ^   / -28.25 to -14.25
              8  4  3  3  3  3  4  3  5  6  7 ^   / -14.25 to -12.25
              8  4  1  9  1  3  4  3  5  6  7 ^   / -12.25 to 3.75
              8  4  1  1  1  3  4  3  5  6  7 ^   /  3.75 to 6.25
              8  4  1  1  1  3  4  3  5  6  7 ^   /  6.25 to 12.25
              8  4  8  8  8  3  4  3  5  6  7 ^   /  12.25 to 13.25
              8  4  3  3  3  3  4  3  5  6  7 ^   /  13.25 to 38.567
              8  4  5  5  5  5  5  5  5  6  7 ^   /  38.567 to 48.817
              8  4  7  7  7  7  7  7  7  7  7 ^   /  48.817 to 65.0

  average     8  4  5  5  5  5  5  5  5  6  7 ^   / -47.29 to -36.25
              8  4  3  3  3  3  4  3  5  6  7 ^   / -36.25 to -28.25
              8  4  3  3  3  3  4  3  5  6  7 ^   / -28.25 to -14.25
              8  4  3  3  3  3  4  3  5  6  7 ^   / -14.25 to -12.25
              8  4  1  9  1  3  4  3  5  6  7 ^   / -12.25 to 3.75
              8  4  1  1  1  3  4  3  5  6  7 ^   /  3.75 to 6.25
              8  4  1  1  1  3  4  3  5  6  7 ^   /  6.25 to 12.25
              8  4  8  8  8  3  4  3  5  6  7 ^   /  12.25 to 13.25
              8  4  3  3  3  3  4  3  5  6  7 ^   /  13.25 to 38.567
              8  4  5  5  5  5  5  5  5  6  7 ^   /  38.567 to 48.817
              8  4  7  7  7  7  7  7  7  7  7 ^   /  48.817 to 65.0

end grid

@@@@@@@@@@@@@@@@@@@@@@@@@@@@@@@@@@@@@@@@@@@@@@@@@@@@@@@@@@@@@@@@@@@@@@@@
@
@ - flux sensors
@
@@@@@@@@@@@@@@@@@@@@@@@@@@@@@@@@@@@@@@@@@@@@@@@@@@@@@@@@@@@@@@@@@@@@@@@@

pnt ps1    0 0 0
sensor scalar ps1
```


المنارة للاستشارات
www.manaraa.com

```
pnt ps2    1.0 0 0
sensor scalar ps2

pnt ps3    2.0 0 0
sensor scalar ps3

pnt ps4    3.0 0 0
sensor scalar ps4

pnt ps5    4.0 0 0
sensor scalar ps5

pnt ps6    5.0 0 0
sensor scalar ps6


@
@ - define boundary conditions
@

bounds on

boundary reflect west
boundary vacuum south east north

fill

data
run
paraview flux
stop
```

C.4.4 EVENT RZ Transient Input Files

C.4.4.1 EVENT RZ Transient – Eigenvalue File

```
title AGN-201 full model, total spectrum - eigenvalue case

@
@ define main problem parameters
@

problem   radiation        @ Radiation problem
case      eigenvalue       @ Keff determination
geometry  rz               @ 2D RZ geometry
angle     1                @ angular flux expansion
scatter   3                @ Order of scattering anisotropy
groups    2                @ Number of energy groups for the problem
upscatter yes              @ upscattering from energy groups
monitor   eigenvalue       @ Monitor the Keff
iter 100 100 1.0e-05 1.0e-04 300 1.0e-9 300   @ Iteration Parameters
dump 99999

normalize power 4.06 total

opposite flux

@
@ - define library
@

library scale work xn2v7.1.wlib.old

@ - distributed volumetric source

source s1 1.0E-06

@
@ - spectrum
@

@spectrum 0.906693 0.093307 4.64109E-9 4.64109E-11 4.33366E-13 0 0 0
@spectrum 9.99617E-1 3.83467E-4 1.16856E-11 0
spectrum 1.0 0

@
@ - define material xs table ( iht, ihs, ihm )
@

xstab 7 8 15

@
@ - Define Isotopes
@

material u-235a    1092235
material u-238a    1092238
```


www.manaraa.com

```
material o1a       1008016
material h1a       1001901
material ca1a      1006000
material u-235j   10092235
material u-238j   10092238
material o1j      10008016
material h1j      10001901
material ca1j     10006000
material ca2     16006312
material pb204   17082204
material pb206   17082206
material pb207   17082207
material pb208   17082208
material o2      18008016
material h2      18001001
@material o3       5008016
@material n        5007014
material alum    15013027
material ca3     19006000
material fe54    19026054
material fe56    19026056
material fe57    19026057
material fe58    19026058

@
@ - mixing instructions
@

@ Uranium-Polyethylene Core - homo - 1
mix c4105
mix c4105 u-235a       1.441848E-04
mix c4105 u-238a       5.877176E-04
mix c4105 ca1a         3.807824E-02
mix c4105 h1a          7.615649E-02
mix c4105 o1a          1.463805E-03
mix c4105 alum         3.367565E-03
@ Uranium-Polyethylene Elements - 2
mix sr1
mix sr1 u-235j         1.170347E-04
mix sr1 u-238j         4.770500E-04
mix sr1 ca1j           2.548332E-02
mix sr1 h1j            5.096665E-02
mix sr1 o1j            1.188169E-03
mix sr1 alum           1.993627E-02

@ Graphite - density 1.2801 g/cc - 3
mix graph
mix graph ca2        8.78149E-02

@ Aluminum - density 2.702 g/cc - 4
mix al
mix al   alum        6.03073E-02

@ Lead - density 10.777 g/cc - 5
mix pb
mix pb   pb204     4.38482E-04
mix pb   pb206     7.54815E-03
mix pb   pb207     6.92175E-03
mix pb   pb208     1.64118E-02

@ Steel - density 7.82120 g/cc - 6
mix steel
mix steel  ca3       3.92153E-03
mix steel  fe54      4.88044E-03
mix steel  fe56      7.66124E-02
mix steel  fe57      1.76931E-03
mix steel  fe58      2.35463E-04

@ Water - density 0.99848 g/cc - 7
mix water
mix water  h2        6.67731E-02
mix water  o2        3.33866E-02

@ Air - 8
mix air
mix air    o2         9.48790E-06
@mix air    n         4.07700E-05
@mix air    o3        9.48790E-06

@ Zone 1 - 9

mix hole1
mix hole1 air  0.5
mix hole1 sr1  0.5

@
@ define the geometry
@

define grid

  xcoord  0.0 1.1875 1.27 5.3 6.30 12.8 15.85 16.1 33.12 44.926 45.72 98.0

  xint       1    2     15        5        25   10     2   10    5      2     5
```


www.manaraa.com

```
  ycoord  -47.29 -36.25 -28.25 -14.25 -12.25 3.75 6.25 12.25 13.25 38.567 48.817 65.0

  yint          5      6      6       3     65   10   25    1     5      5      5

@
@    full core model
@

  material    8  4  5  5  5  5  5  5  5  6  7 ^   / -47.29 to -36.25
              8  4  3  3  3  3  4  3  5  6  7 ^   / -36.25 to -28.25
              8  4  3  3  3  3  4  3  5  6  7 ^   / -28.25 to -14.25
              8  4  3  3  3  3  4  3  5  6  7 ^   / -14.25 to -12.25
              8  4  1  9  1  3  4  3  5  6  7 ^   / -12.25 to 3.75
              8  4  1  1  1  3  4  3  5  6  7 ^   /  3.75 to 6.25
              8  4  1  1  1  3  4  3  5  6  7 ^   /  6.25 to 12.25
              8  4  8  8  8  3  4  3  5  6  7 ^   /  12.25 to 13.25
              8  4  3  3  3  3  4  3  5  6  7 ^   /  13.25 to 38.567
              8  4  5  5  5  5  5  5  5  6  7 ^   /  38.567 to 48.817
              8  4  7  7  7  7  7  7  7  7  7 ^   /  48.817 to 65.0

  source      0  0  0  0  0  0  0  0  0  0  0 ^   / -47.29 to -36.25
              0  0  0  0  0  0  0  0  0  0  0 ^   / -36.25 to -28.25
              0  0  0  0  0  0  0  0  0  0  0 ^   / -28.25 to -14.25
              0  0  0  0  0  0  0  0  0  0  0 ^   / -14.25 to -12.25
              0  0  1  1  1  0  0  0  0  0  0 ^   / -12.25 to  3.75
              0  0  1  1  1  0  0  0  0  0  0 ^   /  3.75 to 6.25
              0  0  1  1  1  0  0  0  0  0  0 ^   /  6.25 to 12.25
              0  0  0  0  0  0  0  0  0  0  0 ^   /  12.25 to 13.25
              0  0  0  0  0  0  0  0  0  0  0 ^   /  13.25 to 38.567
              0  0  0  0  0  0  0  0  0  0  0 ^   /  38.567 to 48.817
              0  0  0  0  0  0  0  0  0  0  0  ^   /  48.817 to 65.0

  average     8  4  5  5  5  5  5  5  5  6  7 ^   / -47.29 to -36.25
              8  4  3  3  3  3  4  3  5  6  7 ^   / -36.25 to -28.25
              8  4  3  3  3  3  4  3  5  6  7 ^   / -28.25 to -14.25
              8  4  3  3  3  3  4  3  5  6  7 ^   / -14.25 to -12.25
              8  4  1  9  1  3  4  3  5  6  7 ^   / -12.25 to 3.75
              8  4  1  1  1  3  4  3  5  6  7 ^   /  3.75 to 6.25
              8  4  1  1  1  3  4  3  5  6  7 ^   /  6.25 to 12.25
              8  4  8  8  8  3  4  3  5  6  7 ^   /  12.25 to 13.25
              8  4  3  3  3  3  4  3  5  6  7 ^   /  13.25 to 38.567
              8  4  5  5  5  5  5  5  5  6  7 ^   /  38.567 to 48.817
              8  4  7  7  7  7  7  7  7  7  7 ^   /  48.817 to 65.0

end grid

@
@ - define boundary conditions
@

bounds on

boundary reflect west
boundary vacuum south east north

@ |--------------------------------------------------------------------------
@ | DELAYED NEUTRON DATA
@ |--------------------------------------------------------------------------

@ - DELAYED NEUTRON PRECURSOR DECAY CONSTANTS - KEEPIN DATA

define delayed

   groups 6

@ - DELAYED NEUTRON PRECURSOR DECAY CONSTANTS

   const 1.241E-02 3.054E-02 1.1101E-01 3.0142E-01 1.1482E+00 3.03737E+00

@ - DELAYED NEUTRON SPECTRUM

   spctrum  1.00E+00 1.00E+00 1.00E+00 1.00E+00 1.00E+00 1.00E+00

@ - DELAYED NEUTRON FRACTIONS

   fractions 2.1557E-04 1.4249E-3 1.2760E-03 2.5790E-03 7.5644E-4 2.7208E-04

end delayed

fill

data
@run
stop
```


www.manaraa.com

C.4.4.2 EVENT RZ Transient

```
title AGN-201 full model, total spectrum - time dependent file

@
@ define main problem parameters
@

problem   radiation        @ Radiation problem
case      time             @ Keff determination
geometry  rz               @ 2D RZ geometry
angle     1                @ angular flux expansion
scatter   3                @ Order of scattering anisotropy
groups    2                @ Number of energy groups for the problem
upscatter yes              @ upscattering from energy groups
monitor   eigenvalue       @ Monitor the Keff
iter 100 100 1.0e-05 1.0e-04 300 1.0e-9 300   @ Iteration Parameters
dump 99999

lump time

normalize eigenvalue

@normalize power 4.06 total

run event RZ_T1_PJ.eig

guess flux RZ_T1_PJ.eig unformatted

@
@ - define library
@

library scale work xn2v7.1.wlib.old

@ - distributed volumetric source

source s1 1.0E-06

@
@ - Define Isotopes
@

material u-235a    1092235
material u-238a    1092238
material o1a       1008016
material h1a       1001901
material ca1a      1006000
material u-235j   10092235
material u-238j   10092238
material o1j      10008016
material h1j      10001901
material ca1j     10006000
material ca2     16006312
material pb204   17082204
material pb206   17082206
material pb207   17082207
material pb208   17082208
material o2      18008016
material h2      18001001
@material o3       5008016
@material n        5007014
material alum    15013027
material ca3     19006000
material fe54    19026054
material fe56    19026056
material fe57    19026057
material fe58    19026058

@
@ - mixing instructions
@

@ Uranium-Polyethylene Core - homo - 1
mix c4105
mix c4105 u-235a       1.441848E-04
mix c4105 u-238a       5.877176E-04
mix c4105 ca1a         3.807824E-02
mix c4105 h1a          7.615649E-02
mix c4105 o1a          1.463805E-03
mix c4105 alum         3.367565E-03
@ Uranium-Polyethylene Elements - 2
mix sr1
mix sr1 u-235j         1.170347E-04
mix sr1 u-238j         4.770500E-04
mix sr1 ca1j           2.548332E-02
mix sr1 h1j            5.096665E-02
mix sr1 o1j            1.188169E-03
mix sr1 alum           1.993627E-02

@ Graphite - density 1.2801 g/cc - 3
mix graph
mix graph ca2       8.78149E-02
```


www.manaraa.com

```
@ Aluminum - density 2.702 g/cc - 4
mix al
mix al   alum        6.03073E-02

@ Lead - density 10.777 g/cc - 5
mix pb
mix pb   pb204     4.38482E-04
mix pb   pb206     7.54815E-03
mix pb   pb207     6.92175E-03
mix pb   pb208     1.64118E-02

@ Steel - density 7.82120 g/cc - 6
mix steel
mix steel  ca3       3.92153E-03
mix steel  fe54      4.88044E-03
mix steel  fe56      7.66124E-02
mix steel  fe57      1.76931E-03
mix steel  fe58      2.35463E-04

@ Water - density 0.99848 g/cc - 7
mix water
mix water  h2        6.67731E-02
mix water  o2        3.33866E-02

@ Air - 8
mix air
mix air    o2         9.48790E-06
@mix air    n         4.07700E-05
@mix air    o3        9.48790E-06

@ Zone 1 - 9

mix hole1
mix hole1 air  0.5
mix hole1 sr1  0.5

@
@ define the geometry
@

define grid

  xcoord  0.0 1.1875 1.27 5.3 6.30 12.8 15.85 16.1 33.12 44.926 45.72 98.0

  xint       1    2     15        5        25   10     2   10    5      2     5

  ycoord  -47.29 -36.25 -28.25 -14.25 -12.25 3.75 6.25 12.25 13.25 38.567 48.817 65.0

  yint          5      6      6       3     65   10   25    1     5      5      5

@
@    full core model
@

  material   8  4  5  5  5  5  5  5  5  6  7 ^   / -47.29 to -36.25
             8  4  3  3  3  3  4  3  5  6  7 ^   / -36.25 to -28.25
             8  4  3  3  3  3  4  3  5  6  7 ^   / -28.25 to -14.25
             8  4  3  3  3  3  4  3  5  6  7 ^   / -14.25 to -12.25
             8  4  1  9  1  3  4  3  5  6  7 ^   / -12.25 to 3.75
             8  4  1  1  1  3  4  3  5  6  7 ^   /  3.75 to 6.25
             8  4  1  1  1  3  4  3  5  6  7 ^   /  6.25 to 12.25
             8  4  8  8  8  3  4  3  5  6  7 ^   /  12.25 to 13.25
             8  4  3  3  3  3  4  3  5  6  7 ^   /  13.25 to 38.567
             8  4  5  5  5  5  5  5  5  6  7 ^   /  38.567 to 48.817
             8  4  7  7  7  7  7  7  7  7  7 ^   /  48.817 to 65.0

  source     0  0  0  0  0  0  0  0  0  0  0 ^   / -47.29 to -36.25
             0  0  0  0  0  0  0  0  0  0  0 ^   / -36.25 to -28.25
             0  0  0  0  0  0  0  0  0  0  0 ^   / -28.25 to -14.25
             0  0  0  0  0  0  0  0  0  0  0 ^   / -14.25 to -12.25
             0  0  1  1  1  0  0  0  0  0  0 ^   / -12.25 to  3.75
             0  0  1  1  1  0  0  0  0  0  0 ^   /  3.75 to 6.25
             0  0  1  1  1  0  0  0  0  0  0 ^   /  6.25 to 12.25
             0  0  0  0  0  0  0  0  0  0  0 ^   /  12.25 to 13.25
             0  0  0  0  0  0  0  0  0  0  0 ^   /  13.25 to 38.567
             0  0  0  0  0  0  0  0  0  0  0 ^   /  38.567 to 48.817
             0  0  0  0  0  0  0  0  0  0  0  ^   /  48.817 to 65.0

  average    8  4  5  5  5  5  5  5  5  6  7 ^   / -47.29 to -36.25
             8  4  3  3  3  3  4  3  5  6  7 ^   / -36.25 to -28.25
             8  4  3  3  3  3  4  3  5  6  7 ^   / -28.25 to -14.25
             8  4  3  3  3  3  4  3  5  6  7 ^   / -14.25 to -12.25
             8  4  1  9  1  3  4  3  5  6  7 ^   / -12.25 to 3.75
             8  4  1  1  1  3  4  3  5  6  7 ^   /  3.75 to 6.25
             8  4  1  1  1  3  4  3  5  6  7 ^   /  6.25 to 12.25
             8  4  8  8  8  3  4  3  5  6  7 ^   /  12.25 to 13.25
             8  4  3  3  3  3  4  3  5  6  7 ^   /  13.25 to 38.567
             8  4  5  5  5  5  5  5  5  6  7 ^   /  38.567 to 48.817
             8  4  7  7  7  7  7  7  7  7  7 ^   /  48.817 to 65.0

end grid

@
@ - define boundary conditions
```


www.manaraa.com

```
@

bounds on

boundary reflect west
boundary vacuum south east north

@read trans1x.time_zones_trans_0-2

@ |---------------------------------------------------------------------|
@ | *********************************************************************|
@ | ******************** TIME ZONE INFORMATION **************************|
@ | *********************************************************************|
@ |---------------------------------------------------------------------|

@ |---------------------------------------------------------------------
@ | TIME ZONE #0 -> uses mixing instructions above
@ |---------------------------------------------------------------------

begin time zone 0

  duration 1.0e+00
  steps -1

end time zone 0

@ |---------------------------------------------------------------------
@ | TIME ZONE #1 -> uses mixing instructions above
@ |---------------------------------------------------------------------

begin time zone 1

  duration 168.0e+00
@  duration 174.0e+00
  steps -1

@
@ - mixing instructions
@

@
@ - Define Isotopes
@

material u-235a    1092235
material u-238a    1092238
material o1a       1008016
material h1a       1001901
material ca1a      1006000
material u-235j   10092235
material u-238j   10092238
material o1j      10008016
material h1j      10001901
material ca1j     10006000
material ca2     1600631
material pb204   17082204
material pb206   17082206
material pb207   17082207
material pb208   17082208
material o2      18008016
material h2      18001001
@material o3       5008016
@material n        5007014
material alum    15013027
material ca3     19006000
material fe54    19026054
material fe56    19026056
material fe57    19026057
material fe58    19026058

@
@ - mixing instructions
@

@ Uranium-Polyethylene Core - homo - 1
mix c4105
mix c4105 u-235a       1.441848E-04
mix c4105 u-238a       5.877176E-04
mix c4105 ca1a         3.807824E-02
mix c4105 h1a          7.615649E-02
mix c4105 o1a          1.463805E-03
mix c4105 alum         3.367565E-03
@ Uranium-Polyethylene Elements - 2
mix sr1
mix sr1 u-235j         1.170347E-04
mix sr1 u-238j         4.770500E-04
mix sr1 ca1j           2.548332E-02
mix sr1 h1j            5.096665E-02
mix sr1 o1j            1.188169E-03
mix sr1 alum           1.993627E-02

@ Graphite - density 1.2801 g/cc - 3
mix graph
mix graph ca2        8.78149E-02
```


www.manaraa.com

```
@ Aluminum - density 2.702 g/cc - 4
mix al
mix al   alum        6.03073E-02

@ Lead - density 10.777 g/cc - 5
mix pb
mix pb   pb204     4.38482E-04
mix pb   pb206     7.54815E-03
mix pb   pb207     6.92175E-03
mix pb   pb208     1.64118E-02

@ Steel - density 7.82120 g/cc - 6
mix steel
mix steel  ca3       3.92153E-03
mix steel  fe54      4.88044E-03
mix steel  fe56      7.66124E-02
mix steel  fe57      1.76931E-03
mix steel  fe58      2.35463E-04

@ Water - density 0.99848 g/cc - 7
mix water
mix water  h2        6.67731E-02
mix water  o2        3.33866E-02

@ Air - 8
mix air
mix air    o2         9.48790E-06
@mix air    n         4.07700E-05
@mix air    o3        9.48790E-06
@ Zone 1 - 9

mix hole1
mix hole1 air  0.43879063
mix hole1 sr1  0.56120937

end time zone 1

@ |-------------------------------------------------------------------------
@ | TIME ZONE #2 -> uses mixing instructions above
@ |-------------------------------------------------------------------------

begin time zone 2

  duration 20.0e+00
  steps -1

@
@ - mixing instructions
@

@
@ - Define Isotopes
@

material u-235a    1092235
material u-238a    1092238
material o1a       1008016
material h1a       1001901
material ca1a      1006000
material u-235j   10092235
material u-238j   10092238
material o1j      10008016
material h1j      10001901
material ca1j     10006000
material ca2     16006312
material pb204   17082204
material pb206   17082206
material pb207   17082207
material pb208   17082208
material o2      18008016
material h2      18001001
@material o3       5008016
@material n        5007014
material alum    15013027
material ca3     19006000
material fe54    19026054
material fe56    19026056
material fe57    19026057
material fe58    19026058

@
@ - mixing instructions
@

@ Uranium-Polyethylene Core - homo - 1
mix c4105
mix c4105 u-235a       1.441848E-04
mix c4105 u-238a       5.877176E-04
mix c4105 ca1a         3.807824E-02
mix c4105 h1a          7.615649E-02
mix c4105 o1a          1.463805E-03
mix c4105 alum         3.367565E-03
@ Uranium-Polyethylene Elements - 2
mix sr1
mix sr1 u-235j         1.170347E-04
```


www.manaraa.com

```
mix sr1 u-238j         4.770500E-04
mix sr1 ca1j           2.548332E-02
mix sr1 h1j            5.096665E-02
mix sr1 o1j            1.188169E-03
mix sr1 alum           1.993627E-02

@ Graphite - density 1.2801 g/cc - 3
mix graph
mix graph ca2        8.78149E-02

@ Aluminum - density 2.702 g/cc - 4
mix al
mix al   alum        6.03073E-02

@ Lead - density 10.777 g/cc - 5
mix pb
mix pb   pb204     4.38482E-04
mix pb   pb206     7.54815E-03
mix pb   pb207     6.92175E-03
mix pb   pb208     1.64118E-02

@ Steel - density 7.82120 g/cc - 6
mix steel
mix steel  ca3       3.92153E-03
mix steel  fe54      4.88044E-03
mix steel  fe56      7.66124E-02
mix steel  fe57      1.76931E-03
mix steel  fe58      2.35463E-04

@ Water - density 0.99848 g/cc - 7
mix water
mix water  h2        6.67731E-02
mix water  o2        3.33866E-02

@ Air - 8
mix air
mix air    o2         9.48790E-06
@mix air    n         4.07700E-05
@mix air    o3        9.48790E-06

@ Zone 1 - 9

mix hole1
mix hole1 air  0.5
mix hole1 sr1  0.5
@mix hole1 air  0.2558
@mix hole1 sr1  0.7442

end time zone 2

@ |-------------------------------------------------------------------------
@ | TIME ZONE #3 -> uses mixing instructions above
@ |-------------------------------------------------------------------------

begin time zone 3

  duration 20.0e+00
  steps -1

@
@ - mixing instructions
@

@
@ - Define Isotopes
@

material u-235a    1092235
material u-238a    1092238
material o1a       1008016
material h1a       1001901
material ca1a      1006000
material u-235j   10092235
material u-238j   10092238
material o1j      10008016
material h1j      10001901
material ca1j     10006000
material ca2     16006312
material pb204   17082204
material pb206   17082206
material pb207   17082207
material pb208   17082208
material o2      18008016
material h2      18001001
@material o3       5008016
@material n        5007014
material alum    15013027
material ca3     19006000
material fe54    19026054
material fe56    19026056
material fe57    19026057
material fe58    19026058

@
@ - mixing instructions
```


www.manaraa.com

```
@

@ Uranium-Polyethylene Core - homo - 1
mix c4105
mix c4105 u-235a       1.441848E-04
mix c4105 u-238a       5.877176E-04
mix c4105 ca1a         3.807824E-02
mix c4105 h1a          7.615649E-02
mix c4105 o1a          1.463805E-03
mix c4105 alum         3.367565E-03
@ Uranium-Polyethylene Elements - 2
mix sr1
mix sr1 u-235j         1.170347E-04
mix sr1 u-238j         4.770500E-04
mix sr1 ca1j           2.548332E-02
mix sr1 h1j            5.096665E-02
mix sr1 o1j            1.188169E-03
mix sr1 alum           1.993627E-02

@ Graphite - density 1.2801 g/cc - 3
mix graph
mix graph ca2        8.78149E-02

@ Aluminum - density 2.702 g/cc - 4
mix al
mix al   alum        6.03073E-02

@ Lead - density 10.777 g/cc - 5
mix pb
mix pb   pb204     4.38482E-04
mix pb   pb206     7.54815E-03
mix pb   pb207     6.92175E-03
mix pb   pb208     1.64118E-02

@ Steel - density 7.82120 g/cc - 6
mix steel
mix steel  ca3       3.92153E-03
mix steel  fe54      4.88044E-03
mix steel  fe56      7.66124E-02
mix steel  fe57      1.76931E-03
mix steel  fe58      2.35463E-04

@ Water - density 0.99848 g/cc - 7
mix water
mix water  h2        6.67731E-02
mix water  o2        3.33866E-02

@ Air - 8
mix air
mix air    o2         9.48790E-06
@mix air    n         4.07700E-05
@mix air    o3        9.48790E-06

@ Zone 1 - 9

mix hole1
mix hole1 air  0.45
mix hole1 sr1  0.55
@mix hole1 air  0.2558
@mix hole1 sr1  0.7442

end time zone 3

@ |-------------------------------------------------------------------------
@ | TIME ZONE #4 -> uses mixing instructions above
@ |-------------------------------------------------------------------------

begin time zone 4

  duration 306.0e+00
  steps -1

@
@ - mixing instructions
@

@
@ - Define Isotopes
@

material u-235a    1092235
material u-238a    1092238
material o1a       1008016
material h1a       1001901
material ca1a      1006000
material u-235j   10092235
material u-238j   10092238
material o1j      10008016
material h1j      10001901
material ca1j     10006000
material ca2     16006312
material pb204   17082204
material pb206   17082206
material pb207   17082207
material pb208   17082208
```


www.manaraa.com

```
material o2      18008016
material h2      18001001
@material o3       5008016
@material n        5007014
material alum    15013027
material ca3     19006000
material fe54    19026054
material fe56    19026056
material fe57    19026057
material fe58    19026058

@
@ - mixing instructions
@

@ Uranium-Polyethylene Core - homo - 1
mix c4105
mix c4105 u-235a       1.441848E-04
mix c4105 u-238a       5.877176E-04
mix c4105 ca1a         3.807824E-02
mix c4105 h1a          7.615649E-02
mix c4105 o1a          1.463805E-03
mix c4105 alum         3.367565E-03
@ Uranium-Polyethylene Elements - 2
mix sr1
mix sr1 u-235j         1.170347E-04
mix sr1 u-238j         4.770500E-04
mix sr1 ca1j           2.548332E-02
mix sr1 h1j            5.096665E-02
mix sr1 o1j            1.188169E-03
mix sr1 alum           1.993627E-02

@ Graphite - density 1.2801 g/cc - 3
mix graph
mix graph ca2        8.78149E-02

@ Aluminum - density 2.702 g/cc - 4
mix al
mix al   alum        6.03073E-02

@ Lead - density 10.777 g/cc - 5
mix pb
mix pb   pb204     4.38482E-04
mix pb   pb206     7.54815E-03
mix pb   pb207     6.92175E-03
mix pb   pb208     1.64118E-02

@ Steel - density 7.82120 g/cc - 6
mix steel
mix steel  ca3       3.92153E-03
mix steel  fe54      4.88044E-03
mix steel  fe56      7.66124E-02
mix steel  fe57      1.76931E-03
mix steel  fe58      2.35463E-04

@ Water - density 0.99848 g/cc - 7
mix water
mix water  h2        6.67731E-02
mix water  o2        3.33866E-02

@ Air - 8
mix air
mix air    o2         9.48790E-06
@mix air    n         4.07700E-05
@mix air    o3        9.48790E-06

@ Zone 1 - 9

mix hole1
mix hole1 air  0.5
mix hole1 sr1  0.5
@mix hole1 air  0.2558
@mix hole1 sr1  0.7442

end time zone 4

@ |-------------------------------------------------------------------------
@ | TIME ZONE #5 -> uses mixing instructions above
@ |-------------------------------------------------------------------------

begin time zone 5

  duration 334.0e+00
  steps -1

@
@ - mixing instructions
@

@
@ - Define Isotopes
@

material u-235a    1092235
material u-238a    1092238
```


www.manaraa.com

```
material o1a       1008016
material h1a       1001901
material ca1a      1006000
material u-235j   10092235
material u-238j   10092238
material o1j      10008016
material h1j      10001901
material ca1j     10006000
material ca2     16006312
material pb204   17082204
material pb206   17082206
material pb207   17082207
material pb208   17082208
material o2      18008016
material h2      18001001
@material o3       5008016
@material n        5007014
material alum    15013027
material ca3     19006000
material fe54    19026054
material fe56    19026056
material fe57    19026057
material fe58    19026058

@
@ - mixing instructions
@

@ Uranium-Polyethylene Core - homo - 1
mix c4105
mix c4105 u-235a       1.441848E-04
mix c4105 u-238a       5.877176E-04
mix c4105 ca1a         3.807824E-02
mix c4105 h1a          7.615649E-02
mix c4105 o1a          1.463805E-03
mix c4105 alum         3.367565E-03
@ Uranium-Polyethylene Elements - 2
mix sr1
mix sr1 u-235j         1.170347E-04
mix sr1 u-238j         4.770500E-04
mix sr1 ca1j           2.548332E-02
mix sr1 h1j            5.096665E-02
mix sr1 o1j            1.188169E-03
mix sr1 alum           1.993627E-02

@ Graphite - density 1.2801 g/cc - 3
mix graph
mix graph ca2        8.78149E-02

@ Aluminum - density 2.702 g/cc - 4
mix al
mix al   alum        6.03073E-02

@ Lead - density 10.777 g/cc - 5
mix pb
mix pb   pb204     4.38482E-04
mix pb   pb206     7.54815E-03
mix pb   pb207     6.92175E-03
mix pb   pb208     1.64118E-02

@ Steel - density 7.82120 g/cc - 6
mix steel
mix steel  ca3       3.92153E-03
mix steel  fe54      4.88044E-03
mix steel  fe56      7.66124E-02
mix steel  fe57      1.76931E-03
mix steel  fe58      2.35463E-04

@ Water - density 0.99848 g/cc - 7
mix water
mix water  h2        6.67731E-02
mix water  o2        3.33866E-02

@ Air - 8
mix air
mix air    o2         9.48790E-06
@mix air    n         4.07700E-05
@mix air    o3        9.48790E-06

@ Zone 1 - 9

mix hole1
mix hole1 air  0.764829194
mix hole1 sr1  0.235170806

end time zone 5

@ |---------------------------------------------------------------------
@ | DELAYED NEUTRON DATA
@ |---------------------------------------------------------------------

@ - DELAYED NEUTRON PRECURSOR DECAY CONSTANTS - KEEPIN DATA

define delayed
```


www.manaraa.com

```
   groups 6
@ - DELAYED NEUTRON PRECURSOR DECAY CONSTANTS
   const 1.241E-02 3.054E-02 1.1101E-01 3.0142E-01 1.1482E+00 3.03737E+00
@ - DELAYED NEUTRON SPECTRUM
   spctrum  1.00E+00 1.00E+00 1.00E+00 1.00E+00 1.00E+00 1.00E+00
@ - DELAYED NEUTRON FRACTIONS
   fractions 2.1557E-04 1.4249E-3 1.2760E-03 2.5790E-03 7.5644E-4 2.7208E-04
end delayed
fill
data
stop
```

C.5 EVENT NETGEN Models

Three EVENT NETGEN models were generated for this work. The purpose of the EVENT NETGEN models were generated to perform the following:

- Detailed eigenvalue model for verification of delayed critical configurations.
- Simplified eigenvalue model for transient testing and and AGN experimental transient analysis.
- Simplified eigenvalue and time-dependent models for AGN transient analysis.

The EVENT NETGEN involve 3-D geometrical configurations that are nearly identical to the MCNP6 model geometry. The EVENT files utilize multigroup cross sections based on ENDF/B-VII.1 neutron cross-section libraries while the MCNP6 files consider continuous-energy cross sections based on ENDF/B-VII neutron cross-section libraries.

www.manaraa.com

C.5.1 Detailed EVENT NETGEN Model

```
Title: AGN201 NETGEN 3D Model

@
@ - AGN 201 NETGEN 3D Model
@ - With Control Rods In and Below Core
@ - Douglas Bowen - 05/02/2013
@

@
@ - Define Main Problem Parameters
@

problem    radiation        @ Radiation problem
geometry   xyz              @ 3D xyz geometry
case       eigenvalue       @ Keff determination
angle      11               @ P3 angular flux expansion
scatter    3                @ Order of scattering anisotropy
groups     2                @ # energy groups for problem
upscatter  yes              @ ? upscattering from energy groups
solution   pcg5             @ Solution scheme
monitor    eigenvalue       @ Monitor the Keff
iter 50 100 1.0e-05 1.0e-05 200 1.0e-08 200   @ Iteration Parameters

@@@@@@@@@@@@@@@@@@@@@@@@@@@@@@@@@@@@@@@@@@@@@@@@@@@@@@@@@@@@@@@@@@@@@@@@
@
@ - csg geometry description
@
@@@@@@@@@@@@@@@@@@@@@@@@@@@@@@@@@@@@@@@@@@@@@@@@@@@@@@@@@@@@@@@@@@@@@@@@

begin csg

algebraic3d

solid glory  =  cylinder (0, 0, -47.29; 0, 0, 78.25;   1.27);
solid core1  =  cylinder (0, 0, -47.29; 0, 0, 78.25;  12.80);
solid baff   =  cylinder (0, 0, -28.25; 0, 0, 13.25;  12.80);
solid graph2 =  cylinder (0, 0, -36.25; 0, 0, 38.567; 33.12);
solid ledd   =  cylinder (0, 0, -46.50; 0, 0, 49.61; 44.926);
solid wat    =  cylinder (0, 0, -47.29; 0, 0, 78.25;  98.00);

# safety rod, coarse rod, and fine rod definitions

solid cyl1   =  cylinder ( 5.869,  5.869, -28.25;  5.869,  5.869, 13.25; 2.75);
solid cyl3   =  cylinder (-5.869,  5.869, -28.25; -5.869,  5.869, 13.25; 2.75);
solid cyl5   =  cylinder ( 5.869, -5.869, -28.25;  5.869, -5.869, 13.25; 2.75);
solid cyl7   =  cylinder (-5.869, -5.869, -28.25; -5.869, -5.869, 13.25; 1.50);

# define AXIAL cutoff planes

solid botps  =  plane (0, 0, -47.29; 0, 0, -1);
solid topps  =  plane (0, 0, -36.25; 0, 0,  1);

solid botpt  =  plane (0, 0, -36.25; 0, 0, -1);
solid toppt  =  plane (0, 0, -34.25; 0, 0,  1);

solid botpt1  =  plane (0, 0, -34.25; 0, 0, -1);
solid toppt1  =  plane (0, 0, -32.25; 0, 0,  1);

solid botpu  =  plane (0, 0, -32.25; 0, 0, -1);
solid toppu  =  plane (0, 0, -30.25; 0, 0,  1);

solid botpu1  =  plane (0, 0, -30.25; 0, 0, -1);
solid toppu1  =  plane (0, 0, -28.25; 0, 0,  1);

solid botpv  =  plane (0, 0, -28.25; 0, 0, -1);
solid toppv  =  plane (0, 0, -26.25; 0, 0,  1);

solid botpv1  =  plane (0, 0, -26.25; 0, 0, -1);
solid toppv1  =  plane (0, 0, -24.25; 0, 0,  1);

solid botpw  =  plane (0, 0, -24.25; 0, 0, -1);
solid toppw  =  plane (0, 0, -22.25; 0, 0,  1);

solid botpw1  =  plane (0, 0, -22.25; 0, 0, -1);
solid toppw1  =  plane (0, 0, -20.25; 0, 0,  1);

solid botpx  =  plane (0, 0, -20.25; 0, 0, -1);
solid toppx  =  plane (0, 0, -18.25; 0, 0,  1);

solid botpx1  =  plane (0, 0, -18.25; 0, 0, -1);
solid toppx1  =  plane (0, 0, -16.25; 0, 0,  1);

solid botpy  =  plane (0, 0, -16.25; 0, 0, -1);
solid toppy  =  plane (0, 0, -14.25; 0, 0,  1);

solid botpy1  =  plane (0, 0, -14.25; 0, 0, -1);
solid toppy1  =  plane (0, 0, -12.25; 0, 0,  1);

solid botpz  =  plane (0, 0, -12.25; 0, 0, -1);
solid toppz  =  plane (0, 0, -10.25; 0, 0,  1);
```


www.manaraa.com

```
solid botpz1  =  plane (0, 0, -10.25; 0, 0, -1);
solid toppz1  =  plane (0, 0,  -8.25; 0, 0,  1);

solid botpza =  plane (0, 0,  -8.25; 0, 0, -1);
solid toppza =  plane (0, 0,  -6.25; 0, 0,  1);

solid botpza1 =  plane (0, 0,  -6.25; 0, 0, -1);
solid toppza1 =  plane (0, 0,  -4.25; 0, 0,  1);

solid botpzb =  plane (0, 0,  -4.25; 0, 0, -1);
solid toppzb =  plane (0, 0,  -2.25; 0, 0,  1);

solid botpzb1 =  plane (0, 0,  -2.25; 0, 0, -1);
solid toppzb1 =  plane (0, 0,  -0.25; 0, 0,  1);

solid botpzc =  plane (0, 0,  -0.25; 0, 0, -1);
solid toppzc =  plane (0, 0,   0.25; 0, 0,  1);

solid botpzd =  plane (0, 0,   0.25; 0, 0, -1);
solid toppzd =  plane (0, 0,   2.25; 0, 0,  1);

solid botpzd1 =  plane (0, 0,   2.25; 0, 0, -1);
solid toppzd1 =  plane (0, 0,   4.25; 0, 0,  1);

solid botpze =  plane (0, 0,   4.25; 0, 0, -1);
solid toppze =  plane (0, 0,   6.25; 0, 0,  1);

solid botpzf =  plane (0, 0,   6.25; 0, 0, -1);
solid toppzf =  plane (0, 0,   8.25; 0, 0,  1);

solid botpzg =  plane (0, 0,   8.25; 0, 0, -1);
solid toppzg =  plane (0, 0,  10.25; 0, 0,  1);

solid botpzh =  plane (0, 0,  10.25; 0, 0, -1);
solid toppzh =  plane (0, 0,  11.25; 0, 0,  1);

solid botpzi =  plane (0, 0,  11.25; 0, 0, -1);
solid toppzi =  plane (0, 0,  12.25; 0, 0,  1);

solid botpzj =  plane (0, 0,  12.25; 0, 0, -1);
solid toppzj =  plane (0, 0,  13.25; 0, 0,  1);

# layer above core region
solid botpzk =  plane (0, 0,  13.25;  0, 0, -1);
solid toppzk =  plane (0, 0,  38.567; 0, 0,  1);

solid botpzl =  plane (0, 0,  38.567; 0, 0, -1);
solid toppzl =  plane (0, 0,  48.817; 0, 0,  1);

solid botpzm =  plane (0, 0,  48.817; 0, 0, -1);
solid toppzm =  plane (0, 0,  65; 0, 0,  1);

# define the fuel and cladding for CR

# sub-level 4
solid CR0v   = cyl1 and toppv and botpv;
solid CR1v   = cyl3 and toppv and botpv;
solid CR2v   = cyl5 and toppv and botpv;
solid CR3v   = cyl7 and toppv and botpv;
solid gl1    = glory and toppv and botpv;

# sub-level 4.1
solid CR0v1   = cyl1 and toppv1 and botpv1;
solid CR1v1   = cyl3 and toppv1 and botpv1;
solid CR2v1   = cyl5 and toppv1 and botpv1;
solid CR3v1   = cyl7 and toppv1 and botpv1;
solid gl2     = glory and toppv1 and botpv1;

# sub-level 3
solid CR0w   = cyl1 and toppw and botpw;
solid CR1w   = cyl3 and toppw and botpw;
solid CR2w   = cyl5 and toppw and botpw;
solid CR3w   = cyl7 and toppw and botpw;
solid gl3    = glory and toppw and botpw;

# sub-level 3.1
solid CR0w1   = cyl1 and toppw1 and botpw1;
solid CR1w1   = cyl3 and toppw1 and botpw1;
solid CR2w1   = cyl5 and toppw1 and botpw1;
solid CR3w1   = cyl7 and toppw1 and botpw1;
solid gl4     = glory and toppw1 and botpw1;

# sub-level 2
solid CR0x   = cyl1 and toppx and botpx;
solid CR1x   = cyl3 and toppx and botpx;
solid CR2x   = cyl5 and toppx and botpx;
solid CR3x   = cyl7 and toppx and botpx;
solid gl5    = glory and toppx and botpx;

# sub-level 2.1
solid CR0x1   = cyl1 and toppx1 and botpx1;
solid CR1x1   = cyl3 and toppx1 and botpx1;
solid CR2x1   = cyl5 and toppx1 and botpx1;
solid CR3x1   = cyl7 and toppx1 and botpx1;
```


www.manaraa.com

```
solid gl6     = glory and toppx1 and botpx1;

# sub-level 1
solid CR0y    = cyl1 and toppy and botpy;
solid CR1y    = cyl3 and toppy and botpy;
solid CR2y    = cyl5 and toppy and botpy;
solid CR3y    = cyl7 and toppy and botpy;
solid gl7     = glory and toppy and botpy;

# sub-level 1.1
solid CR0y1    = cyl1 and toppy1 and botpy1;
solid CR1y1    = cyl3 and toppy1 and botpy1;
solid CR2y1    = cyl5 and toppy1 and botpy1;
solid CR3y1    = cyl7 and toppy1 and botpy1;
solid gl8      = glory and toppy1 and botpy1;

# level 1
solid CR0    = cyl1 and toppz and botpz;
solid CR1    = cyl3 and toppz and botpz;
solid CR2    = cyl5 and toppz and botpz;
solid CR3    = cyl7 and toppz and botpz;
solid gl9    = glory and toppz and botpz;

# level 1.1
solid CR01    = cyl1 and toppz1 and botpz1;
solid CR11    = cyl3 and toppz1 and botpz1;
solid CR21    = cyl5 and toppz1 and botpz1;
solid CR31    = cyl7 and toppz1 and botpz1;
solid gl10    = glory and toppz1 and botpz1;

# level 2
solid CR0a    = cyl1 and toppza and botpza;
solid CR1a    = cyl3 and toppza and botpza;
solid CR2a    = cyl5 and toppza and botpza;
solid CR3a    = cyl7 and toppza and botpza;
solid gl11    = glory and toppza and botpza;

# level 2.1
solid CR0a1    = cyl1 and toppza1 and botpza1;
solid CR1a1    = cyl3 and toppza1 and botpza1;
solid CR2a1    = cyl5 and toppza1 and botpza1;
solid CR3a1    = cyl7 and toppza1 and botpza1;
solid gl12     = glory and toppza1 and botpza1;

# level 3
solid CR0b    = cyl1 and toppzb and botpzb;
solid CR1b    = cyl3 and toppzb and botpzb;
solid CR2b    = cyl5 and toppzb and botpzb;
solid CR3b    = cyl7 and toppzb and botpzb;
solid gl13    = glory and toppzb and botpzb;

# level 3.1
solid CR0b1    = cyl1 and toppzb1 and botpzb1;
solid CR1b1    = cyl3 and toppzb1 and botpzb1;
solid CR2b1    = cyl5 and toppzb1 and botpzb1;
solid CR3b1    = cyl7 and toppzb1 and botpzb1;
solid gl14    = glory and toppzb1 and botpzb1;

# level 4
solid CR0c    = cyl1 and toppzc and botpzc;
solid CR1c    = cyl3 and toppzc and botpzc;
solid CR2c    = cyl5 and toppzc and botpzc;
solid CR3c    = cyl7 and toppzc and botpzc;
solid gl15    = glory and toppzc and botpzc;

# level 5
solid CR0d    = cyl1 and toppzd and botpzd;
solid CR1d    = cyl3 and toppzd and botpzd;
solid CR2d    = cyl5 and toppzd and botpzd;
solid CR3d    = cyl7 and toppzd and botpzd;
solid gl16    = glory and toppzd and botpzd;

# level 5.1
solid CR0d1    = cyl1 and toppzd1 and botpzd1;
solid CR1d1    = cyl3 and toppzd1 and botpzd1;
solid CR2d1    = cyl5 and toppzd1 and botpzd1;
solid CR3d1    = cyl7 and toppzd1 and botpzd1;
solid gl17    = glory and toppzd1 and botpzd1;

# level 6
solid gl18    = glory and botpze and toppzi;

# level 7
solid gl19    = glory and botpzj and toppzj;

# core definitions

solid clev6a  = core1
                      and topps and botps;

solid clev7a  = core1
                      and botpt and toppu1;

solid clev4a  = core1  and not glory
                      and not CR0v
```


www.manaraa.com

```
                    and not CR1v
                    and not CR2v
                    and not CR3v
                    and toppv and botpv;

solid clev4a1  = core1 and not glory
                    and not CR0v1
                    and not CR1v1
                    and not CR2v1
                    and not CR3v1
                    and toppv1 and botpv1;

solid clev3a  = core1 and not glory
                    and not CR0w
                    and not CR1w
                    and not CR2w
                    and not CR3w
                    and toppw and botpw;

solid clev3a1  = core1 and not glory
                    and not CR0w1
                    and not CR1w1
                    and not CR2w1
                    and not CR3w1
                    and toppw1 and botpw1;

solid clev2a  = core1 and not glory
                    and not CR0x
                    and not CR1x
                    and not CR2x
                    and not CR3x
                    and toppx and botpx;

solid clev2a1  = core1 and not glory
                    and not CR0x1
                    and not CR1x1
                    and not CR2x1
                    and not CR3x1
                    and toppx1 and botpx1;

solid clev1a  = core1 and not glory
                   and not CR0y
                   and not CR1y
                   and not CR2y
                   and not CR3y
                   and toppy and botpy;

solid clev1a1  = core1 and not glory
                   and not CR0y1
                   and not CR1y1
                   and not CR2y1
                   and not CR3y1
                   and toppy1 and botpy1;

solid clev1  = core1 and not glory
                    and not CR0
                    and not CR1
                    and not CR2
                    and not CR3
                    and toppz and botpz;

solid clev11  = core1 and not glory
                    and not CR01
                    and not CR11
                    and not CR21
                    and not CR31
                    and toppz1 and botpz1;

solid clev2  = core1 and not glory
                   and not CR0a
                   and not CR1a
                   and not CR2a
                   and not CR3a
                   and toppza and botpza;

solid clev21  = core1 and not glory
                   and not CR0a1
                   and not CR1a1
                   and not CR2a1
                   and not CR3a1
                   and toppza1 and botpza1;

solid clev3  = core1 and not glory
                   and not CR0b
                   and not CR1b
                   and not CR2b
                   and not CR3b
                   and toppzb and botpzb;

solid clev31  = core1 and not glory
                   and not CR0b1
                   and not CR1b1
                   and not CR2b1
                   and not CR3b1
                   and toppzb1 and botpzb1;
```


www.manaraa.com

```
solid clev4  = baff and not glory
                    and not CR0c
                    and not CR1c
                    and not CR2c
                    and not CR3c
                    and toppzc and botpzc;

solid clev5  = core1 and not glory
                    and not CR0d
                    and not CR1d
                    and not CR2d
                    and not CR3d
                    and toppzd and botpzd;

solid clev51  = core1 and not glory
                    and not CR0d1
                    and not CR1d1
                    and not CR2d1
                    and not CR3d1
                    and toppzd1 and botpzd1;

solid clev6  = core1 and not glory
                    and botpze and toppzi;

solid clev7  = core1 and not glory
                    and botpzj and toppzj;

#####

solid gr1    = graph2 and not core1
                    and botpz and toppzj;

#####

solid ld1    = ledd and not graph2
                    and botpz and toppzj;

#####

solid wa1    = wat and not ledd
                    and botpz and toppzj;

#####

# Upper Reflector

solid uref1a  = graph2 and botpzk and toppzk;
solid uref1b  = ledd and not graph2 and botpzk and toppzk;
solid uref1c  = wat and not ledd and botpzk and toppzk;

solid uref2a  = graph2 and botpzl and toppzl;
solid uref2b  = ledd and not graph2 and botpzl and toppzl;
solid uref2c  = wat and not ledd and botpzl and toppzl;

solid uref3a  = graph2 and botpzm and toppzm;
solid uref3b  = ledd and not graph2 and botpzm and toppzm;
solid uref3c  = wat and not ledd and botpzm and toppzm;

# Lower Reflector

solid lref1a  = graph2 and not core1 and botps and topps;
solid lref1b  = ledd and not graph2 and botps and topps;
solid lref1c  = wat and not ledd and botps and topps;

solid lref2a  = graph2 and not core1 and botpt and toppy1;
solid lref2b  = ledd and not graph2 and botpt and toppy1;
solid lref2c  = wat and not ledd and botpt and toppy1;

# Top Level Objects
# level 1
tlo CR0;
tlo CR1;
tlo CR2;
tlo CR3;
# level 1.1
tlo CR01;
tlo CR11;
tlo CR21;
tlo CR31;
# level 2
tlo CR0a;
tlo CR1a;
tlo CR2a;
tlo CR3a;
# level 2.1
tlo CR0a1;
tlo CR1a1;
tlo CR2a1;
tlo CR3a1;
# level 3
tlo CR0b;
tlo CR1b;
tlo CR2b;
tlo CR3b;
# level 3.1
```


www.manaraa.com

```
tlo CR0b1;
tlo CR1b1;
tlo CR2b1;
tlo CR3b1;
# level 4
tlo CR0c;
tlo CR1c;
tlo CR2c;
tlo CR3c;
# level 5
tlo CR0d;
tlo CR1d;
tlo CR2d;
tlo CR3d;
# level 5.1
tlo CR0d1;
tlo CR1d1;
tlo CR2d1;
tlo CR3d1;
# sublevel 4
tlo CR0v;
tlo CR1v;
tlo CR2v;
tlo CR3v;
# sublevel 4.1
tlo CR0v1;
tlo CR1v1;
tlo CR2v1;
tlo CR3v1;
# sublevel 3
tlo CR0w;
tlo CR1w;
tlo CR2w;
tlo CR3w;
# sublevel 3.1
tlo CR0w1;
tlo CR1w1;
tlo CR2w1;
tlo CR3w1;
# sublevel 2
tlo CR0x;
tlo CR1x;
tlo CR2x;
tlo CR3x;
# sublevel 2.1
tlo CR0x1;
tlo CR1x1;
tlo CR2x1;
tlo CR3x1;
# sublevel 1
tlo CR0y;
tlo CR1y;
tlo CR2y;
tlo CR3y;
# sublevel 1.1
tlo CR0y1;
tlo CR1y1;
tlo CR2y1;
tlo CR3y1;
# core levels
tlo clev1;
tlo clev2;
tlo clev3;
tlo clev4;
tlo clev5;
tlo clev6;
tlo clev7;
# core sublevels
tlo clev1a;
tlo clev2a;
tlo clev3a;
tlo clev4a;
tlo clev7a;
# core levels
tlo clev11;
tlo clev21;
tlo clev31;
tlo clev51;
# core sublevels
tlo clev1a1;
tlo clev2a1;
tlo clev3a1;
tlo clev4a1;
#
tlo gr1;
#
tlo ld1;
#
tlo wa1;
#
tlo uref1a;
tlo uref1b;
tlo uref1c;
#
tlo uref2a;
```


www.manaraa.com

```
tlo uref2b;
tlo uref2c;
#
tlo uref3a;
tlo uref3b;
tlo uref3c;
#
tlo lref1a;
tlo lref1b;
tlo lref1c;
#
tlo lref2a;
tlo lref2b;
tlo lref2c;
#
tlo clev6a;
#
tlo gl1;
tlo gl2;
tlo gl3;
tlo gl4;
tlo gl5;
tlo gl6;
tlo gl7;
tlo gl8;
tlo gl9;
tlo gl10;
tlo gl11;
tlo gl12;
tlo gl13;
tlo gl14;
tlo gl15;
tlo gl16;
tlo gl17;
tlo gl18;
tlo gl19;
#

end csg

@
@ - Define Boundary Conditions
@

boundary vacuum clev1
boundary vacuum clev2
boundary vacuum clev3
boundary vacuum clev4
boundary vacuum clev5
boundary vacuum clev6
boundary vacuum gr1
boundary vacuum ld1
boundary vacuum wa1
boundary vacuum uref1a
boundary vacuum uref1b
boundary vacuum uref1c
boundary vacuum uref2a
boundary vacuum uref2b
boundary vacuum uref2c
boundary vacuum lref1a
boundary vacuum lref1b
boundary vacuum lref1c

@@@@@@@@@@@@@@@@@@@@@@@@@@@@@@@@@@@@@@@@@@@@@@@@@@@@@@@@@@@@@@@@@@@@@@@@@
@
@ - create mesh
@
@@@@@@@@@@@@@@@@@@@@@@@@@@@@@@@@@@@@@@@@@@@@@@@@@@@@@@@@@@@@@@@@@@@@@@@@@

netgen

@list constraints

@
@ - define library
@

library scale work xn2v7.1.wlib.old
@library scale work scale_8g_wlib.old

@
@ - spectrum
@

@spectrum 0.906693 0.093307 4.64109E-9 4.64109E-11 4.33366E-13 0 0 0
@spectrum 9.99617E-1 3.83467E-4 1.16856E-11 0
spectrum 1 0

@
@ - define material xs table ( iht, ihs, ihm )
@

xstab 7 8 15

@
```


المنارة للاستشارات
www.manaraa.com

```
@ - Define Isotopes
@

material u-235a    1092235
material u-238a    1092238
material o1a       1008016
material h1a       1001901
material ca1a      1006000
material u-235b    2092235
material u-238b    2092238
material o1b       2008016
material h1b       2001901
material ca1b      2006000
material u-235c    3092235
material u-238c    3092238
material o1c       3008016
material h1c       3001901
material ca1c      3006000
material u-235d    4092235
material u-238d    4092238
material o1d       4008016
material h1d       4001901
material ca1d      4006000
material u-235e    5092235
material u-238e    5092238
material o1e       5008016
material h1e       5001901
material ca1e      5006000
material u-235f    6092235
material u-238f    6092238
material o1f       6008016
material h1f       6001901
material ca1f      6006000
material u-235g    7092235
material u-238g    7092238
material o1g       7008016
material h1g       7001901
material ca1g      7006000
material u-235h    8092235
material u-238h    8092238
material o1h       8008016
material h1h       8001901
material ca1h      8006000
material u-235i    9092235
material u-238i    9092238
material o1i       9008016
material h1i       9001901
material ca1i      9006000
material u-235j   10092235
material u-238j   10092238
material o1j      10008016
material h1j      10001901
material ca1j     10006000
material u-235k   11092235
material u-238k   11092238
material o1k      11008016
material h1k      11001901
material ca1k     11006000
material u-235l   12092235
material u-238l   12092238
material o1l      12008016
material h1l      12001901
material ca1l     12006000
material u-235m   13092235
material u-238m   13092238
material o1m      13008016
material h1m      13001901
material ca1m     13006000
material ca2      16006312
material pb204    17082204
material pb206    17082206
material pb207    17082207
material pb208    17082208
material o2       18008016
material h2       18001001
@material o3        5008016
@material n         5007014
material alum     15013027
material ca3      19006000
material fe54     19026054
material fe56     19026056
material fe57     19026057
material fe58     19026058

@
@ - mixing instructions
@
@ Uranium-Polyethylene Core -1
mix c497
mix c497 u-235a       1.4536E-04
mix c497 u-238a       5.9251E-04
mix c497 ca1a         3.8307E-02
mix c497 h1a          7.6615E-02
mix c497 o1a          1.4757E-03
@ Uranium-Polyethylene Core - 2
```


www.manaraa.com

```
mix c498
mix c498 u-235b       1.4570E-04
mix c498 u-238b       5.9389E-04
mix c498 ca1b         3.8305E-02
mix c498 h1b          7.6609E-02
mix c498 o1b          1.4792E-03
@ Uranium-Polyethylene Core - 3
mix c499
mix c499 u-235c       1.4224E-04
mix c499 u-238c       5.7978E-04
mix c499 ca1c         3.8333E-02
mix c499 h1c          7.6666E-02
mix c499 o1c          1.4440E-03
@ Uranium-Polyethylene Core - 4
mix c4100
mix c4100 u-235d       1.4410E-04
mix c4100 u-238d       5.8737E-04
mix c4100 ca1d         3.8318E-02
mix c4100 h1d          7.6635E-02
mix c4100 o1d          1.4629E-03
@ Uranium-Polyethylene Core - 5
mix chomo
mix chomo u-235e       1.451808E-04
mix chomo u-238e       5.917778E-04
mix chomo ca1e         3.830883E-02
mix chomo h1e          7.661766E-02
mix chomo o1e          1.473917E-03
@ Uranium-Polyethylene Elements - 10
mix sr1
mix sr1 u-235j         1.170347E-04
mix sr1 u-238j         4.770500E-04
mix sr1 ca1j           2.548332E-02
mix sr1 h1j            5.096665E-02
mix sr1 o1j            1.188169E-03
mix sr1 alum           1.993627E-02

@ Graphite - density 1.2801 g/cc - 11
mix graph
mix graph ca2        8.78149E-02

@ Aluminum - density 2.702 g/cc - 12
mix al
mix al   alum        6.03073E-02

@ Lead - density 10.777 g/cc - 13
mix pb
mix pb   pb204     4.38482E-04
mix pb   pb206     7.54815E-03
mix pb   pb207     6.92175E-03
mix pb   pb208     1.64118E-02

@ Steel - density 7.82120 g/cc - 14
mix steel
mix steel  ca3       3.92153E-03
mix steel  fe54      4.88044E-03
mix steel  fe56      7.66124E-02
mix steel  fe57      1.76931E-03
mix steel  fe58      2.35463E-04

@ Water - density 0.99848 g/cc - 15
mix water
mix water  h2        6.67731E-02
mix water  o2        3.33866E-02

@ Air - 16
mix air
@mix air    h2         4.07700E-05
mix air    o2         1.0E-06
@mix air    n         4.07700E-05
@mix air    o3        9.48790E-06

@ Aluminum - density 2.702 g/cc - 12
mix al5
mix al5   alum        7.5805E-03

@
@ - Assign Sources and Material Properties to Regions
@
property glory al
@ core sub-level 4
property CR0v     air
property CR1v     air
property CR2v     air
property CR3v     air
@ core sub-level 4.1
property CR0v1     air
property CR1v1     air
property CR2v1     air
property CR3v1     air
@ core sub-level 3
property CR0w     air
property CR1w     air
property CR2w     air
property CR3w     air
@ core sub-level 3.3
```


www.manaraa.com

```
property CR0w1     air
property CR1w1     air
property CR2w1     air
property CR3w1     air
@ core sub-level 2
property CR0x     air
property CR1x     air
property CR2x     air
property CR3x     air
@ core sub-level 2.1
property CR0x1     air
property CR1x1     air
property CR2x1     air
property CR3x1     air
@ core sub-level 1
property CR0y     air
property CR1y     air
property CR2y     air
property CR3y     air
@ core sub-level 1.1
property CR0y1     air
property CR1y1     air
property CR2y1     air
property CR3y1     air
@ core level 1
property CR0     sr1
property CR1     sr1
property CR2     sr1
property CR3     sr1
@ core level 1.1
property CR01     sr1
property CR11     sr1
property CR21     sr1
property CR31     sr1
@ core level 2
property CR0a    sr1
property CR1a    sr1
property CR2a    sr1
property CR3a    sr1
@ core level 2.1
property CR0a1    sr1
property CR1a1    sr1
property CR2a1    sr1
property CR3a1    sr1
@ core level 3
property CR0b    sr1
property CR1b    sr1
property CR2b    sr1
property CR3b    sr1
@ core level 3.1
property CR0b1    sr1
property CR1b1    sr1
property CR2b1    sr1
property CR3b1    sr1
@ baffle level 4
property CR0c    al
property CR1c    al
property CR2c    al
property CR3c    al
@ core level 5
property CR0d    sr1
property CR1d    sr1
property CR2d    sr1
property CR3d    sr1
@ core level 5.1
property CR0d1    sr1
property CR1d1    sr1
property CR2d1    sr1
property CR3d1    sr1
@ sublevel core plates
property clev1a   graph
property clev2a   graph
property clev3a   graph
property clev4a   graph
property clev7a   pb
@ sublevel core plates - other segments
property clev1a1   graph
property clev2a1   graph
property clev3a1   graph
property clev4a1   graph
property clev7a    graph
@ core level plates
property clev1   c497
property clev11  c497
property clev2   c498
property clev21  c498
property clev3   c499
property clev31  c499
property clev4   al
property clev5   c4100
property clev51  c4100
property clev6   chomo
property clev7   air
@
property gr1     graph
```


www.manaraa.com

```
@
property ld1    pb
@
property wa1    water
@
property uref1a graph
property uref1b pb
property uref1c water
@
property uref2a pb
property uref2b pb
property uref2c water
@
property uref3a water
property uref3b water
property uref3c water
@
property lref1a pb
property lref1b pb
property lref1c water
@
property lref2a graph
property lref2b pb
property lref2c water
@
property clev6a pb
@
property gl1 al5
property gl2 al5
property gl3 al5
property gl4 al5
property gl5 al5
property gl6 al5
property gl7 al5
property gl8 al5
property gl9 al5
property gl10 al5
property gl11 al5
property gl12 al5
property gl13 al5
property gl14 al5
property gl15 al5
property gl16 al5
property gl17 al5
property gl18 al5
property gl19 air

@
@ - Define Mesh Type
@

@ mesh r1  delaunay


@
@ - Mesh Problem
@

@fill

@
@ - Plotting Device
@

@ dev x11

@
@ - Output Data to Default File
@
paraview

data

@
@ - Stop the GEM Run
@

stop
```


www.manaraa.com

C.5.2 Simplified EVENT NETGEN Model

```
Title: AGN201 NETGEN 3D Model

@
@ - AGN 201 NETGEN 3D Model
@ - With Control Rods In and Below Core
@ - Douglas Bowen - 05/02/2013
@

@
@ - Define Main Problem Parameters
@

problem    radiation        @ Radiation problem
geometry   xyz              @ 3D xyz geometry
case       eigenvalue       @ Keff determination
angle      7                @ P3 angular flux expansion
scatter    3                @ Order of scattering anisotropy
groups     2                @ # energy groups for problem
upscatter  yes              @ ? upscattering from energy groups
solution   pcg5             @ Solution scheme
monitor    eigenvalue       @ Monitor the Keff
iter 100 100 1.0e-05 1.0e-05 300 1.0e-9 300   @ Iteration Parameters
dump 99999

@normalize power 4.06 total

@opposite flux

@@@@@@@@@@@@@@@@@@@@@@@@@@@@@@@@@@@@@@@@@@@@@@@@@@@@@@@@@@@@@@@@@@@@@@@@
@
@ - csg geometry description
@
@@@@@@@@@@@@@@@@@@@@@@@@@@@@@@@@@@@@@@@@@@@@@@@@@@@@@@@@@@@@@@@@@@@@@@@@

begin csg

algebraic3d
solid gloryhole = cylinder (-100, 0, 0; 100, 0, 0; 1.27);
solid core1  =  cylinder (0, 0, -47.29; 0, 0, 78.25;  12.80);
solid graph2 =  cylinder (0, 0, -36.25; 0, 0, 38.567; 33.12);
solid ledd   =  cylinder (0, 0, -46.50; 0, 0, 49.61; 44.926);
solid wat    =  cylinder (0, 0, -47.29; 0, 0, 78.25;  98.00);

# safety rod, coarse rod, and fine rod definitions
# 0/1=CCR, 4/5=FCR
solid cyl0   =  cylinder ( 5.869,  5.869, -28.25;  5.869,  5.869, 13.25; 2.25);
solid cyl1   =  cylinder ( 5.869,  5.869, -28.25;  5.869,  5.869, 13.25; 2.75);
solid cyl4   =  cylinder (-5.869, -5.869, -28.25; -5.869, -5.869, 13.25; 1.00);
solid cyl5   =  cylinder (-5.869, -5.869, -28.25; -5.869, -5.869, 13.25; 1.50);

# define AXIAL cutoff planes

solid botpz   =  plane (0, 0, -12.25;  0, 0, -1);
solid toppz   =  plane (0, 0,  12.25;  0, 0,  1);

solid botpp   =  plane (0, 0, 12.25;   0, 0, -1);
solid toppp   =  plane (0, 0, 13.25;   0, 0,  1);

solid botpz1   =  plane (0, 0, -28.25; 0, 0, -1);
solid toppz1   =  plane (0, 0, -12.25; 0, 0,  1);

#---------------------------------------------------------CCR
solid botpv1  =  plane (0, 0, -12.25;  0, 0, -1);
solid toppv1  =  plane (0, 0,   3.75;  0, 0,  1);
#---------------------------------------------------------CCR

#---------------------------------------------------------FCR
solid botpe1  =  plane (0, 0, -12.25;  0, 0, -1);
solid toppe1  =  plane (0, 0,   3.75;  0, 0,  1);
#---------------------------------------------------------FCR

solid botps  =  plane (0, 0, -47.29;   0, 0, -1);
solid topps  =  plane (0, 0, -36.25;   0, 0,  1);

solid botpt  =  plane (0, 0, -36.25;   0, 0, -1);
solid toppt  =  plane (0, 0,  38.567;  0, 0,  1);

solid botpzl =  plane (0, 0,  38.567;  0, 0, -1);
solid toppzl =  plane (0, 0,  48.817;  0, 0,  1);

solid botpzm =  plane (0, 0,  48.817;  0, 0, -1);
solid toppzm =  plane (0, 0,  65.000;  0, 0,  1);

# define the fuel and cladding for CR

# Core Zone 1 (bottom)
# v=CCR , e=FCR
solid fuelv1 = cyl0 and toppv1 and botpv1;
solid cladv1 = cyl1 and not fuelv1 and toppv1 and botpv1;
solid fuele1 = cyl4 and toppe1 and botpe1;
```


www.manaraa.com

```
solid clade1 = cyl5 and not fuele1 and toppe1 and botpe1;

solid gh    = gloryhole and core1;

solid rx1   = core1
                      and not fuelv1
                      and not cladv1
                      and not fuele1
                      and not clade1
                      and not gloryhole
                      and toppz and botpz;

solid rx2    = core1 and toppz1 and botpz1;

solid vd     = core1 and botpp and toppp;


solid gh1    = gloryhole and not core1 and graph2;

solid gr1    = graph2 and not rx2 and not rx1
                      and not fuelv1
                      and not cladv1
                      and not fuele1
                      and not clade1
                      and not vd
                      and not gloryhole
                      and botpt and toppt;

solid gh2     = gloryhole and ledd and not graph2;

solid lea1    = ledd and not gr1 and not rx2 and not rx1
                      and not fuelv1
                      and not cladv1
                      and not fuele1
                      and not clade1
                      and not vd
                      and not gloryhole
                      and botps and toppzl;

solid gh3     = gloryhole and wat and not ledd;

solid wa1    = wat and not lea1 and not gr1
                      and not rx2
                      and not rx1
                      and not fuelv1
                      and not cladv1
                      and not fuele1
                      and not clade1
                      and not vd
                      and not gloryhole
                      and botps and toppzm;

# core2
tlo fuelv1;
tlo cladv1;
tlo fuele1;
tlo clade1;
# core levels
tlo rx1;
tlo rx2;
tlo vd;
tlo gr1;
tlo lea1;
tlo wa1;
# glory hole
tlo gh;
tlo gh1;
tlo gh2;
tlo gh3;
end csg

@
@ - Define Boundary Conditions
@

boundary vacuum wa1

@@@@@@@@@@@@@@@@@@@@@@@@@@@@@@@@@@@@@@@@@@@@@@@@@@@@@@@@@@@@@@@@@@@@@@@@
@
@ - create mesh
@
@@@@@@@@@@@@@@@@@@@@@@@@@@@@@@@@@@@@@@@@@@@@@@@@@@@@@@@@@@@@@@@@@@@@@@@@

netgen

@list constraints

@
@ - define library
@

library scale work xn2v7.1.wlib.old
@library scale work scale_8g_wlib.old

@
```


المنارة للاستشارات
www.manaraa.com

```
@ - spectrum
@

@spectrum 0.906693 0.093307 4.64109E-9 4.64109E-11 4.33366E-13 0 0 0
@spectrum 9.99617E-1 3.83467E-4 1.16856E-11 0
spectrum 1 0

@
@ - define material xs table ( iht, ihs, ihm )
@

xstab 7 8 15

@
@ - Define Isotopes
@

material u-235e    5092235
material u-238e    5092238
material o1e       5008016
material h1e       5001901
material ca1e      5006000
material u-235j   10092235
material u-238j   10092238
material o1j      10008016
material h1j      10001901
material ca1j     10006000
material ca2     16006312
material pb204   17082204
material pb206   17082206
material pb207   17082207
material pb208   17082208
material o2      18008016
material h2      18001001
@material o3       5008016
@material n        5007014
material alum    15013027
material ca3     19006000
material fe54    19026054
material fe56    19026056
material fe57    19026057
material fe58    19026058

@
@ - mixing instructions
@

@ Uranium-Polyethylene Core - 5
mix chomo
mix chomo u-235e       1.332532E-04
mix chomo u-238e       5.431592E-04
mix chomo ca1e         3.813831E-02
mix chomo h1e          7.627662E-02
mix chomo o1e          1.352825E-03
mix chomo alum         2.529110E-03
@ Uranium-Polyethylene Elements - 10
mix sr1
mix sr1 u-235j         1.463033E-04
mix sr1 u-238j         5.963529E-04
mix sr1 ca1j           3.806768E-02
mix sr1 h1j            7.613536E-02
mix sr1 o1j            1.485312E-03

@ Graphite - density 1.2801 g/cc - 11
mix graph
mix graph ca2        8.78149E-02

@ Aluminum - density 2.702 g/cc - 12
mix al
mix al   alum        6.03073E-02

@ Aluminum - density 2.702 g/cc - 12
mix al2
mix al2   alum        7.5805E-03

@ Lead - density 10.777 g/cc - 13
mix pb
mix pb   pb204     4.38482E-04
mix pb   pb206     7.54815E-03
mix pb   pb207     6.92175E-03
mix pb   pb208     1.64118E-02

@ Steel - density 7.82120 g/cc - 14
mix steel
mix steel  ca3       3.92153E-03
mix steel  fe54      4.88044E-03
mix steel  fe56      7.66124E-02
mix steel  fe57      1.76931E-03
mix steel  fe58      2.35463E-04

@ Water - density 0.99848 g/cc - 15
mix water
mix water  h2        6.67731E-02
mix water  o2        3.33866E-02
```


www.manaraa.com

```
@ Air - 16
mix air
mix air    o2         9.48790E-06
@mix air    n         4.07700E-05
@mix air    o3        9.48790E-06

@ HOLE 17 - CCR
mix hole17
mix hole17 air  0.0
mix hole17 sr1  1.0

@ HOLE 18 - FCR
mix hole18
mix hole18 air  1.0
mix hole18 sr1  0.0

@
@ - Assign Sources and Material Properties to Regions
@

@ glory hole
property gh     al2
property gh1    al2
property gh2    al2
property gh3    al2
@ rod rods/clad
property fuelv1  hole17
property cladv1  al
property fuele1  hole18
property clade1  al
@ core level plates
property rx1    chomo
property rx2    graph
property vd     air
@ graphite reflector
property gr1    graph
property lea1   pb
property wa1    water

@
@ - Define Mesh Type
@

@ mesh r1  delaunay


@
@ - Mesh Problem
@

@fill

@
@ - Plotting Device
@

@ dev x11

@
@ - Output Data to Default File
@
@run
@paraview flux
paraview
data

@
@ - Stop the GEM Run
@

stop
```


www.manaraa.com

C.5.3 EVENT NETGEN Transient Input Files

C.5.3.1 EVENT NETGEN Transient – Eigenvalue File

```
Title: AGN201 NETGEN 3D Model

@
@ - AGN 201 NETGEN 3D Model
@ - With Control Rods In and Below Core
@ - Douglas Bowen - 05/02/2013
@

@
@ - Define Main Problem Parameters
@

problem    radiation        @ Radiation problem
geometry   xyz              @ 3D xyz geometry
case       eigenvalue       @ Keff determination
angle      1                @ P3 angular flux expansion
scatter    3                @ Order of scattering anisotropy
groups     2                @ # energy groups for problem
upscatter  yes              @ ? upscattering from energy groups
solution   pcg5             @ Solution scheme
monitor    eigenvalue       @ Monitor the Keff
iter 100 100 1.0e-06 1.0e-06 300 1.0e-11 300   @ Iteration Parameters
dump 99999

normalize power 4.06 total

opposite flux

@@@@@@@@@@@@@@@@@@@@@@@@@@@@@@@@@@@@@@@@@@@@@@@@@@@@@@@@@@@@@@@@@@@@@@@@
@
@ - csg geometry description
@
@@@@@@@@@@@@@@@@@@@@@@@@@@@@@@@@@@@@@@@@@@@@@@@@@@@@@@@@@@@@@@@@@@@@@@@@

begin csg

algebraic3d
solid gloryvoid = cylinder (-100, 0, 0; 100, 0, 0; 1.27);
solid gloryhole = cylinder (-100, 0, 0; 100, 0, 0; 1.47);
solid core1  =  cylinder (0, 0, -47.29; 0, 0, 78.25;  12.80);
solid graph2 =  cylinder (0, 0, -36.25; 0, 0, 38.567; 33.12);
solid ledd   =  cylinder (0, 0, -46.50; 0, 0, 49.61; 44.926);
solid wat    =  cylinder (0, 0, -47.29; 0, 0, 78.25;  98.00);

# safety rod, coarse rod, and fine rod definitions
# 0/1=CCR, 4/5=FCR
solid cyl0   =  cylinder ( 5.869,  5.869, -28.25;  5.869,  5.869, 13.25; 2.25);
solid cyl1   =  cylinder ( 5.869,  5.869, -28.25;  5.869,  5.869, 13.25; 2.75);
solid cyl4   =  cylinder (-5.869, -5.869, -28.25; -5.869, -5.869, 13.25; 1.00);
solid cyl5   =  cylinder (-5.869, -5.869, -28.25; -5.869, -5.869, 13.25; 1.50);

# define AXIAL cutoff planes

solid botpz   =  plane (0, 0, -12.25;  0, 0, -1);
solid toppz   =  plane (0, 0,  12.25;  0, 0,  1);

solid botpp   =  plane (0, 0, 12.25;   0, 0, -1);
solid toppp   =  plane (0, 0, 13.25;   0, 0,  1);

solid botpz1   =  plane (0, 0, -28.25; 0, 0, -1);
solid toppz1   =  plane (0, 0, -12.25; 0, 0,  1);

#---------------------------------------------------------CCR
solid botpv1  =  plane (0, 0, -12.25;  0, 0, -1);
solid toppv1  =  plane (0, 0,   3.75;  0, 0,  1);
#---------------------------------------------------------CCR

#---------------------------------------------------------FCR
solid botpe1  =  plane (0, 0, -12.25;  0, 0, -1);
solid toppe1  =  plane (0, 0,   3.75;  0, 0,  1);
#---------------------------------------------------------FCR

solid botps  =  plane (0, 0, -47.29;   0, 0, -1);
solid topps  =  plane (0, 0, -36.25;   0, 0,  1);

solid botpt  =  plane (0, 0, -36.25;   0, 0, -1);
solid toppt  =  plane (0, 0,  38.567;  0, 0,  1);

solid botpzl =  plane (0, 0,  38.567;  0, 0, -1);
solid toppzl =  plane (0, 0,  48.817;  0, 0,  1);

solid botpzm =  plane (0, 0,  48.817;  0, 0, -1);
solid toppzm =  plane (0, 0,  65.000;  0, 0,  1);

# define the fuel and cladding for CR
```


www.manaraa.com

```
# Core Zone 1 (bottom)
# v=CCR , e=FCR
solid fuelv1 = cyl0 and toppv1 and botpv1;
solid cladv1 = cyl1 and not fuelv1 and toppv1 and botpv1;
solid fuele1 = cyl4 and toppe1 and botpe1;
solid clade1 = cyl5 and not fuele1 and toppe1 and botpe1;

solid gv    = gloryvoid and core1;

solid gh    = gloryhole and not gloryvoid and core1;

solid rx1   = core1
                        and not fuelv1
                        and not cladv1
                        and not fuele1
                        and not clade1
                        and not gloryhole
                        and not gloryvoid
                        and toppz and botpz;

solid rx2    = core1 and toppz1 and botpz1;

solid vd     = core1 and botpp and toppp;

solid gv1    = gloryvoid and not core1 and graph2;

solid gh1    = gloryhole and not gloryvoid and not core1 and graph2;

solid gr1    = graph2 and not rx2 and not rx1
                        and not fuelv1
                        and not cladv1
                        and not fuele1
                        and not clade1
                        and not vd
                        and not gloryhole
                        and not gloryvoid
                        and botpt and toppt;

solid gv2     = gloryvoid and ledd and not graph2;

solid gh2     = gloryhole and not gloryvoid and ledd and not graph2;

solid lea1    = ledd and not gr1 and not rx2 and not rx1
                        and not fuelv1
                        and not cladv1
                        and not fuele1
                        and not clade1
                        and not vd
                        and not gloryhole
                        and not gloryvoid
                        and botps and toppz1;

solid gv3     = gloryvoid and wat and not ledd;

solid gh3     = gloryhole and not gloryvoid and wat and not ledd;

solid wa1    = wat and not lea1 and not gr1
                        and not rx2
                        and not rx1
                        and not fuelv1
                        and not cladv1
                        and not fuele1
                        and not clade1
                        and not vd
                        and not gloryhole
                        and not gloryvoid
                        and botps and toppzm;

# core2
tlo fuelv1;
tlo cladv1;
tlo fuele1;
tlo clade1;
# core levels
tlo rx1;
tlo rx2;
tlo vd;
tlo gr1;
tlo lea1;
tlo wa1;
# glory hole
tlo gh;
tlo gv;
tlo gh1;
tlo gv1;
tlo gh2;
tlo gv2;
tlo gh3;
tlo gv3;
end csg

@
@ - Define Boundary Conditions
@
```


www.manaraa.com

```
boundary vacuum wa1

@@@@@@@@@@@@@@@@@@@@@@@@@@@@@@@@@@@@@@@@@@@@@@@@@@@@@@@@@@@@@@@@@@@@@@@@
@
@ - create mesh
@
@@@@@@@@@@@@@@@@@@@@@@@@@@@@@@@@@@@@@@@@@@@@@@@@@@@@@@@@@@@@@@@@@@@@@@@@

netgen

@list constraints

@
@ - define library
@

library scale work xn2v7.1.wlib.old
@library scale work scale_8g_wlib.old

@
@ - spectrum
@

@spectrum 0.906693 0.093307 4.64109E-9 4.64109E-11 4.33366E-13 0 0 0
@spectrum 9.99617E-1 3.83467E-4 1.16856E-11 0
spectrum 1 0

@
@ - define material xs table ( iht, ihs, ihm )
@

xstab 7 8 15

@
@ - Define Isotopes
@

material u-235e    5092235
material u-238e    5092238
material o1e       5008016
material h1e       5001901
material ca1e      5006000
material u-235j   10092235
material u-238j   10092238
material o1j      10008016
material h1j      10001901
material ca1j     10006000
material ca2     16006312
material pb204   17082204
material pb206   17082206
material pb207   17082207
material pb208   17082208
material o2      18008016
material h2      18001001
@material o3       5008016
@material n        5007014
material alum    15013027
material ca3     19006000
material fe54    19026054
material fe56    19026056
material fe57    19026057
material fe58    19026058

@
@ - mixing instructions
@
@ Uranium-Polyethylene Core - 5
mix chomo
mix chomo u-235e       1.40281E-04
mix chomo u-238e       5.71806E-04
mix chomo ca1e         3.83490E-02
mix chomo h1e          7.66981E-02
mix chomo o1e          1.42418E-03
@ Uranium-Polyethylene Elements - 10
mix sr1
mix sr1 u-235j         9.7919E-05
mix sr1 u-238j         3.9913E-04
mix sr1 ca1j           3.8697E-02
mix sr1 h1j            7.7393E-02
mix sr1 o1j            9.9410E-04

@ Graphite - density 1.2801 g/cc - 11
mix graph
mix graph ca2        8.78149E-02

@ Aluminum - density 2.702 g/cc - 12
mix al
mix al   alum        6.03073E-02

@ Lead - density 10.777 g/cc - 13
mix pb
mix pb   pb204     4.38482E-04
mix pb   pb206     7.54815E-03
mix pb   pb207     6.92175E-03
```


www.manaraa.com

```
mix pb   pb208     1.64118E-02

@ Steel - density 7.82120 g/cc - 14
mix steel
mix steel  ca3       3.92153E-03
mix steel  fe54      4.88044E-03
mix steel  fe56      7.66124E-02
mix steel  fe57      1.76931E-03
mix steel  fe58      2.35463E-04

@ Water - density 0.99848 g/cc - 15
mix water
mix water  h2        6.67731E-02
mix water  o2        3.33866E-02

@ Air - 16
mix air
mix air    o2         9.48790E-06
@mix air    n         4.07700E-05
@mix air    o3        9.48790E-06

@ HOLE 17 - CCR
mix hole17
mix hole17 air  0.2
mix hole17 sr1  0.8

@ HOLE 18 - FCR
mix hole18
mix hole18 air  0.7
mix hole18 sr1  0.3

@
@ - Assign Sources and Material Properties to Regions
@

@ glory hole
property gh     al
property gv     air
property gh1    al
property gv1    air
property gh2    al
property gv2    air
property gh3    al
property gv3    air
@ rod rods/clad
property fuelv1  hole17
property cladv1  al
property fuele1  hole18
property clade1  al
@ core level plates
property rx1    chomo
property rx2    graph
property vd     air
@ graphite reflector
property gr1    graph
property lea1   pb
property wa1    water

@
@ - Define Mesh Type
@

@ mesh r1  delaunay


@
@ - Mesh Problem
@

@fill

@
@ - Plotting Device
@

@ dev x11

@
@ - Output Data to Default File
@
@run
@paraview flux
@paraview
data

@
@ - Stop the GEM Run
@

stop
```


www.manaraa.com

C.5.3.2 EVENT NETGEN Transient – Time-Dependent File

```
Title: AGN201 NETGEN 3D Model

@
@ - AGN 201 NETGEN 3D Model
@ - With Control Rods In and Below Core
@ - Douglas Bowen - 05/02/2013
@

@
@ - Define Main Problem Parameters
@
problem    radiation        @ RADIATION PROBLEM
geometry   xyz              @ 3D XYZ GEOMETRY
case       time             @ TIME DEPENDENT RUN
angle      1                @ P3 angular flux expansion
scatter    3                @ Order of scattering anisotropy
groups     2                @ NUMBER OF ENERGY GROUPS IN X-SECTION LIB
upscatter  yes              @ CONSIDER UPSCATTERING FROM ENERGY GROUPS
solution   pcg5             @ SOLUTION SCHEME
monitor    eigenvalue       @ MONITOR THE PROBLEM EIGENVALUE (KEFF)
iter 100 100 1.0e-06 1.0e-06 300 1.0e-11 300   @ Iteration Parameters
dump 99999

lump time

normalize eigenvalue

@normalize power 4.06 total

run event NG_T11_HGH.eig

guess flux NG_T11_HGH.eig unformatted

@@@@@@@@@@@@@@@@@@@@@@@@@@@@@@@@@@@@@@@@@@@@@@@@@@@@@@@@@@@@@@@@@@@@@@@@
@
@ - csg geometry description
@
@@@@@@@@@@@@@@@@@@@@@@@@@@@@@@@@@@@@@@@@@@@@@@@@@@@@@@@@@@@@@@@@@@@@@@@@

begin csg

algebraic3d
solid gloryvoid = cylinder (-100, 0, 0; 100, 0, 0; 1.27);
solid gloryhole = cylinder (-100, 0, 0; 100, 0, 0; 1.47);
solid core1  =  cylinder (0, 0, -47.29; 0, 0, 78.25;  12.80);
solid graph2 =  cylinder (0, 0, -36.25; 0, 0, 38.567; 33.12);
solid ledd   =  cylinder (0, 0, -46.50; 0, 0, 49.61; 44.926);
solid wat    =  cylinder (0, 0, -47.29; 0, 0, 78.25;  98.00);

# safety rod, coarse rod, and fine rod definitions
# 0/1=CCR, 4/5=FCR
solid cyl0   =  cylinder ( 5.869,  5.869, -28.25;  5.869,  5.869, 13.25; 2.25);
solid cyl1   =  cylinder ( 5.869,  5.869, -28.25;  5.869,  5.869, 13.25; 2.75);
solid cyl4   =  cylinder (-5.869, -5.869, -28.25; -5.869, -5.869, 13.25; 1.00);
solid cyl5   =  cylinder (-5.869, -5.869, -28.25; -5.869, -5.869, 13.25; 1.50);

# define AXIAL cutoff planes

solid botpz   =  plane (0, 0, -12.25;  0, 0, -1);
solid toppz   =  plane (0, 0,  12.25;  0, 0,  1);

solid botpp   =  plane (0, 0, 12.25;   0, 0, -1);
solid toppp   =  plane (0, 0, 13.25;   0, 0,  1);

solid botpz1   =  plane (0, 0, -28.25; 0, 0, -1);
solid toppz1   =  plane (0, 0, -12.25; 0, 0,  1);

#---------------------------------------------------------CCR
solid botpv1  =  plane (0, 0, -12.25;  0, 0, -1);
solid toppv1  =  plane (0, 0,   3.75;  0, 0,  1);
#---------------------------------------------------------CCR

#---------------------------------------------------------FCR
solid botpe1  =  plane (0, 0, -12.25;  0, 0, -1);
solid toppe1  =  plane (0, 0,   3.75;  0, 0,  1);
#---------------------------------------------------------FCR

solid botps  =  plane (0, 0, -47.29;   0, 0, -1);
solid topps  =  plane (0, 0, -36.25;   0, 0,  1);

solid botpt  =  plane (0, 0, -36.25;   0, 0, -1);
solid toppt  =  plane (0, 0,  38.567;  0, 0,  1);

solid botpzl =  plane (0, 0,  38.567;  0, 0, -1);
solid toppzl =  plane (0, 0,  48.817;  0, 0,  1);

solid botpzm =  plane (0, 0,  48.817;  0, 0, -1);
solid toppzm =  plane (0, 0,  65.000;  0, 0,  1);

# define the fuel and cladding for CR
```


المنارة للاستشارات
www.manaraa.com

```
# Core Zone 1 (bottom)
# v=CCR , e=FCR
solid fuelv1 = cyl0 and toppv1 and botpv1;
solid cladv1 = cyl1 and not fuelv1 and toppv1 and botpv1;
solid fuele1 = cyl4 and toppe1 and botpe1;
solid clade1 = cyl5 and not fuele1 and toppe1 and botpe1;

solid gv    = gloryvoid and core1;

solid gh    = gloryhole and not gloryvoid and core1;

solid rx1   = core1
                        and not fuelv1
                        and not cladv1
                        and not fuele1
                        and not clade1
                        and not gloryhole
                        and not gloryvoid
                        and toppz and botpz;

solid rx2    = core1 and toppz1 and botpz1;

solid vd     = core1 and botpp and toppp;

solid gv1    = gloryvoid and not core1 and graph2;

solid gh1    = gloryhole and not gloryvoid and not core1 and graph2;

solid gr1    = graph2 and not rx2 and not rx1
                        and not fuelv1
                        and not cladv1
                        and not fuele1
                        and not clade1
                        and not vd
                        and not gloryhole
                        and not gloryvoid
                        and botpt and toppt;

solid gv2     = gloryvoid and ledd and not graph2;

solid gh2     = gloryhole and not gloryvoid and ledd and not graph2;

solid lea1    = ledd and not gr1 and not rx2 and not rx1
                        and not fuelv1
                        and not cladv1
                        and not fuele1
                        and not clade1
                        and not vd
                        and not gloryhole
                        and not gloryvoid
                        and botps and toppz1;

solid gv3     = gloryvoid and wat and not ledd;

solid gh3     = gloryhole and not gloryvoid and wat and not ledd;

solid wa1    = wat and not lea1 and not gr1
                        and not rx2
                        and not rx1
                        and not fuelv1
                        and not cladv1
                        and not fuele1
                        and not clade1
                        and not vd
                        and not gloryhole
                        and not gloryvoid
                        and botps and toppzm;

# core2
tlo fuelv1;
tlo cladv1;
tlo fuele1;
tlo clade1;
# core levels
tlo rx1;
tlo rx2;
tlo vd;
tlo gr1;
tlo lea1;
tlo wa1;
# glory hole
tlo gh;
tlo gv;
tlo gh1;
tlo gv1;
tlo gh2;
tlo gv2;
tlo gh3;
tlo gv3;
end csg

@
@ - Define Boundary Conditions
@
```


www.manaraa.com

```
boundary vacuum wa1

@@@@@@@@@@@@@@@@@@@@@@@@@@@@@@@@@@@@@@@@@@@@@@@@@@@@@@@@@@@@@@@@@@@@@@@@
@
@ - create mesh
@
@@@@@@@@@@@@@@@@@@@@@@@@@@@@@@@@@@@@@@@@@@@@@@@@@@@@@@@@@@@@@@@@@@@@@@@@

netgen

@list constraints

@
@ - define library
@

library scale work xn2v7.1.wlib.old
@library scale work scale_8g_wlib.old

@
@ - spectrum
@

@spectrum 0.906693 0.093307 4.64109E-9 4.64109E-11 4.33366E-13 0 0 0
@spectrum 9.99617E-1 3.83467E-4 1.16856E-11 0
spectrum 1 0

@
@ - define material xs table ( iht, ihs, ihm )
@

xstab 7 8 15

@
@ - Define Isotopes
@

material u-235e    5092235
material u-238e    5092238
material o1e       5008016
material h1e       5001901
material ca1e      5006000
material u-235j   10092235
material u-238j   10092238
material o1j      10008016
material h1j      10001901
material ca1j     10006000
material ca2     16006312
material pb204   17082204
material pb206   17082206
material pb207   17082207
material pb208   17082208
material o2      18008016
material h2      18001001
@material o3       5008016
@material n        5007014
material alum    15013027
material ca3     19006000
material fe54    19026054
material fe56    19026056
material fe57    19026057
material fe58    19026058

@
@ - mixing instructions
@
@ Uranium-Polyethylene Core - 5
mix chomo
mix chomo u-235e       1.40281E-04
mix chomo u-238e       5.71806E-04
mix chomo ca1e         3.83490E-02
mix chomo h1e          7.66981E-02
mix chomo o1e          1.42418E-03
@ Uranium-Polyethylene Elements - 10
mix sr1
mix sr1 u-235j         9.7919E-05
mix sr1 u-238j         3.9913E-04
mix sr1 ca1j           3.8697E-02
mix sr1 h1j            7.7393E-02
mix sr1 o1j            9.9410E-04

@ Graphite - density 1.2801 g/cc - 11
mix graph
mix graph ca2        8.78149E-02

@ Aluminum - density 2.702 g/cc - 12
mix al
mix al   alum        6.03073E-02

@ Lead - density 10.777 g/cc - 13
mix pb
mix pb   pb204     4.38482E-04
mix pb   pb206     7.54815E-03
mix pb   pb207     6.92175E-03
mix pb   pb208     1.64118E-02
```


www.manaraa.com

```
@ Steel - density 7.82120 g/cc - 14
mix steel
mix steel  ca3       3.92153E-03
mix steel  fe54      4.88044E-03
mix steel  fe56      7.66124E-02
mix steel  fe57      1.76931E-03
mix steel  fe58      2.35463E-04

@ Water - density 0.99848 g/cc - 15
mix water
mix water  h2        6.67731E-02
mix water  o2        3.33866E-02

@ Air - 16
mix air
mix air    o2         9.48790E-06
@mix air    n         4.07700E-05
@mix air    o3        9.48790E-06

@ HOLE 17 - CCR
mix hole17
mix hole17 air  0.2
mix hole17 sr1  0.8

@ HOLE 18 - FCR
mix hole18
mix hole18 air  0.7
mix hole18 sr1  0.3

@
@ - Assign Sources and Material Properties to Regions
@

@ glory hole
property gh     al
property gv     air
property gh1    al
property gv1    air
property gh2    al
property gv2    air
property gh3    al
property gv3    air
@ rod rods/clad
property fuelv1  hole17
property cladv1  al
property fuele1  hole18
property clade1  al
@ core level plates
property rx1    chomo
property rx2    graph
property vd     air
@ graphite reflector
property gr1    graph
property lea1   pb
property wa1    water

@ |-------------------------------------------------------------------------|
@ | *********************************************************************** |
@ | ******************** TIME ZONE INFORMATION **************************** |
@ | *********************************************************************** |
@ |-------------------------------------------------------------------------|

@ |-------------------------------------------------------------------------
@ | TIME ZONE #0 -> uses mixing instructions above
@ |-------------------------------------------------------------------------

begin time zone 0

  duration 1.0e+00
  steps -1

end time zone 0

@ |-------------------------------------------------------------------------
@ | TIME ZONE #1 -> uses mixing instructions above
@ |-------------------------------------------------------------------------

begin time zone 1

  duration 1.0e+00
  steps -1

@
@ - mixing instructions
@
@ Uranium-Polyethylene Core - 5
mix chomo
mix chomo u-235e       1.40281E-04
mix chomo u-238e       5.71806E-04
mix chomo ca1e         3.83490E-02
mix chomo h1e          7.66981E-02
mix chomo o1e          1.42418E-03
@ Uranium-Polyethylene Elements - 10
mix sr1
```


www.manaraa.com

```
mix sr1 u-235j         9.7919E-05
mix sr1 u-238j         3.9913E-04
mix sr1 ca1j           3.8697E-02
mix sr1 h1j            7.7393E-02
mix sr1 o1j            9.9410E-04

@ Graphite - density 1.2801 g/cc - 11
mix graph
mix graph ca2        8.78149E-02

@ Aluminum - density 2.702 g/cc - 12
mix al
mix al   alum        6.03073E-02

@ Lead - density 10.777 g/cc - 13
mix pb
mix pb   pb204     4.38482E-04
mix pb   pb206     7.54815E-03
mix pb   pb207     6.92175E-03
mix pb   pb208     1.64118E-02

@ Steel - density 7.82120 g/cc - 14
mix steel
mix steel  ca3       3.92153E-03
mix steel  fe54      4.88044E-03
mix steel  fe56      7.66124E-02
mix steel  fe57      1.76931E-03
mix steel  fe58      2.35463E-04

@ Water - density 0.99848 g/cc - 15
mix water
mix water  h2        6.67731E-02
mix water  o2        3.33866E-02

@ Air - 16
mix air
mix air    o2         9.48790E-06
@mix air    n         4.07700E-05
@mix air    o3        9.48790E-06

@ HOLE 17 - CCR
mix hole17
mix hole17 air  0.2
mix hole17 sr1  0.8

@ HOLE 18 - FCR
mix hole18
mix hole18 air  0.7
mix hole18 sr1  0.3

end time zone 1

@ |-------------------------------------------------------------------------
@ | TIME ZONE #2 -> uses mixing instructions above
@ |-------------------------------------------------------------------------

begin time zone 2

  duration 60.0
  steps -1

@
@ - mixing instructions
@
@ Uranium-Polyethylene Core - 5
mix chomo
mix chomo u-235e       1.40281E-04
mix chomo u-238e       5.71806E-04
mix chomo ca1e         3.83490E-02
mix chomo h1e          7.66981E-02
mix chomo o1e          1.42418E-03
@ Uranium-Polyethylene Elements - 10
mix sr1
mix sr1 u-235j         9.7919E-05
mix sr1 u-238j         3.9913E-04
mix sr1 ca1j           3.8697E-02
mix sr1 h1j            7.7393E-02
mix sr1 o1j            9.9410E-04

@ Graphite - density 1.2801 g/cc - 11
mix graph
mix graph ca2        8.78149E-02

@ Aluminum - density 2.702 g/cc - 12
mix al
mix al   alum        6.03073E-02

@ Lead - density 10.777 g/cc - 13
mix pb
mix pb   pb204     4.38482E-04
mix pb   pb206     7.54815E-03
mix pb   pb207     6.92175E-03
mix pb   pb208     1.64118E-02

@ Steel - density 7.82120 g/cc - 14
```


www.manaraa.com

```
mix steel
mix steel  ca3       3.92153E-03
mix steel  fe54      4.88044E-03
mix steel  fe56      7.66124E-02
mix steel  fe57      1.76931E-03
mix steel  fe58      2.35463E-04

@ Water - density 0.99848 g/cc - 15
mix water
mix water  h2        6.67731E-02
mix water  o2        3.33866E-02

@ Air - 16
mix air
mix air    o2         9.48790E-06
@mix air    n         4.07700E-05
@mix air    o3        9.48790E-06

@ HOLE 17 - CCR
mix hole17
mix hole17 air  0.2
mix hole17 sr1  0.8

@ HOLE 18 - FCR
mix hole18
mix hole18 air  0.018609314
mix hole18 sr1  0.981390686

end time zone 2

@ |-------------------------------------------------------------------------
@ | TIME ZONE #3 -> uses mixing instructions above
@ |-------------------------------------------------------------------------

begin time zone 3

  duration 10.0
  steps -1

@
@ - mixing instructions
@
@ Uranium-Polyethylene Core - 5
mix chomo
mix chomo u-235e       1.40281E-04
mix chomo u-238e       5.71806E-04
mix chomo ca1e         3.83490E-02
mix chomo h1e          7.66981E-02
mix chomo o1e          1.42418E-03
@ Uranium-Polyethylene Elements - 10
mix sr1
mix sr1 u-235j         9.7919E-05
mix sr1 u-238j         3.9913E-04
mix sr1 ca1j           3.8697E-02
mix sr1 h1j            7.7393E-02
mix sr1 o1j            9.9410E-04

@ Graphite - density 1.2801 g/cc - 11
mix graph
mix graph ca2        8.78149E-02

@ Aluminum - density 2.702 g/cc - 12
mix al
mix al   alum        6.03073E-02

@ Lead - density 10.777 g/cc - 13
mix pb
mix pb   pb204     4.38482E-04
mix pb   pb206     7.54815E-03
mix pb   pb207     6.92175E-03
mix pb   pb208     1.64118E-02

@ Steel - density 7.82120 g/cc - 14
mix steel
mix steel  ca3       3.92153E-03
mix steel  fe54      4.88044E-03
mix steel  fe56      7.66124E-02
mix steel  fe57      1.76931E-03
mix steel  fe58      2.35463E-04

@ Water - density 0.99848 g/cc - 15
mix water
mix water  h2        6.67731E-02
mix water  o2        3.33866E-02

@ Air - 16
mix air
mix air    o2         9.48790E-06
@mix air    n         4.07700E-05
@mix air    o3        9.48790E-06

@ HOLE 17 - CCR
mix hole17
mix hole17 air  0.2
mix hole17 sr1  0.8
```


www.manaraa.com

```
@ HOLE 18 - FCR
mix hole18
mix hole18 air  0.342147617
mix hole18 sr1  0.657852383

end time zone 3

@ |---------------------------------------------------------------------
@ | TIME ZONE #4 -> uses mixing instructions above
@ |---------------------------------------------------------------------

begin time zone 4

  duration 45.0
  steps -1

@
@ - mixing instructions
@
@ Uranium-Polyethylene Core - 5
mix chomo
mix chomo u-235e       1.40281E-04
mix chomo u-238e       5.71806E-04
mix chomo ca1e         3.83490E-02
mix chomo h1e          7.66981E-02
mix chomo o1e          1.42418E-03
@ Uranium-Polyethylene Elements - 10
mix sr1
mix sr1 u-235j         9.7919E-05
mix sr1 u-238j         3.9913E-04
mix sr1 ca1j           3.8697E-02
mix sr1 h1j            7.7393E-02
mix sr1 o1j            9.9410E-04

@ Graphite - density 1.2801 g/cc - 11
mix graph
mix graph ca2        8.78149E-02

@ Aluminum - density 2.702 g/cc - 12
mix al
mix al   alum        6.03073E-02

@ Lead - density 10.777 g/cc - 13
mix pb
mix pb   pb204     4.38482E-04
mix pb   pb206     7.54815E-03
mix pb   pb207     6.92175E-03
mix pb   pb208     1.64118E-02

@ Steel - density 7.82120 g/cc - 14
mix steel
mix steel  ca3       3.92153E-03
mix steel  fe54      4.88044E-03
mix steel  fe56      7.66124E-02
mix steel  fe57      1.76931E-03
mix steel  fe58      2.35463E-04

@ Water - density 0.99848 g/cc - 15
mix water
mix water  h2        6.67731E-02
mix water  o2        3.33866E-02

@ Air - 16
mix air
mix air    o2         9.48790E-06
@mix air    n         4.07700E-05
@mix air    o3        9.48790E-06

@ HOLE 17 - CCR
mix hole17
mix hole17 air  0.14
mix hole17 sr1  0.86

@ HOLE 18 - FCR
mix hole18
mix hole18 air  0.7
mix hole18 sr1  0.3

end time zone 4

@ |---------------------------------------------------------------------
@ | TIME ZONE #5 -> uses mixing instructions above
@ |---------------------------------------------------------------------

begin time zone 5

  duration 229.0
  steps -1

@
@ - mixing instructions
@
@ Uranium-Polyethylene Core - 5
mix chomo
```


www.manaraa.com

```
mix chomo u-235e       1.40281E-04
mix chomo u-238e       5.71806E-04
mix chomo ca1e         3.83490E-02
mix chomo h1e          7.66981E-02
mix chomo o1e          1.42418E-03
@ Uranium-Polyethylene Elements - 10
mix sr1
mix sr1 u-235j         9.7919E-05
mix sr1 u-238j         3.9913E-04
mix sr1 ca1j           3.8697E-02
mix sr1 h1j            7.7393E-02
mix sr1 o1j            9.9410E-04

@ Graphite - density 1.2801 g/cc - 11
mix graph
mix graph ca2        8.78149E-02

@ Aluminum - density 2.702 g/cc - 12
mix al
mix al   alum        6.03073E-02

@ Lead - density 10.777 g/cc - 13
mix pb
mix pb   pb204     4.38482E-04
mix pb   pb206     7.54815E-03
mix pb   pb207     6.92175E-03
mix pb   pb208     1.64118E-02

@ Steel - density 7.82120 g/cc - 14
mix steel
mix steel  ca3       3.92153E-03
mix steel  fe54      4.88044E-03
mix steel  fe56      7.66124E-02
mix steel  fe57      1.76931E-03
mix steel  fe58      2.35463E-04

@ Water - density 0.99848 g/cc - 15
mix water
mix water  h2        6.67731E-02
mix water  o2        3.33866E-02

@ Air - 16
mix air
mix air    o2         9.48790E-06
@mix air    n         4.07700E-05
@mix air    o3        9.48790E-06

@ HOLE 17 - CCR
mix hole17
mix hole17 air  0.20
mix hole17 sr1  0.80

@ HOLE 18 - FCR
mix hole18
mix hole18 air  0.7
mix hole18 sr1  0.3

end time zone 5

@ |-------------------------------------------------------------------------
@ | TIME ZONE #6 -> uses mixing instructions above
@ |-------------------------------------------------------------------------

begin time zone 6

  duration 347.0
  steps -1

@
@ - mixing instructions
@
@ Uranium-Polyethylene Core - 5
mix chomo
mix chomo u-235e       1.40281E-04
mix chomo u-238e       5.71806E-04
mix chomo ca1e         3.83490E-02
mix chomo h1e          7.66981E-02
mix chomo o1e          1.42418E-03
@ Uranium-Polyethylene Elements - 10
mix sr1
mix sr1 u-235j         9.7919E-05
mix sr1 u-238j         3.9913E-04
mix sr1 ca1j           3.8697E-02
mix sr1 h1j            7.7393E-02
mix sr1 o1j            9.9410E-04

@ Graphite - density 1.2801 g/cc - 11
mix graph
mix graph ca2        8.78149E-02

@ Aluminum - density 2.702 g/cc - 12
mix al
mix al   alum        6.03073E-02

@ Lead - density 10.777 g/cc - 13
```


www.manaraa.com

```
mix pb
mix pb   pb204     4.38482E-04
mix pb   pb206     7.54815E-03
mix pb   pb207     6.92175E-03
mix pb   pb208     1.64118E-02

@ Steel - density 7.82120 g/cc - 14
mix steel
mix steel  ca3       3.92153E-03
mix steel  fe54      4.88044E-03
mix steel  fe56      7.66124E-02
mix steel  fe57      1.76931E-03
mix steel  fe58      2.35463E-04

@ Water - density 0.99848 g/cc - 15
mix water
mix water  h2        6.67731E-02
mix water  o2        3.33866E-02

@ Air - 16
mix air
mix air    o2         9.48790E-06
@mix air    n         4.07700E-05
@mix air    o3        9.48790E-06

@ HOLE 17 - CCR
mix hole17
mix hole17 air  0.991096431
mix hole17 sr1  0.008903569

@ HOLE 18 - FCR
mix hole18
mix hole18 air  0.7
mix hole18 sr1  0.3

end time zone 6

@ |---------------------------------------------------------------------
@ | DELAYED NEUTRON DATA
@ |---------------------------------------------------------------------

@ - DELAYED NEUTRON PRECURSOR DECAY CONSTANTS - KEEPIN DATA

define delayed

   groups 6

@ - DELAYED NEUTRON PRECURSOR DECAY CONSTANTS

   const 1.241E-02 3.054E-02 1.1101E-01 3.0142E-01 1.1482E+00 3.03737E+00

@ - DELAYED NEUTRON SPECTRUM

   spctrum  1.00E+00 1.00E+00 1.00E+00 1.00E+00 1.00E+00 1.00E+00

@ - DELAYED NEUTRON FRACTIONS

   fractions 2.1557E-04 1.4249E-3 1.2760E-03 2.5790E-03 7.5644E-4 2.7208E-04

end delayed

@
@ - Mesh Problem
@

@fill

@
@ - Plotting Device
@

@ dev x11

@
@ - Output Data to Default File
@
@paraview

data

@
@ - Stop the GEM Run
@

stop
```


www.manaraa.com

C.5.4 EVENT Transient Testing Files

Extensive scoping computations were performed prior as the EVENT transient models were developed. A uranium-polyethylene annular cylinder with an cylinidrical control rod was assumed for the EVENT transient testing model. The material composition of the uranium-polyethylene cylinder is essentially identical to the core region of the AGN. The control rod is intended to represent the CCR in the AGN core. An EVENT eigenvalue case and a time-dependent case were developed to simulate transients based on the control rod movement. The EVENT results were compared to both an analytical and a numerical solution to the point kinetics equations. The analytical solution was a solution to the point kinetics equations based on the assumption there is only one delayed neutron group. The numerial solution was based on a solution to the point kinetics equations for one delayed neutron group using the NDSOLVE function in Mathematica. The Mathematica notebook file is shown below.

C.5.4.1 EVENT U-Polyethylene Cylinder Transient Input Files

C.5.4.1.1 Eigenvalue GEM Input File

```
Title: 3D Uranium-Polyethylene Cylinder with Inner Region

@
@ - Define Main Problem Parameters
@

problem    radiation        @ Radiation problem
geometry   xy               @ 2D xyz geometry
case       eigenvalue       @ eigenvalue run
angle      1                @ P3 angular flux expansion
scatter    3                @ Order of scattering anisotropy
groups     2                @ No. of energy group for problem
upscatter  yes              @ # upscattering from energy groups
solution   pcg5             @ Solution scheme
monitor    eigenvalue       @ Monitor the Keff
iter 100 100 5.0e-05 5.0e-05 300 1.0e-11 300   @ Iteration Parameters
normalize eigenvalue
dump 99999

@normalize power 1 total
```


www.manaraa.com

```
opposite flux

@
@ --> DEFINE GEOMETRY
@

@
@ - Define Points
@

@ Cylinder Center

pnt p1  0.000  0.000

@
@ - Define Default Line Interval
@

default itv 5

@
@ - Define Inner and Outer regions
@

@
@ Main Reactor Sections
@

circle   c1   p1    2.0      10
circle   c2   p1   12.5        10

@
@ - Define Regions
@
@
@ Main Reactor Sections
@

region r1 c1
region r2 c2 c1

@ - distributed volumetric source

source s1 1.0E-06

@
@ - Define Boundary Conditions
@

boundary vacuum c2

@
@ - define library
@

library scale work xn2v7.1.wlib.old

@
@ - spectrum
@

@spectrum 9.99617E-1 3.83467E-4 1.16856E-11 0
spectrum 1 0

@
@ - Define Isotopes
@

material u-235a    1092235
material u-238a    1092238
material o1a       1008016
material h1a       1001901
material ca1a      1006000
material u-235j   10092235
material u-238j   10092238
material o1j      10008016
material h1j      10001901
material ca1j     10006000
material ca2     16006312
material pb204   17082204
material pb206   17082206
material pb207   17082207
material pb208   17082208
material o2      18008016
material h2      18001001
@material o3       5008016
@material n        5007014
material alum    15013027
material ca3     19006000
material fe54    19026054
material fe56    19026056
material fe57    19026057
material fe58    19026058
```


www.manaraa.com

```
@
@ - mixing instructions
@

@ Uranium-Polyethylene Core - homo - 1
mix core
mix core u-235a       1.40281E-04
mix core u-238a       5.71806E-04
mix core ca1a         3.83490E-02
mix core h1a          7.66981E-02
mix core o1a          1.42418E-03

@ Air - 8
mix air
mix air    o2         9.48790E-06

@ Zone 1 - 9

mix hole1
mix hole1 air  0.32056
mix hole1 core 0.67944

@
@ - assign materials and sources
@

@
@ - define averaging regions
@

average 1 r1
average 2 r2

@
@ - define sources, material properties, mesh
@

property r1  hole1  s1
property r2  core   s1

mesh r1  delaunay
mesh r2  delaunay

@ |--------------------------------------------------------------------------
@ | DELAYED NEUTRON DATA
@ |--------------------------------------------------------------------------

@ - DELAYED NEUTRON PRECURSOR DECAY CONSTANTS - KEEPIN DATA

define delayed

   groups 1

@ - DELAYED NEUTRON PRECURSOR DECAY CONSTANTS

   const 4.0775E-01

@ - DELAYED NEUTRON SPECTRUM

   spctrum  1.00E+00

@ - DELAYED NEUTRON FRACTIONS

   fractions 6.5240E-03

end delayed

@
@ - Mesh Problem
@

fill

@
@ - Plotting Device
@

paraview
@run
@
@ - Output Data to Default File
@

data

@
@ - Stop the GEM Run
@

stop
```


www.manaraa.com

C.5.4.1.2 Time-Dependent GEM Input File

```
Title: 3D Uranium-Polyethylene Cylinder with Inner Region

@
@ - Define Main Problem Parameters
@

problem    radiation        @ Radiation problem
geometry   xy               @ 2D xyz geometry
case       time             @ time run
angle      1                @ P3 angular flux expansion
scatter    3                @ Order of scattering anisotropy
groups     2                @ # energy group problem
upscatter  yes               @ No upscattering from energy groups
solution   pcg5             @ Solution scheme
monitor    eigenvalue       @ Monitor the Keff
iter 100 100 5.0e-05 5.0e-05 300 1.0e-11 300   @ Iteration Parameters
dump 99999

lump time

@normalize eigenvalue

@normalize power 1 total

run event uslug.eig

guess flux uslug.eig unformatted

@
@ --> DEFINE GEOMETRY
@

@
@ - Define Points
@

@ Cylinder Center

pnt p1  0.000  0.000

@
@ - Define Default Line Interval
@

default itv 5

@
@ - Define Inner and Outer regions
@

@
@ Main Reactor Sections
@

circle   c1   p1    2.0      10
circle   c2   p1   12.5        10

@
@ - Define Regions
@
@
@ Main Reactor Sections
@

region r1 c1
region r2 c2 c1

@ - distributed volumetric source

source s1 1.0E-06

@
@ - Define Boundary Conditions
@

boundary vacuum c2

@
@ - define library
@

library scale work xn2v7.1.wlib.old

@
@ - spectrum
@

@spectrum 9.99617E-1 3.83467E-4 1.16856E-11 0
spectrum 1 0
```


www.manaraa.com

```
@
@ - Define Isotopes
@

material u-235a    1092235
material u-238a    1092238
material o1a       1008016
material h1a       1001901
material ca1a      1006000
material u-235j   10092235
material u-238j   10092238
material o1j      10008016
material h1j      10001901
material ca1j     10006000
material ca2     16006312
material pb204   17082204
material pb206   17082206
material pb207   17082207
material pb208   17082208
material o2      18008016
material h2      18001001
@material o3       5008016
@material n        5007014
material alum    15013027
material ca3     19006000
material fe54    19026054
material fe56    19026056
material fe57    19026057
material fe58    19026058

@
@ - mixing instructions
@

@ Uranium-Polyethylene Core - homo - 1
mix core
mix core u-235a       1.40281E-04
mix core u-238a       5.71806E-04
mix core ca1a         3.83490E-02
mix core h1a          7.66981E-02
mix core o1a          1.42418E-03

@ Air - 8
mix air
mix air    o2         9.48790E-06

@ Zone 1 - 9

mix hole1
mix hole1 air  0.32056
mix hole1 core 0.67944

@
@ - assign materials and sources
@

@
@ - define averaging regions
@

average 1 r1
average 2 r2

@
@ - define sources, material properties, mesh
@

property r1  hole1  s1
property r2  core   s1

mesh r1  delaunay
mesh r2  delaunay

@ |--------------------------------------------------------------------------
@ | TIME ZONE #1 -> uses mixing instructions above
@ |--------------------------------------------------------------------------

begin time zone 1

  duration 1.0
  steps -1

@
@ - mixing instructions
@

@ Uranium-Polyethylene Core - homo - 1
mix core
mix core u-235a       1.40281E-04
mix core u-238a       5.71806E-04
mix core ca1a         3.83490E-02
mix core h1a          7.66981E-02
mix core o1a          1.42418E-03

@ Air - 8
```


www.manaraa.com

```
mix air
mix air    o2         9.48790E-06

@ Zone 1 - 9

mix hole1
mix hole1 air  0.23345
mix hole1 core 0.76655

end time zone 1

@ |---------------------------------------------------------------------
@ | DELAYED NEUTRON DATA
@ |---------------------------------------------------------------------

@ - DELAYED NEUTRON PRECURSOR DECAY CONSTANTS - KEEPIN DATA

define delayed

   groups 1

@ - DELAYED NEUTRON PRECURSOR DECAY CONSTANTS

   const 4.0775E-01

@ - DELAYED NEUTRON SPECTRUM

   spctrum  1.00E+00

@ - DELAYED NEUTRON FRACTIONS

   fractions 6.5240E-03

end delayed

@
@ - Mesh Problem
@

fill

@
@ - Plotting Device
@

@paraview

@
@ - Output Data to Default File
@

data

@
@ - Stop the GEM Run
@

Stop
```

C.5.5 *Mathematica* Notebook File

Mathematica was used to test time-dependent EVENT results for some simple cylindrical LEU-polyethylene cylinders. These calculations involved the point kinetics equations with only one effective group of delayed neutrons. The *Mathematica* results were also compared to the results of an analytic solution to the point kinetics equations for the AGN. The *Mathematica* notebook file is listed below.

www.manaraa.com

AGN 201M Reactivity Calculations

Define Constants for Point Kinetics Equations

In[1021]:=
```
lambda = 0.4263;
```

In[1022]:=
```
beff = 0.00734;
```

In[1023]:=
```
rho1 = 0.00235;
rho2 = 0.00235;
```

In[1025]:=
```
lambda2 = 0.000073126;
```

Define Coefficients for Point Kinetics Equations

In[1026]:=
```
A1 = (rho1 - beff) / lambda2;
```

In[1027]:=
```
B1 = lambda;
```

In[1028]:=
```
C1 = beff / lambda2;
```

In[1029]:=
```
D1 = lambda;
```

Define Coefficients for Point Kinetics Equations

In[1030]:=
```
A11 = (rho2 - beff) / lambda2;
```

In[1031]:=
```
B11 = lambda;
```

In[1032]:=
```
C11 = beff / lambda2;
```

In[1033]:=
```
D11 = lambda;
```

Numerical Solution Point Kinetics Equations

In[1034]:=
```
sol2 = NDSolve[{P1'[t] == A11 P1[t] + B11 Z1[t],
    Z1'[t] == C11 P1[t] - D11 Z1[t],
    P1[0] == 1, Z1[0] == beff / (lambda lambda2)},
  {P1, Z1}, {t, 0, 100}, Method → Automatic];
```


www.manaraa.com

In[1035]:=
```
big2 = LogPlot[Evaluate[{P1[t]} /. sol2], {t, 0, 5}]
```

Out[1035]=

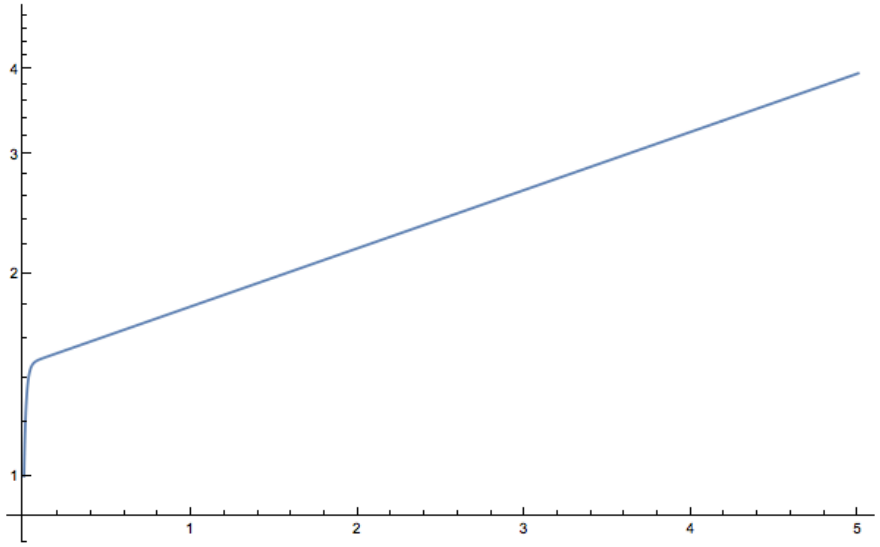

In[1036]:=
```
num2 = LogPlot[Evaluate[{P1[t] / P1[0]} /. sol2], {t, 0, 1}]
```

Out[1036]=

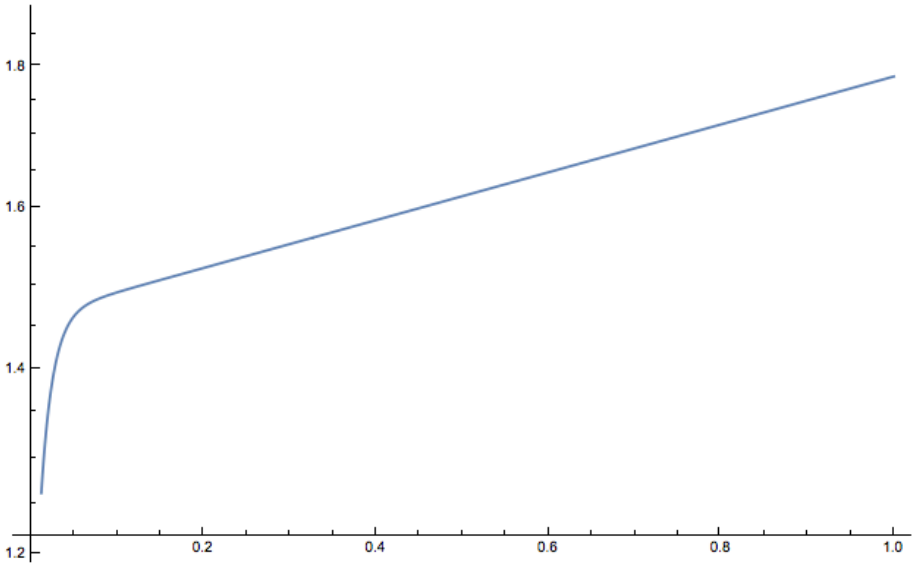

Analytic Solution to One Delay Family Approximation

In[1037]:=
```
P0 = 1;
```


www.manaraa.com

```
In[1038]:= P2[t] = P0 * ((rho1 / (rho1 - beff)) * Exp[((rho1 - beff) / lambda2) t] -
              (beff / (rho1 - beff)) * Exp[(- (rho1 * lambda) / (rho1 - beff)) t])
Out[1038]= -0.470942 e^(-68.2384 t) + 1.47094 e^(0.200763 t)

In[1039]:= big3 = LogPlot[Evaluate[{P2[t]}], {t, 0, 1}]
```

Out[1039]=

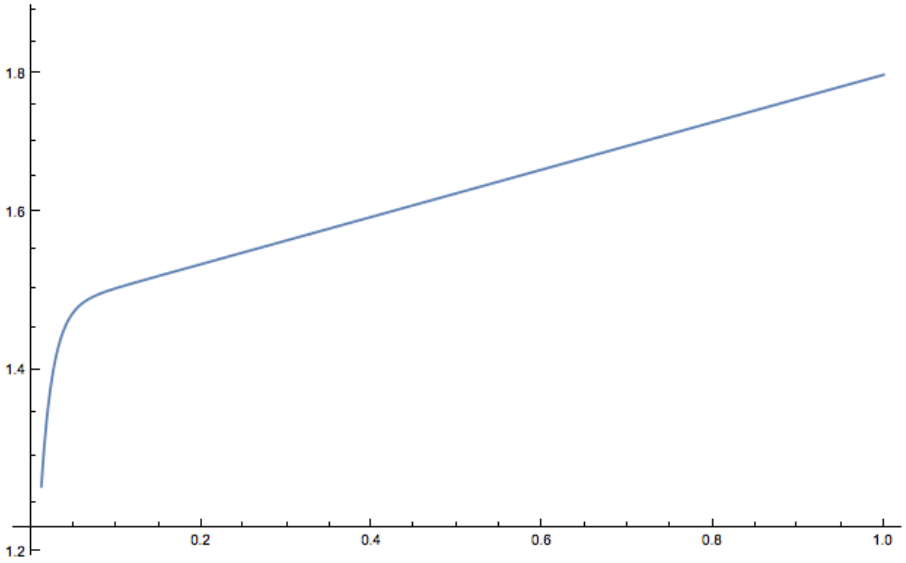


```
In[1040]:= big2 = LogPlot[Evaluate[{P1[t]} /. sol2], {t, 0, 5}]
```

Out[1040]=

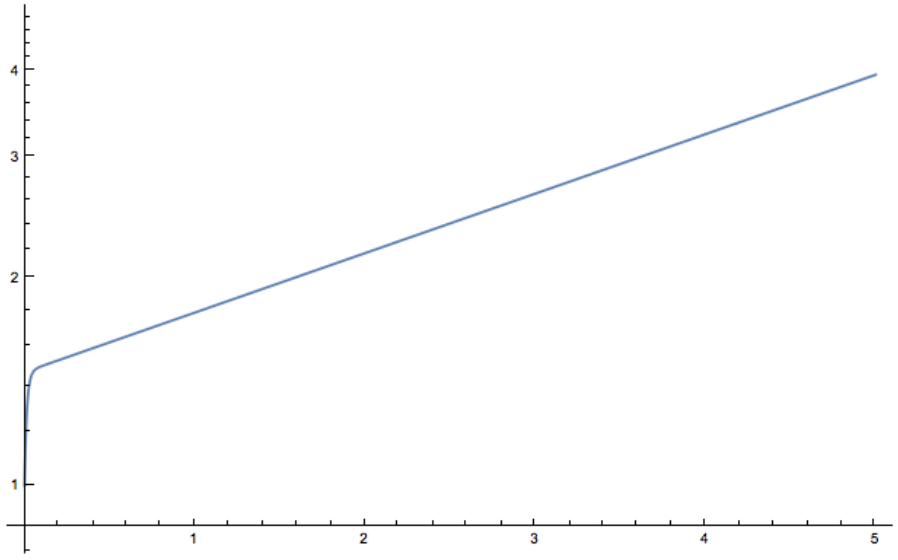

www.manaraa.com

References

[1] Federal Register, Vol. 75, No. 93, Friday, May 14, 2010, University of New Mexico AGN-201M Reactor; Environmental Assessment and Finding of No Significant Impact, Docket No. 50-252; NRC-2008-0557.

[2] A. T. Biehl, R. P. Geckler, S. Kahn, and R. Mainhardt, "Elementary Reactor Experimentation," Aerojet General Nucleonics, October 1957.

[3] C.R.E. de Oliviera, "EVENT – A Multigroup, Finite Element-Spherical Harmonics Program for the Solution of Steady-State and Time-Dependent Radiation Transport Problems in Arbitrary Geometry," Imperial College of Science, Technology, and Medicine, London, June 2001.

[4] L. Wetzel, "Critical Experiment Report for the AGN-201M Reactor at the University of New Mexico, NCS-2007-214, October 23, 2007.

[5] L. M. Petrie et al, "KENO V.a: An Improved Monte Carlo Criticality Program," Oak Ridge National Laboratory, ORNL/TM-2005/39 Version 6.1 Sect. F11, June 2011.

[6] Los Alamos National Laboratory, "MCNP6™ User's Manual, Version 1.0," LA-CP-13-00634, Rev. 0, May 2013.

[7] M. L. Gorham, "Experimental Parameterization of the Idaho State University AGN-201 Research and Training Reactor," M.S. Thesis, Idaho State University, 2012.

www.manaraa.com

[8] The University of New Mexico, "The University of New Mexico AGN-201M Reactor – Reactor Operation and Training Manual," Department of Chemical and Nuclear Engineering, June 2011.

[9] D. A. Daavettila et al, "A Manual of Reactor Laboratory Experiments," Argonne National Laboratory, ANL-6990, January 1965.

[10] M. A. Jessee and M. D. DeHart, "NEWT: A New Transport Algorithm for Two-Dimensional Discrete-Ordinates Analysis in Non-Orthogonal Geometries," Oak Ridge National Laboratory, ORNL/TM-2005/39 Version 6.1 Sect. F21, June 2011.

[11] University of New Mexico, "License Renewal Application, Safety Analysis Report, Technical Specifications, Environmental Considerations, and Operator Requalification Program," Redacted Version, February 21, 2007.

[12] D. Chandler, "Spatially-Dependent Reactor Kinetics and Supporting Physics Validation Studies at the High Flux Isotope Reactor," PhD Dissertation, University of Tennessee, 2011.

[13] R. H. Kimpland, "A Multi-region Computer Model for Predicting Nuclear Excursions in Aqueous Homogeneous Solution Assemblies," Dissertation, University of Arizona, 1993.

[14] S. Goluoglu, "A Deterministic Method for Transient, Three-Dimensional Neutron Transport," PhD Dissertation, University of Tennessee, 1997.

[15] S. Goluoglu and H.L. Dodds, "A Time-Dependent, Three-Dimensional Neutron Transport Methodology," *Nucl. Sci. Eng.*, **139**, 248-261, 2001.

[16] Argonne Code Center: Benchmark Problem Book, ANL-7416, Supplement No. 3, Argonne National Laboratory, December 1985.

[17] C. L. Bentley, "Improvements in a Hybrid Stochastic/Deterministic Method for Transient Three-Dimensional Neutron Transport," PhD Dissertation, University of Tennessee, December 1996.

[18] M. W. Waddell Jr. and H.L. Dodds, "A Hybrid Stochastic/Deterministic Method for Transient, Three-Dimensional Neutron Transport, PhD Dissertation, University of Tennessee, Transactions of the American Nuclear Society, Volume 66, 1992.

www.manaraa.com

[19] T. H. Newton, Jr., "Development of a Low Enriched Uranium Core for the MIT Reactor," PhD Dissertation, Massachusetts Institute of Technology, February 2006.

[20] W. L. Woodruff, "A Kinetics and Thermal-Hydraulics Capability for the Analysis of Research Reactors," *Nucl. Tech.*, **64**, February, 1984.

[21] C. C. Pain, A. J. H. Goddard and C. R. E. de Oliviera, "The Finite Element Transient Criticality Code FETCH – Verification and Validation," *Proceedings of the Second NUCEF International Symposium on Nuclear Fuel Cycle*," Hitachinaka, Ibaraki, Japan, pp. 139, 1998.

[22] C. C. Pain, C. R. E. de Oliveira, A. J. H. Goddard and A. P. Umpleby, "Criticality Behaviour of Dilute Plutonium Solutions," *Nucl. Sci. Tech.*, **135**, pp. 194-215, 2001.

[23] C. C. Pain, C. R. E. de Oliviera, A. J. H. Goddard, M. D. Eaton, S. Gundry and A. P. Umpleby, "Transient Analysis and Dosimetry of the Tokaimura Criticality Accident," *Nuclear Technology*, **144**, No. 1, pp. 16-33, 2003.

[24] C. C. Pain, C. R. E. de Oliveira, A. J. H. Goddard, and A. P. Umpleby, "Transient Criticality in Fissile Solutions–Compressibility Effects," *Nuclear Science and Engineering*, **138**, pp. 78-95, 2001.

[25] R. A. Knief, *Nuclear Criticality Safety – Theory and Practice*, American Nuclear Society, 1985.

[26] SCALE: A Modular Code System for Performing Standardized Computer Analyses for Licensing Evaluation, ORNL/TM-2005/39, Version 6, Vols. I–III, January 2009. (Available from Radiation Safety Information Computational Center at Oak Ridge National Laboratory as CCC-750).

[27] D. F. Hollenbach, L. M. Petrie, S. Goluoglu, N. F. Landers, and M. E. Dunn, "KENO-VI: A General Quadratic Version of the KENO Program," Oak Ridge National Laboratory, ORNL/TM-2005/39, Version 6.1, Sect. F17, June 2011.

[28] L. M. Petrie et al, "CSAS6: Control Module for Enhanced Criticality Safety Analysis Sequences with KENO-VI," Oak Ridge National Laboratory, ORNL/TM-2005/39 Version 6.1 Sect. C6, June 2011.

www.manaraa.com

[29] M. L. Williams and D. F. Hollenbach, "CENTRM: A One-Dimensional Neutron Transport Code for Computing Pointwise Energy Specta," Oak Ridge National Laboratory, ORNL/TM-2005/39 Version 6.1 Sect. F18, June 2011.

[30] M. A. Jessee and M. D. DeHart, "NEWT: A New Transport Algorith for Two-Dimensional Discrete Ordinates Analysis in Non-Orthogonal Geometries, ORNL/TM-2005/39, Version 6.1, Sect. F21, Oak Ridge National Laboratory, June 2011.

[31] N. M. Greene, L. M. Petrie, and M. L. Williams, "XSDRNPM: A One Dimensional Discrete-Ordinance Code for Transport Analysis," ORNL/TM-2005/39, Version 6.1, Sect. F3, Oak Ridge National Laboratory, June 2011.

[32] Oak Ridge National Laboratory Radiation Shielding Information Center, "RSICC Data Library DLC-023 – CASK-81: 22 Neutron, 18 Gamma-Ray Group, P3, Cross Sections for Shipping Cask Analysis," 1987.

[33] G. E. Hansen and W. H. Roach, "Six and Sixteen Group Cross Sections for Fast and Intermediate Critical Assemblies, LA-2543-MS, Los Alamos Scientific Library, November 1961.

[34] M. L. Williams, D. Wiarda, K. S. Kim, M. E. Dunn and B. T. Rearden, "SCALE 6.2 Beta 3 Manual, Ch. 11 SCALE Cross-Section Libraries," Oak Ridge National Laboratory, April 2014.

[35] D. Brown, "Release of the ENDF/B-VII.1 Evaluated Nuclear Data File," *Transactions of the American Nuclear Society*, 107, pp. 679-682, 2012.

[36] C.R.E. de Oliviera, "GEM – A Finite Element Mesh Generator and Data Preparation Program for Radiation Transport and Fluids Codes," Imperial College of Science, Technology, and Medicine, London, June 2001.

[37] J. Wood and M. M. R. Williams, Recent Progress in the Application of the Finite Element Method to the Neutron Transport Equation, Progress in Nuclear Energy, 14, No. 1, pp. 21-40, 1984.

[38] J. Schöberl, "NETGEN – 4X – An Automatic Mesh Generation Tool," RWTH Aachen University, Germany, March 3, 2010.

[39] C. R. E. Oliviera, "Solving Radiation Transport Problems with the GEM/EVENT Codes, Code Manual, University of New Mexico, September 2011.

www.manaraa.com

[40] C.R.E. de Oliviera, "EVENT – A Multigroup, Finite Element-Spherical Harmonics Program for the Solution of Steady-State and Time-Dependent Radiation Transport Problems in Arbitrary Geometry," Imperial College of Science, Technology, and Medicine, London, June 2001.

[41] R. T. Ackroyd, et al., "Recent Developments in Finite Element Methods for Neutron Transport Theory," Advances in Nuclear Science and Technology, Vol. 19, 1987.

[42] C. R. E de Oliviera, C. C. Pain, and A. J. H. Goddard, "The Finite Element-Spherical Harmonics Method for Time-dependent Radiation Transport Applications," Proceedings of the 1998 Radiation Protection and Shielding Topical Conference, Nashville, USA, April 19-23, 1998.

[43] C. R. E. de Oliviera, C. C. Pain, and A. H. Goddard, "The Finite Element-Spherical Harmonics Method for Time-dependent Radiation Transport Applications," The American Nuclear Society Radiation Protection and Shielding Topical Conference, Nashville, TN, 1998.

[44] J. C. Stone, Adaptive Discrete-Ordinates Algorithms and Strategies, PhD Dissertation, Texas A&M University, 2007.

[45] W. R. Martin, The Application of the Finite Element Method to the Neutron Transport Equation," PhD Dissertation, University of Michigan, 1976.

[46] K. Moreland, "The ParaView Tutorial, Version 4.1," Sandia National Laboratories, 2012.

[47] Wci.llnl.gov, (2014). *VisIt*. [online] Available at: https://wci.llnl.gov/simulation/computer-codes/visit [Accessed 19 Sep. 2014].

[48] S. Wolfram, *Mathematica*, Second Edition, Addison-Wesley Publishing Co., Redwood City, CA, 1991.

[49] K.C. Ruzich and W.J. Sturm, "Hazard Summary Report for the Argonne AGN-201 Reactor," Argonne National Laboratory, ANL-6510, February 1962.

[50] J. J. Duderstadt and L.J. Hamilton, *Nuclear Reactor Analysis*, John Wiley & Sons, 1976.

[51] A. F. Henry, *Nuclear-Reactor Analysis*, The MIT Press, Cambridge, MA, 1975.

www.manaraa.com

[52] R. A. Rydin, *Nuclear Reactor Theory and Design*, 3rd Edition, 2003.

[53] S. Michálek, J. Haščík, F. Farkas, "MCNP5 Delayed Neutron Fractions (β_{eff}) Calculation in Training Reactor VR-1," Journal of Electrical Engineering, **59**, No. 4, pp. 221-224, 2008.

[54] G. D. Spriggs, R. D. Busch, and J. M. Campbell, "Calculation of the Delayed Neutron Effectiveness Factor Using Ratios of k-eigenvalues," Annals of Nuclear Energy, **28**, pp. 477-487, 2001.

[55] R. K. Meulekamp and S. C. van der Marck, "Calculating the Effective Delayed Neutron Fraction with Monte Carlo," *Nuc. Sci. Engr.*, **152**, 142-148, 2006.

[56] B. Kiedrowski, F. Brown, and P. Wilson, "Calculating Kinetics Parameters and Reactivity Changes with Continuous Energy Monte Carlo," American Nuclear Society, PHYSOR-2010 Conference Presentation, Pittsburg, PA, LA-UR-09-06786, 2010.

[57] Busch, Robert, *Email Communication Regarding Control Rod Annual Measurement Results,* March 2015.

[58] G. R. Keepin, *Physics of Nuclear Kinetics*, Addison-Wesley Publishing Co. Inc., 1965.

[59] M. C. Brady, "Evaluation and Application of Delayed Neutron Precursor Data," Los Alamos National Laboratory, LA-11534-T, April 1989.

[60] Busch, Robert, *Personal Communication*, January 2015.

www.manaraa.com